CONTINUUM ANALYSIS OF UNSTIFFENED AND STIFFENED COUPLED SHEAR WALLS

by

LAMRI BENSMAIL

Ingenieur d'Etat en Constructions

Civiles et Industrielles

Universite de CONSTANTINE.

A Thesis Submitted for the Degree of

Master of Science

Department of Civil Engineering,

University of Glasgow.

March, 1990.

ProQuest LLC.
789 East Eisenhower Parkway
P.O. Box 1346
Ann Arbor, MI 48106 – 1346

CONTENTS

ACKNOWLEDGEMENTS

The work described here in was carried out in the Department of Civil Engineering at the University of Glasgow, under the supervision and guidance of Professor A. Coull

The author wishes to express his gratitude to Professor A. Coull, Regius Professor of Civil Engineering in the University of Glasgow, for his supervision and guidance during the course of this research programme.

Thanks are due to D. R. Green, for the facilities of the department, for Dr I. McConnochie for the administrative matters and for the computing consultants and staff for their assistance and the computing facilities provided for the numerical work.

The author also wishes to thank the Algerian Ministry of Higher Education and the Algerian Embassy for their scolarship without which this research would not have been possible.

My grateful thanks are due to **"ALLAH"** first for giving me the opportunity to do this study and helping me to accomplish it, and then to:

* My family, Notably, my mother for her moral support, my father, and my brothers and sisters, for their encouragement and material support throughout the years.

* My friends T. Bouden, S. Djellab, A. Bensalem, M. Bendahgane, and Y. K. To, for their useful discussion and cooperation.

* My friends K. Belkheir, A. Bouazza, and M. Sellougha for their encouragement.

SUMMARY

The basic approach of the continuum analysis of coupled shear wall structures subjected to lateral loads has been reassessed, and a discretisation of the method has been established. It has been demonstrated that consistent results are achieved for the case of equal walls on identical supports.

Inconsistencies occur in the traditional theory if the walls are unequal. A top concentrated interactive force is found to exist in the connecting medium at the top of the structure, and statical conditions may be violated. Although good results are still obtained for slightly unsymmetrical shear wall structures, the accuracy falls sharply when the unsymmetry of the structure becomes important, especially in the extreme case of a wall connected by beams to a column. For such cases, the results given by the continuum method show very poor agreement with those given by an accurate stiffness–matrix frame analysis if the conventional assumption of a line of contraflexure occuring at the mid–span position of the lintel beams is adopted. It is found that a revised analysis using a modified line of contraflexure greatly improves the accuracy of the results obtained for the forces in the slender wall, and also reduces the intensity of the top fictitious force.

Guidance on the best method of modelling for an analysis by the continuum method is presented. A revised line of contraflexure is adopted, and guidance on the incorporation of the top boundary condition is established. Best results for the internal forces are achieved if the revised line of contraflexure is used, provided the top boundary condition is properly considered, and if the beam moment is distributed equally between the stories above and below the level concerned in the discretisation procedure.

The continuum analysis for coupled shear walls is extended to cover the inclusion of one or two stiffening beams along the height for walls supported on elastically flexible foundations. Good agreement is obtained between the results given by this extended method and those from the frame analysis. Where stiffening beams are provided to enhance the rigidity of the structure, best results are obtained when the two stiffening beams are located at roughly one third and two thirds of the height of the structure. In the case of one stiffening beam only, the best location is between one third and one half of the height of the structure.

NOMENCLATURE

A_1, A_2	cross–section area of wall 1 and wall 2 respectively
A	A_1+A_2
A_b, A_{b1}, A_{b2}	cross–section areas of lintel beams and stiffening beams 1 and 2 respectively
b	clear span length of lintel beams
C_f, C_{f1}, C_{f2}	reduction factors due to the shift in the line of contraflexure.
c_1, c_2	distances from the centroidal axes of walls to the outer edges of the walls
D, D_1, D_2	depth of lintel beams and stiffening beams 1 and 2
d_1, d_2	distances from the centroidal axes of walls to the inner edges of the walls
E, E_{m1}, E_{m2}	elastic modulus of walls and stiffening beams 1 and 2 respectively
f	shape factor
G_f	reduction factor due to shear deformations in the continuous medium
H	structural height
h	storey height
I_1, I_2	second moment of area of wall 1 and wall 2 respectively
I	$I_1+ I_2$
I'	second moment of area of the composite cantilever (I'=I+ml)

I_b, I_{f_1}, I_{f_2} second moment of area of lintel beams and of stiffening beam 1 and 2 respectively

I_d, I_{m_1}, I_{m_2} reduced second moment of area of lintel beams and of stiffening beams 1 and 2 respectively

J H/h (number of stories)

k relative flexural rigidity of lintel beams, αH

K_δ vertical stiffness of soil foundation

K_r rotational stiffness of soil foundation

K_1, K_2 percentage of individual and composite cantilever action

L_1, L_2 distances from the mid-span position of lintel beams to the centroidal axes of walls 1 and 2 respectively.

L distance between centroidal axes of walls ($L = L_1 + L_2$)

M_e moment due to external loads

M_{e0} moment at base Level due to externaL loads

M_0 bending moment in walls at base Level [as defined in equation (2.51)]

m $A_1A_2.L/A$(sum of the static moments of the walls)

m_1,m_2 moments at the extremities of the connecting beams

M_1, M_2 bending moments in walls

M_t $M_1 + M_2$

$(M_m)_s$, $(M_d)_s$ concentrated moments in the stiffening beams for the discrete system and the equivalent continuous system respectively.

n	axial force distribution in the connecting medium
N_f	axial force in lintel beam f
P	concentrated load at top of the structure
q	laminar shear in the connecting medium
q_0	laminar shear in the connecting medium at the base level
Q_t	concentrated interactive top force
Q_f	shear force in lintel beam f
R_f	reduction factor of the second moment of area of lintel beams [as defined in equation (2.35)]
R_1, R_2	reduction factors of the second moment of area of stiffening beams 1 and 2 respectively
S_{m1}, S_{m2}	relative flexural second moments of inertia of the stiffening beams 1 and 2 respectively [as defined in equations (4.24)]
S_1, S_2	shear forces in walls
T	axial force in walls
T_0	axial force in walls at the base level
t	thickness of walls
U	total uniformly distributed load
V_{m1}, V_{m2}	shear forces in the stiffening beams 1 and 2 respectively
W	total triangularly distributed load
x	height co-ordinate
x_1, x_2	positions of the stiffening beams 1 and 2 respectively
y	lateral deflection

Greek letters

σ_A, σ_B	maximum extreme fibre stresses in wall 1
σ_C, σ_D	maximum extreme fibre stresses in wall 2
δ	relative settlement of walls
α, β	structural parameters [see equations (2.40) and (2.39)]
γ_1, γ_2	relative flexural rigidities of the stiffening beams [see equations (4.23)]
θ	base rotation
Δ	shift in the line of contraflexure from the mid-span position of lintel beams
ν	Poisson's ratio
ξ, ξ_1, ξ_2	height ratios ($\xi = x/H$, $\xi_1 = x_1/H$, $\xi_2 = x_2/H$)
μ	$1/(2J) + \xi$
φ	$1/(2J) - \xi$
τ	$\xi_1 + 1/(2J)$
ρ	$\xi_1 - 1/(2J)$
χ	$\xi_2 + 1/(2J)$
υ	$\xi_2 - 1/(2J)$
λ_1	d_1/d_2
λ_2	b/d_2
λ_3	$(I_2 b)/(I_b h)$

Subscripts

o	denotes base of the structure
i	denotes the zone number of the shear wall
s	denotes the stiffening beam number

CHAPTER ONE

INTRODUCTION

1.1 Tall buildings and shear walls

A modern trend is to build high. Tall buildings or high rise constructions are buildings for which the effects of horizontal loads are significant from the structural point of view. They are mainly used for residential and office purposes, for economical reasons. Tall building structures may consist of vertical elements of frames, shear walls or a combination of both. The causes of lateral loads affecting tall buildings are wind, seismic activities and blast loadings which refer to vibrations induced in the soil due to man-made explosions. However the most frequent cause of horizontal loads is wind, whose intensity depends mainly on its velocity and the shape and the lateral stiffness of the structure. Therefore the provision of lateral stiffness becomes increasingly important especially for structures over about twenty storeys in height. The determination of wind forces on a structure is basically a dynamic problem. However since the structure as a whole adapts itself as though for quasi-static loads, it has been the usual practice to treat the wind as a statically applied pressure and to neglect its dynamic nature unless the structure is very flexible.

The shear wall is an economical and basic component of tall building structures. It includes elevators, shafts, stairwells, core units, plane walls and coupled shear walls. Coupled shear walls are walls perforated by openings for doors, windows or corridors. They are introduced into multistorey structures mainly to resist lateral loads and to provide lateral stability of the structure against wind or seismic loading. The structures considered in the present work are those comprising shear walls connected by beams which

form part of the wall, or floor slabs, or a combination of both.

In recent years, much research has been carried out on the development of analytical techniques for shear walls which are commonly used in residential structures. A comprehensive review of the methods of analysis and sources of information on the subgect have been presented by Fintel et al[1], Coull and Stafford Smith[2] and Coull[3]. Coupled shear walls may be analysed by four distinct methods, namely

1. the finite element method
2. the finite strip method
3. the frame analogy method
4. the continuum method

The finite element method which is a powerful method usually referring to systems of two or three dimensional elements. In this method of analysis, walls and beams are divided into small elements. The accuracy of the method depends on the type and size of the elements used. These elements are connected to each other at discrete nodes. A stiffness analysis of the various force actions on the structure involves the solution of many simultaneous equations. This analysis has the disadvantage of the large number of elements and nodes required for the modelling of the shear wall structure, which leads to to a costly computer analysis and it is time consuming. However the finite element method is more appropriate for the investigation of particular problems in greater detail.

The finite strip method, in which the shear wall is modelled as an assemblage of strip elements with each element always stretching from the base to the top of the structure. The number of degrees of freedom is high and independent of the height. It is an accurate and relatively economic method for carrying out static, dynamic and stability analyses of shear walls.

The frame analogy method of analysis of shear walls is based on matrix procedures, using the stiffness matrix method. In this method,

columns and beams are represented by line elements joining node points. Plane walls are replaced by columns positioned along their centroidal axes. When connected to other members, the finite width of the wall is incorporated at each floor level by a stiff horizontal arm connecting the centroidal axis to the external fibres. This device effectively ensures that plane sections remain plane as the wall deflects and that the effects of the wall rotations are correctly included at the junction with an external connection. However in modern computer programs the effects of the stiff arms are more conveniently included by the constraint technique, which consists of constraining the nodes at the junction wall– beam to have the same rotation and lateral deflection as the column nodes. The method is relatively versatile in dealing with the geometry of the structure and the combination of loads applied to it. The analysis requires the solution of a set of equations, and as so it needs the use of a computer.

The continuum method is the most appropriate method for hand calculations for regular or partially regular structures. Its simplicity and ability to produce design curves and charts make it a suitable method for design offices calculations. Although subjected to some limitations, the continuum method has proved able to give solutions to relatively complex problems using small computers. In this method, the discrete system of connections, formed by lintel beams or floor slabs, is replaced by an equivalent continuous medium which is assumed to be rigidly attached to the walls. Axial deformations of the connecting beams are assumed to be negligible. The behaviour of the system is governed by a second order differential equation, enabling a general closed solution to the problem to be obtained. Since a deep wall panel will appear as a slender cantilever beam when viewed in the context of the complete building height, the shear deformations in the walls may be safely neglected and the shear wall will be dominated by its flexural behaviour when subjected to lateral loading.

1.2 Review of previous research.

Attention is only paid to the previous work related to the work presented in this thesis.

The application of the continuum technique to tall buildings was first used by Chitty and Wan[4]. Since then several investigators helped in the development of the technique, notably Beck[5], who was the first to apply the continuum method to coupled shear walls, and Rosman[6,7,8] who developed the technique to include the finite depths of the walls, and to deal with such topics as non-uniform structures. A comprehensive treatment has also been carried out by Coull[9,10] who extended the basic method to deal with the cases where the wall thickness and cross sections are variable. The case of flexible foundations and its effects on the behaviour of the structure has also been considered by Coull[11]. Where a top stiff beam is added to the coupled shear wall to limit the foundation movement due to support condition of flexible foundations, an analytical solution has been presented by Coull[12]. Curves[14,15,16] which illustrate the behaviour of coupled shear walls and give assistance in design offices have also been produced.

The insertion of additional stiffening beams between two solid walls may greatly affect the structural behaviour. Coull and Choo[25] investigated coupled shear walls stiffened by a top and/or a bottom stiffening beam, and showed the importance of a stiffening beam in increasing the stiffness of the structure and reducing the bending stresses in the walls. Chan and Kuang[26,31] carried out an analogous study on coupled shear walls with a stiffening beam somewhere along the height and showed the importance of the locations of the stiffening beam in affecting the structural actions.

The degree of coupling of coupled shear walls and the effect of the openings on the overall behaviour of the structure and the overal stress, has been conveniently expressed in terms of a non-dimensional geometrical

parameter (αH) defining the relative stiffness[17] of the connecting beams with respect to that of the walls. Pearce and Mathews[18] showed that when the value of this non-dimensional parameter, which appears in the second order differential equation governing the structural behaviour, is very small, the effect of the openings on the overall stress is small. However larger openings correspond to a bigger relative stiffness of the connecting beams with regard to the stiffnes of the walls, and the behaviour of the coupled shear wall will be similar to that of a frame.

For the case of unequal coupled shear walls and especially for the limiting case of a wall connected to a column by lintel beams, when the bending stiffness of the slender wall section is flexible in comparison with the adjacent section and approaches that of the connecting beams, the continuum method can produce significant errors[27,28,29]. This is due to the basic assumption that there are points of contraflexure on the centre lines of the connecting beams. Deschappelles[27] used the continuum method theory and gave an alternative solution for the extreme case of a wall connected by beams to a column by developing a new line of contraflexure. Development of a criterion for assessing when the effect of the comparative walls stiffness on the beam's stiffness may be important has been carried out by Macleod[28] for coupled shear walls with one and two rows of openings. Similar work has been carried out by Arvidsson[29], who presented a method based on the continuous theory which takes into consideration the effect of door openings near the edge of the wall.

Ungureanu[19] proposed a new structural model, by which the continuous uniform connection is replaced by a continuous connection of variable stiffness defined by a Fourier series which includes more efficiently the local effects of the joints between horizontal and vertical elements.

The study of shear walls by the frame method required the incorporation and modelling of the assumed stiff arms joining the ends of

the lintel beams to the centroidal axes of the walls. Schwaighofer and Microys[20] presented a method for analysing shear walls by standard computer programs. The method treats the rigid arms, which are theoretically of infinite sectional area and moment of inertia, as additional members of high but finite values of cross-sectional area and moment of inertia. This procedure increases the number of nodes in the structural model. For the special case of symmetrical structures, Stafford Smith[21] replaced the rigid-ended beam by an analogous uniform beam with the same rotational end stiffness, which allowed standard computer programs to be used without any increase in the number of nodes. The increase of the flexibility of the connecting beams due to the local deformations at the wall junction has been estimated[22] by assuming the wall to act as a semi-infinite elastic plane, and the effects of the deformations were calculated as reduction factors for the beam stiffness. From the results of the experimental investigations carried out by Michael[22], the latter concluded that for most span-to-depth ratios of lintel beams likely to occur in practice, the extra flexibility of the beam can be taken into account by assuming an effective span of the beam equal to the real clear span increased by half its depth on each side. Using the finite element method, similar work has been carried out[23] and comparative charts have been introduced. Bhatt[23] considered the problem of local deformations occuring at the junction wall-beam due to the high local stress concentrations and their effect on the lintel beam's flexibility. He pointed out that when the ratio of beam length to depth is less than 5, the effect of junction deformations becomes important. However for ratios less than 3, the effects of the ratio of the wall width to the beam depth becomes also important and can be taken into account by the charts provided. The results obtained by the latter author are applicable to the analysis of shear walls by both countinuum and wide column frame methods of analysis. For

the former method, the extra flexibility of the beam is taken into account by increasing the length of the beam by using deflection factors given in graphs provided by the same authur, or by dividing the non-dimensional parameter, αH by the same factor. For the wide-column frame method, the correction is achieved either by increasing the flexible portion or by the provision of rotational springs between the rigid and elastic portions of the beam.

1.3 Scope of present research

The continuum method has always been well accepted for the analysis of symmetrical coupled shear wall systems because of the inherent simplicity in its approach. However, the continuum method has been criticised as not having the flexibility of the wide-column frame method to cover the case of unsymmetrical structures. This is particularly true when one wall becomes very slender compared to the other wall, that is the slender wall which may be regarded as a column whose stiffness approaches the stiffness of the connecting beams. This criticism is justified when the analytical solution is employed using the assumption of points of contraflexure at the mid-span position of the lintel beams. The error has been shown by a comparative study[28] against the frame method, which does not employ the assumption of the points of contraflexure. The study showed that the inaccuracy increases with the increase of the ratio of the inertias of the walls, and reaches a maximum in the extreme case of a very slender wall or column connected to a relatively much stiffer wall.

The structural response of laterally loaded coupled shear walls depends on the degree of coupling afforded by the connecting beams. Coupled shear walls with weak connecting beams will behave more like two independant cantilevered walls. Where the connecting beams are significantly stiffer, the two walls will tend to act as a monolithic cantilever and the system is

structurally more efficient. The structural response of a coupled shear wall with weak coupling beams may be improved by introducing stiffer beams at convenient positions along the height of the structure. Also, where the foundations are flexible, the use of stiffening beams may also improve the base conditions if a stiff beam is positioned at the base or at a position near the base level.

Additional errors arise if a roof beam is included to stiffen the structure and to induce additional axial forces in the walls to reduce the bending moments. The inaccuracy is due to the assumption of equal curvatures, which leads to moments at the top of the structure which are not consistent with those given by statics.

A third problem arises with non rigid foundations when differential settlement and rotation occurs.

The object of the present work is to attempt to study the reasons for the discrepancies in the continuum analysis of unequal coupled walls, to improve the solution by a more accurate representation of the model used in the analysis, based on the continuous connection technique, to assess the accuracy of the analytical solution of the continuous connection method against the wide column frame method, to investigate the position of the points of contraflexure, and to examine the effect of the different points of contraflexure on the results obtained for the case of unsymmetrical coupled shear wall systems, and particularly the extreme case of a column connected to a wall by lintel beams.

The investigation of unequal uniform coupled shear wall systems and the particular case of a wall connected to a column is reported in chapter 2.

The case of a coupled shear wall structure, stiffened by one or two stiffening beams at any position along the height of the structure is reported in chapter 4. The effects of the stiffening beams and their positions which

have a great effect on the structure are also considered in the present work in chapter 4. The numerical results for the latter case have been carried out, using a program written in "Fortran 77" on an ICL 3980 computer, and are reported in chapter 5. The results related to the analysis carried out in chapter 2 are reported in chapter 3. For both cases reported in chapters 2 and 4, a comparative study has been carried out with the more exact analogous frame method in which beams and walls are represented by bar elements along their centroidal axes. The general purpose program used is "Flash" (Finite Element Analysis of Shells). A series of tests has been carried out on different coupled wall structures with different wall inertias, with or without stiffening beams, to asses the accuracy of the modified theory. The results obtained for the two cases reported in chapters 2 and 4 are presented in chapters 3 and 5, respectively.

CHAPTER TWO

CONTINUUM ANALYSIS OF UNEQUAL COUPLED SHEAR WALLS

2. 1 Introduction

In the analysis of coupled shear walls using the equivalent distributed lamina method, an assumption is made that a point of contraflexure occurs at the mid–point of the connecting lamina.

Herein, the problem is reformulated in more general form so that no assumption is made that the mid–points of the connecting beams are points of contraflexure. And so any pair of coupled shear walls can be analysed regardless of the relative flexural rigidities of the two walls. However special care is paid to the limiting case of a wide wall connected to a relatively very slender wall by lintel beams in which the points of contraflexure of the connecting beams can move considerably off–centre.

2. 2 Analysis

Consider a coupled shear wall system resting on a flexible foundation and assumed to be subjected to three kinds of typical lateral loads, namely a uniformly distributed load of intensity w, an upper triangularly distributed load of intensity w_1 at the top, and a concentrated load P acting at the top of the structure, as shown in Fig. 2.1 (a). The following assumptions are considered in the analysis

(1) The structure is uniform throughout the height, and the storey heights remain constant.

(2) Plane sections before bending remain plane after bending for all structural members.

(3) The discrete set of connecting beams, each of flexural rigidity EI_b (Fig. 2.1(a)) may be replaced by an equivalent continuous uniform connecting medium of stiffness EI_b/h per unit height, where h is the storey height (Fig. 2.1 (b)).

(4) Due to the high in-plane rigidity of the surrounding floor slabs and axial stiffness of the connecting beams, the axial deformations of the connecting beams are assumed to be negligible, so that the vertical elements deflect equally in the horizontal plane at any level. It follows that the slopes and the curvatures of the walls in the continuum model are everywhere equal along the height, and so the bending moment in each wall will be proportional to its flexural rigidity.

(5) The connecting beams, and hence the equivalent connecting medium, deform with a point of contraflexure at distance Δ for the intermediate lintel beams and Δ_t for the top lintel beam from the mid-span position of the connecting medium towards the less stiff wall. The values of the two distances Δ and Δ_t will be considered later. The two distances Δ and Δ_t will both be equal to zero for the case of equal walls because of symmetry.

(6) The discrete structure (Fig. 2.1 (a)) and the equivalent connecting medium (Fig. 2.1 (b)) are assumed cut along a vertical line passing through the points of contraflexure of the connecting medium at the distance Δ from the centre line of the lamina towards the less stiff wall. The discrete set of axial forces, N and shear forces, Q in the connecting beams (Fig. 2.2 (a)) may then be replaced by equivalent continuous distributions of intensity 'n' and 'q' per unit height respectively (Fig. 2.2 (b)). Also, the discrete system will carry a concentrated moment, M_p at the top lintel beam in the cut position

due to the difference in the shift of the point of contraflexure between the top beam and the lintel beams underneath, $(\Delta_t - \Delta)$ as will be shown later. This moment is asssumed to be concentrated at the top of the continuous medium. M_p is zero in the particular case of two equal walls.

For the three types of loading considered, the external moment, M_e is given by

$$M_e = H.M\ (\xi) \qquad \ldots\ldots (2.1)$$

where

$$M\ (\xi) = \frac{1}{2}\ U.(1-\xi)^2 + P.(1-\xi) + \frac{1}{3}\ W.\left[\ 2 - \xi\ \{\ 3 - (\xi)^2\ \}\ \right] \qquad (2.2)$$

$U = wH$ (Total uniformly distributed load)

$W = 1/2\ w_1 H$ (Total triangularly distributed load)

H is the structural height

and ξ is the height ratio x/H

Consider a small vertical element subjected to the set of stress resultants shown in Fig. 2.3. The conditions of vertical and rotational equilibrium become

$$q = -\frac{dT}{dx} \qquad \ldots\ldots (2.3)$$

$$\frac{dM_1}{dx} + S_1 - (\ L_1 + \Delta\ )q = 0 \qquad \ldots\ldots (2.4)$$

$$\frac{dM_2}{dx} + S_2 - (\ L_2 - \Delta\ )q = 0 \qquad \ldots\ldots (2.5)$$

The addition of the latter two equations yields the overall condition

$$\frac{dM_1}{dx} + \frac{dM_2}{dx} + S_1 + S_2 - Lq = 0 \quad \ldots\ldots\ldots\ldots\ldots\ldots \quad (2.6)$$

where L is the distance between centroidal axes of the two walls (equal to L_1+L_2)

The moment–curvature relationship for each wall is

$$EI_1 \frac{d^2y}{dx^2} = M_1 = M_e - M_{t1} - M_A \quad \ldots\ldots\ldots\ldots\ldots\ldots \quad (2.7)$$

$$EI_2 \frac{d^2y}{dx^2} = M_2 = - M_{t2} + M_A \quad \ldots\ldots\ldots\ldots\ldots\ldots \quad (2.8)$$

where M_{t1} and M_{t2} are the moments due to shear forces in the continuous medium, given by

$$M_{t1} = (L_1+\Delta)T + M_p \quad , \qquad M_{t2} = (L_2-\Delta)T - M_p$$

where

$$T = \int_x^H q \, dx \quad \ldots\ldots\ldots\ldots\ldots\ldots \quad (2.9)$$

The moment, M_A due to the axial forces n in the connecting medium is given by,

$$M_A = \int_x^H n(\lambda)(\lambda-x)\, d\lambda + Q_t (H-x) \quad \ldots\ldots\ldots\ldots\ldots\ldots \quad (2.10)$$

in which λ is a dummy variable of integration, and Q_t is a concentrated interactive force which exists at the top of the structure, as will be discussed later.

The addition of equations (2.7) and (2.8) yields the overall moment–curvature relationship,

$$EI \frac{d^2y}{dx^2} = M_t = M_e - L\,T \qquad \ldots\ldots\ldots\ldots\ldots\ldots\ldots\ldots \quad (2.11)$$

Since the curvatures in the two walls are equal at all levels, it follows from equation (2.11) that

$$M_1 = \frac{I_1}{I} (M_e - T.L) \qquad \ldots\ldots\ldots\ldots\ldots\ldots\ldots\ldots \quad (2.12)$$

$$M_2 = \frac{I_2}{I} (M_e - T.L) \qquad \ldots\ldots\ldots\ldots\ldots\ldots\ldots\ldots \quad (2.13)$$

where M_1 and M_2 are the bending moments in walls 1 and 2 respectively

and $I = I_1 + I_2$

From equations (2.7) and (2.11),

$$M_A = \frac{I_2}{I} M_e + \frac{I_1}{I} L\,T - M_{t_1} \qquad \ldots\ldots\ldots\ldots\ldots\ldots\ldots\ldots \quad (2.14)$$

and hence, from equation (2.10),

$$n_i = \frac{d^2M_A}{dx^2} = \frac{I_2}{I} \frac{d^2M_e}{dx^2} + \left(\frac{I_1}{I} L - \Delta - L_1\right) \frac{d^2T}{dx^2} \qquad \ldots\ldots\ldots \quad (2.15)$$

where

$$\frac{d^2M_e}{dx^2} = \frac{1}{H} (U + 2W.\xi) \qquad \ldots\ldots\ldots\ldots\ldots\ldots\ldots\ldots\ldots \quad (2.16)$$

and

$$\frac{d^2T}{dx^2} = - \frac{dq}{dx}$$

Substitution of equations (2.12), (2.13) and (2.3) into (2.4) and (2.5) yields the shear force in each wall,

$$S_1 = \left(\frac{I_1}{I} L - \Delta - L_1\right) \frac{dT}{dx} - \frac{I_1}{I} \frac{dM_e}{dx} \qquad \ldots\ldots\ldots\ldots\ldots\ldots (2.17)$$

$$S_2 = \left(\frac{I_2}{I} L + \Delta - L_2\right) \frac{dT}{dx} - \frac{I_2}{I} \frac{dM_e}{dx} \qquad \ldots\ldots\ldots\ldots\ldots\ldots (2.18)$$

where

$$\frac{dM_e}{dx} = - P - U (1-\xi) - W (1-\xi^2)$$

The first term of the shears will be equal to zero in the special case of equal walls and the shears will then be proportional to their inertias and reduce to

$$S_1 = - \frac{I_1}{I} \frac{dM_e}{dx}$$

$$S_2 = - \frac{I_2}{I} \frac{dM_e}{dx} \qquad \ldots\ldots\ldots (2.19)$$

In each case the total shear, S (x) is given by the sum of the two shears as

$$S (x) = S_1 + S_2$$

$$= - \frac{dM_e}{dx} \qquad \ldots\ldots\ldots\ldots\ldots\ldots\ldots\ldots\ldots\ldots\ldots\ldots (2.20)$$

At the top of the structure, equations (2.17) and (2.18) become,

$$S_1(H) = \left(\frac{I_1}{I} L - \Delta - L_1\right) \frac{dT}{dx}(H) - \frac{I_1}{I} \frac{dM_e}{dx}(H)$$

$$S_2(H) = \left(\frac{I_2}{I} L + \Delta - L_2\right) \frac{dT}{dx}(H) - \frac{I_2}{I} \frac{dM_e}{dx}(H) \quad \ldots\ldots (2.21)$$

In the case of a distributed loading, the static shear force is zero at the top, that is

$$\frac{dM_e}{dx} = 0$$

and since

$$\frac{I_1}{I} L - \Delta - L_1 = -\left(\frac{I_2}{I} L + \Delta - L_2\right)$$

the top shears given by equation (2.21), become

$$S_1(H) = -S_2(H) = \left(\frac{I_1}{I} L - \Delta - L_1\right) \frac{dT}{dx}(H) \quad \ldots \quad (2.22)$$

which is true for any distributed loading. It must therefore be deduced that, in order to produce a shear force at the top of the continuous structure, a concentrated interactive force Q_t must exist at the top of the connecting medium, of magnitude

$$Q_t = \left(\frac{I_1}{I} L - \Delta - L_1\right) q(H)$$

$$= -\left(\frac{I_2}{I} L + \Delta - L_2\right) q(H) \quad \ldots\ldots\ldots\ldots\ldots (2.23)$$

where

$$q\ (H) = -\ \frac{dT}{dx}\ (H)$$

The force Q_t will be tensile or compressive according as the top shear force $S_1(H)$ is negative or positive.

At the base, the shear forces in the walls are given by

$$S_1\ (0) = -\ \frac{I_1}{I}\ \frac{dM_e}{dx}\ (0) + \left(\frac{I_1}{I}\ L - \Delta - L_1\right)\ \frac{dT}{dx}\ (0)$$

..... (2.24)

$$S_2\ (0) = -\ \frac{I_2}{I}\ \frac{dM_e}{dx}\ (0) + \left(\frac{I_2}{I}\ L + \Delta - d_2\right)\ \frac{dT}{dx}\ (0)$$

For the case of a rigid foundation, it will be shown later from the base compatibility equation (2.52), that

$$\frac{dT}{dx}\ (0) = 0$$

and equations (2.24) reduce to

$$S_1\ (0) = -\ \frac{I_1}{I}\ \frac{dM_e}{dx}\ (0)$$

..... (2.25)

$$S_2\ (0) = -\ \frac{I_2}{I}\ \frac{dM_e}{dx}\ (0)$$

and the shears at the base become proportional to their flexural rigidities

The effect of the coupling can be assessed by considering two limiting cases, the case of coupled shear walls connected by weak beams and the case of a shear wall connected by relatively stiff beams. In the former case the walls are assumed to be acting completly independently, with the neutral axis at

the centroid of each wall. However, for the latter case, the wall system is assumed to be acting as a single composite cantilever, the neutral axis being situated at the centroid of the two wall elements. The stress distribution at any section, for the two walls shown in Fig. 2.4 (a) under the action of the bending moments M_1 and M_2 and the axial forces T, will be as shown in Fig. 2.4 (b). Taking tensile stresses as positive, the maximum extreme fibre stresses in walls 1 and 2 will be given by:

$$\sigma_A = \frac{M_1 c_1}{I_1} + \frac{T}{A_1} = (M_e - T.L)\frac{c_1}{I} + \frac{T}{A_1}$$

$$\sigma_B = -\frac{M_1 d_1}{I_1} + \frac{T}{A_1} = -(M_e - T.L)\frac{d_1}{I} + \frac{T}{A_1}$$

$$\sigma_C = \frac{M_2 . d_2}{I_2} - \frac{T}{A_2} = (M_e - T.L)\frac{d_2}{I} - \frac{T}{A_2} \quad \ldots\ldots \quad (2.26)$$

$$\sigma_D = -\frac{M_2 . c_2}{I_2} - \frac{T}{A_2} = -(M_e - T.L)\frac{c_2}{I} - \frac{T}{A_2}$$

This stress distribution may be considered to be derived from an alternative superposition of two pure bending stress distributions[14,15]: (a) a bending stress obtained on the assumption that the wall system acts as a single composite cantilever, as shown in Fig. 2.4 (c), (b) two linear stress distributions obtained on the assumption that the walls act completely independently, as shown in Fig. 2.4 (d).

Suppose that K_1, is the percentage of the load carried by independent cantilever action and that K_2, is the percentage carried by composite cantilever action and consider the two component stress distributions.

(a) *Composite cantilever action* (see Fig. 2.4 (c))

The total bending moment, M_t in the walls at any section is equal to:

$$M_t = M_e \frac{K_2}{100}$$

and the extreme fibre stresses in wall 1 will be given by:

$$\sigma_A = \frac{M_e}{I'} \left(\frac{A_2 L}{A} + c_1\right) \frac{K_2}{100}$$

$$\sigma_B = \frac{M_e}{I'} \left(\frac{A_2 L}{A} - d_1\right) \frac{K_2}{100} \qquad \ldots\ldots\ldots\ldots\ldots\ldots \quad (2.27)$$

in which

$I' = (I + mL)$, which is the second moment of area of the structure acting as a composite cantilever. .. (2.28)

$m = \frac{A_1 A_2 L}{A}$, which is the sum of the static moments of area of the walls. ..... (2.29)

$A = A_1 + A_2$ (sum of the cross sectional areas of wall 1 and 2)

Similar expressions hold for wall 2

(b) *Individual cantilever action* (see Fig. 2.4 (d))

The loads carried by the walls are proportional to their moments of inertia. The bending moments in walls 1 and 2 will thus be given by:

$$M_1 = M_e \frac{I_1}{I} \frac{K_1}{100}$$

$$M_2 = M_e \frac{I_2}{I} \frac{K_1}{100}$$

and the extreme fibre stresses in wall 1 become:

$$\sigma_A = \frac{M_1 . c_1}{I_1} = M_e \frac{c_1}{I} \frac{K_1}{100}$$

$$\sigma_B = - \frac{M_1 . d_1}{I_1} = - M_e \frac{d_1}{I} \frac{K_1}{100} \quad \ldots\ldots\ldots\ldots\ldots\ldots \quad (2.30)$$

Similar expressions again hold for wall 2.

On equating corresponding stresses at the four extreme fibre positions from equations (2.26), (2.27) and (2.30) for wall 1, with the corresponding expressions for wall 2, the composite action proportional function K_2 may finally shown to be:

$$K_2 = 100 \frac{\alpha^2}{\beta^2} \frac{T}{M_e} \quad \ldots\ldots\ldots\ldots\ldots\ldots\ldots\ldots\ldots\ldots\ldots\ldots \quad (2.31)$$

and

$$K_1 = 100 - K_2 \quad \ldots\ldots\ldots\ldots\ldots\ldots\ldots\ldots\ldots\ldots\ldots\ldots \quad (2.32)$$

The compatibility of the vertical displacements at the cut position requires that

$$L \frac{dy}{dx} - \frac{hb^3}{12EI_d} q - \frac{1}{E} \left(\frac{1}{A_1} + \frac{1}{A_2} \right) \int_0^x T \, dx - \delta = 0 \quad \ldots\ldots\ldots\ldots \quad (2.33)$$

where A_1 and A_2 are the cross sectional areas of walls 1 and 2 respectively, E is the modulus of elasticity.

The four successive terms in the compatibility equation denote the relative displacement at the cut due to bending of the walls, deformation of the laminae due to both bending and shear deformations in the connecting medium, axial deformation of the walls and the relative vertical foundation settlement.

The effect of shearing deformation in the lintel connecting beams may be included by replacing the true second moment of area I_b by a reduced second moment of area I_d, given by

$$I_d = I_b . R_f \quad \ldots\ldots\ldots\ldots\ldots\ldots\ldots\ldots\ldots\ldots\ldots\ldots\ldots\ldots \quad (2.34)$$

where R_f is a reduction factor given by

$$R_f = G_f . C_f \quad \ldots\ldots\ldots\ldots\ldots\ldots\ldots\ldots\ldots\ldots\ldots\ldots\ldots\ldots \quad (2.35)$$

G_f is a reduction factor due to the shear deformations in the connecting medium, given by

$$G_f = \left(1 - \frac{S_f}{1 + S_f} \right) \quad \ldots\ldots\ldots\ldots\ldots\ldots\ldots\ldots\ldots\ldots\ldots\ldots\ldots\ldots \quad (2.36)$$

and

$$S_f = 24 \, f \, \frac{I_b}{A_b} \, \frac{1 + \nu}{b^2} \, C_f$$

where

A_b is the cross-sectional area of the lintel beams, f, is a shape factor and ν, is Poisson's ratio.

C_f is a reduction factor due to the shift in the line of contraflexure, Δ from the mid span-position of the clear span b of the lintel beams and is given by

$$C_f = 1 - \frac{12\ (\Delta/b)^2}{1 + 12\ (\Delta/b)^2} \quad \ldots\ldots\ldots\ldots\ldots\ldots\ldots\ldots\ldots\ldots\ (2.37)$$

For the special case when the centre—line of the lamina passes through the points of contraflexure of the lintel beams, that is $\Delta = 0$, the reduction factor C_f will be equal to unity. And if the shear deformations in the continuous medium are neglected, the reduction factor G_f will also be equal to unity.

For a beam of a depth D and a thickness t, the shape factor, $f \simeq 6/5$

and $S_f = 2.4\ (D/b)^2\ (1+\nu)\ C_f$

Differentiating equation (2.33) and combining equations (2.3) and (2.11) to eliminate the variables y and q yields the governing differential equations for the axial force T

$$\frac{d^2T}{dx^2} - \alpha^2 T = -\beta^2 M_e \quad \ldots\ldots\ldots\ldots\ldots\ldots\ldots\ldots\ldots\ldots\ (2.38)$$

where

$$\beta^2 = \frac{12\ I_d.L}{hb^3 I} \quad \ldots\ldots\ldots\ldots\ldots\ldots\ldots\ldots\ldots\ldots\ (2.39)$$

$$\alpha^2 = \beta^2\ \frac{I'}{m} \quad \ldots\ldots\ldots\ldots\ldots\ldots\ldots\ldots\ldots\ldots\ (2.40)$$

The complete solution to equation (2.36) is as follows

$$T = B.\cosh k\xi + C.\sinh k\xi + \frac{\beta^2}{\alpha^2} H \left(M(\xi) + \frac{U + 2W\xi}{k^2} \right). \quad (2.41)$$

where k is the relative flexural rigidity of the lintel beams, (αH).

The corresponding expression for the laminar shear can then be derived by

using equation (2.3), and is given as follows

$$q = -\frac{1}{H}\left[k \left(B.\sinh k\xi + C.\cosh k\xi \right) + \frac{\beta^2}{\alpha^2} H \left(\frac{dMe}{dx} + \frac{2W}{k^2} \right) \right] \quad \ldots\ (2.42)$$

The axial force in the walls and the laminar shear at the base level can be obtained respectively as, at $x = 0$,

$$T_0 = B + \frac{\beta^2}{\alpha^2} H \left[U \left(\frac{1}{2} + \frac{1}{k^2} \right) + \frac{2}{3} W + P \right] \quad \ldots\ (2.43)$$

$$q_0 = -\left[C.\alpha - \frac{\beta^2}{\alpha^2} \left\{ U + P + W \left(1 - \frac{2}{k^2} \right) \right\} \right] \quad \ldots\ (2.44)$$

$$\frac{d^2T}{dx^2} = -\frac{dq}{dx}$$

$$= \frac{1}{H^2} k^2 \left[B \cosh k\xi + C \sinh k\xi \right] + \frac{\beta^2}{\alpha^2} \frac{1}{H} \left[U + 2W.\xi \right] \quad \ldots\ (2.45)$$

The values of the integration constants B and C can be determined by considering the boundary conditions for the problem.

Boundary conditions

(1) At the top of the structure $x = H$, the axial force in each wall is equal to zero, that is

$$T(H) = 0 \quad \ldots\ (2.46)$$

Therefore, equation (2.41) results in

$$B = -C \tanh k + \mu_1 \quad \ldots\ (2.47)$$

where

$$\mu_1 = -\frac{\beta^2}{\alpha^2} H \frac{(U + 2W)}{k^2 \cosh k}$$

(2) The boundary condition at the base depends on whether the foundation on which the coupled shear walls rest is considered to be elastically flexible or fully rigid.

Considering the the compatibility equation (2.31) at the base level, x = 0, where the separate wall bases rest on elastic foundations, both vertical and rotational deformations of the separate bases will be considered and the base compatibility equation can be expressed as

$$L\theta - \frac{h\, b^3}{12EI_d} q_0 - \delta = 0 \quad \ldots\ldots\ldots\ldots\ldots\ldots\ldots\ldots \quad (2.48)$$

where the rotation θ and the relative settlement δ of the walls at the foundation are given by

$$\theta = \frac{M_0}{K_r} \quad \ldots\ldots\ldots\ldots\ldots\ldots\ldots\ldots\ldots\ldots\ldots\ldots\ldots\ldots \quad (2.49)$$

$$\delta = \frac{T_0}{K_\delta} \quad \ldots\ldots\ldots\ldots\ldots\ldots\ldots\ldots\ldots\ldots\ldots\ldots\ldots\ldots \quad (2.50)$$

where

$$M_0 = M_{e0} - T_0.L = M_1\,(0) + M_2\,(0) \quad \ldots\ldots\ldots\ldots\ldots\ldots \quad (2.51)$$

K_r and K_δ are the rotational and translational elastic stiffnes of the soil foundation and M_{e0} is the moment at the base level due to external load.

Substituting equations (2.49) and (2.50) into equation (2.48) yields

$$\lambda r/L\ Me_0 - q_0 - \mu_f\ T_0 = 0 \quad \ldots\ldots\ldots\ldots\ldots\ldots\ldots \quad (2.52)$$

in which

$$\mu_f = \lambda_\delta + \lambda_r = \frac{\beta^2 EI}{L}\left[\frac{L^2}{K_r} + \frac{1}{K_\delta}\right] = \frac{12\,EI_d}{hb^3}\left[\frac{L^2}{K_r} + \frac{1}{K_\delta}\right]$$

$$\lambda_\delta = \frac{\beta^2 EI}{L}\,\frac{1}{K_\delta} = \frac{12\,EI_d}{K_\delta\, hb^3}$$

$$\lambda_r = \frac{\beta^2 EI\, L}{K_r} = \frac{12\,EI_d\, L^2}{K_r\, hb^3}$$

and λ_δ and λ_r can be interpreted as the settlement and rotational flexibility of the soil foundations.

Substituting equations (2.43) and (2.44) into equation (2.52) and simplifying yields

$$C = H/k\,[\,B.\mu_f - \mu_5\,] \qquad \ldots\ldots (2.53)$$

where

$$\mu_5 = -\frac{\beta^2}{\alpha^2}\left[U+P+W\left(1-\frac{2}{k^2}\right) + \mu_f H\left(M(0)+\frac{U}{k^2}\right)\right]+\frac{\lambda r}{L} H M(0)$$

The solutions of the simultaneous equations (2.47) and (2.53) give the expressions of the integration constants as follows

$$B = \frac{\mu_5.H/k \tanh k + \mu_1}{1 + H/k.\mu_f \tanh k}$$

$$C = H/k\,[\,B.\mu_f - \mu_5\,]$$

Analysis of lateral deflection

By integrating equation (2.11) twice and using the boundary conditions

$$y\ (0) = 0$$

$$\frac{dy}{dx}\ (0) = \theta$$

the lateral deflection of the structure can be found as

$$y = \frac{1}{EI} H^2 \left[\left(1 - S_d \right) \Pi\ (\xi)\ H + \frac{L}{k^2} F\ (\xi) - S_d\ H \left(\frac{U\ \xi^2}{2\ k^2} + \frac{W\ \xi^3}{3\ k^2} \right) \right] + \theta H.\xi \quad \ldots\ldots\ldots\ldots\ldots\ldots \quad (2.54)$$

where

$$S_d = \frac{\beta^2}{\alpha^2} L = \frac{m\ L}{I'}$$

$$\Pi\ (\xi) = 1/120.\xi^2 \left[5\ U \left(\xi^2 - 4\ \xi + 6 \right) + 2\ W \left(\xi^3 - 10\ \xi + 20 \right) + 20\ P \left(3 - \xi \right) \right]$$

$$F\ (\xi) = B\ (1 - \cosh k\xi) + C \left(k\xi - \sinh k\xi \right)$$

Coupled shear wall on rigid foundation

For the case of a coupled shear wall on rigid foundation, $\mu_f = \lambda_\delta = \lambda_r = 0$, $\delta = \theta = 0$ and the boundary condition represented in equation (2.52) can be reduced to the condition $q_0 = 0$. The expressions of the integration constants can then be expressed as follows

$$B = \mu_5.H/k \tanh k + \mu_1$$

$$C = - H/k.\mu_5$$

where the expressions for μ_5 become,

$$\mu_5 = - \frac{\beta^2}{\alpha^2} [U + P + W (1 - \frac{2}{k^2})]$$

The base shears in equations (2.15) become proportional to their inertias and reduce to

$$S_1 (0) = - \frac{I_1}{I} \frac{dM_e}{dx} (0)$$

$$\qquad \qquad \qquad \qquad (2.55)$$

$$S_2 (0) = - \frac{I_2}{I} \frac{dM_e}{dx} (0)$$

However, it is useful to express the equations for q, T, y, K_1 and K_2 in dimensionless form for a coupled shear wall on rigid foundations to enable design curves to be drawn, and these will have the following expressions,

$$q = \frac{\beta^2}{\alpha^2} q^* \qquad \ldots\ldots \qquad (2.56)$$

$$T = \frac{\beta^2}{\alpha^2} H T^* \qquad \ldots\ldots \qquad (2.57)$$

$$y = \frac{H^3}{EI} y^* \qquad \ldots\ldots \qquad (2.58)$$

where

$$T^* = B^*.\cosh k\xi + C^*.\sinh k\xi + M (\xi) + \frac{U + 2W \xi}{k^2} \qquad \ldots\ldots \qquad (2.59)$$

$$q^* = - [B^*.k \sinh k\xi + C^*.k \cosh k\xi + \frac{dMe}{dx} + \frac{2W}{k^2}] \qquad \cdots \qquad (2.60)$$

$$y^* = (1 - S_d) \Pi (\xi) + \frac{L}{k^2} F^*(\xi) -$$

$$S_d H \left(\frac{U \xi^2}{2 k^2} + \frac{W \xi^3}{3 k^2} \right) \qquad \ldots\ldots\ldots\ldots\ldots\ldots\ldots \quad (2.61)$$

$$C^* = 1/k \left[U+P+W (1-2/k^2) \right]$$

$$\ldots\ldots\ldots\ldots\ldots\ldots \quad (2.62)$$

$$B^* = \mu_1^* - C^*.\tanh k$$

in which

$$\mu_1^* = - \frac{(U + 2W)}{k^2 \cosh k}$$

and the expression for $F^*(\xi)$, becomes,

$$F^*(\xi) = B^*(1 - \cosh k\xi) + C^*(k\xi - \sinh k\xi)$$

For the special case of a uniformly distributed wind loading, $P = W = 0$, and the expressions of q^*, T^* and y^*, become,

$$q^* = U q' \qquad \ldots\ldots\ldots\ldots\ldots\ldots\ldots\ldots\ldots\ldots\ldots\ldots\ldots \quad (2.63)$$

$$T^* = \frac{1}{2} U T' \qquad \ldots\ldots\ldots\ldots\ldots\ldots\ldots\ldots\ldots\ldots\ldots\ldots\ldots \quad (2.64)$$

$$y^* = \frac{1}{8} U \bar{y} \qquad \ldots\ldots\ldots\ldots\ldots\ldots\ldots\ldots\ldots\ldots\ldots\ldots\ldots \quad (2.65)$$

where

$$q' = 1 - \xi + \frac{1}{k.\cosh k} \left[\sinh k\xi - k \cosh k(1-\xi) \right] \quad \ldots\ldots \quad (2.66)$$

$$T' = (1 - \xi)^2 + \frac{2}{k^2.\cosh k}\left[\cosh k - \cosh k\xi - k \sinh k(1-\xi) \right] \quad \ldots\ldots \quad (2.67)$$

$$\bar{y} = \frac{1}{3}\left[1 - \frac{\beta^2}{\alpha^2} L \right]\left[(1-\xi)^4 + 4\xi - 1 \right] + \frac{8}{k^2}\frac{\beta^2}{\alpha^2} L \left[\xi(1 - \frac{1}{2}\xi) - \frac{1}{k^2.\cosh k}\{ 1 + k \sinh k - \cosh k\xi - K \sinh k(1-\xi) \} \right]. \quad (2.68)$$

$$\bar{y}_{max} = \left(1 - \frac{\beta^2}{\alpha^2} L \right) + \frac{1}{k^2}\frac{\beta^2}{\alpha^2}\left[4 - \frac{8}{k^2.\cosh k}\{ 1 + k \sinh k - \cosh k \} \right]. \quad (2.69)$$

$$C' = 1/k \quad \ldots\ldots\ldots \quad (2.70)$$

$$B' = \mu_1' - C'.\tanh k$$

$$\mu_1' = - \frac{1}{k^2 \cosh k}$$

The expression of $F'(\xi)$ becomes,

$$F'(\xi) = B'(1 - \cosh k\xi) + C'(k\xi - \sinh k\xi)$$

2.3 Discretisation

The previous expressions for force actions are referred to the substitute continuum structure, and must be transformed into the real discrete system of beams and walls.

The expressions for the discrete shear force, Q_f, and the axial force, N_f, in any internal lintel beam, f, may be obtained respectively in each zone from the corresponding continuous distributed forces, once the laminar shears q_i and

the axial distributions n_i are determined (see Fig. 2.5) as,

$$Q_f = \int_{x-h/2}^{x+h/2} q.dx$$

$$= - [B \{ \cosh k\mu - \cosh k\varphi \} +$$

$$C \{ \sinh k\mu - \sinh k\varphi \}] +$$

$$\frac{\beta^2}{\alpha^2} H.N(\xi). \qquad \ldots\ldots\ldots\ldots \qquad (2.71)$$

$$N_f = \int_{x-h/2}^{x+h/2} n.dx$$

$$= \frac{I_2}{I} Z_f(\xi) +$$

$$\left(\frac{I_1}{I} L - \Delta - L_1 \right) \left[\frac{k}{H} \right. [B \{ \sinh k\mu - \sinh k\varphi \} +$$

$$C \{ \cosh k\mu - \cosh k\varphi \}] +$$

$$\left. \frac{\beta^2}{\alpha^2} Z_f(\xi) \right] \qquad \ldots\ldots\ldots \qquad (2.72)$$

where

$$\varphi = \xi - \frac{1}{2J}, \qquad \mu = \xi + \frac{1}{2J} \qquad \ldots\ldots\ldots \qquad (2.73)$$

$$N(\xi) = \frac{1}{3} \left[6 (\mu - \xi) [(1 - \xi) U + P] - [6 (\mu - \xi) \{ -1 +$$

$$(\mu - \xi)\xi\} + 2\xi^3 + \frac{12}{k^2}(\mu - \xi)\ \Big]\ W \Big] \quad \ldots\ldots (2.74)$$

However the shear and axial forces in the top lintel beam are given by

$$Q(H) = \int_{H-h/2}^{H} q.dx$$

$$= -\Big[\ B\ \{\ \cosh k - \cosh k\varphi\ \} +$$

$$C\ \{\ \sinh k - \sinh k\varphi\ \}\ \Big] + \frac{\beta^2}{\alpha^2} H N_1 \quad \ldots\ldots\ (2.75)$$

$$N(H) = \int_{H-h/2}^{H} n.dx + Q_t$$

$$= \frac{I_2}{I}\Big[\ Z(1) - P\ \Big] +$$

$$\Big(\frac{I_1}{I} L - \Delta - L_1\Big) \Big[\frac{k}{H} \Big[\ B\ \{\ \sinh k - \sinh k\varphi\ \} +$$

$$C\ \{\ \cosh k - \cosh k\varphi\ \}\ \Big] +$$

$$\frac{\beta^2}{\alpha^2}\Big[\ Z(1) - P\ \Big]\ \Big] + Q_t \quad . \quad (2.76)$$

where

$$N_1 = \frac{1}{6}\Big[\ 3\ \frac{1}{2J}\ \Big\{\ \frac{1}{2J}\ U + 2\ P\ \Big\} -$$

$$2\left\{-\frac{1}{8J^3}+\frac{3}{4J^2}-\frac{3}{J}+2+\frac{1}{2J}\frac{6}{k^2}\right\}W\Big] \quad \ldots\ldots \quad (2.77)$$

The static shear at the internal beam's level, and the top beam level, will be respectively given by

$$Z_f(\xi) = \frac{dM_e}{dx}(x-h/2) - \frac{dM_e}{dx}(x+h/2) = \frac{1}{J}\left[\, U + 2\xi\, W \,\right]$$

$$\ldots\ldots \quad (2.78)$$

$$Z(1) = \frac{dM_e}{dx}(H-h/2) - \frac{dM_e}{dx}(H) + P = \frac{1}{2\,J}\left[U + \frac{1}{2\,J}\{4J-1\}\,W\right] + P$$

in which

$$\frac{dMe}{dx} = -\left[\, U\,(1-\xi) + W\,(1-(\xi)^2) + P \,\right] \ldots\ldots\ldots\ldots \quad (2.79)$$

and J = H/h (number of storeys)

The shear forces, the axial forces and the moments in walls (see Fig. 2.5), are respectively given by

$$(S_1)_{f_1} = \sum_{f-1}^{j=1}(Z_j - N_j) \quad , \qquad (S_2)_{f_1} = \sum_{f-1}^{j=1} N_j$$

$$\ldots\ldots \quad (2.80)$$

$$(S_1)_{f_2} = (S_1)_{f_1} - N_f + Z_f \quad , \qquad (S_2)_{f_2} = (S_2)_{f_1} + N_f$$

$$(T)_{f_1} = \sum_{f-1}^{j=1} Q_j$$

$$\ldots\ldots\ldots \quad (2.81)$$

$$(T)_{f_2} = (T)_{f_1} + Q_f$$

$$(M_1)_{f_1} = h \sum_{f}^{j=1} (S_1{}^{f_1})_j - (T)_{f_1}(L_1+\Delta) - M_p$$

$$(M_2)_{f_1} = h \sum_{f}^{j=1} (S_2{}^{f_1})_j - (T)_{f_1}(L_2-\Delta) + M_p \qquad \ldots\ldots (2.82)$$

$$(M_1)_{f_2} = (M_1)_{f_1} - Q_f(L_1+\Delta)$$

$$(M_2)_{f_2} = (M_2)_{f_1} - Q_f(L_2-\Delta) \qquad \ldots\ldots (2.83)$$

where

$$M_p = (\Delta_t-\Delta)\, Q_f(H) = (\Delta_t-\Delta) \int_{H-h/2}^{H} q.dx \qquad \ldots\ldots (2.84)$$

Note that in the special case when $\Delta = \Delta_t$, the moment M_p will be equal to zero, that is the line of contraflexure will pass through the centre line of the connecting medium or lintel beams from top to bottom.

Alternative calculation of moments

By assuming that the beam moment is distributed equally between the stories above and below the level concerned, the bending moments in the discrete set of walls can alternatively be given by

$$(M_1)_{f_1} = M_1 + 0.5\,[Q_f(L_1+\Delta)+\hat{M}]$$
$$(M_2)_{f_1} = M_2 + 0.5\,[Q_f(L_2-\Delta)-\hat{M}] \qquad \ldots\ldots (2.85)$$

$$(M_1)_{f_2} = M_1 - 0.5\,[Q_f(L_1+\Delta)+\hat{M}]$$
$$(M_2)_{f_2} = M_2 - 0.5\,[Q_f(L_2-\Delta)-\hat{M}] \qquad \ldots\ldots (2.86)$$

The extra moment $\hat{M}$ is given by

$\hat{M} = M_p$ for $X = H$

$\hat{M} = 0$ for $X \neq H$

2. 4 Difficulties and Inconsistencies.

Some inconsistencies occur in the continuum method theory due basically to some of the assumptions made in the method

(a) Top interactive force

It has been shown by equation (2.23) that a top concentrated interactive force Q_t exists at the top of the cut continuous medium, which is not possible physically for a continuous system.

For the special case when, $\Delta + L_1 = \frac{I_1}{I} L$ and $L_2 - \Delta = \frac{I_2}{I} L$

that is

$$\frac{I_1}{I_2} = \frac{L_1 + \Delta}{L_2 - \Delta} \quad \text{or} \quad \Delta = \frac{I_1 L_2 - I_2 L_1}{I} \quad \ldots\ldots\ldots\ldots \quad (2.87)$$

which can be rewritten as

$$\frac{\Delta}{L_2} = \frac{\frac{I_1}{I_2} - \frac{L_1}{L_2}}{1 + \frac{I_1}{I_2}} \quad \ldots\ldots\ldots\ldots\ldots\ldots\ldots\ldots\ldots\ldots \quad (2.88)$$

the top interactive shear force Q_t vanishes. That is, the top shear force Q_t vanishes always if the line of contraflexure occurs at distances $I_1/I.L$ and $I_2/I.L$ from the centroidal axes of walls 1 and 2 respectively. That is, its distance from the centroidal axis of a wall is proportional to the flexural rigidity of that wall.

However this force will always exist in the special case of a point load at the top of wall 1, in order to transfer a component of the shear to wall 2.

The expression of Q_t, given by equation (2.23), may be rewritten for the case of rigid foundations, as,

$$Q_t = Z_1 . q^*(H) \quad \ldots\ldots\ldots\ldots\ldots\ldots\ldots\ldots\ldots \quad (2.89)$$

where

$$Z_1 = \left(\frac{I_1}{I} L - \Delta - L_1\right) \frac{\beta^2}{\alpha^2}$$

For the most common situation of a pair of coupled walls, subjected to a uniformly distributed wind loading, the function $q^*(H)$ is given by

$$q^*(H) = U\, q'(H) \quad \ldots\ldots\ldots\ldots\ldots\ldots\ldots\ldots\ldots \quad (2.90)$$

where

$$q'(H) = \frac{1}{k.\cosh k} [\, \sinh k - k \,] \quad \ldots\ldots\ldots\ldots\ldots\ldots \quad (2.91)$$

The function q'(H) depends only on the relative stiffness parameter k, which depends also on the flexural rigidity of the connecting beams, as well as on the storey height and number of storeys.

(b) Case of a coupled shear wall with a top stiffening beam

Where a beam of flexural rigidity $E_m I_s$ and cross sectional area A_s, relatively stiff compared to the rest of the coupling beams, is present at the top of the structure x = H, to help stiffen the structure, the axial force in the walls at the top of the structure is equal to the shear force in the stiff top beam. The compatibility equation at the top becomes,

$$L \frac{dy}{dx} - \frac{b^3}{12E_m I_m} T(H) - \frac{1}{E}\left(\frac{1}{A_1} + \frac{1}{A_2}\right) \int_0^x T\, dx - \delta = 0 \quad \ldots\ldots \quad (2.92)$$

where

$$I_m = R.I_n$$

in which

$$R = [\ 1 - S_{ft} / (1+S_{ft})\ ].C_{ft}$$

where

$$S_{ft} = 24\ f \frac{I_n}{A_n} \frac{1+\nu}{b^2} C_{ft}$$

$$C_{ft} = 1 - \frac{12(\Delta_t/b)^2}{1 + 12(\Delta_t/b)^2}$$

$$A_n = A_s - A_b$$

and

$$I_n = I_s - I_b$$

By equating the compatibility equation at the top stiff beam and the corresponding compatibility equation given by equation (2.33) at x = H, the top boundary coundition becomes,

$$T(H) = \gamma.H\ q(H) \quad \ldots\ldots \quad (2.93)$$

where

$$\gamma = \frac{1}{J} \frac{E_m I_m}{EI_d} \quad \ldots\ldots \quad (2.94)$$

Therefore, the substitution of equations (2.41) and (2.42) in equation (2.93), results in

$$B = -\bar{B} - \bar{C}.C \quad \ldots\ldots\ldots\ldots\ldots\ldots\ldots\ldots \quad (2.95)$$

where

$$\bar{B} = -\frac{\beta^2}{\alpha^2} H \frac{U + 2W + k^2\gamma\,(2W/k^2 - P)}{k^2 \cosh k}$$

$$\bar{C} = \frac{\sinh k + k\gamma.\cosh k}{\cosh k + k\gamma.\sinh k}$$

It should be noted that where $\gamma = 0$, the above equation reduces to equation (2.47).

Since the walls deflect equally, the slopes are the same at the tops of the walls. If the shear force at the point of contraflexure of the beam is T (H), the moments at the tops of walls 1 and 2 will be

$$M_1(H) = T\,(H)\,(L_1 + \Delta_t), \quad M_2(H) = T\,(H)\,(L_2 - \Delta_t). \quad (2.96)$$

However, as the curvatures are equal at all levels, the top moments are proportional also to their flexural rigidities, as

$$M_1(H) = EI_1 \frac{d^2y}{dx^2}(H), \qquad M_2(H) = EI_2 \frac{d^2y}{dx^2} \quad \ldots\ldots \quad (2.97)$$

The equations (2.96) and (2.97) will be consistent only in the special cases where

$$\frac{I_1}{I_2} = \frac{L_1 + \Delta_t}{L_2 - \Delta_t} \quad \text{or} \quad \Delta_t = \frac{I_1L_2 - I_2L_1}{I} \quad \ldots\ldots\ldots\ldots\ldots \quad (2.98)$$

which again can be rewritten as

$$\frac{\Delta_t}{L_2} = \frac{\frac{I_1}{I_2} - \frac{L_1}{L_2}}{1 + \frac{I_1}{I_2}} \qquad \ldots\ldots\ldots\ldots\ldots\ldots\ldots\ldots\ldots\ldots \quad (2.99)$$

Hence, the shears in walls and the axial flow distributions in the continuous medium, at the top of the structure, respectively reduce to

$$S_1(H) = -\frac{I_1}{I}\frac{dM_e}{dx}, \qquad S_2(H) = -\frac{I_2}{I}\frac{dM_e}{dx}$$

and (2.100)

$$n(H) = \frac{I_2}{I}\frac{d^2M_e}{dx^2}$$

(c) Case of a coupled shear wall resting on elastic soil foundations

In the case of shear wall bases resting on separate bases in an elastic soil, the vertical elastic stiffness K_δ is given by

$$\frac{1}{K_\delta} = \frac{1}{k_1\ a_1} + \frac{1}{k_2\ a_2} \qquad \ldots\ldots\ldots \quad (2.101)$$

where

k_1 = modulus of subgrade reaction of the soil under wall 1

k_2 = modulus of subgrade reaction of the soil under wall 2

a_1 = area of base 1

a_2 = area of base 2

However, the rotational deformations of the wall bases, θ_{w1} and θ_{w2} are respectively given by

$$\theta_{w1} = K_{r1}M_1(0) = \frac{K_{r1}I_1M_0}{I}$$

..... (2.102)

$$\theta_{w2} = K_{r2}M_2(0) = \frac{K_{r2}I_2M_0}{I}$$

where K_{r1} and K_{r2} are rotational elastic stiffnesses of the soil foundations under wall 1 and 2 respectively and are given by

$$K_{r1} = \frac{1}{k_1 I_{b1}}$$

..... (2.103)

$$K_{r2} = \frac{1}{k_2 I_{b2}}$$

I_{b1} = second moment of area of wall base 1

I_{b2} = second moment of area of wall base 2

Since the walls deflect equally, the rotations of the two wall bases must be the same and the slope at the base of the walls θ is given by

$$\theta = \theta_{w1} = \theta_{w2}$$

which may be rewritten as

$$\theta = \frac{M_0}{K_r}$$

where

$$K_r = \frac{1}{K_{r1}} + \frac{1}{K_{r2}} \qquad \text{.....} \quad (2.104)$$

Hence

$$I : I_1 : I_2 = \frac{1}{K_r} : \frac{1}{K_{r1}} : \frac{1}{K_{r2}}$$

Thus to be consistent with the basic assumption that the walls deflect equally there is the additional requirement that

$$\frac{K_{r2}}{K_{r1}} = \frac{I_1}{I_2}$$

or ..... (2.105)

$$\frac{k_1 I_{b1}}{k_2 I_{b2}} = \frac{I_1}{I_2}$$

Where $k_1 = k_2$, the latter equation becomes

$$\frac{I_{b1}}{I_{b2}} = \frac{I_1}{I_2} \qquad (2.106)$$

Obviously this requirement is not necessarily true since the wall bases may not be constructed such that their respective second moments of area are proportional to that of the walls.

This problem can be solved if the analysis takes account of axial deformations of the laminae. By so doing the walls need not be assumed to deflect equally and the additional requirement of equation (2.105) need not be maintained but a second differential equation for the deflection of the second wall will be required. This latter matter has only been considered for the case of a coupled shear wall resting on rigid foundation[30] and is not considered in the present work.

2. 5 Investigation of the position of the points of contraflexure

If the position of the line of contraflexure is considered given by the expression in equation (2.88), for the case of plane walls of rectangular cross section, this expression reduces to

$$\frac{\Delta}{L_2} = \frac{\lambda_1^3 - \dfrac{\lambda_1 + 1/2\ \lambda_2}{1 + 1/2\ \lambda_2}}{1 + \lambda_1^3} \qquad \ldots\ldots\ldots\ldots \qquad (2.107)$$

where $\lambda_1 = \dfrac{d_1}{d_2}$ and $\lambda_2 = \dfrac{b}{d_2}$

The shift in the points of contraflexure, Δ may be determined from an approximate analysis of an isolated storey height panel (Fig. 2.6 (a)). This panel is assumed to behave as if it was a frame with the walls behaving as columns. It is then assumed that the vertical members of the structure bend with double curvature causing a point of contraflexure at mid-storey height above and below the panel's beam (Fig. 2.6 (a)). If the panel is assumed cut at distances $L_1 + \Delta$ and $L_2 - \Delta$ respectively from the centroidal axes of the walls, that is at the line of contraflexure, the bending of the beam will give at the line of contraflexure two angles v_{11} and v_{12} (Fig. 2.6 (c)) due to the shear force at the continuous medium and the rotation of the columns (Fig. 2.6 (b)) causes an angle φ_{11} in wall 1 and φ_{12} in wall 2 under the action of the moments $Q_f\ (L_1 + \Delta)$ and $Q_f\ (L_2 - \Delta)$.

By taking the positive sense of these angles to be clockwise, the angles are

$$\varphi_{11} = -\frac{Q_f(L_1+\Delta)h}{12EI_1} \quad , \quad v_{11} = -\frac{Q_f(b+2\Delta)^2}{8EI_b}$$

$$\varphi_{12} = - \frac{Q_f (L_2 - \Delta) h}{12 E I_2} \quad , \quad v_{12} = - \frac{Q_f (b - 2\Delta)^2}{8 E I_b}$$

where I_b is the inertia of the lintel beams, and L_1 and L_2 are the distances from the mid-span position of lintel beams to the centroidal axes of wall 1 and 2 respectively, given by.

$$L_1 = \frac{b}{2} + d_1 \quad , \quad L_2 = \frac{b}{2} + d_2$$

The total angles will be

$$\psi_{11} = \varphi_{11} + v_{11} = - \frac{Q_f}{4E} \left[\frac{(L_1 + \Delta) . h}{3 I_1} + \frac{(b + 2\Delta)^2}{2 E I_b} \right]$$

$$\psi_{12} = \varphi_{12} + v_{12} = - \frac{Q_f}{4E} \left[\frac{(L_2 - \Delta) . h}{3 I_2} + \frac{(b - 2\Delta)^2}{2 E I_b} \right]$$

Since ψ_{11} must be equal to ψ_{12}, it follows that

$$\Delta = L_2 \frac{\frac{I_1}{I_2} - \frac{L_1}{L_2}}{1 + \frac{I_1}{I_2} + 12 \frac{b I_1}{h I_b}} = L_2 \frac{1 - \frac{L_1}{L_2} \frac{I_2}{I_1}}{1 + \frac{I_2}{I_1} + 12 \lambda_3} \quad .... \qquad (2.108)$$

where

$$\lambda_3 = \frac{b I_2}{h I_b} \quad ..... \qquad (2.109)$$

The determination of Δ_t, may also be carried out, using a similar procedure and the same assumptions as before by analysing the top half storey panel (Fig. 2.7 (a)), the values of the angles φ_{11}, φ_{12} (Fig. 2.7 (b)), v_{11} and v_{12} (Fig. 2.7 (c)) will be given by,

$$\varphi_{11} = -\frac{Q_f(H)(L_1+\Delta_t)h}{6EI_1} \quad , \quad v_{11} = -\frac{Q_f(H)(b+2\Delta_t)^2}{8EI_b}$$

$$\varphi_{12} = -\frac{Q_f(H)(L_2-\Delta_t)h}{6EI_2} \quad , \quad v_{12} = -\frac{Q_f(H)(b-2\Delta_t)^2}{8EI_b}$$

The total angles ψ_{11} and ψ_{12} are respectively given by

$$\psi_{11} = \varphi_{11} + v_{11} = -\frac{Q_f(H)}{2E}\left[\frac{(L_1+\Delta_t)h}{3I_1} + \frac{(b+2\Delta_t)^2}{4I_b}\right]$$

$$\psi_{12} = \varphi_{12} + v_{12} = -\frac{Q_f(H)}{2E}\left[\frac{(L_2-\Delta_t)h}{3I_2} + \frac{(b-2\Delta_t)^2}{4I_b}\right]$$

Since $\psi_{11} = \psi_{12}$, it follows that,

$$\Delta_t = L_2 \frac{\frac{I_1}{I_2} - \frac{L_1}{L_2}}{1 + \frac{I_1}{I_2} + 6\frac{bI_1}{hI_b}} = L_2 \frac{1 - \frac{L_1}{L_2}\frac{I_2}{I_1}}{1 + \frac{I_2}{I_1} + 6\lambda_3} \quad \ldots\ldots \quad (2.110)$$

Equations (2.108) and (2.110) yield the interesting fact that, whenever the second moments of inertias of the walls are proportional to the distances from the mid-span position of the connecting beams to the centroidal axes of the walls, that is

$$\frac{I_1}{I_2} = \frac{L_1}{L_2}$$

the values of the shifts Δ and Δ_t, will be equal to zero, that is the line of contraflexure will pass through the continuous lamina at the mid-span position of the lintel beams. However it is only in the special case of two equal plane walls that this line of contraflexure of the system coincides with the centre line of the lamina and the previous identity in this special case becomes

$$\frac{I_1}{I_2} = \frac{L_1}{L_2} = 1$$

2. 6 Shear wall connected by beams to a column.

If one wall is very slender relative to the other much stiffer wall, such that the smaller wall becomes relatively very flexible, equations (2.108) and (2.110) reduce to

$$\Delta = L_2 \left(1 - \frac{12\lambda_3}{1 + 12\,\lambda_3} \right) \ldots\ldots\ldots\ldots \quad (2.111)$$

$$\Delta_t = L_2 \left(1 - \frac{6\lambda_3}{1 + 6\,\lambda_3} \right) \ldots\ldots\ldots\ldots \quad (2.112)$$

However when the smaller wall becomes very slender such that the distance from its centroidal axis to its inner edge becomes negligible that is $d_2 \simeq 0$ and $L_2 \simeq b/2$, the behaviour of the slender wall will be similar to that of a column which bends in double curvature with points of contraflexure at mid-height of each storey. An approximate solution to this case can be found using the continuous medium method as follows.

Consider the coupled shear wall shown in Fig. 2.8. The column has a double curvature deformation curve as shown in Fig. 2.9, from which the following relations can be deduced

$$m_1 + m_2 = q.h.b \quad (\text{equilibrium in node A}) \ldots\ldots\ldots\ldots \quad (2.113)$$

$$m_2 = 0.5\, m_3 \quad (\text{equilibrium in node B}) \ldots\ldots\ldots\ldots \quad (2.114)$$

where m_1 and m_2 are the moments at the extrimities A and B of the connecting beam respectively (Fig. 2.9).

From the slope-deflection equations, it can be deduced that

$$m_2 = \frac{6EI_2}{h}\,\theta_B \qquad \ldots\ldots (2.115)$$

$$\theta_B = \frac{1}{2EI_b}\left[\, q.h.b^2 - 2m_3.b \,\right] \qquad \ldots\ldots (2.116)$$

From equations (2.114), (2.115) and (2.116), it follows that

$$m_3 = \frac{6\,\lambda_3'\,q.h.b}{1 + 12\,\lambda_3'} \qquad \ldots\ldots (2.117)$$

where

$$\lambda_3' = \frac{I_2{}^e.b}{I_b.h} \qquad \ldots\ldots (2.118)$$

in which $I_2{}^e$ is the reduced moment of inertia of the column, which includes the effects of shear deformations in the column, and is given by,

$$I_2{}^e = \frac{I_2}{1 + \dfrac{24f(1+\nu)I_2}{h^2.A_2}}$$

However, if a point of contraflexure is assumed to occur at a distance Δ from the mid-span of the connecting beam towards the column, the moment m_3 at the junction beam-column will be given by

$$m_3 = (L_2 - \Delta).qh \qquad \ldots\ldots (2.119)$$

By comparing the latter equation with equation (2.117), it follows that

$$\Delta = L_2\left[\, 1 - \frac{12\,\lambda_3'}{1 + 12\lambda_3'}\,\right]$$

which can be rewritten as

$$\frac{\Delta}{L_2} = \left[1 - \frac{12\,\lambda_3'}{1 + 12\lambda_3'} \right]$$

and the remaining analysis will be the same as stated before.

Another method of finding Δ for the case of a slender wall connected to a stiff one is as follows :

Considering the slope deflection equations for the continuous medium (Fig. 2.10), and neglecting the deformations due to normal and shear forces for the sake of simplicity, the moments at the beam—wall and beam—column junctions will be respectively given by

$$m_1 = 2\,EK' \left(2\theta_1 + \theta_2 + 3\,\frac{c_1\theta_1 + c_2\theta_2}{b} \right)$$

$$m_2 = 2\,EK' \left(2\theta_2 + \theta_1 + 3\,\frac{c_1\theta_1 + c_2\theta_2}{b} \right)$$

or

$$(b/2 + \Delta)q = EK' \left[\left(3\,\frac{c_1}{b} + 2\right)\theta_1 + \left(3\,\frac{c_2}{b} + 1\right)\theta_2 \right] \ldots\ldots \quad (2.120)$$

$$(b/2 - \Delta)q = EK' \left[\left(3\,\frac{c_1}{b} + 1\right)\theta_1 + \left(3\,\frac{c_2}{b} + 2\right)\theta_2 \right] \ldots\ldots \quad (2.121)$$

where

$$K' = \frac{I_b}{bh}$$

Considering the slope deflection equations for the vertical members between two consecutive floors [see Fig. 2.11], the moments at the two extremities of the two vertical members will be given by

$$M_{Ai} = -2EK_i \left[2\theta_{Ai} + \theta_{Bi} - 3\, R_i\right] + (F_{AB})$$

$$i = 1,2 \qquad (2.122)$$

$$M_{Bi} = -2EK_i \left[2\theta_{Bi} + \theta_{Ai} - 3\, R_i\right] + (F_{BA})$$

where

$$K_i = \frac{I_i}{h}, \qquad R_i = \frac{\delta_i}{h}$$

and F_{AB} and F_{BA} are fixed end moments due to lateral load.

For the leeward wall $F_{AB} = F_{BA} = 0$ and for the windward wall $F_{AB} = -F_{BA}$ for a uniformly distributed wind load, and the summation of equations (2.122) for each vertical member yields

$$R_i = \frac{\theta_{Ai} + \theta_{Bi}}{2} + \frac{M_{Ai} + M_{Bi}}{12\ EK_i} \quad \ldots\ldots\ldots\ldots\ldots\ldots \qquad (2.123)$$

In the shear wall, the contribution of the term involving the moments in equation (2.123) is insignificant and in the column the value of the sum of the moments will be approximately $(m_2 + d_2 q)h$. The angles R_i then become

$$R_1 = \frac{\theta_{A1} + \theta_{B1}}{2} = \theta_1$$

$$R_2 = \frac{\theta_{A2} + \theta_{B2}}{2} + \frac{(m_2 + d_2 q)}{12\ EK_2}\, h = \theta_2 + \frac{(L_2 - \Delta)qh}{12\ EK_2}$$

Therefore, since the horizontal displacements of both vertical members are equal, equality of angles R at both vertical members may be written as

$$\theta_1 = \theta_2 + \frac{(L_2 - \Delta)qh}{12\ EK_2} \quad \ldots\ldots\ldots\ldots\ldots\ldots\ldots\ldots \qquad (2.124)$$

The angles θ_1 and θ_2 are given from equations (2.120) and (2.121) as

$$\theta_1 = \frac{b^2 \left[3\left(\frac{1}{2} + \frac{\Delta}{b}\right)\left(2\frac{c_2}{b} + 1\right) - \left(3\frac{c_2}{b} + 1\right)\right]}{6\,EK'L} q \quad \ldots\ldots\ldots\ldots \quad (2.125)$$

$$\theta_2 = \frac{b^2 \left[-3\left(\frac{1}{2} + \frac{\Delta}{b}\right)\left(2\frac{c_1}{b} + 1\right) + \left(3\frac{c_1}{b} + 2\right)\right]}{6\,EK'L} q \quad \ldots\ldots\ldots\ldots \quad (2.126)$$

By substituting equations (2.125) and (2.126) into equation (2.124), it follows that

$$\frac{\Delta}{L_2} = \frac{1}{12\,\lambda_3/L.(c_1+c_2+b) + 1} \quad \ldots\ldots\ldots\ldots\ldots\ldots \quad (2.127)$$

In the case of plane walls, $L = c_1 + c_2 + b$, and equation (2.127) reduces to

$$\frac{\Delta}{L_2} = 1 - \frac{12\lambda_3}{1 + 12\,\lambda_3} \quad \ldots\ldots\ldots\ldots\ldots\ldots\ldots\ldots\ldots \quad (2.128)$$

2. 7 Coupled shear walls with a top rigid beam.

When a coupled shear wall is provided with a top stiff beam of a very high stiffness so that in the limiting case the bending deformations in the beam can be neglected, the top beam can then be considered rigid. The analysis will then be slightly different since the top compatibility equation becomes

$$L\frac{dy}{dx} - \frac{1}{E}\left(\frac{1}{A_1} + \frac{1}{A_2}\right)\int_0^H T\,dx - \delta = 0 \quad \ldots\ldots\ldots\ldots\ldots \quad (2.129)$$

The top boundary equation will be found by comparing equation (2.82), with

the compatibility equation given by equation (2.31) at x = H, which results in

$$q(H) = 0$$

Hence from equation (2.42)

$$B = - C \operatorname{ctanh} \alpha H + \mu_6 \quad \ldots\ldots\ldots\ldots\ldots\ldots\ldots\ldots\ldots\ldots \quad (2.130)$$

where

$$\mu_6 = - \frac{\beta^2}{\alpha^2} H \frac{- P + \frac{2W}{k^2}}{k . \sinh k}$$

The lower boundary coundition will be as given by equation (2.53). Then by substitution of equation (2.130) in equation (2.53) the constant of integration C will be given by

$$C = \frac{\mu_6 . \mu_f H - \mu_5 H}{k + \mu_f H . \operatorname{ctanh} k} \quad \ldots\ldots\ldots\ldots\ldots\ldots\ldots\ldots\ldots\ldots \quad (2.131)$$

The shift in the point of contraflexure Δ_t at the top will be given by

$$\Delta_t = L_2 \frac{\frac{I_1}{I_2} - \frac{L_1}{L_2}}{1 + \frac{I_1}{I_2}} \quad \ldots\ldots\ldots\ldots\ldots\ldots\ldots\ldots\ldots\ldots \quad (2.132)$$

The following analysis will be exactly the same as before.

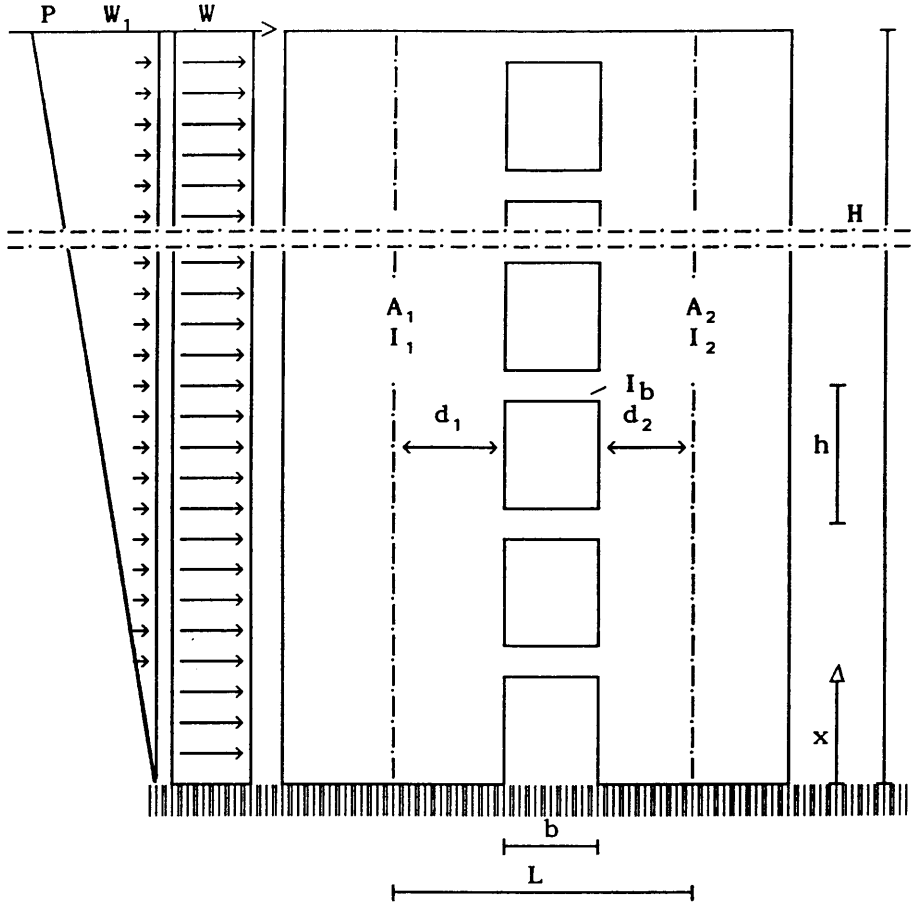

Fig. 2.1 (a) Coupled shear wall.

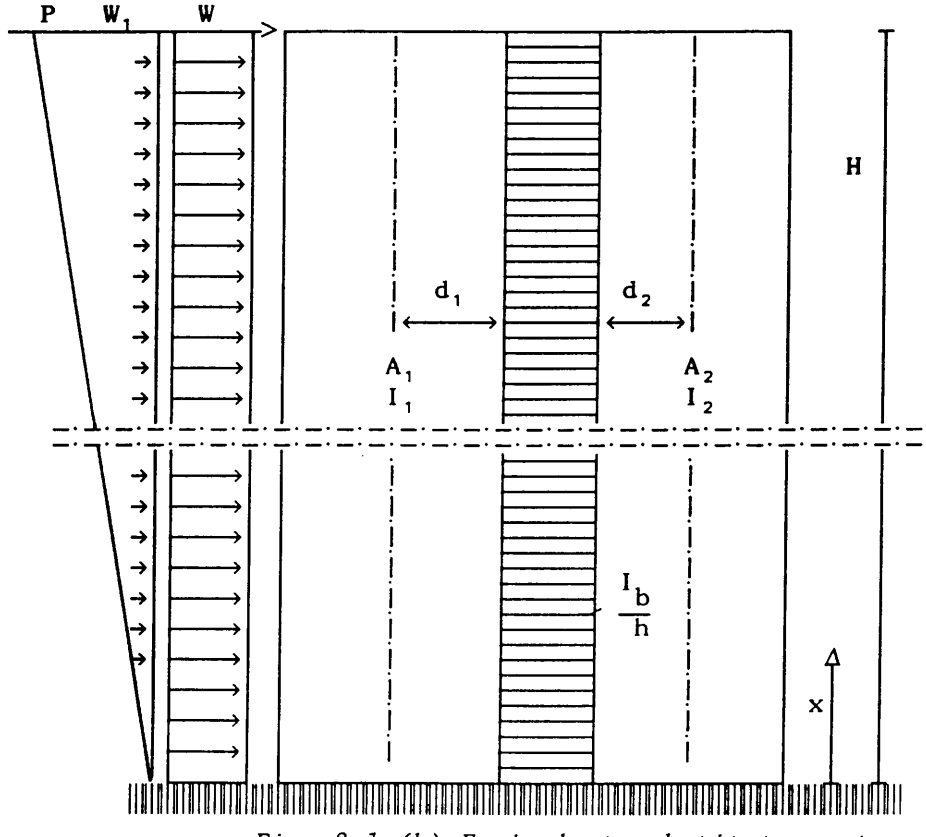

Fig. 2.1 (b) Equivalent substitute system.

Fig. 2.1

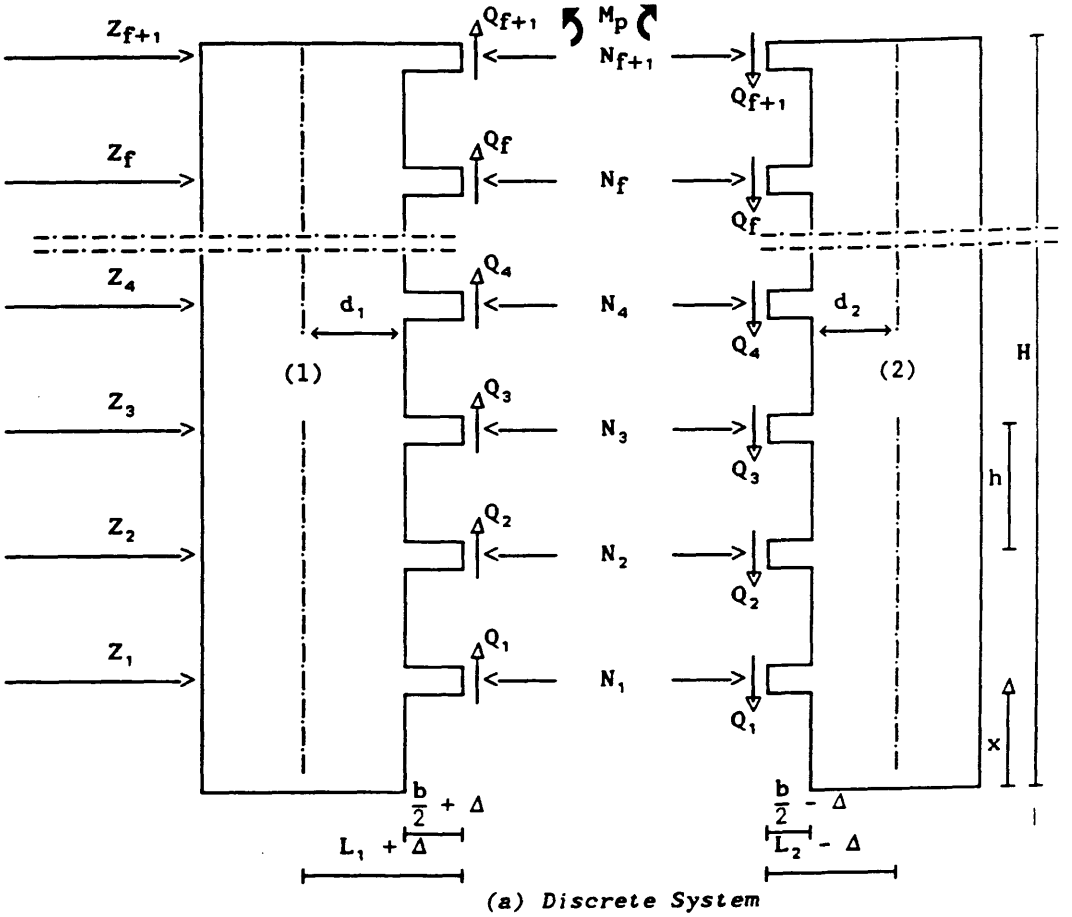

(a) Discrete System

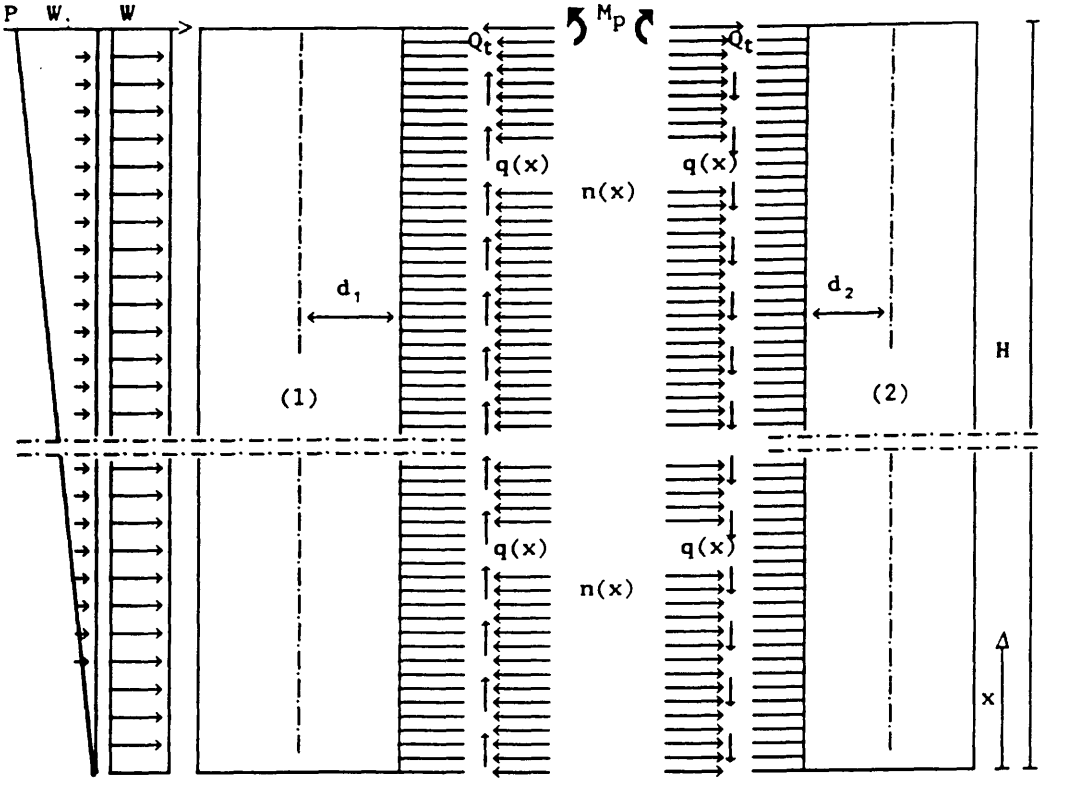

(b) Substitute system

Fig. 2.2

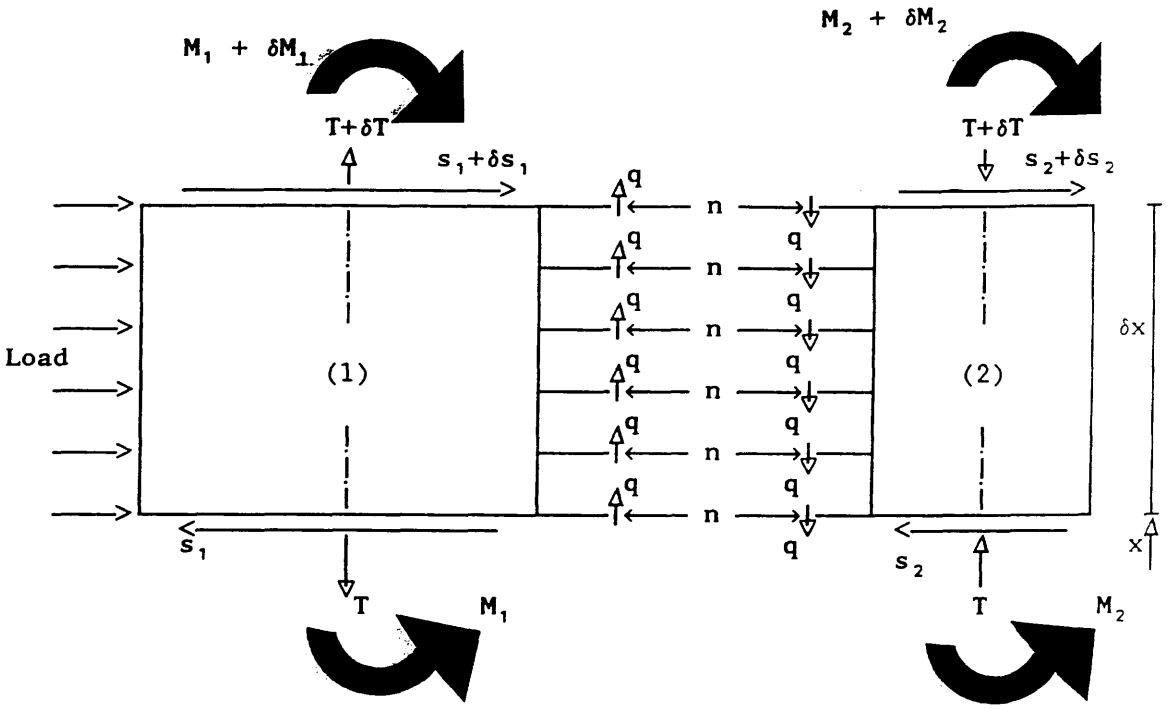

Equilibrium of an element dx

Fig. 2.3

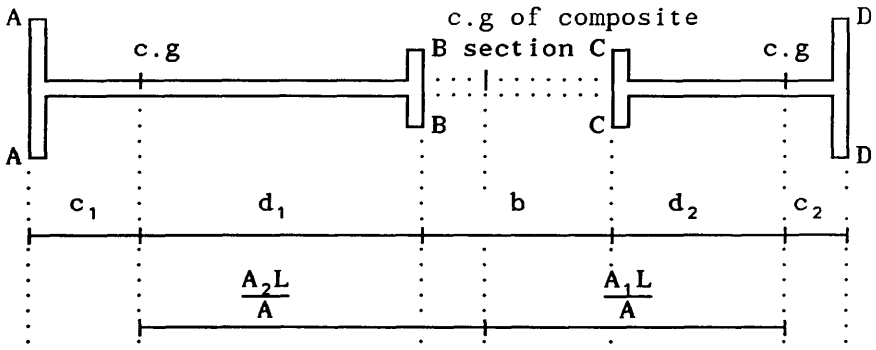

(a) Wall cross section

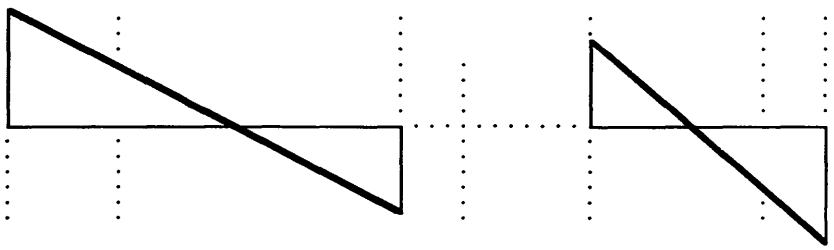

(b) Actual stress distribution

=

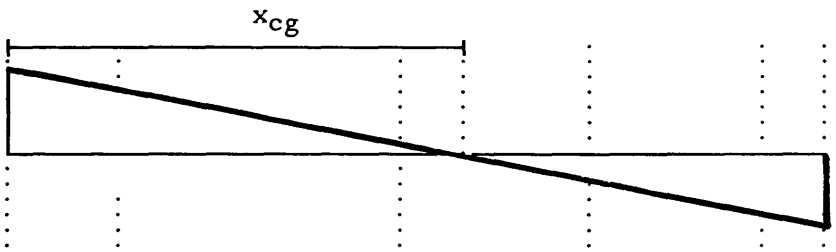

(c) Composite cantilever stresses

+

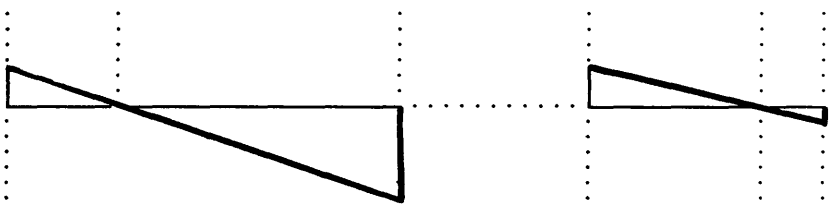

(d) Individual cantilever stresses

Fig. 2.4

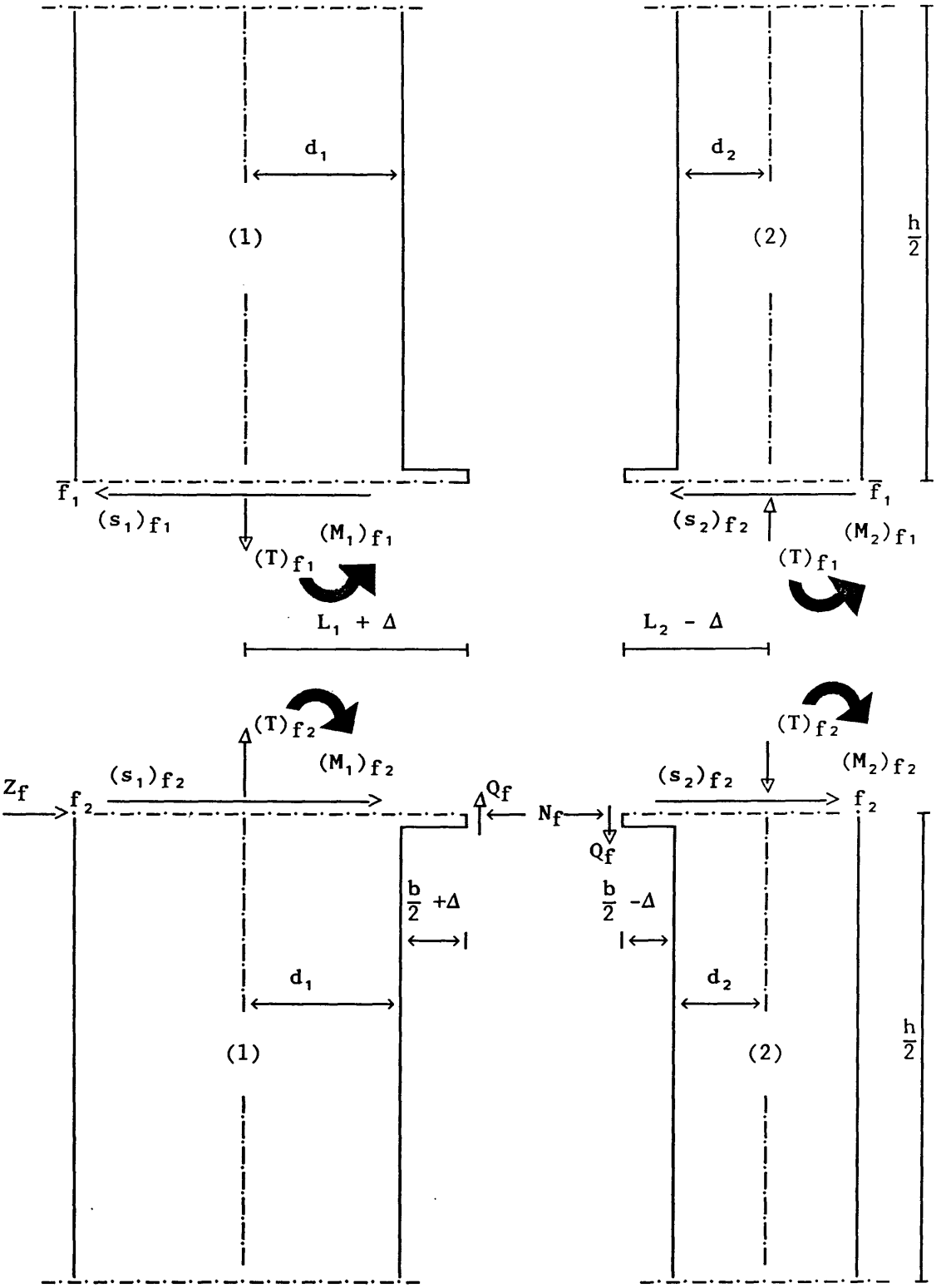
d1
(1)
f1
(s1)f1
(M1)f1
(T)f1
L1 + Δ
d2
(2)
h/2
f1
(s2)f2
(M2)f1
(T)f1
L2 - Δ
(T)f2
(M1)f2
Zf
f2
(s1)f2
Qf
b/2 +Δ
d1
(1)
(T)f2
(M2)f2
Nf
Qf
(s2)f2
f2
b/2 -Δ
d2
(2)
h/2

Fig. 2.5

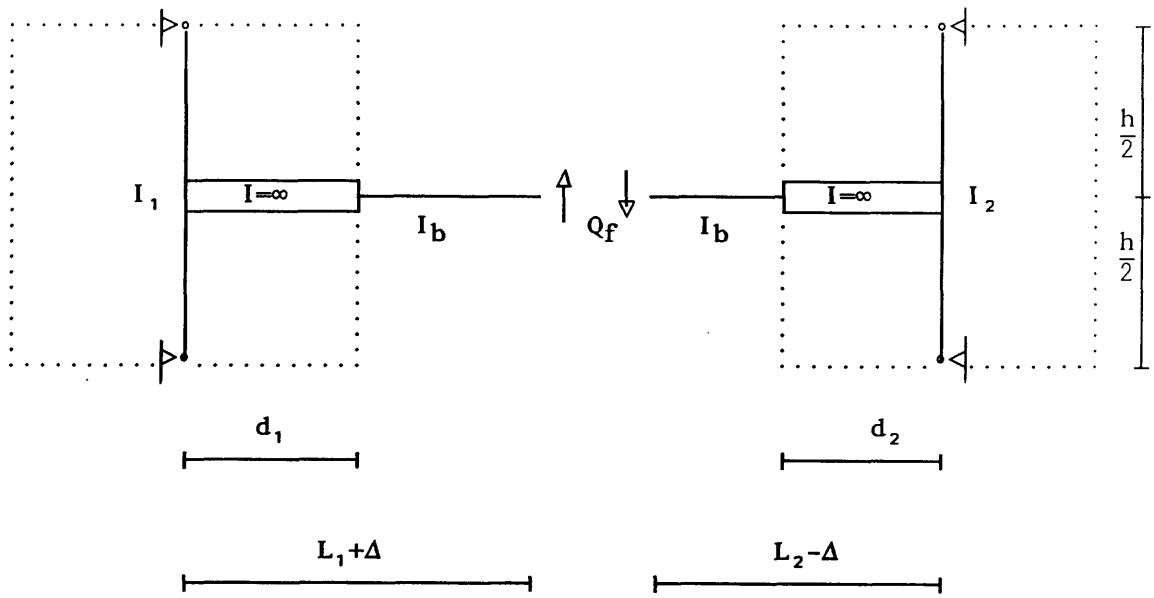
I₁
I=∞
Ib
Qf
Ib
I=∞
I₂
h/2
h/2
d₁
d₂
L₁+Δ
L₂-Δ

(a)

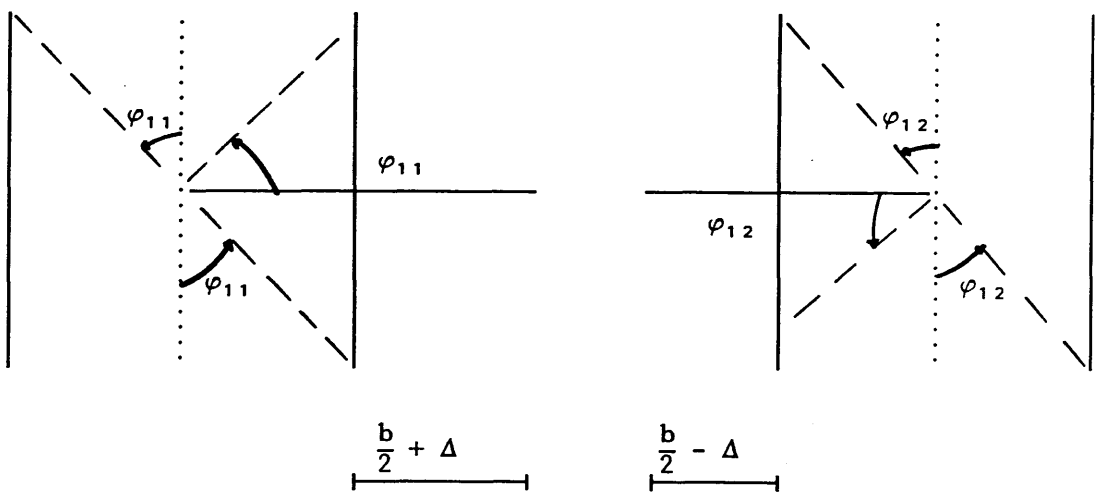
φ11
φ11
φ11
φ12
φ12
φ12
b/2 + Δ
b/2 - Δ

(b)

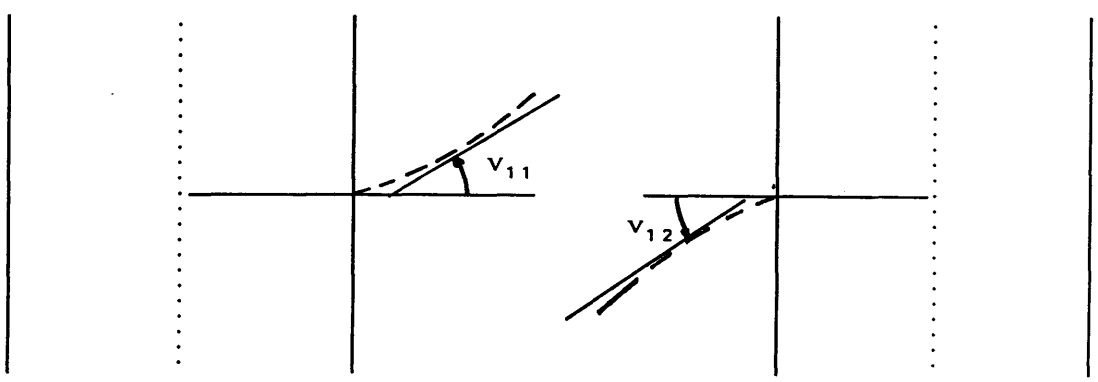
v11
v12

(c)

Fig. 2.6

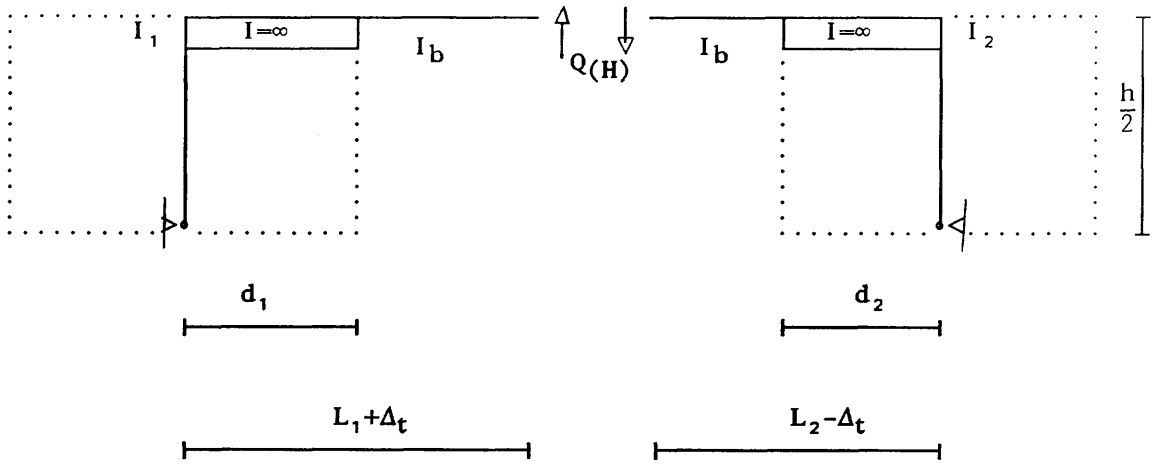
I 1
I=∞
I b
Q(H)
I b
I=∞
I 2
h/2
d 1
d 2
L 1+Δt
L 2-Δt

(a)

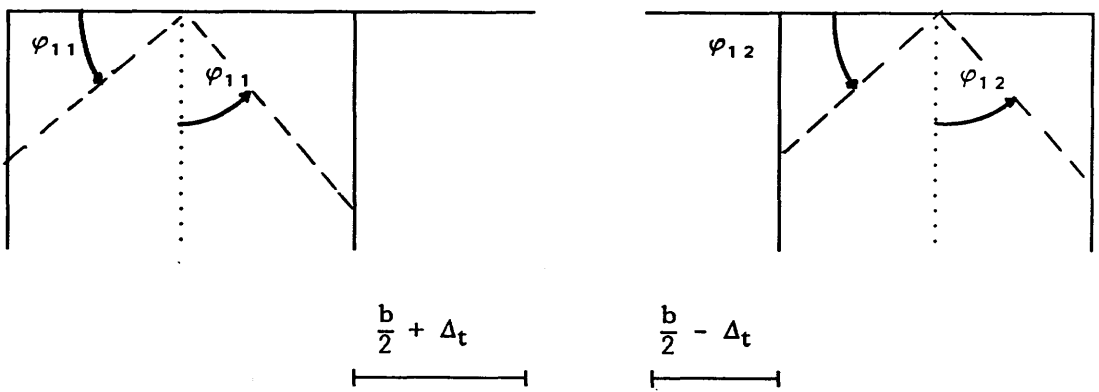
φ11
φ11
φ12
φ12
b/2 + Δt
b/2 - Δt

(b)

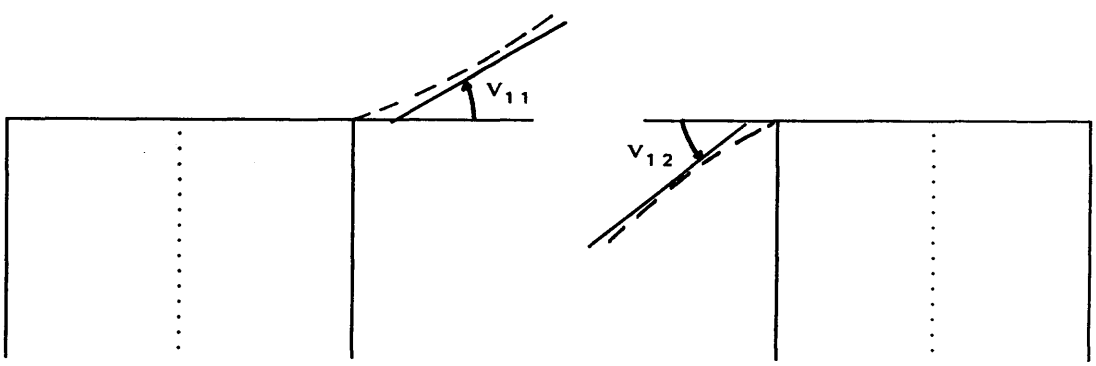
v11
v12

(c)

Fig. 2.7

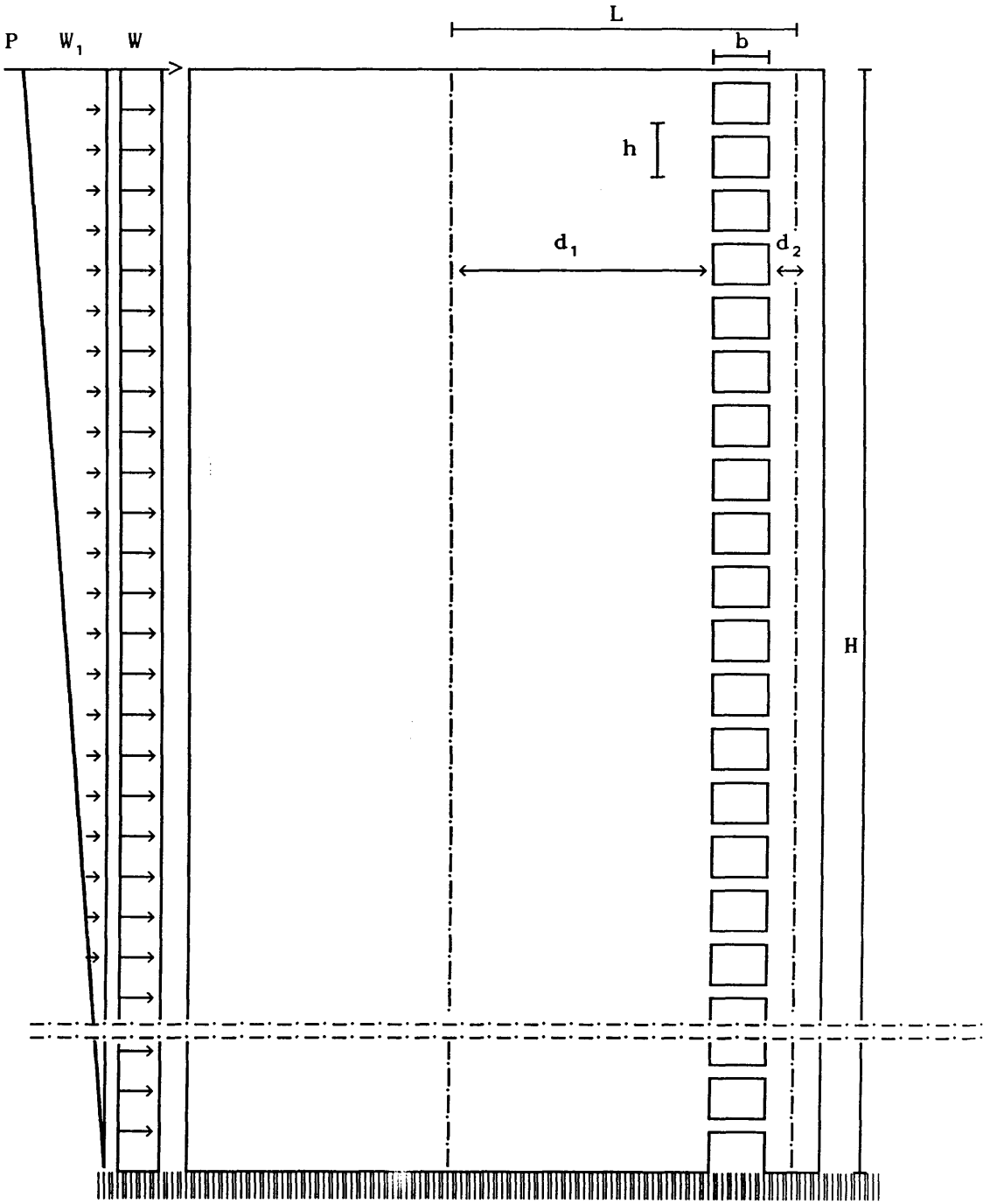

Fig. 2.8

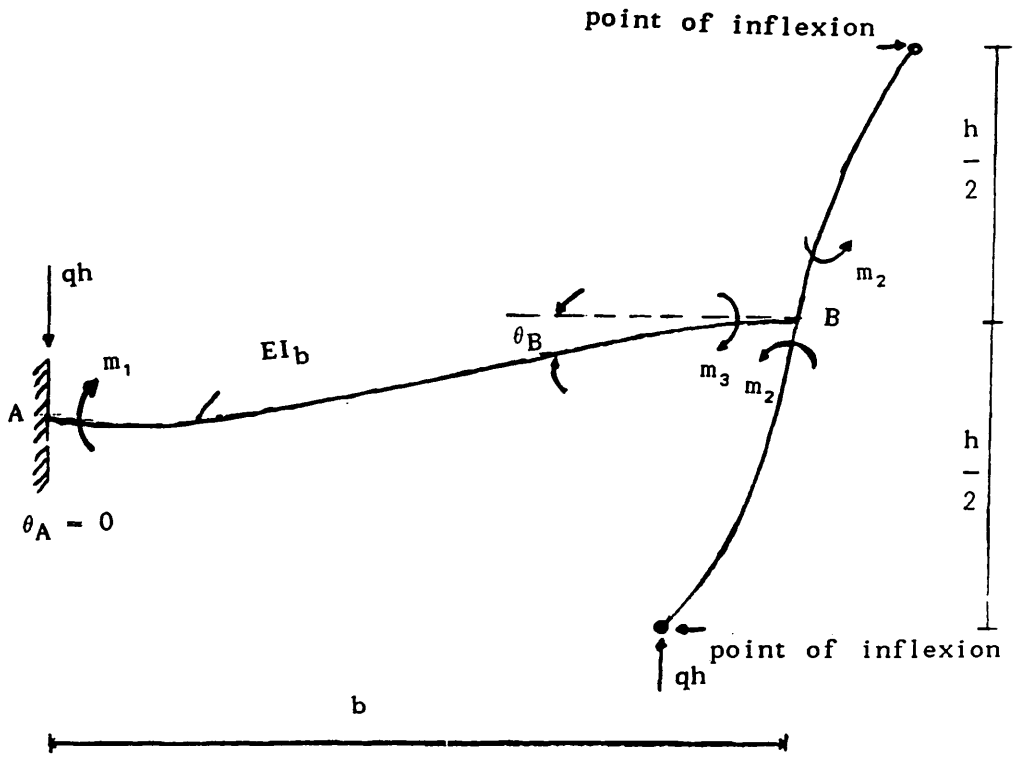
point of inflexion
h/2
qh
m2
EIb
θB
B
m1
m3
m2
A
θA = 0
h/2
point of inflexion
qh
b

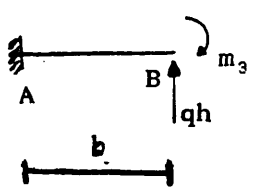
m3
A
B
qh
b

Fig. 2.9

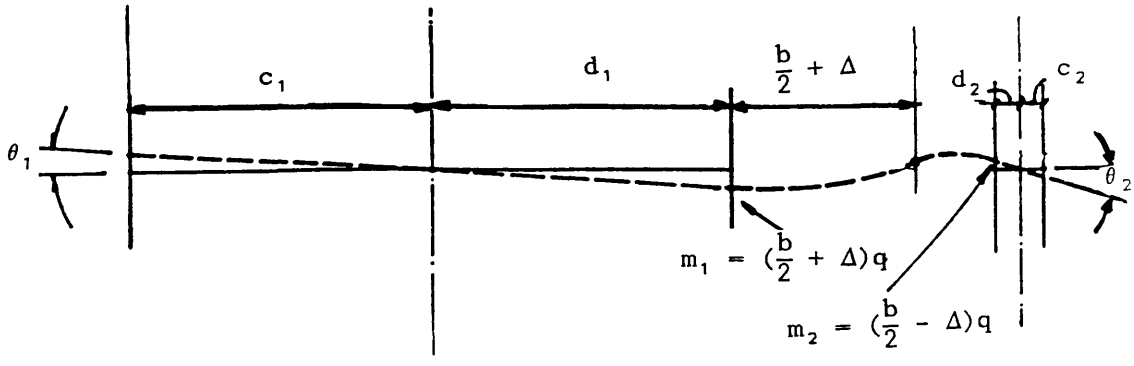
c_1
d_1
$\frac{b}{2} + \Delta$
d_2
c_2
θ_1
θ_2
$m_1 = (\frac{b}{2} + \Delta)q$
$m_2 = (\frac{b}{2} - \Delta)q$

Fig. 2.10

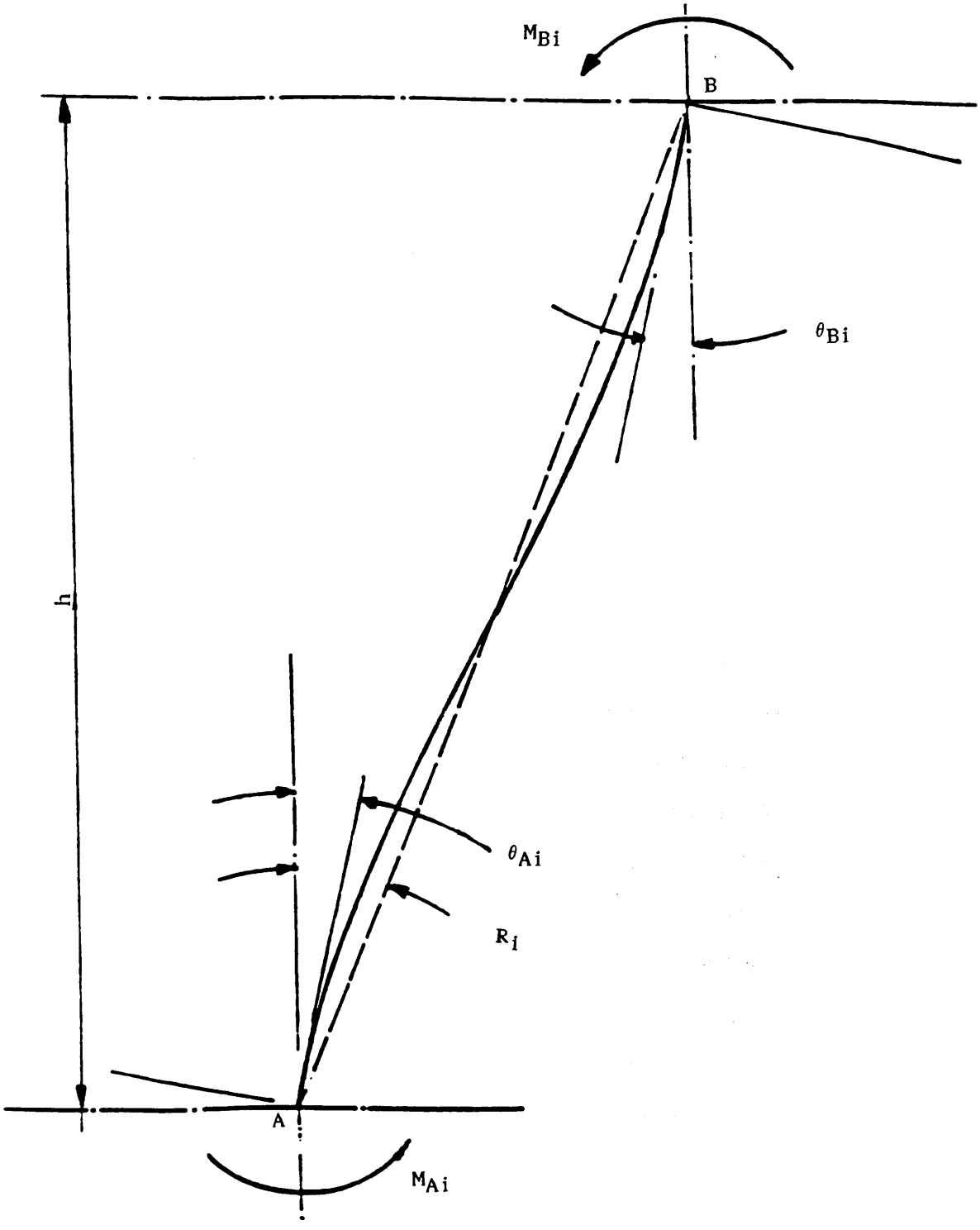

Fig. 2.11

CHAPTER THREE

NUMERICAL INVESTIGATIONS OF UNEQUAL COUPLED SHEAR WALLS

3. 1 Introduction

As discussed in Chapter 2, the continuum analysis of unequal shear walls shows some inconsistencies due basically to some of the assumptions made in the method. The first inconsistency is the presence of a fictitious top concentrated interactive shear force (Chapter 2, Sections 2.2 and 2.4 (a)) at the top of the cut continuous medium for the case of unequal walls. As it will be shown later, this force, which can be relatively large, is greatly reduced if a revised line of contraflexure (Chapter 2, section 2.5) is adopted. This revised line of contraflexure considers two positions of the points of contaflexure, one for the main beams and one for the top beam. As the position of the point of contraflexure is related to the inertia of the corresponding beam, the position of the point of contraflexure at the top beam may be different from the position of the line of contraflexure in the other beams according to the top boundary condition. It was hoped that the use of the revised line of contraflexure would give more accurate results, especially for the extreme case of a wall connected to a column by beams. The second inconsistency arises from the particular form of the top boundary condition associated with a stiffening beam (Chapter 2, Section 2.4 (b)). The inconsistency is that the top wall moments given by statics are not compatible with those given from the assumption of equal curvatures in the walls. This incompatibility increases as one wall gets bigger compared to the other. Again, it was expected that the use of the revised line of contraflexure would have the effect of reducing this incompatibility.

The object of this Chapter is to investigate how best to model a coupled shear wall structure for a continuum analysis, how to choose the line of contraflexure and how to reduce the magnitude of the top concentrated interactive shear force. The continuum method results are tested against the frame analogy ones using the general purpose program "Flash" (Finite Element Analysis of Shells).

3. 2 Numerical results

The numerical investigations conducted on the analysis of unequal coupled shear walls are presented in this chapter. Firstly, general curves for the top concentrated fictitious force and the reduction factors are presented. The top concentrated interactive shear force can be very important, since it is shown that, for certain geometrical situations, the magnitude of this force may be quite large. For a structure subjected to a uniformly distributed wind loading, this force may constitute up to 10% of the total load. Secondly, a numerical investigation is carried out on a representative example structure. Because of the amount of data generated, the results shown are only those which are of the greatest importance. For a structure with unequal walls, especially when one wall is much larger than the other, the results for the larger wall always show very good agreement with the frame analysis, and therefore only the results for the smaller wall are shown. The moments in the smaller wall given by the continuum method discretisation and the corresponding values given by the alternative calculation of the moments, which are both explained in Chapter 2 (Section 2.3) are the most important to show together with the plots showing the shift in the line of contraflexure. The plots of the discrete beam shears and the wall discrete axial forces are also of importance and are shown in parallel with the moments. However, the deflections calculated from the continuum analogy have always shown very good agreement with

those from the frame analogy and only a few representative plots are shown. Concerning the shears in the walls, a few plots only are presented to show the shears in the smaller wall. The set of plots illustrating the results are shown for a range of structures of various ratios of the widths, and hence inertias, of the walls to illustrate the effect on the shift of the line of contraflexure from the conventional mid-span position. All these plots are given for different top beam inertias since these affect the top boundary condition of the structure. The plots also show a comparison between the results obtained from the continuum method presented in Chapter 2 and the corresponding results obtained by the frame method; these show also the difference between these two results and those given by the continuum method employing the conventional assumption of the mid-span position of the line of contraflexure. Since the modelling of the structure is influenced by the top beam conditions, calculations are performed to investigate its effect.

For the sake of simplicity the results are based on the assumption that shear deformations are neglected in the structural members and the foundation is fully rigid.

3. 2.1 Curves

The magnitude of the top concentrated interactive force depends on the parameter Z_1, defined in Capter 2 (Section 2.4 (a)), which is a function only of the spacing of the two walls and of Δ and $q'(H)$, which is given by equation 2.91 and depends on the relative stiffness parameter k (= αH). For the most common situation of a pair of plane coupled walls of uniform thickness t, and depths $(2d_1)$ and $(2d_2)$, and for a given value of the ratio of the shift of the line of contraflexure to the span of the beam, Δ/b, the parameter Z_1 depends only on the two ratios, the wall width ratio, λ_1 (= d_1/d_2) and the ratio of the beam span to half the depth of

the smaller wall, λ_2 (= b/d_2). The expression of Z_1 is then given by,

$$Z_1 = \frac{3\lambda_1(\lambda_1+\lambda_2+1)}{(\lambda_1+1)(\lambda_1{}^3+1)+3\lambda_1(\lambda_1+\lambda_2+1)^2}\left[\frac{\lambda_1{}^3}{\lambda_1{}^3+1}(\lambda_1+\lambda_2+1) - \frac{\Delta}{b}\lambda_2 - \frac{1}{2}\lambda_2 - \lambda_1\right]. \quad (3.1)$$

The variations of Z_1 with λ_1 and λ_2, for a wide range of practical situations, are shown in Fig. 3.1 for $\Delta/b = 0$, in Fig. 3.2 for $\Delta/b = 0.20$ and in Fig 3.3 for $\Delta/b = 0.50$. The corresponding variation of the function q'(H) with the parameter k for a structure subjected to a uniformly distributed wind loading and resting on a fully rigid base is shown in Fig. 3. 4. It is seen that the maximum value of Z_1 occurs for the case of $\Delta/b = 0.0$, and when λ_1 and λ_2 are around 3 and 20 respectively. However, q'(H) is maximum for a value of k around 3. This situation corresponds to a magnitude of the top concentrated interactive force of nearly 10% of the total lateral load on the structure. However for the same values of λ_1 and λ_2 and for $\Delta/b = 0.2$, the parameter Z_1 reduces by about 40%. Also, for $\Delta/b = 0.5$, the parameter Z_1 reduces by a further 78%. By adopting the same value of q'(H), the corresponding magnitude of the top force will be between 4% and 5% for $\Delta/b = 0.2$ and between 1% and 2% for $\Delta/b = 0.5$. These figures show the significance of the position of the mid–span line of contraflexure. As far as the top concentrated force is concerned, greatest errors occur with the mid–span position.

If the top fictitious force is to be equal to zero, the position of the line of contraflexure will be given according to equation 2.88 and hence from equation 2.107 as

$$\frac{\Delta}{b} = \left[\frac{1}{2} + \frac{1}{\lambda_2}\right]\left[\frac{\lambda_1{}^3 - \dfrac{\lambda_1 + 1/2\ \lambda_2}{1 + 1/2\ \lambda_2}}{1 + \lambda_1{}^3}\right] \ldots\ldots \quad (3.2)$$

Thus the ratio of the distance Δ, measured from the mid-span position of the connecting beams to the point of contraflexure to the span of the connecting beams b will be function only of the parameters λ_1 ($= d_1/d_2$) and λ_2 ($= b/d_2$). The variation of the ratio Δ/b for a wide range of ratios of λ_1 and λ_2 is shown in Fig. 3.5. The figure shows that the line of contraflexure does go off-centre quickly, even for small ratios of λ_1, especially when λ_2 is relatively small. However, as will be shown later by the frame method, the line of contraflexure will not move all that amount. The alternative positions of the points of contraflexure are given by equations 2.108 and 2.110. However, the relationship between the position of the point of contraflexure in the top beam and the position of the points of contraflexure in the main beams is expressed by the ratio Δ_t/Δ and is given from equations 2.108 and 2.110 for the case of uniform connecting beams of second moment of inertia I_b as

$$\frac{\Delta_t}{\Delta} = \frac{1 + \lambda_1^3 + 12\,\lambda_3}{1 + \lambda_1^3 + 6\,\lambda_3} \qquad \ldots\ldots\ldots\ldots\ldots\ldots \qquad (3.3)$$

The variation of the ratio Δ_t/Δ with λ_1 and λ_3 [$= (I_2/h)/(I_b/b)$] is shown in Fig. 3.6. For the extreme case of a wall connected to a column by beams, the variation of the line of contraflexure is expressed by the ratio Δ/b obtained from equation 2.111 as

$$\frac{\Delta}{b} = \left[\frac{1}{2} + \frac{1}{\lambda_2}\right]\left[1 - \frac{12\,\lambda_3}{1 + 12\,\lambda_3}\right] \qquad \ldots\ldots\ldots\ldots \qquad (3.4)$$

Thus the ratio Δ/b will be function only of the parameters λ_2 and λ_3 and its variation with these parameters is shown in Fig. 3.7.

The reduction factor C_f by which the second moment of inertia is reduced by the shift in the line of contraflexure is given by equation 2.37. The relation between this factor and the ratio Δ/b is shown in Fig. 3.8. If

k' is the parameter αH for the case when the line of contraflexure is assumed to lie at the mid-span position of the connecting beams, and k is the parameter αH for the case of the revised line of contraflexure, the relationship between the two parameters will be as follows,

$$k = A_f . k' \quad \ldots\ldots\ldots\ldots\ldots\ldots\ldots\ldots \quad (3.5)$$

where

$$A_f = \sqrt{C_f}$$

$$= \sqrt{1 - \frac{12(\Delta/b)^2}{1 + 12\ (\Delta/b)^2}} \quad \ldots\ldots\ldots\ldots \quad (3.6)$$

The variation of the reduction factor A_f with the ratio Δ/b, is given in Fig. 3.9.

The two figures 3.8 and 3.9 show the importance of the shift in the line of contaflexure Δ. As the line of contraflexure moves from the mid span position towards the smaller wall, the reduction factors C_f and A_f decrease considerably. As a consequence the relative flexural rigidity k is reduced by an amount A_f.

3. 2.2 Example structure

The representative structure which has been used for parameter studies is the model originally investigated by Macleod[28]. The structure consists of a twenty storey shear wall with a single row of openings resting on a fully rigid base and subjected to a uniformly distributed load. The dimensions of the structure are shown in Fig. 3.10. To illustrate the effects of the top boundary condition and the modelling of the beams, three different ratios of the inertia of the top beam to that of the main beams have been taken, and for each case the investigation has covered five different ratios of the

widths of the walls λ_1. In each case the distance between the centroidal axes of the walls is kept constant. The investigation has covered the forces, deflections and moments, and for each configuration are shown two curves relating to the continuum method discretisation, the first using the revised position of the line of contraflexure, and the second using the conventional mid-span position, a curve showing the comparative results given by the frame method, and a curve given by the continuum method using the continuous medium results before discretisation.

The beam inertia ratio S_m, that is, the ratio of the inertia of the top beam to that of the main beams ($S_m = I_s/I_b$), is initially assumed to be a half, which agrees with the modelling assumption that the connecting beams are smeared over half a storey height above and below each beam level with the top beam being smeared over the half storey height immediately below it. The second case, and the most common, is that when S_m is taken to be equal to unity, which corresponds to a different type of modelling in which the beams can be considered either to be smeared over a storey height below to cover the entire height of structure or the top effect is neglected. The third case is the special case of a coupled shear wall with a relatively stiff top beam, for which S_m is taken to be equal to ten. For this case, a part of the inertia of the top stiff beam, equal to that of the ordinary beams, is considered smeared over the storey height immediately below the top beam level leaving the top beam inertia to be $(I_s - I_b)$. In each case, the wall width ratios λ_1 range between the case of equal walls to the extreme case of a wall connected to a column, represented by width ratios of 1, 3, 10, 25 and 54. A large amount of data has been produced, so only a representative sample of the results is presented to show the main conclusions reached. In general the case of equal symmetrical walls has shown good agreement between the continuum method results and the frame method results. Results for a value of the

ratio λ_1 equal to 3 are very similar to those for $\lambda_1 = 1$, and hence the results for a ratio of 3 are shown rather than those for a ratio of 1. Also, for λ_1 equal to 10 and 25, the results obtained show approximately the same accuracy and for this reason the important results for the ratio of 10 are shown, and the ones for a ratio of 25 are omitted except for the case of the deflection where the ratio of 25 is taken as a representative example. However, the most important wall width ratio is the value of 54 which represents the extreme case of a wall connected to a column by beams.

(a) Positon of the line of contraflexure

The variation of the position of the points of contraflexure in the corresponding beams is shown to be constant over the height of the structure for different values of the ratio λ_1. Only when the top stiff beam becomes stiffer does the position of the top point of contraflexure become considerably different from the position of the line of contraflexure in the main beams. This has been proved by both the frame method and the continuum method using the revised line of contraflexure defined in section 2.5.

Fig. 3.11 shows the position of the line of contraflexure as given by the frame method for λ_1 equal to 1, 10, 25 and 54 and for two different values of beam inertia ratio S_m of 0.5 and 1. The figure shows that the points of contraflexure for each ratio λ_1 have an essentially constant position for each beam and show approximately a vertical line stretching from the bottom up to the nineteenth storey. The position of this line is affected only by the wall width ratio and is not affected by the stiffness of the top beam. However, the point of contraflexure in the top beam is affected by both ratios λ_1 and S_m. For a ratio of S_m equal to 0.5, the top point of contraflexure has the same position as the other points of

contraflexure in the remaining beams. However, as the top beam gets stiffer, the top point of contraflexure moves towards the smaller wall and even for a value of the ratio S_m of 1 the change is significant. This phenomenon is accentuated for the case of a top stiffening beam, as shown in Fig. 3.12 for S_m equal to 10. However, Fig. 3.13 shows the corresponding results given by the theory presented in Chapter 2, section 2.5 (equations 2.108 and 2.110) in addition to those given by the frame method and shows good agreement between the two for S_m equal to 0.5 and 1. Similarly Fig. 3.14 shows the comparative case of a top stiffening beam for which S_m is equal to 10. The figures show a relatively constant position of the line of contraflexure from top to bottom apart from the top beam in which the point of contraflexure moves quickly away towards the smaller wall as the ratio λ_1 gets bigger and the top beam becomes stiffer. This is better presented in Fig. 3.15 which plots the variation of the top point of contraflexure against λ_1 for the three set of values of S_m.

(b) Lateral deflections

The prediction of deflections has always been very satisfactory, and the results given by the continuum method give very good agreement with those given by the frame method. To demonstrate the accuracy generally obtained, representative curves for the deflections are shown in Figs. 3.16 and 3.17. These represent a ratio S_m of 1 for the first one and 10 for the second one and a ratio λ_1 of 25 and 54 respectively. Although the wall width ratio λ_1 is very large, the curves given by the frame method and the continuum method are indistinguishable from each other.

(c) Discrete moments in the smaller wall

The discrete moments in the larger wall given by the continuum method have always shown good agreement with those given by the frame

method, and hence the only results which will be shown here are those for the smaller wall. The results are given in two parts as follows

– Unstiffened coupled shear wall

For the case of an unstiffened coupled shear wall, the moments given by the continuum method discretisation and the alternative moment approach using the revised line of contraflexure position always gave good agreement with the results from the frame method. As a sample of that, Fig. 3.18 shows the moments in the smaller wall for λ_1 equal to 3 and S_m equal to 0.5. It shows good agreement apart from the very bottom where a small difference occurs between the continuum discretisation and the frame method. Fig. 3.19 shows the results for the same wall width ratio but for a different beam inertia ratio S_m equal to 1. The only difference arises at the top beam where there is a small difference in the moments. For such a small ratio λ_1, the line of contraflexure does not alter very much, and thus the moments given by the continuum method discretisation are not effectively altered by the revised line of contraflexure. A similar situation occurs for a ratio λ_1 of 10 as shown in Fig. 3.20. However, for a ratio λ_1 of 54, the results given by the continuum method discretisation using the mid–span line of contraflexure assumption show very large discrepancies compared to those from either the frame method or the revised theory using the revised position of the line of contraflexure. The latter two are in good agreement. This is shown by Fig. 3.21 for a ratio S_m of 0.5 and by Fig. 3.22 for the most common case of a beam inertia ratio of 1. The two figures show good agreement, even at the top where the greatest discrepancies occur.

– Stiffened coupled shear wall with a beam inertia ratio S_m of 10

For the case of a top stiffening beam, the results are similar to those

for unstiffened coupled shear walls but the envelope given by the continuum method discretisation is displaced due to the top boundary condition. The results given by the continuum method discretisation and the results given by the alternative calculation diverge. While the continuum method discretisation results show much poorer agreement with those from the frame method, the alternative approach results are accurate enough. Fig. 3.23 shows that for a ratio S_m of 10 and even for a small ratio λ_1 of 3 the moments given by the continuum method discretisation using the mid-span position of the line of contraflexure or the revised line of contraflexure are in good agreement but are significantly different from the ones given by the frame method. However, using the alternative approach (presented in Chapter 2) for the calculation of the moments, Fig. 3.24 shows very good agreement apart from a very small difference at the top and bottom of the structure. The same things happen with a ratio λ_1 of 10, where Fig. 3.25 and Fig. 3.26 correspond to Fig. 3.23 and Fig. 3.24 respectively. For the extreme case of λ_1 equal to 54, the results given by the frame method and the results given by the continuum method discretisation using the revised line of contraflexure diverge greatly, and the continuum method envelope is displaced by a large amount as shown in Fig. 3.27. However, this time the curve shows a very big disagreement in the results given by the continuum method discretisation using the mid-span position of the line of contraflexure compared to those given using the revised line of contraflexure. Fig. 3.28, however, using the alternative calculation, gives good results apart from at the top storey, where a relatively large difference occurs; the results from the continuum method discretisation using the mid-span position still show large discrepancies from those from the frame method.

(d) Discrete shears in the beams and axial forces in walls

The beam shears and the axial forces are related since the axial forces are simply the integral of the shears. Representative results are shown for three wall width ratios of 3, 10 and 54.

– Wall width ratio of 3

For S_m equal to 0.5, the beam shears shown by Fig. 3.29 show accurate results. Comparatively Fig. 3.30 shows a small disagreement in the shears given by the continuum method discretisation and the frame method at the top floors for a ratio S_m of 1, whereas Fig. 3.31 gives better results for the case of a top stiffening beam corresponding to a ratio S_m of 10. In general good results are achieved in most of the structure apart from discrepancies which arise at the top beam level

The axial forces in the walls also show satisfactory results. Figs. 3.32 and 3.33 show the axial forces for ratios S_m of 0.5 and 10 respectively. Similar results where obtained for the other configurations examined.

– Wall width ratio of 10

For a beam inertia ratio S_m equal to 1. Fig. 3.34 shows the shears in the beams and Fig. 3.35 shows the axial forces in walls. The overall shears are still accurate enough apart from at the top where the discrepancy increases. However, the axial forces are reasonably accurate.

– Extreme case of wall width ratio of 54

In this case, Fig. 3.36 show that the results given by the continuum method discretisation using the revised line of contraflexure give better agreement when compared with the frame method than the results given by the continuum method discretisation using the mid–span line of contraflexure position. Figs. 3.36 and 3.37 give approximately the same

results for ratios S_m of 0.5 and 1 respectively. However, for the case of a stiffening beam corresponding to a beam inertia ratio of 10, Fig. 3.38 shows that the top shears become relatively much more important and there is better agreement between the continuum method and the frame method when using the revised line of contraflexure rather than using the mid-span line of contraflexure.

Figs. 3.39, 3.40 and 3.41 show the axial forces in the walls for ratios S_m of 0.5, 1 and 10 respectively. The three figures show good agreement although the accuracy decreases from top to bottom.

(e) Discrete shears in the smaller wall

Again the discrete shears in the larger wall are generally predicted accurately and only some representative plots of the shears in the smaller wall are shown here. The smaller the ratio λ_1, the better the agreement achieved between the continuum method results and the frame method results.

For a beam inertia ratio of 1, Figs. 3.42 and 3.43 show the wall shears for the cases of a wall width ratio of 10 and 54 respectively. The first figure generally shows good agreement apart from at the top, while the second gives good results compared to the ones given by the continuum method using the mid-span position of the line of contraflexure.

For a ratio S_m of 10, Fig. 3.44 shows the shears for a ratio λ_1 of 3. It shows a relatively large discrepancy at the top. Fig. 3.45 shows better results relative to the previous one in respect of the top beam for a ratio λ_1 of 54. The figure also shows a large disagreement between the results given by the continuum method using the mid-span assumption and the ones using the revised line of contraflexure which is the best in terms of a comparison with the frame method.

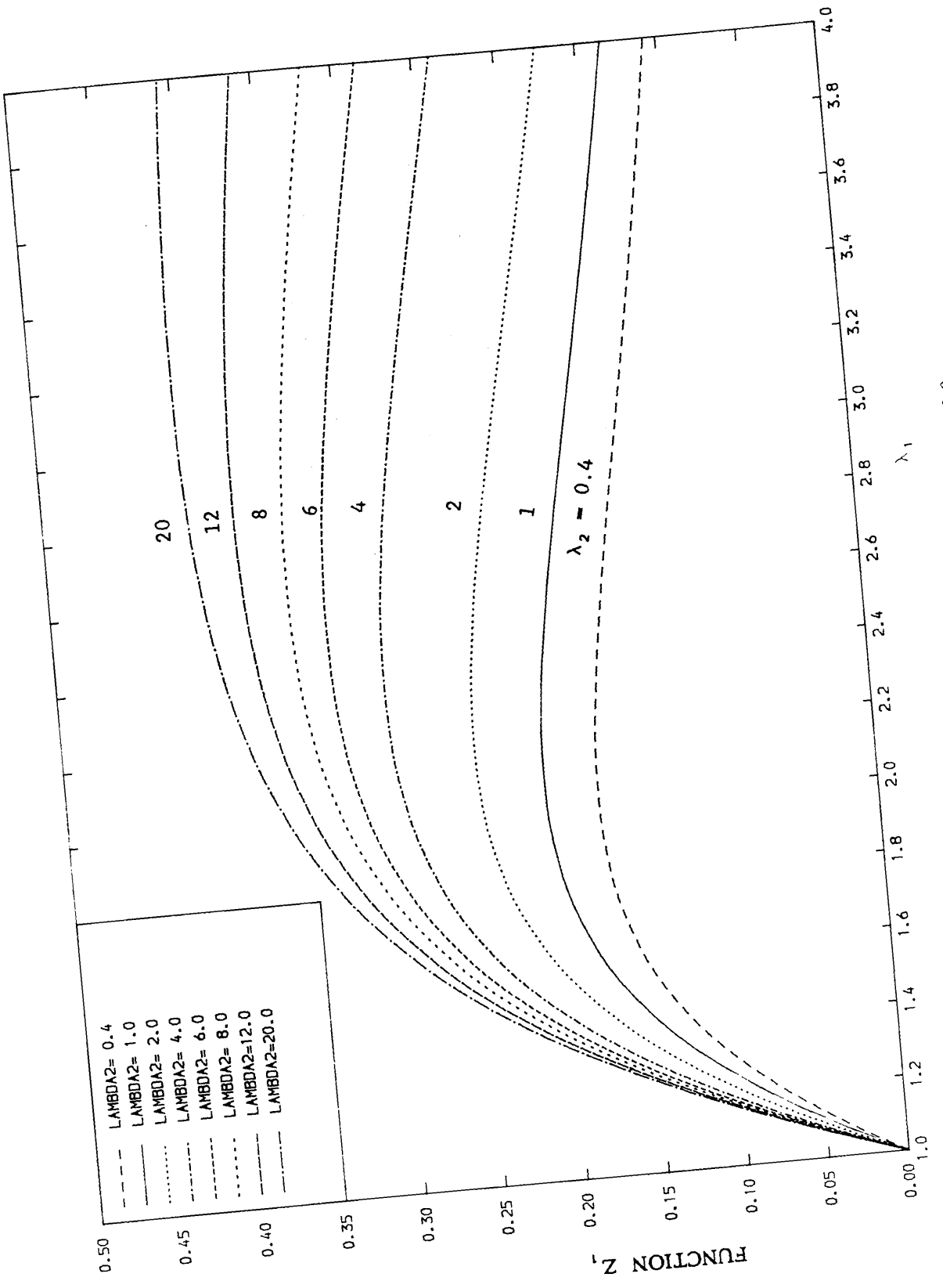

Fig. 3.1. VALUES OF Z_1 *AGAINST* λ_1 *and* λ_2 *FOR* $\Delta / b = 0.0$.

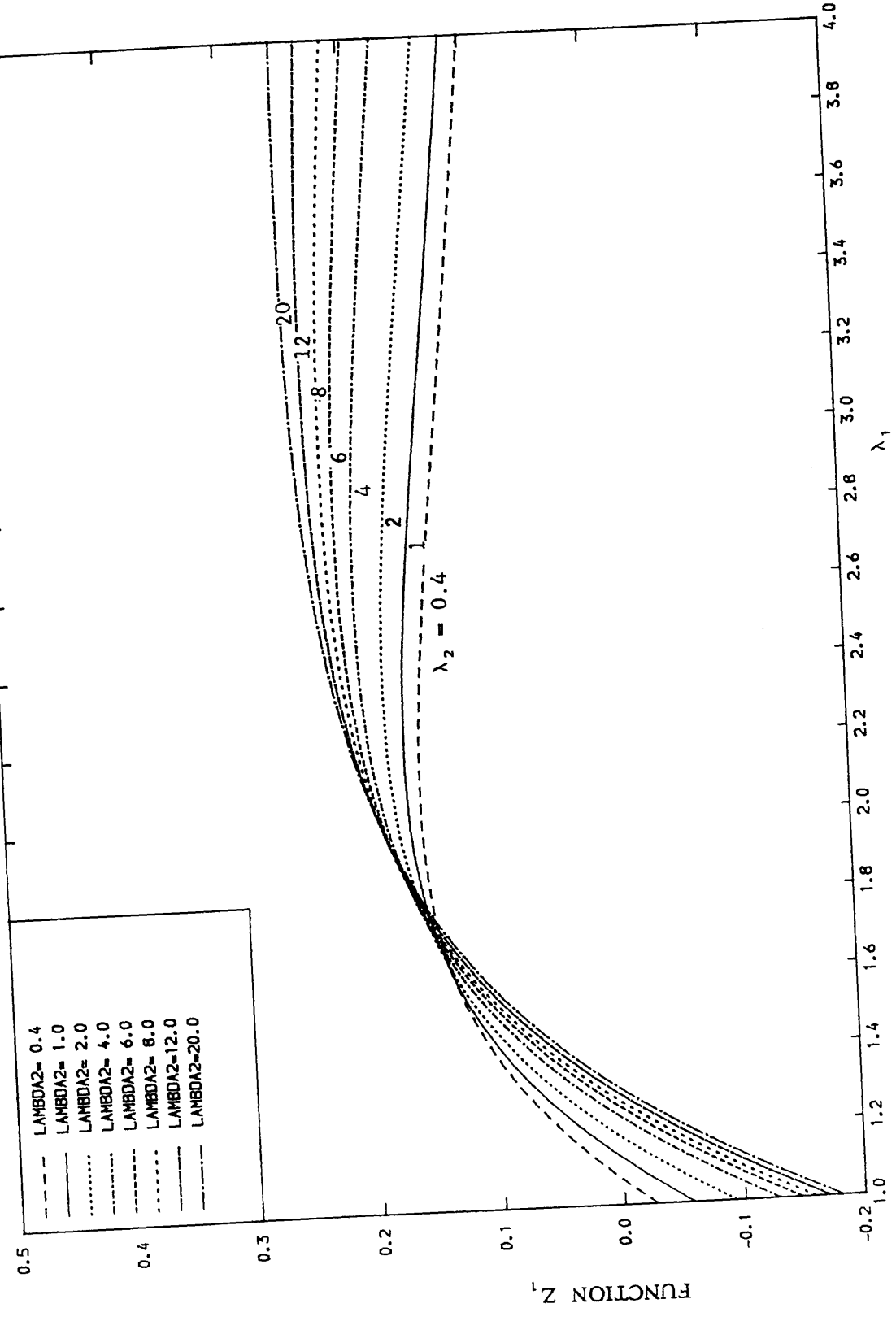

Fig. 3.2. VALUES OF Z_1 AGAINST λ_1 and λ_2 FOR $\Delta/b = 0.20$.

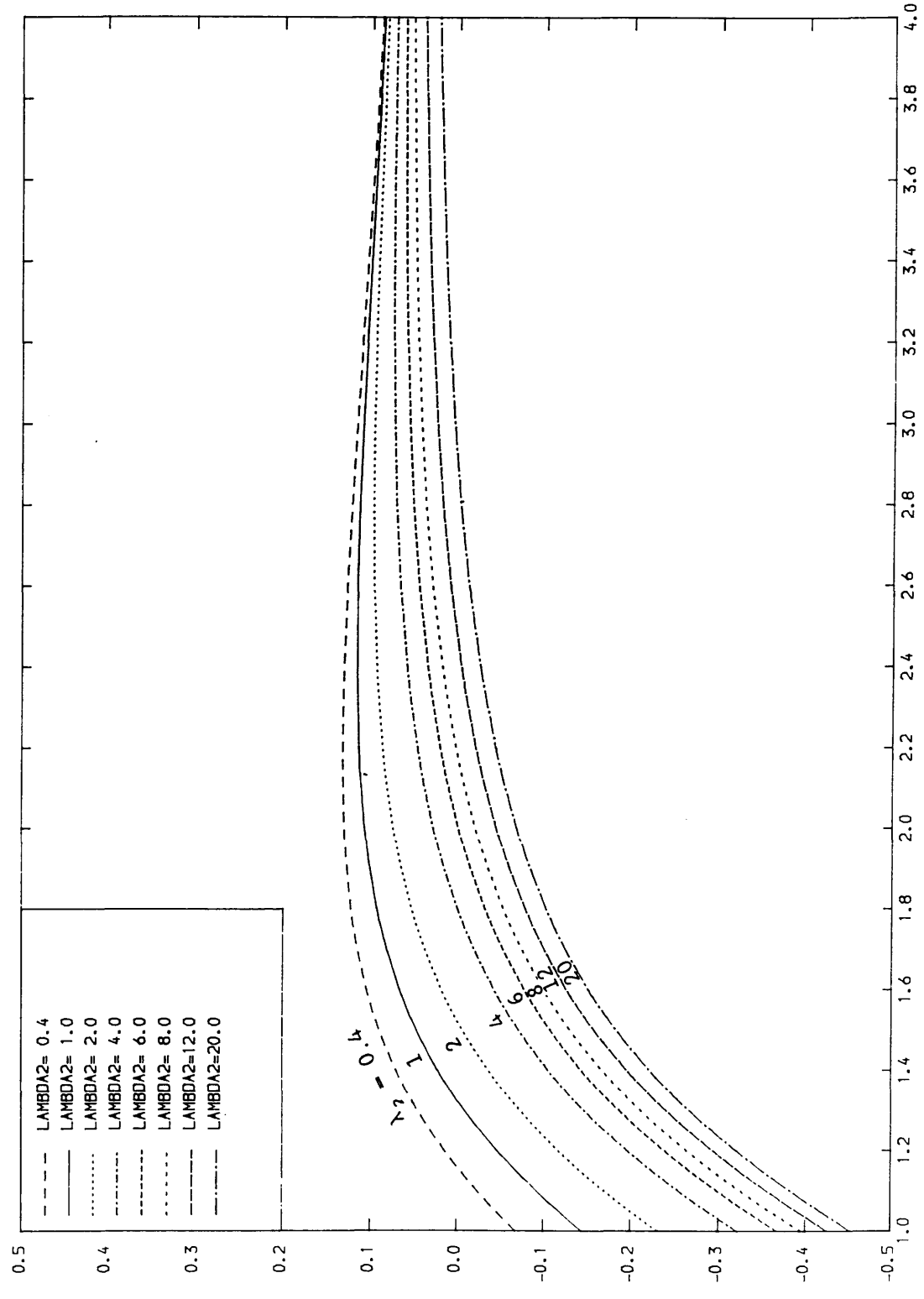

Fig. 3.3. VALUES OF Z_1 *AGAINST* λ_1 *and* λ_2 *FOR* $\Delta / b = 0.50$.

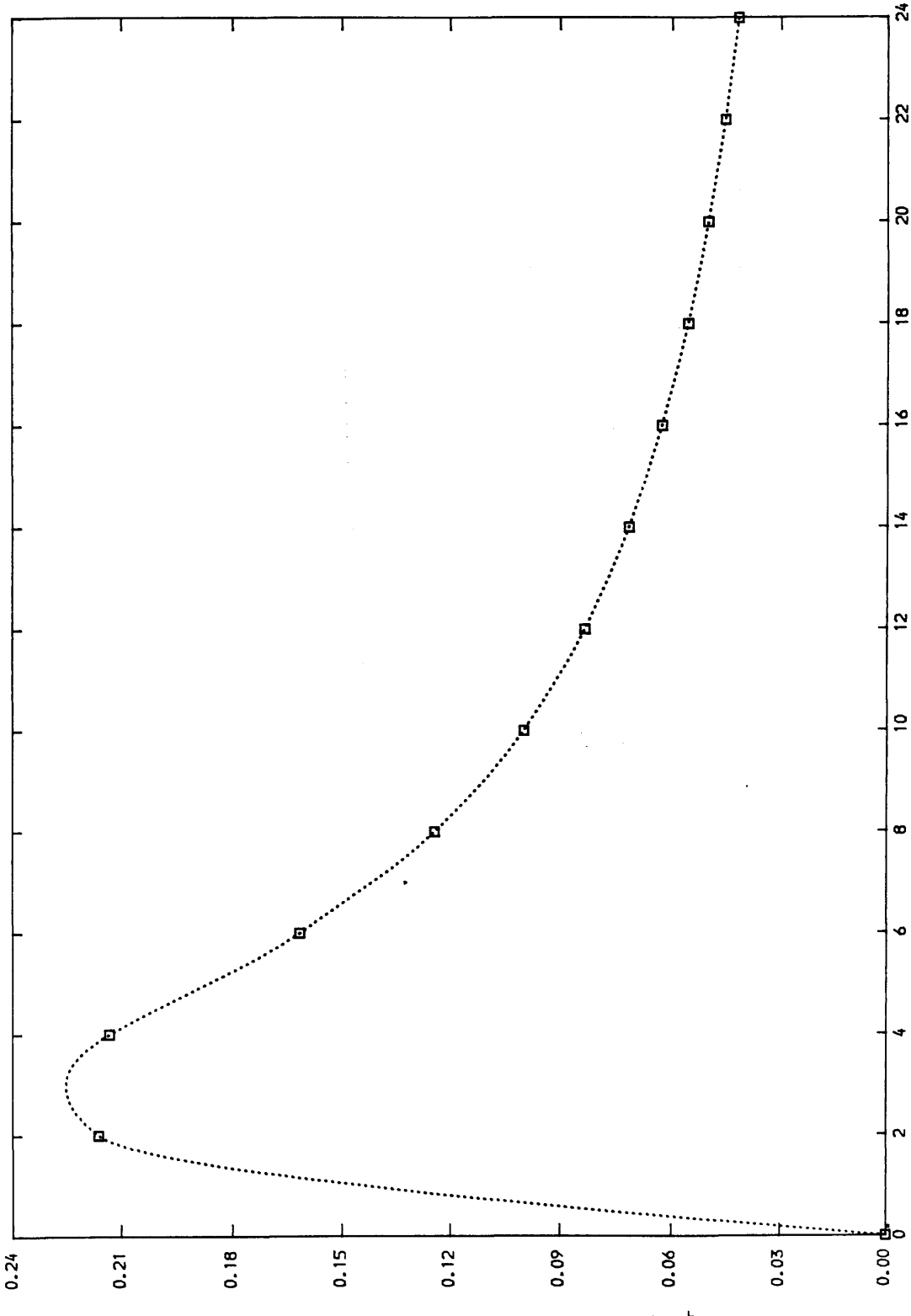

Fig. 3.4. Variation of the function q' (H) with the relative flexural rigidity of lintel beams, k_1 for a uniform load case

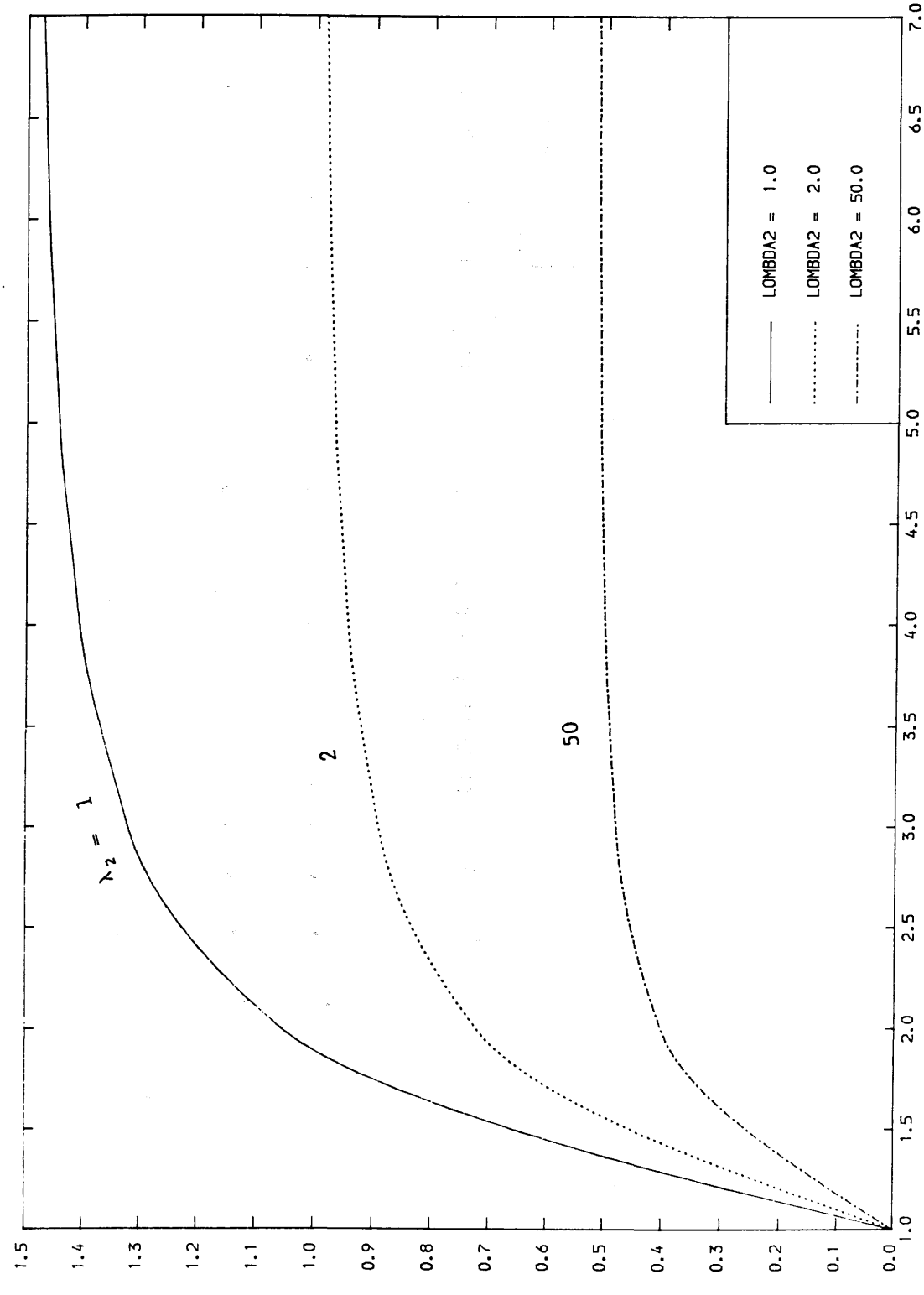

Fig. 3.5. VARIATION OF Δ/b AGAINST λ_1, FOR DIFFERENT VALUES OF λ_2

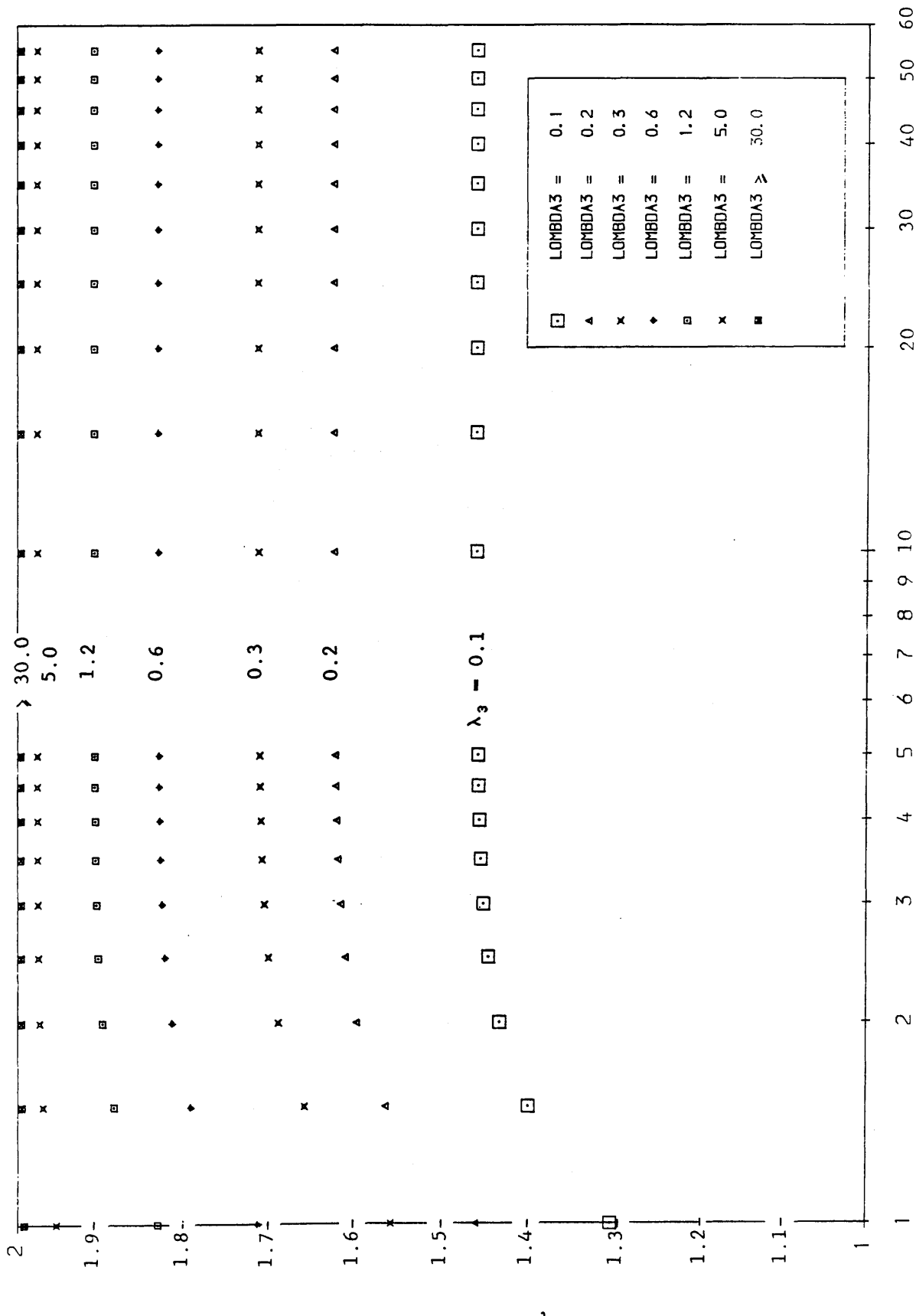

Fig. 3.6. RELATION BETWEEN Δ_t AND Δ FOR $S_m = 1.0$

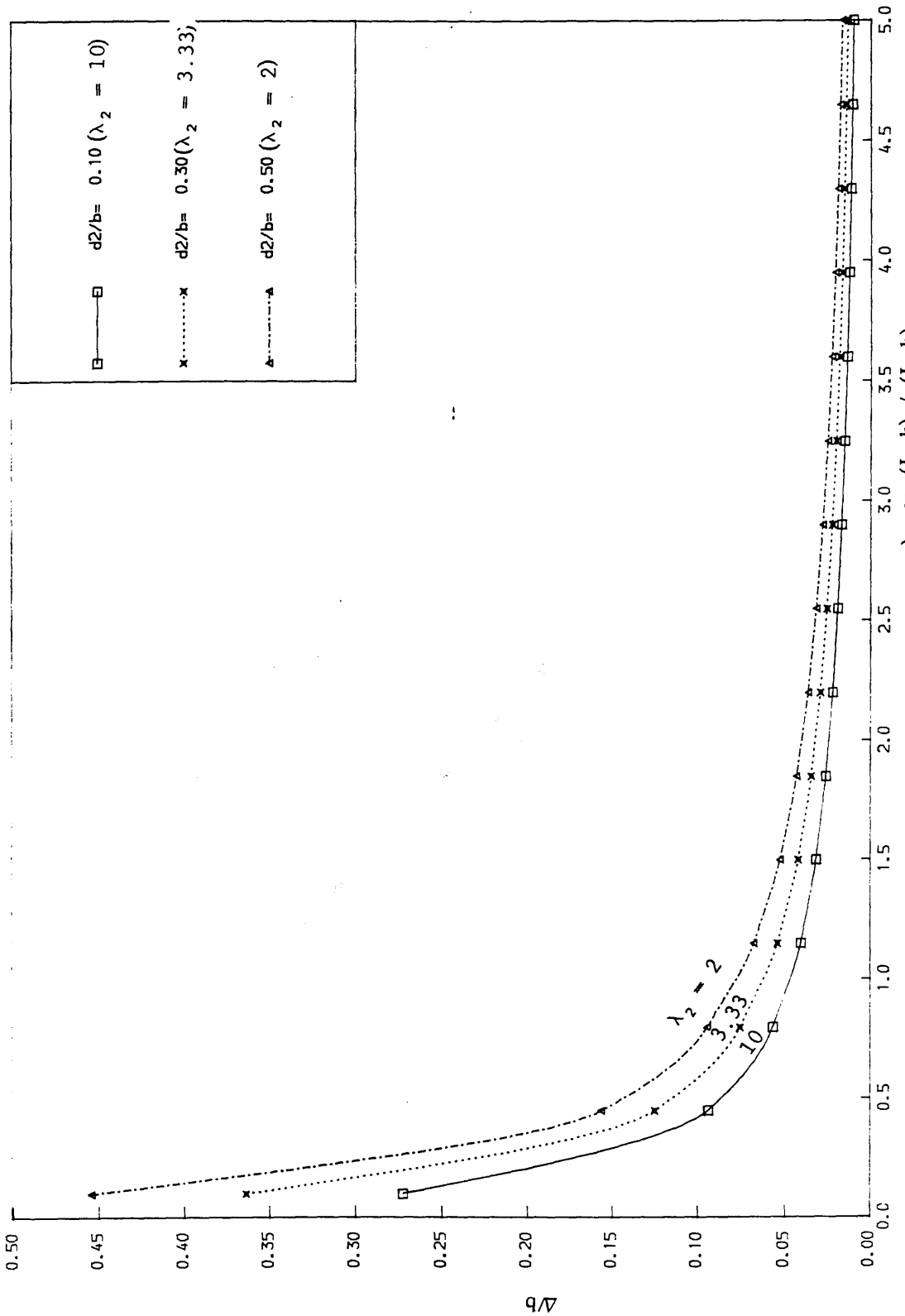

Fig. 3.7. SHIFT OF THE LINE OF CONTRAFLEXURE FOR THE EXTREME CASE OF A WALL CONNECTED TO A COLUMN BY BEAMS.

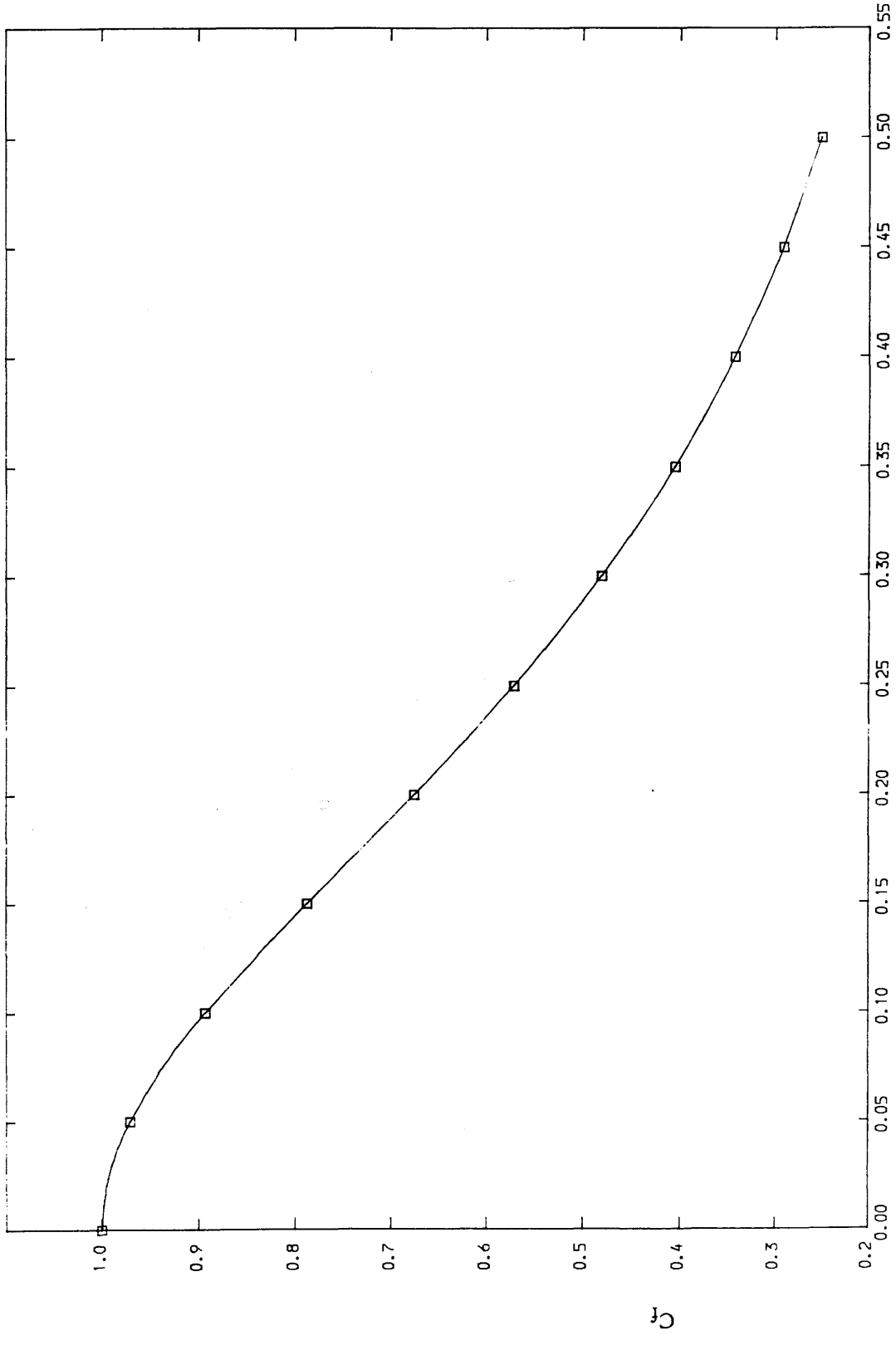

Fig. 3.8. Reduction factor C_f due to the shift of the point of contraflexure

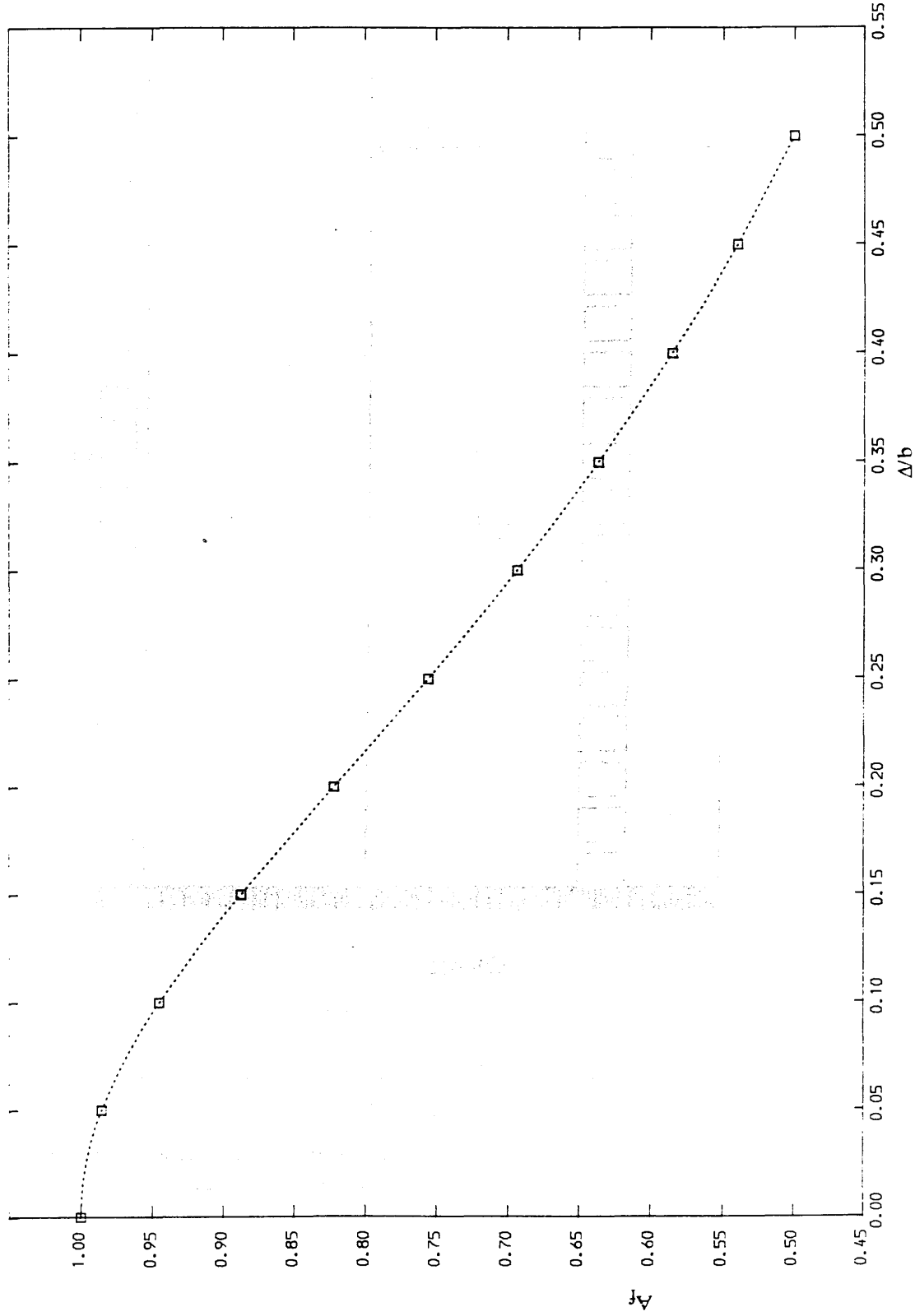

Fig. 3.9. Reduction factor A_f due to the shift of the point of contraflexure

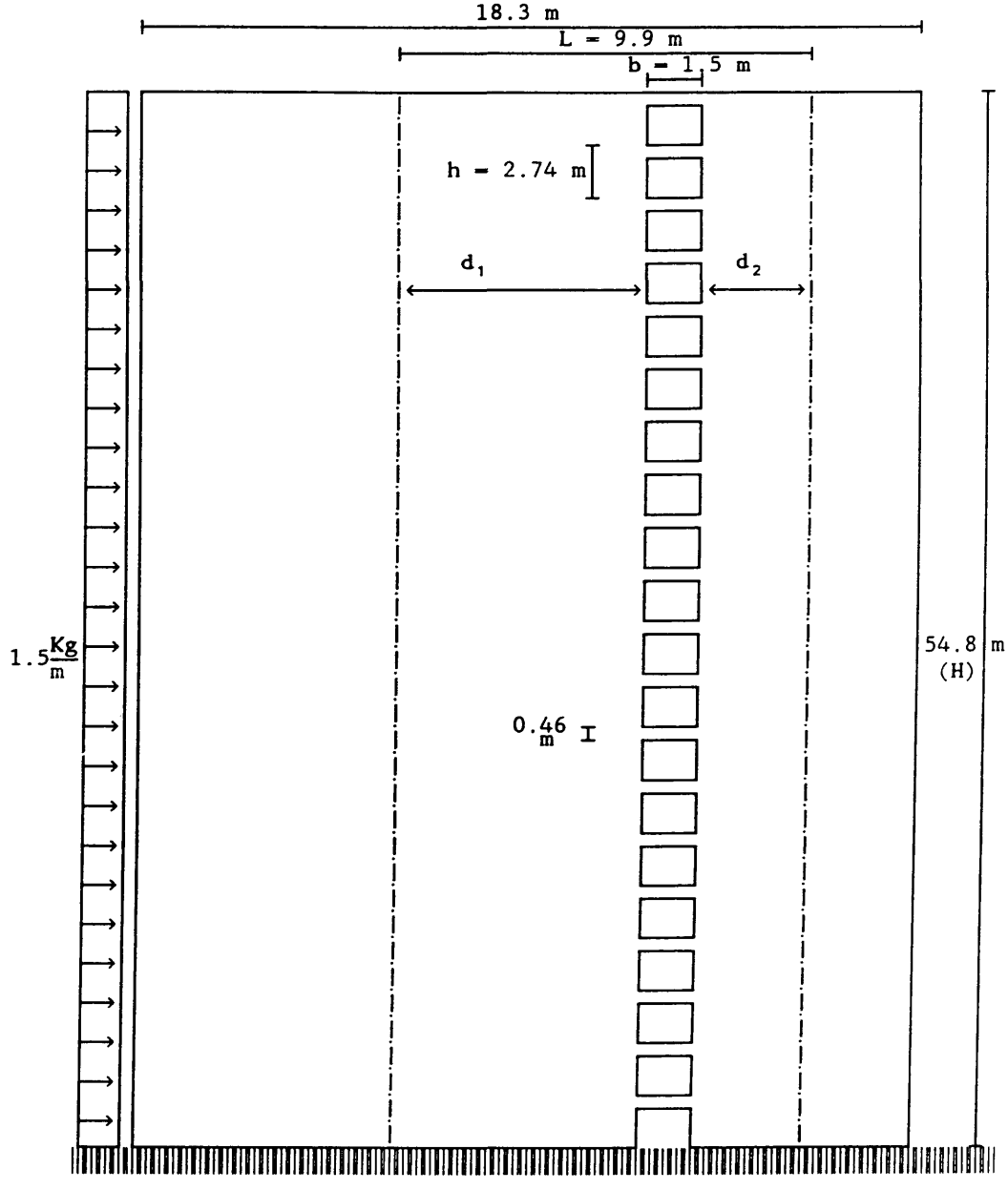

Elevation

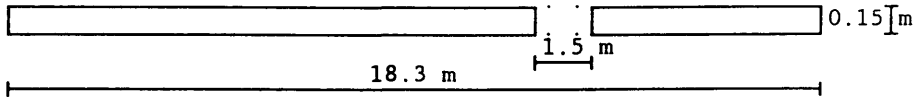

Shear wall cross section

Coupling beam section (0.46 × 0.15 m)

Inertia of main beams 12 10^{-4} m^4

$E = 2.0\ 10^{-7}\ KN/m^2$

$d_1 + d_2 = 8.4\ m$

$b = 1.5\ m$

$h = 2.74\ m$

$H = 54.8\ m$

Fig. 3.10

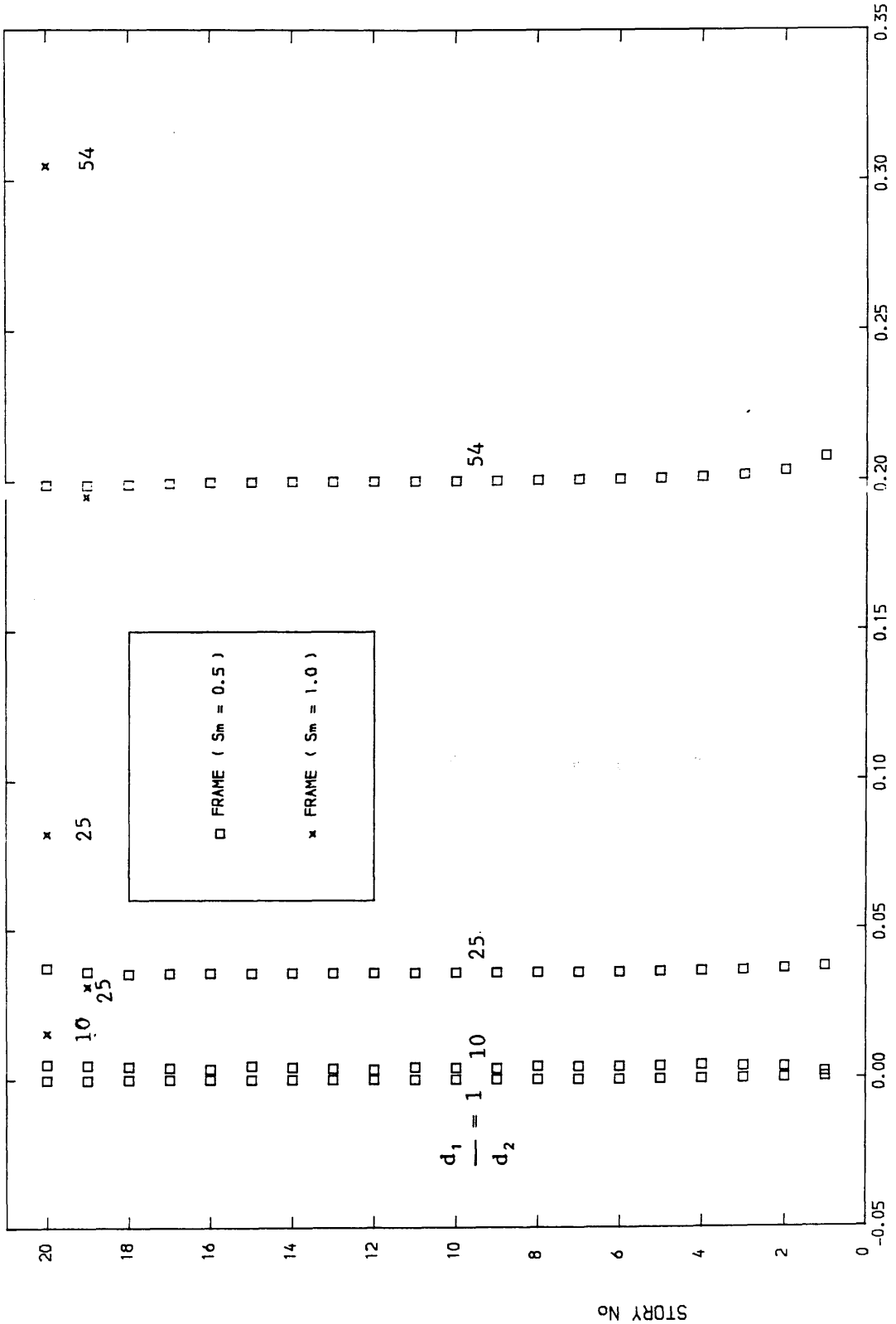

Fig. 3.11. SHIFT OF THE POINT OF CONTRAFLEXURE

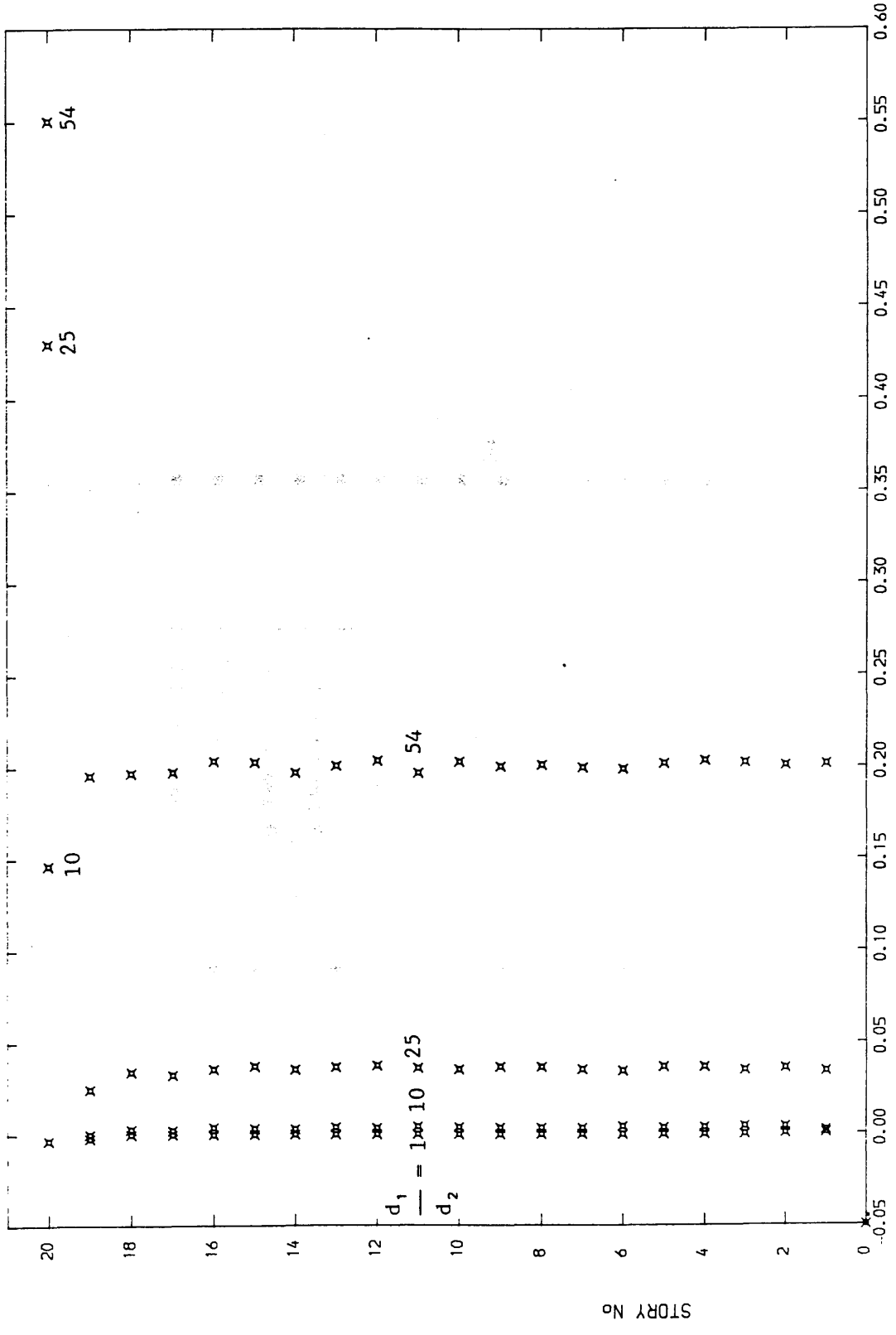

Fig. 3.12. SHIFT OF THE POINT OF CONTRAFLEXURE
FRAME (Sm = 10.0)

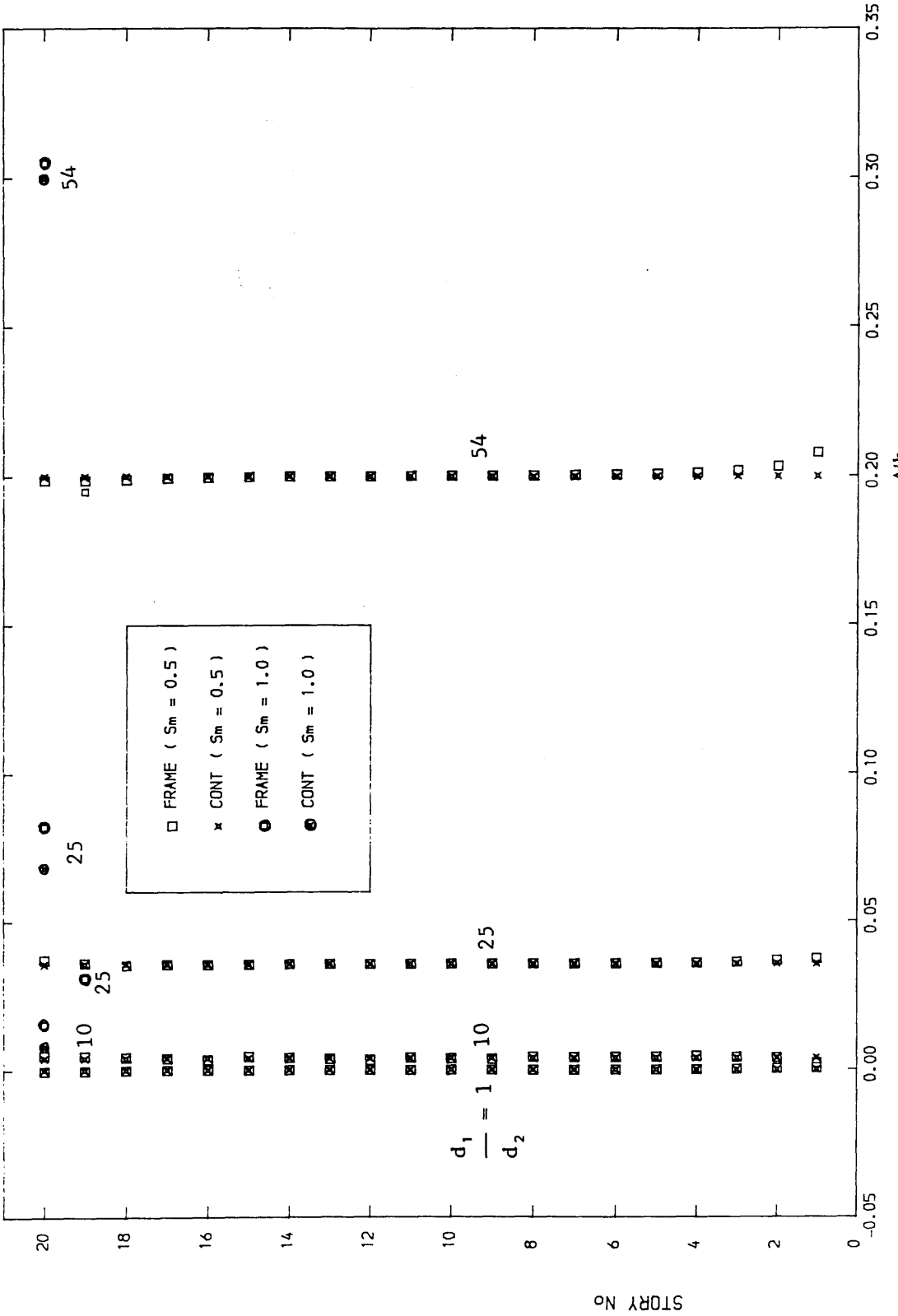

Fig. 3.13. SHIFT OF THE POINT OF CONTRAFLEXURE

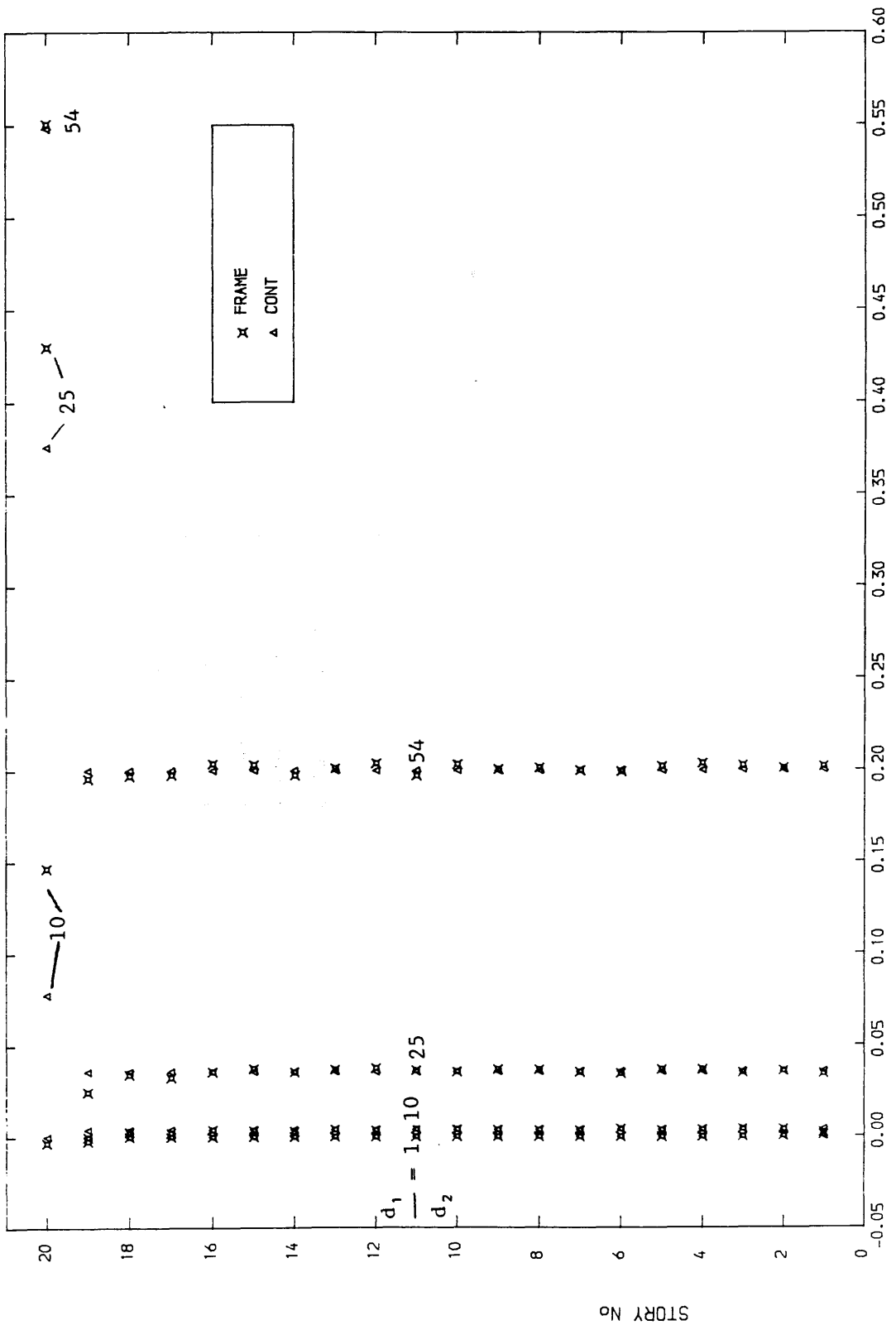

Fig. 3.14. SHIFT OF THE POINT OF CONTRAFLEXURE
Sm = 10.0

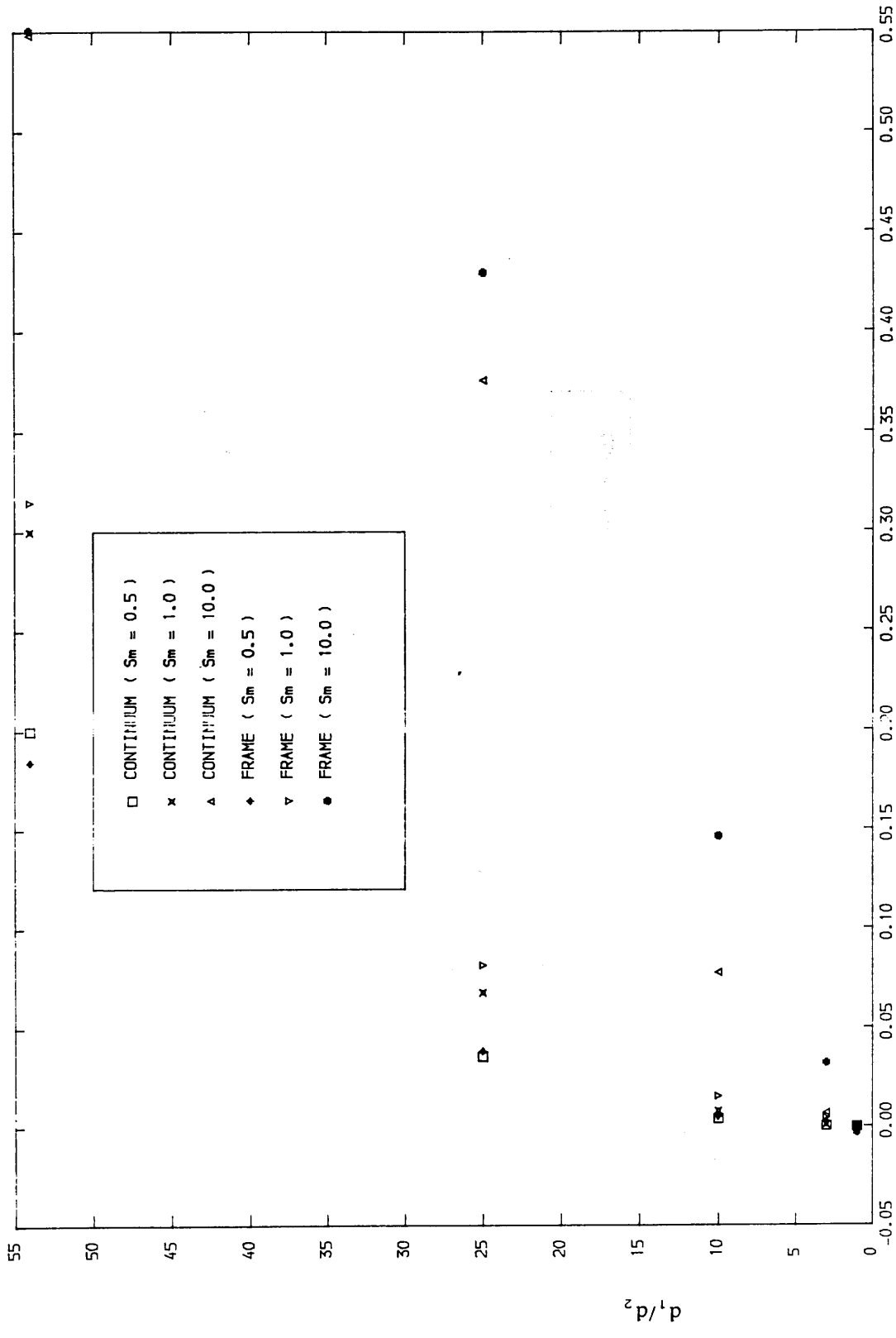

Fig. 3.15. SHIFT OF THE TOP POINT OF CONTRAFLEXURE

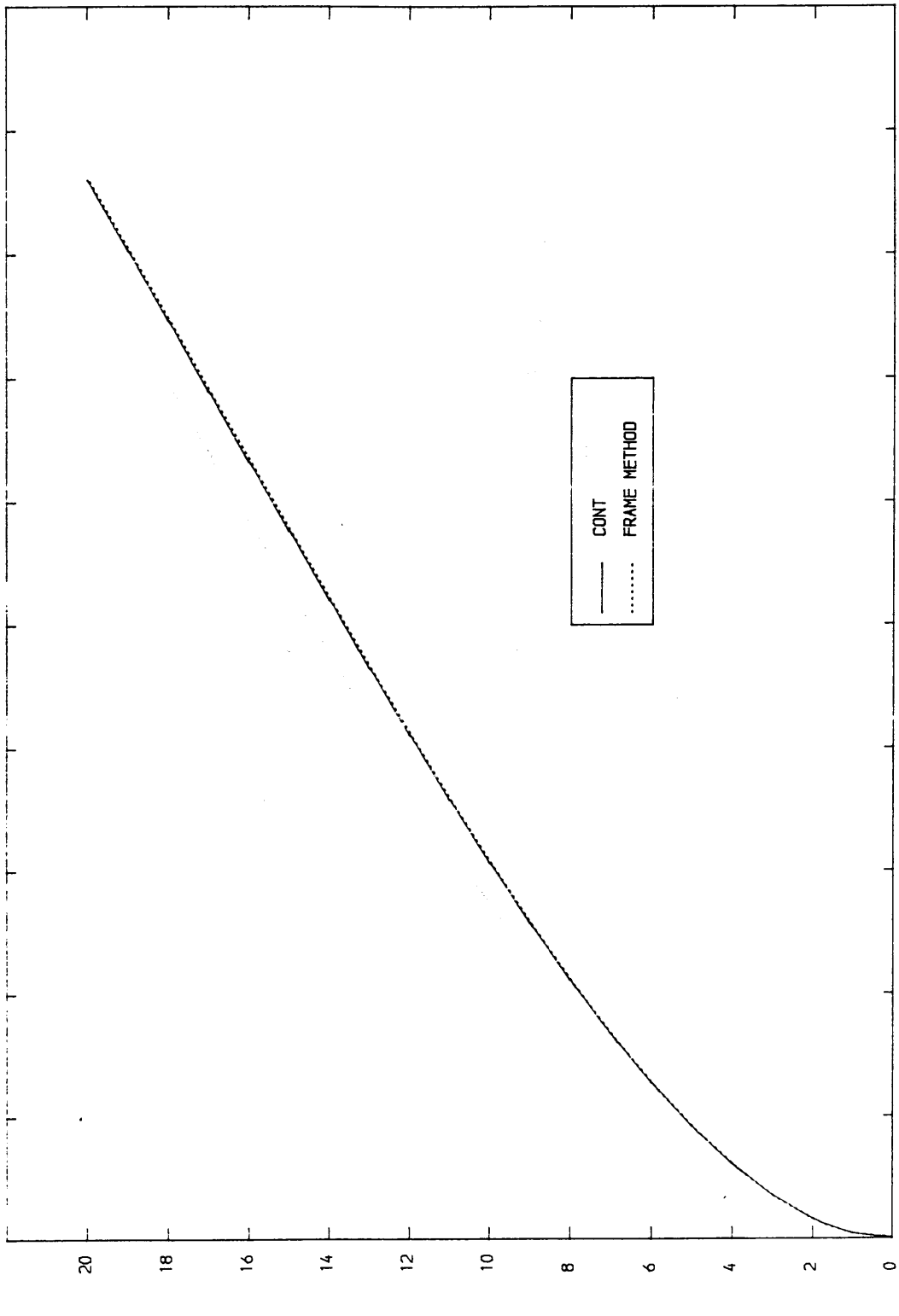

Fig. 3.16. LATERAL DEFLECTION ($\lambda_1 = d_1 / d_2 = 25$)

Sm = 1.0

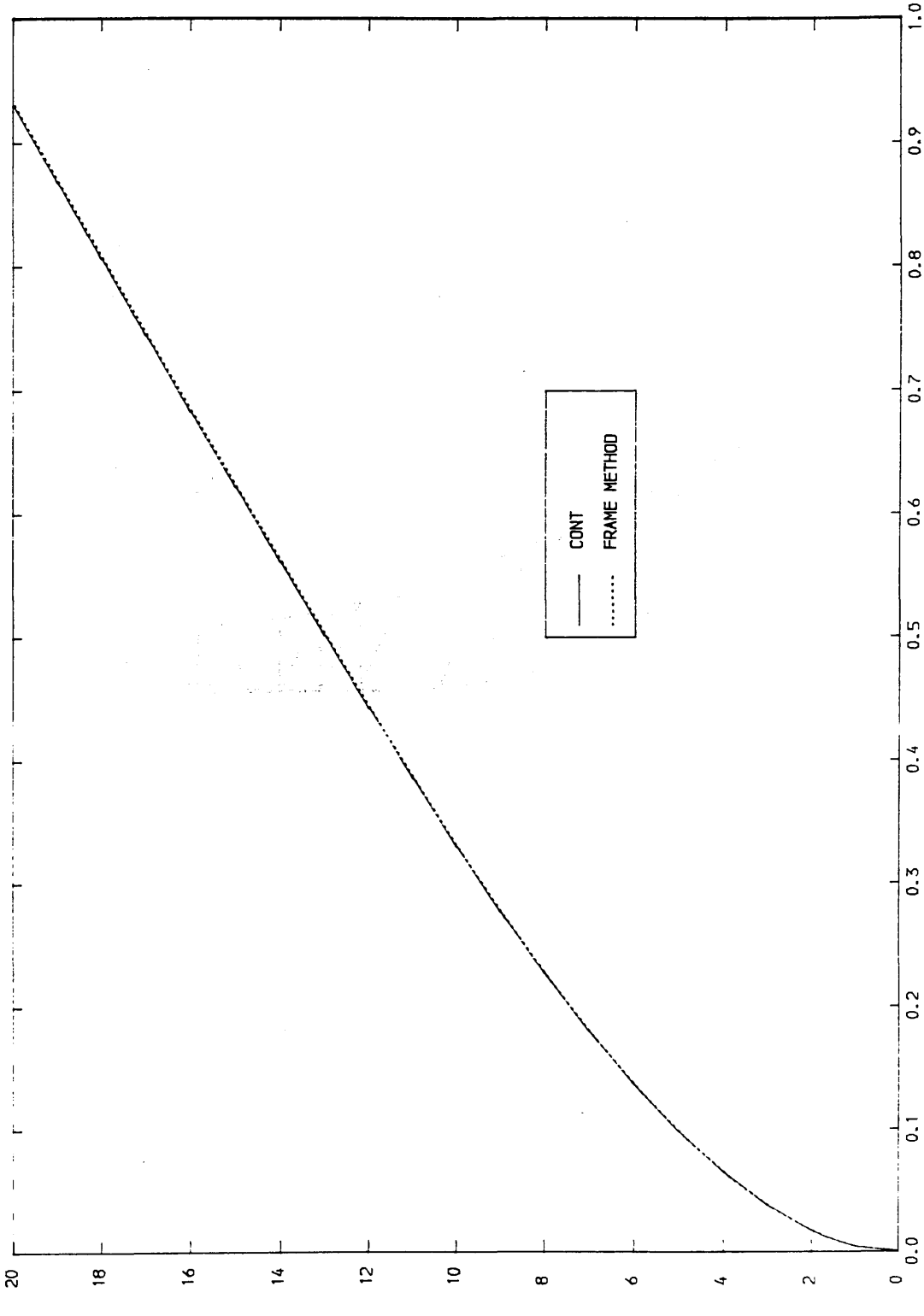

Fig. 3.17. LATERAL DEFLECTION ($\lambda_1 = d_1 / d_2 = 54$)

Sm = 10.0

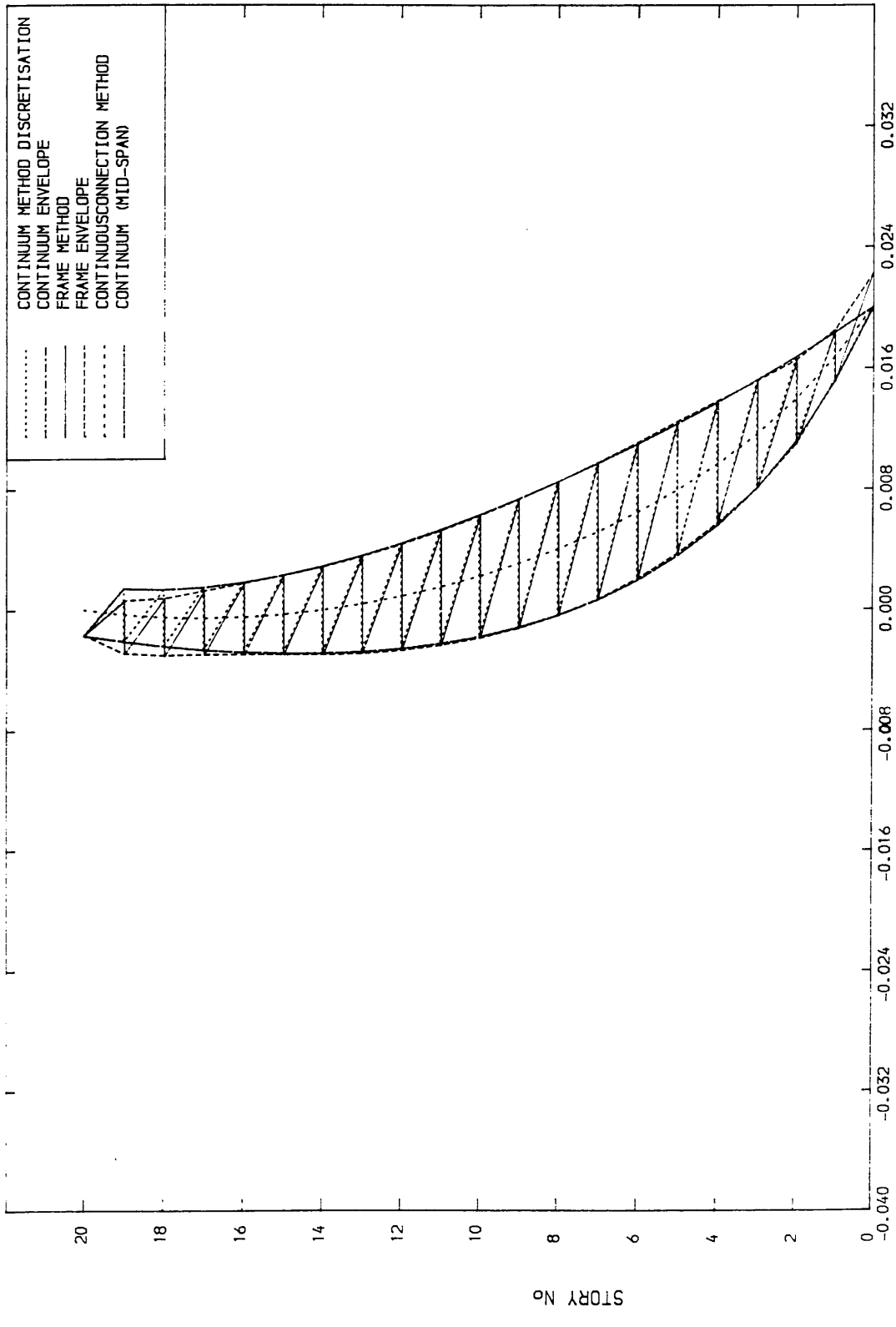

Fig. 3.18. MOMENTS IN WALL2 ($\lambda_1 = d_1 / d_2 = 3$)
Sm = 0.5, ALTERNATIVE CALCULATION

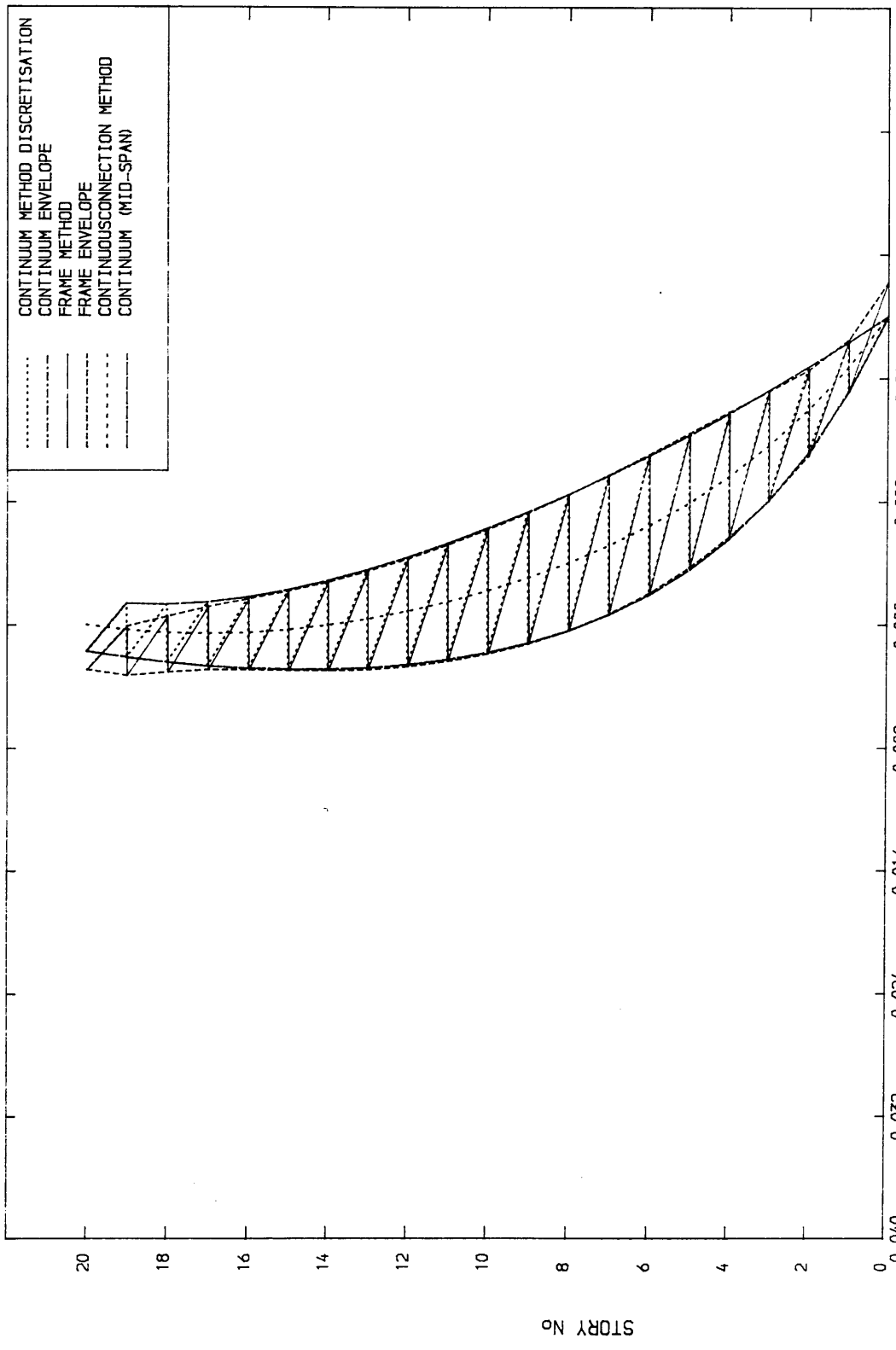

Fig. 3.19. MOMENTS IN WALL2 ($\lambda_1 = d_1 / d_2 = 3$)
Sm = 1.0, ALTERNATIVE CALCULATION

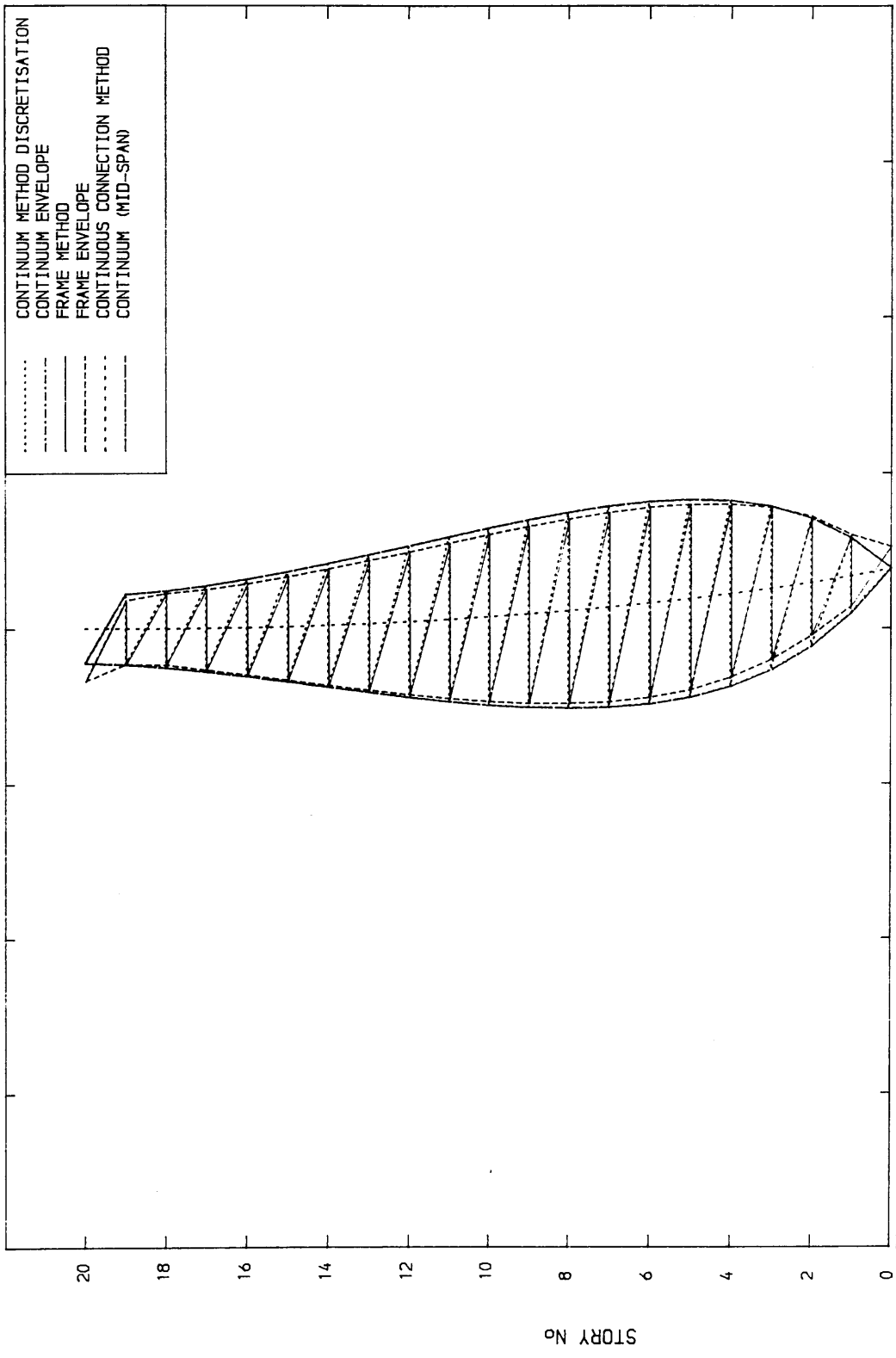

Fig. 3.20. MOMENTS IN WALL2 ($\lambda_1 = d_1 / d_2 = 10$)
Sm = 1.0, ALTERNATIVE CALCULATION

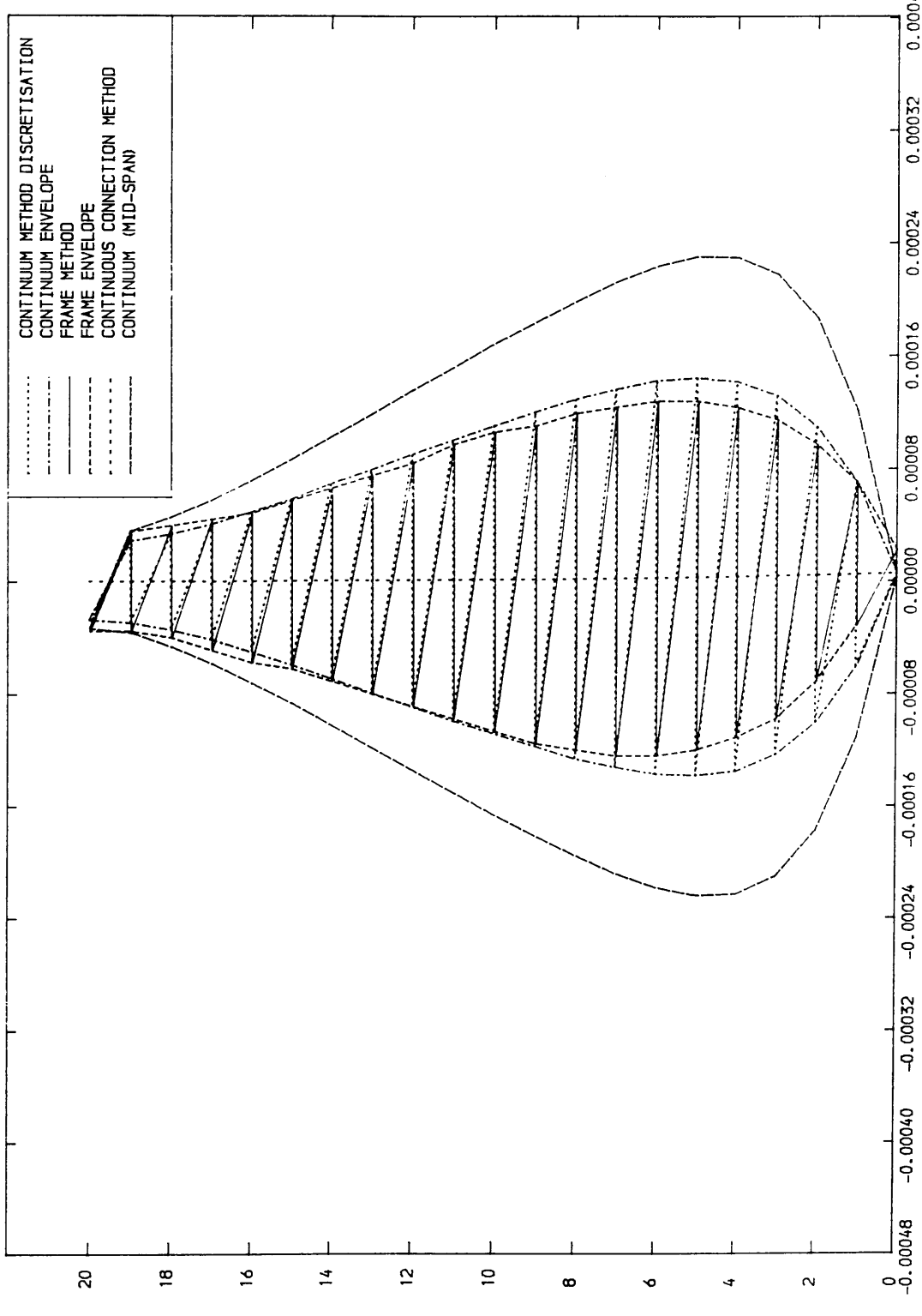

Fig. 3.21. MOMENTS IN WALL2 ($\lambda_1 = d_1 / d_2 = 5.4$)
Sm = 0.5, ALTERNATIVE CALCULATION

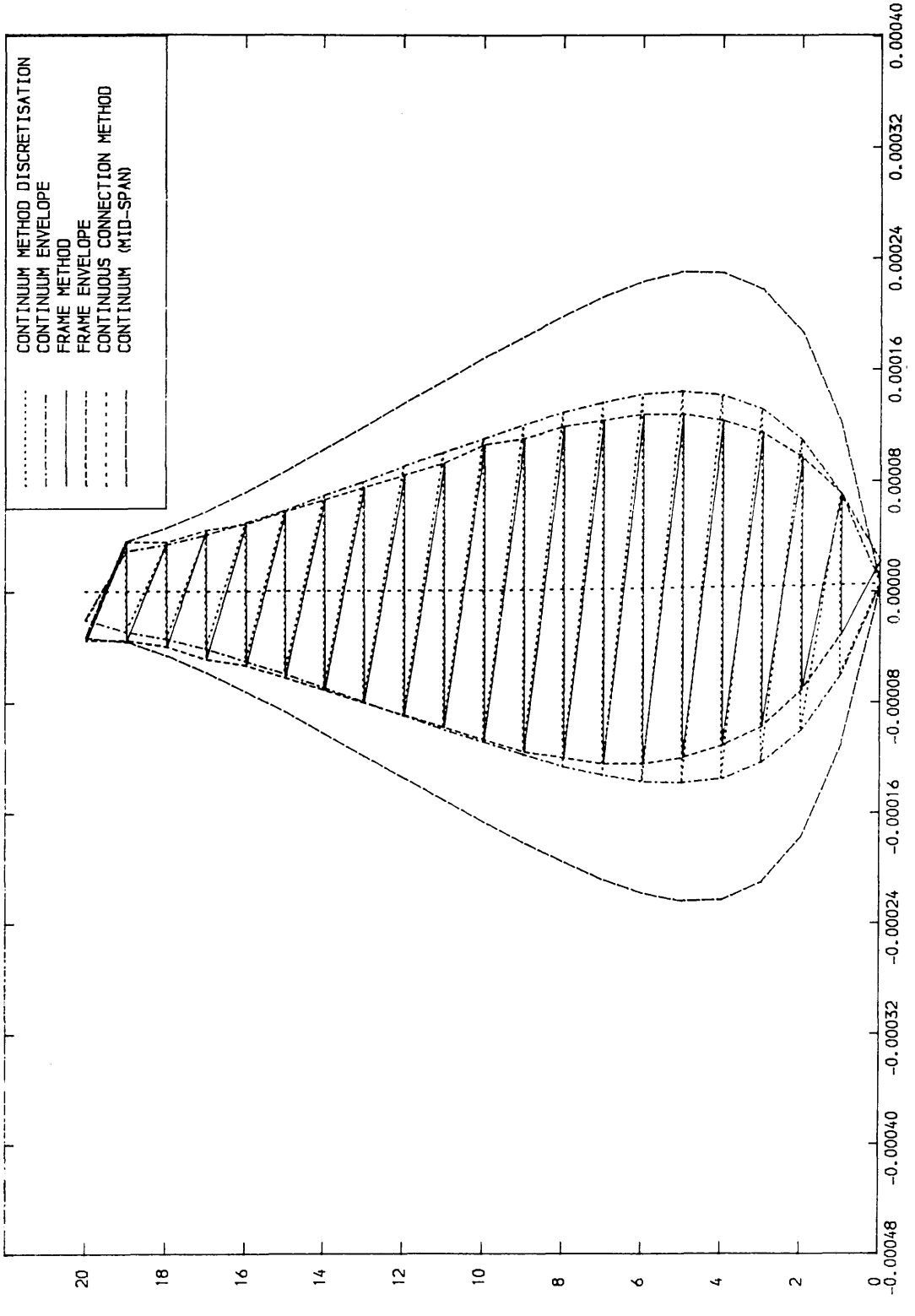

Fig. 3.22. MOMENTS IN WALL2 ($\lambda_1 = d_1 / d_2 = 54$)
Sm = 1.0, ALTERNATIVE CALCULATION

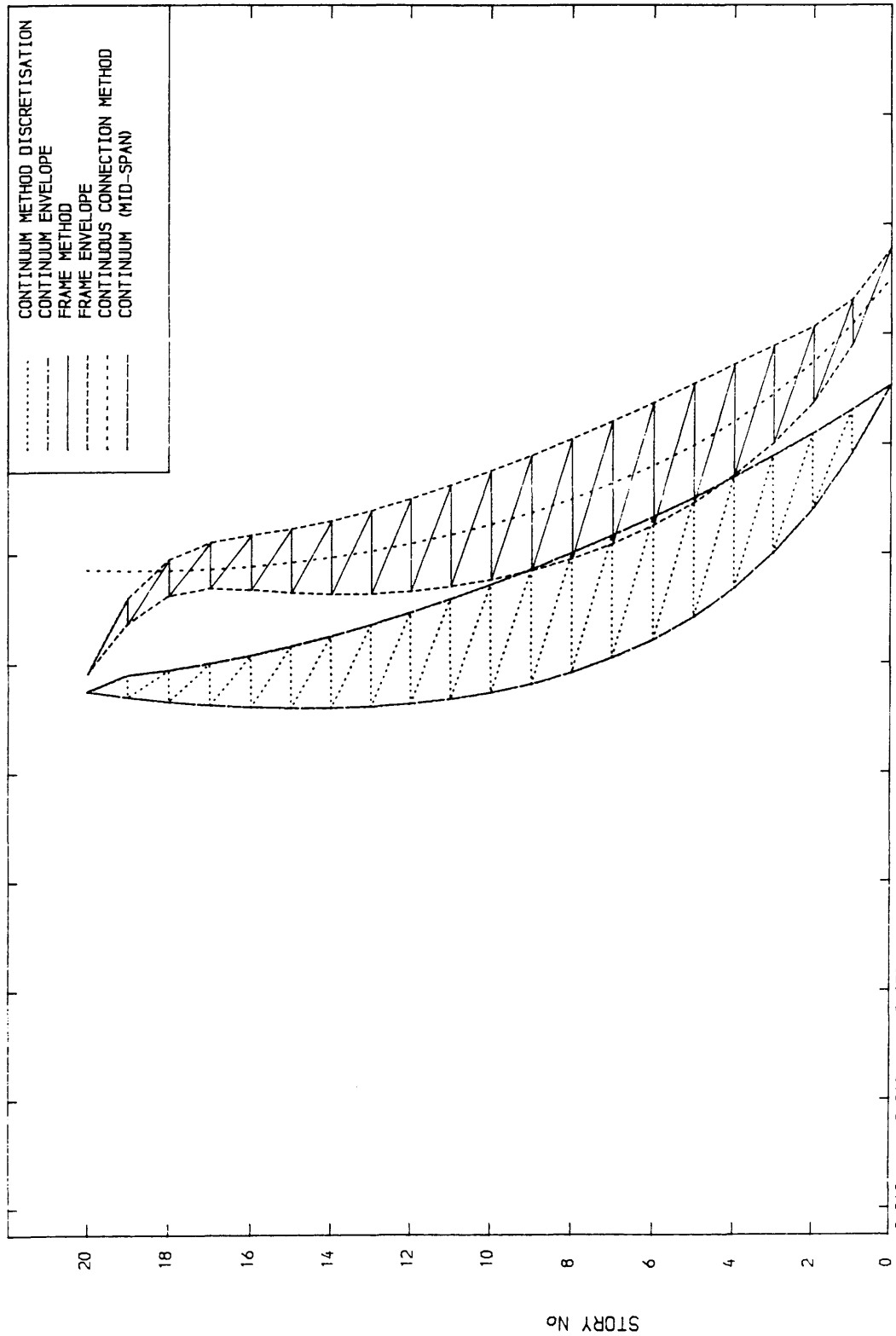

Fig. 3.23. MOMENTS IN WALL2 ($\lambda_1 = d_1 / d_2 = 3$)
$S_m = 10.0$

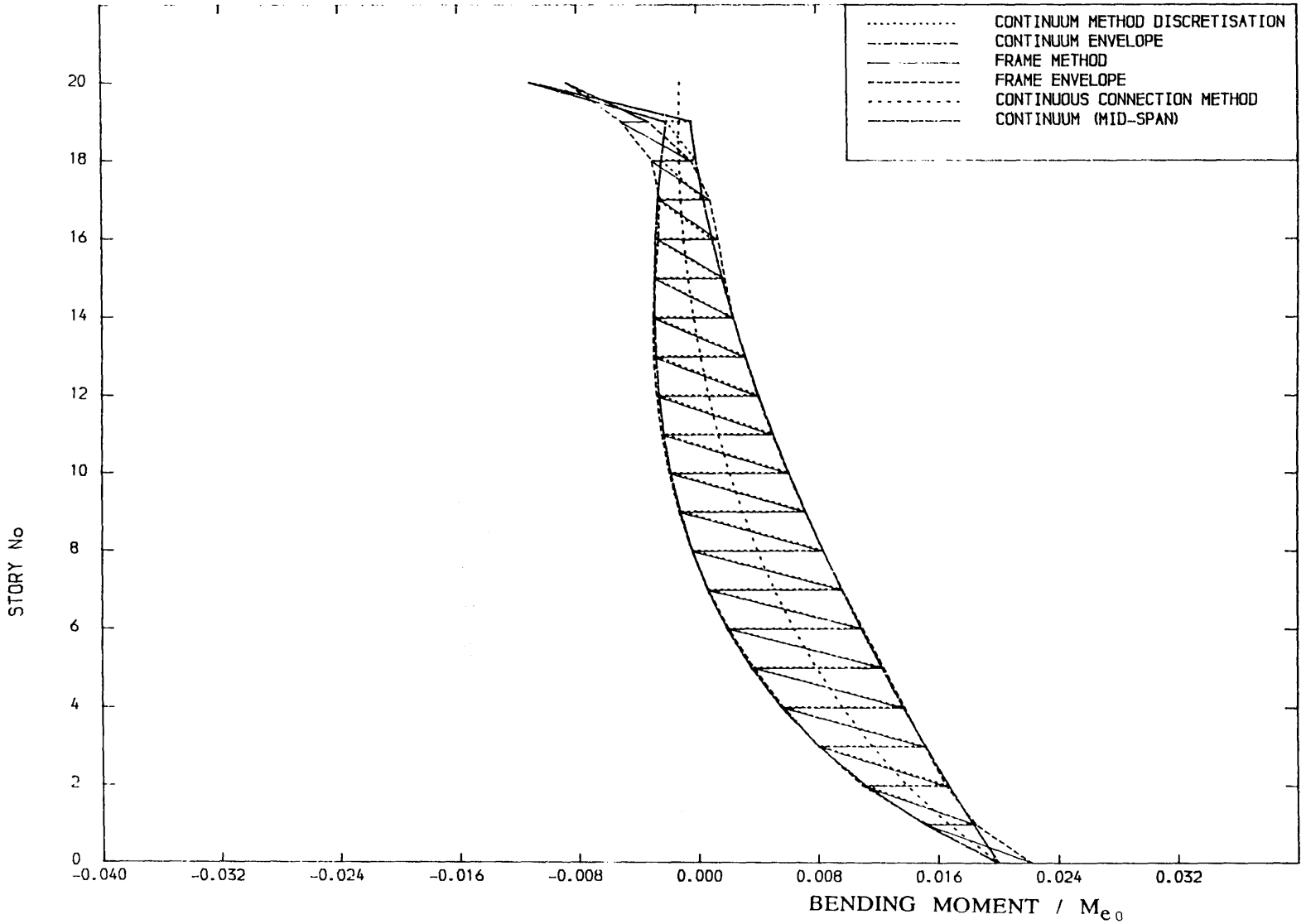

Fig. 3.24. MOMENTS IN WALL 2 ($\lambda_1 = d_1 / d_2 = 3$)
Sm = 10.0, ALTERNATIVE CALCULATION

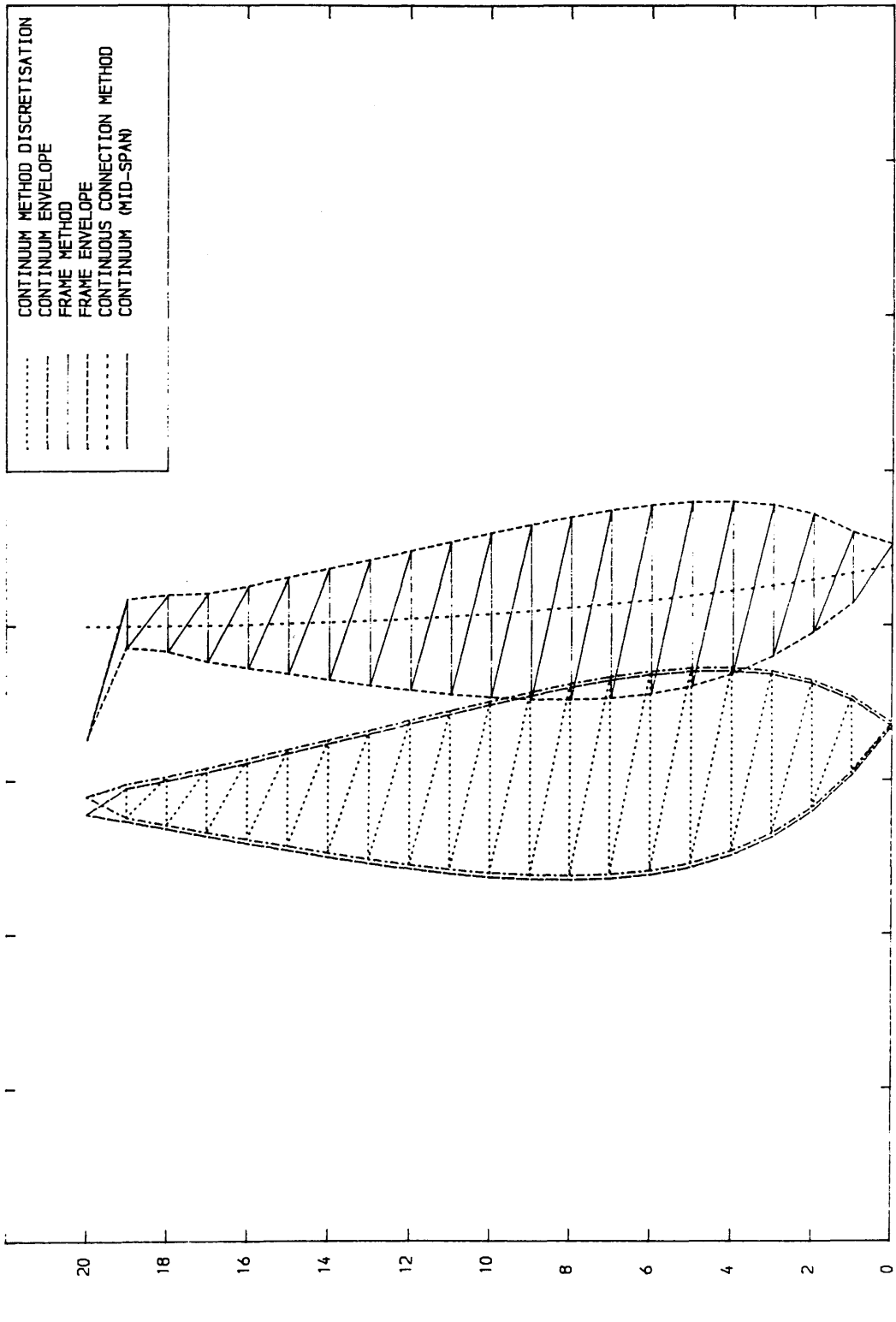

Fig. 3.25. MOMENTS IN WALL2 ($\lambda_1 = d_1 / d_2 = 10$)
Sm = 10.0

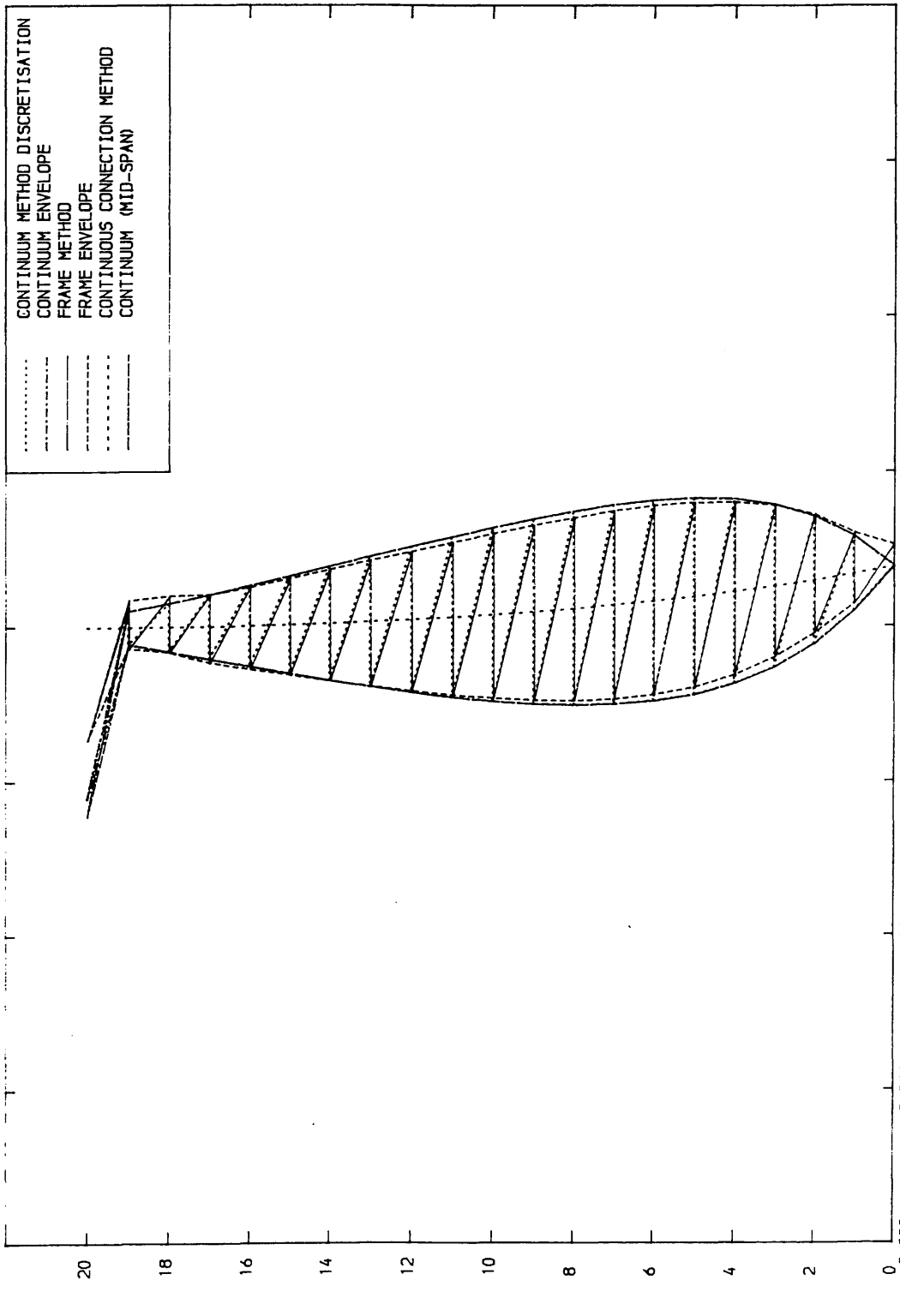

Fig. 3.26. MOMENTS IN WALL2 ($\lambda_1 = d_1 / d_2 = 10$)
Sm = 10.0, ALTERNATIVE CALCULATION

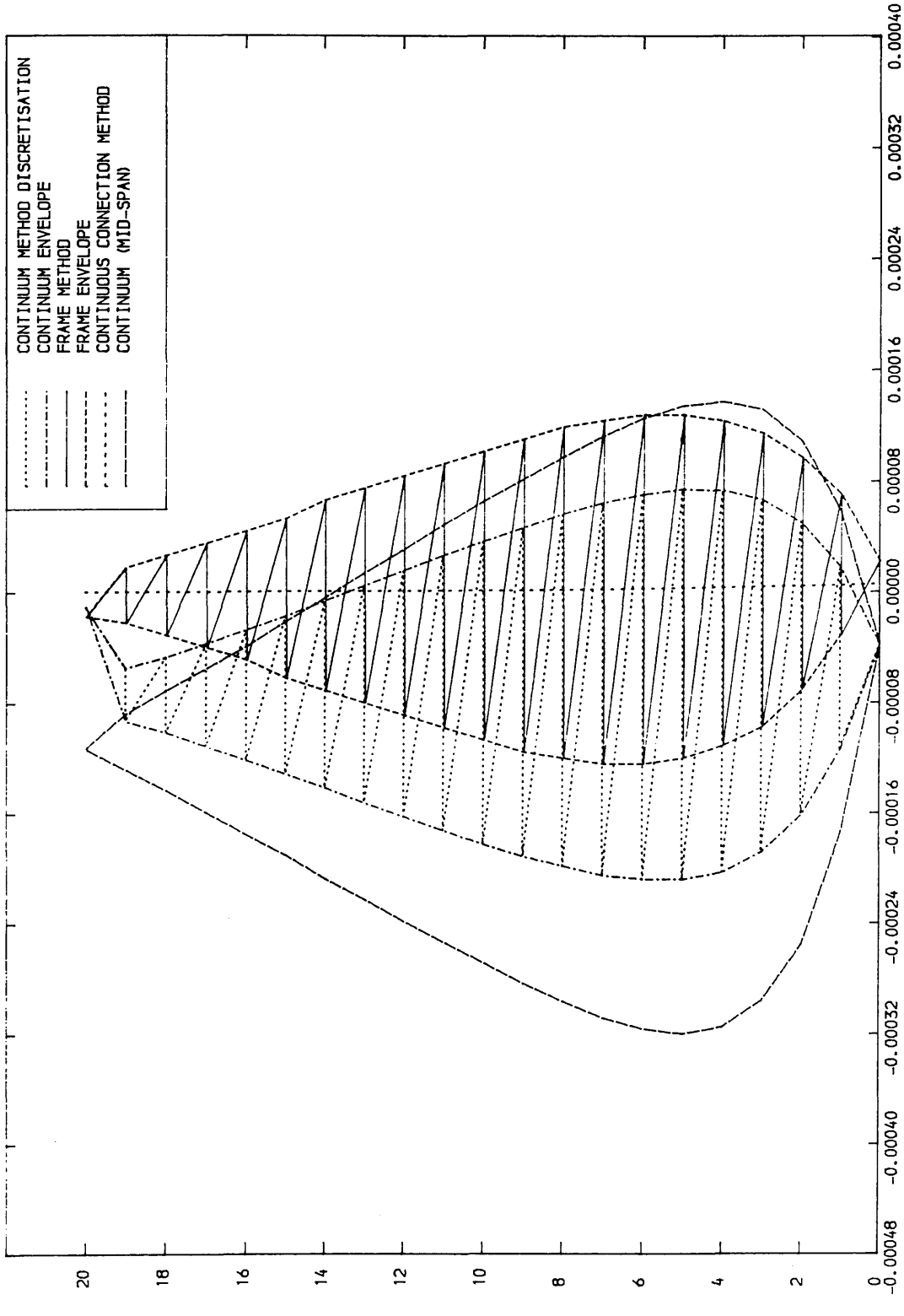

Fig. 3.27. MOMENTS IN WALL2 ($\lambda_1 = d_1 / d_2 = 54$)
Sm = 10.0

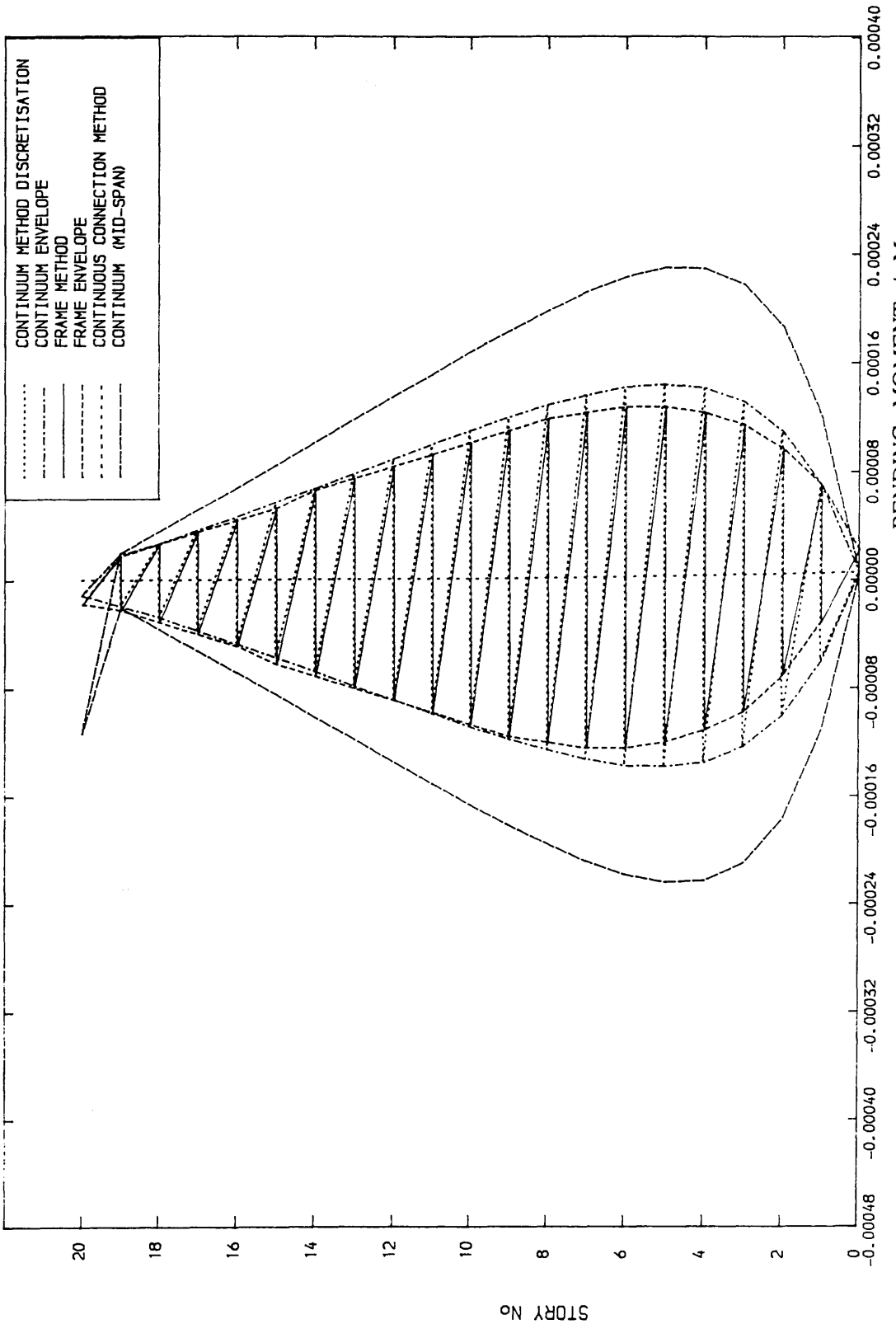

Fig. 3.28. MOMENTS IN WALL2 ($\lambda_1 = d_1 / d_2 = 54$)
Sm = 10.0, ALTERNATIVE CALCULATION

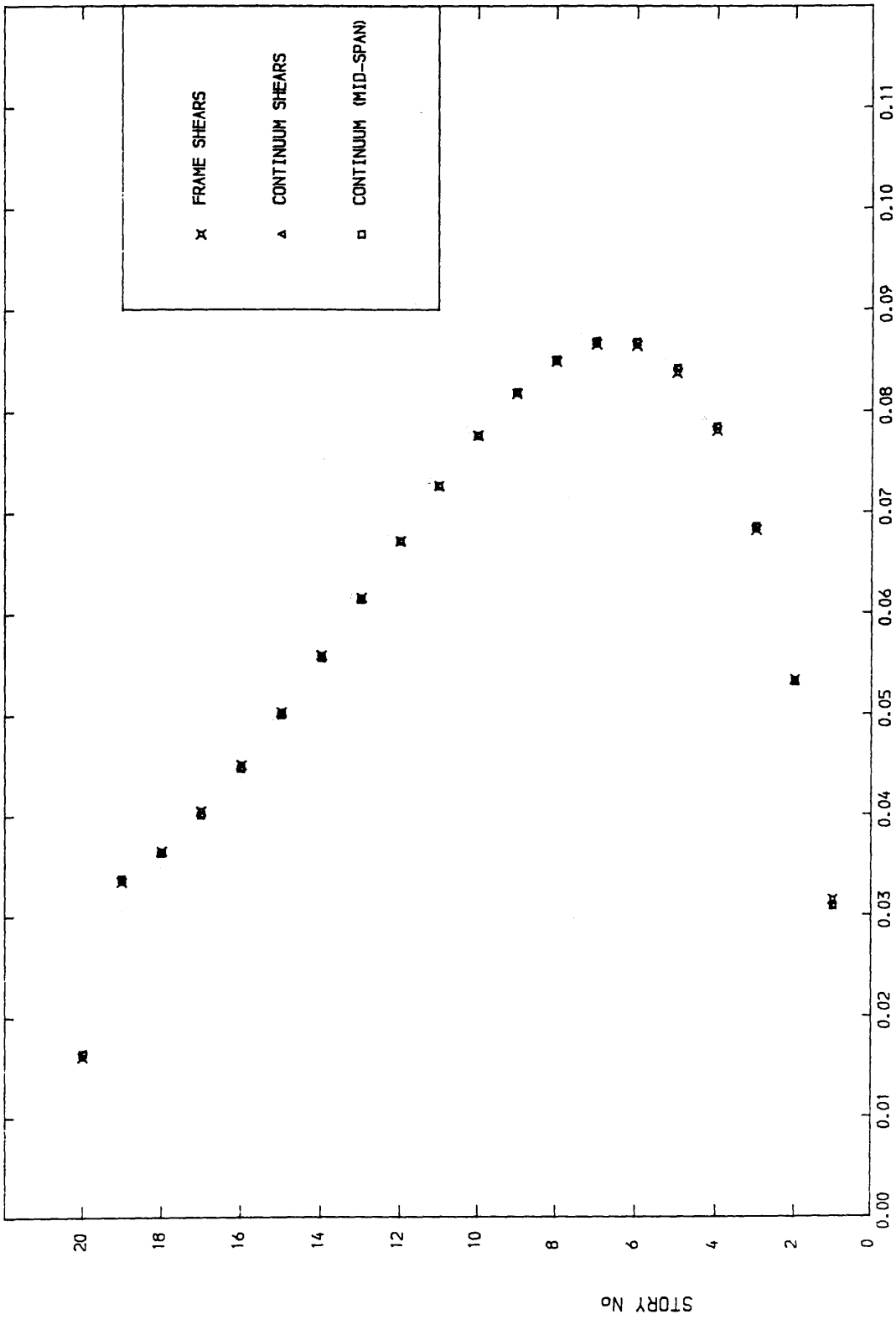

Fig. 3.29. SHEARS IN BEAMS ($\lambda_1 = d_1 / d_2 = 3$)
$S_m = 0.5$

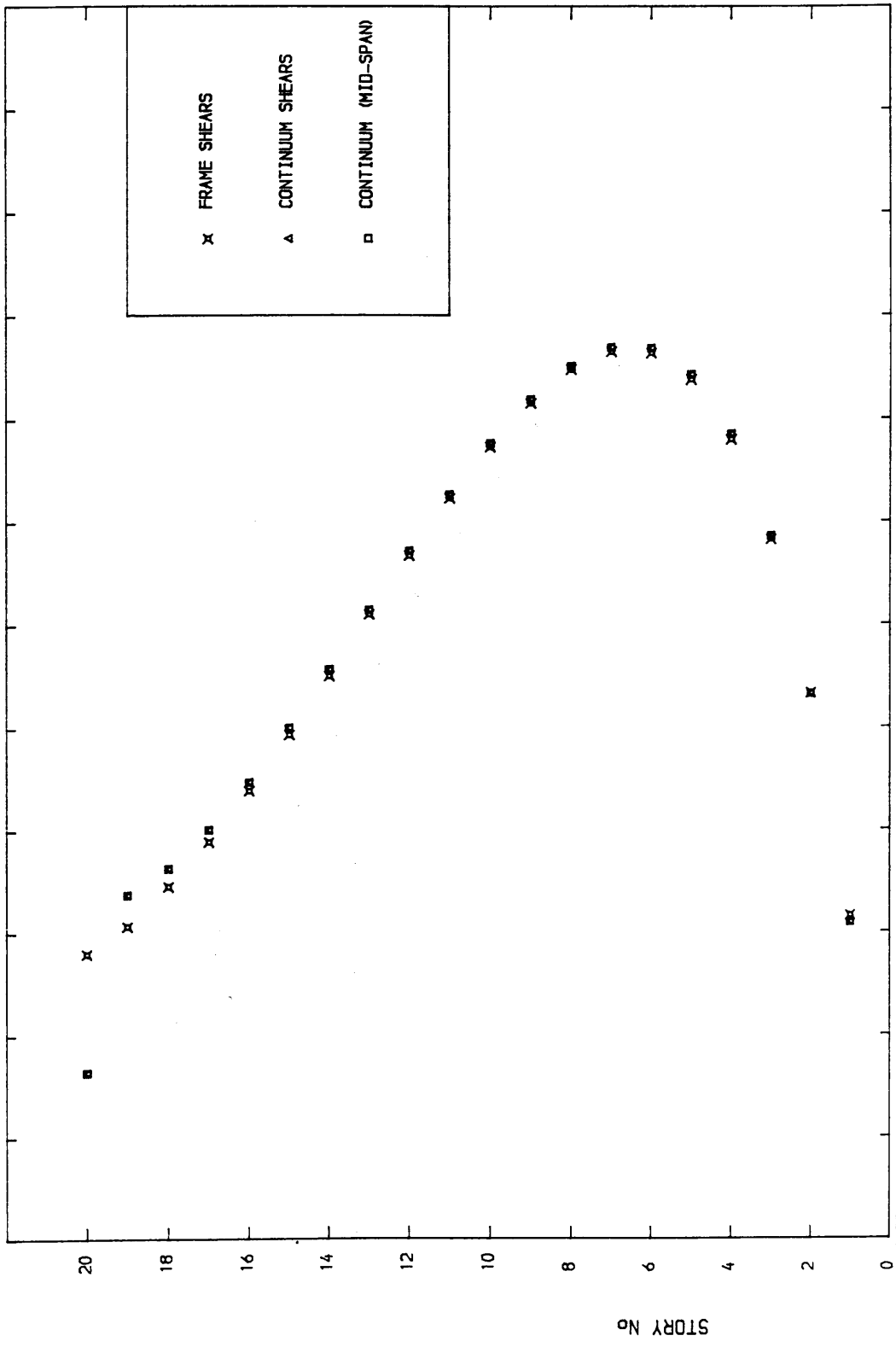

Fig. 3.30. SHEARS IN BEAMS ($\lambda_1 = d_1 / d_2 = 3$)
Sm = 1.0

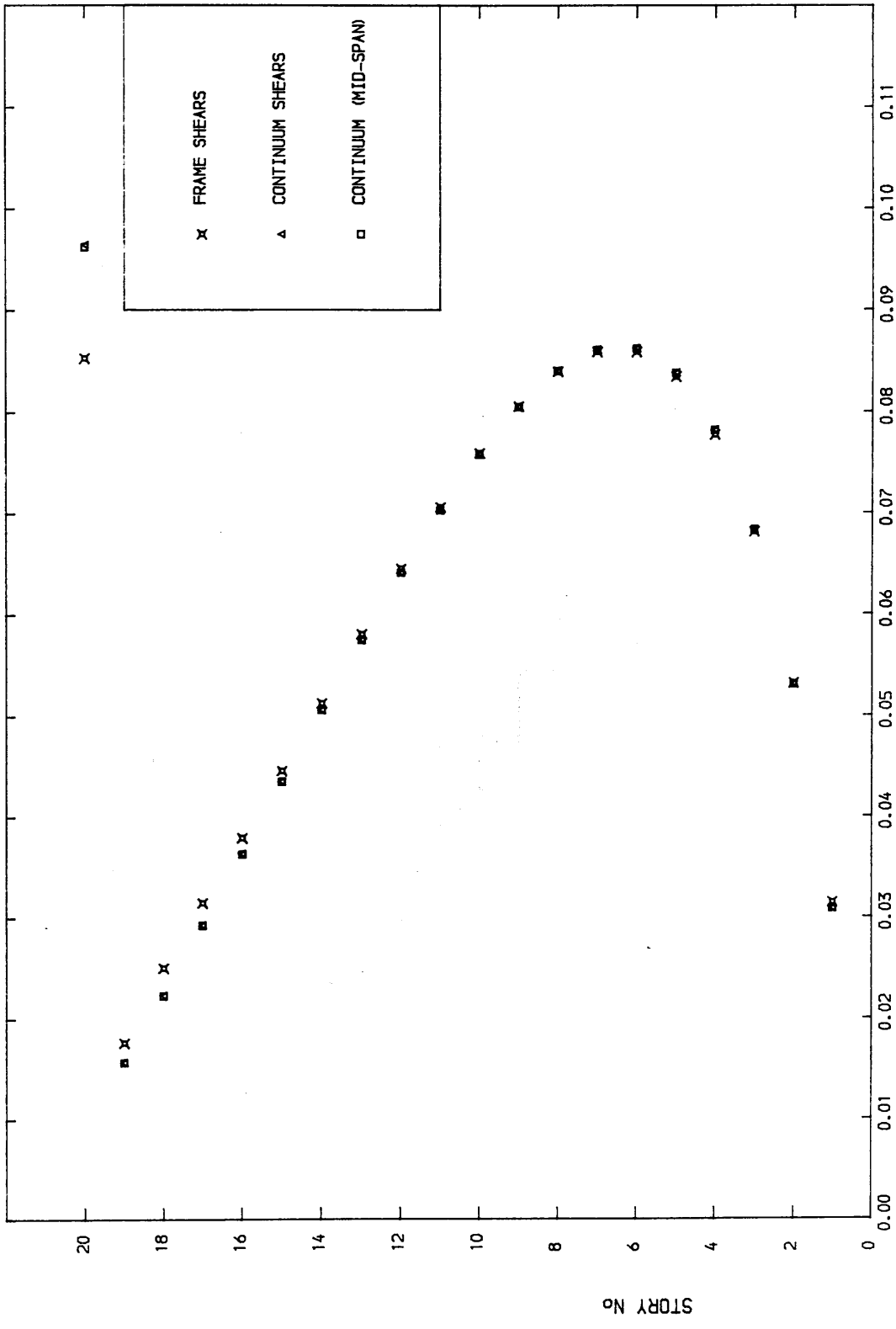

Fig. 3.31. SHEARS IN BEAMS ($\lambda_1 = d_1 / d_2 = 3$)
Sm = 10.0

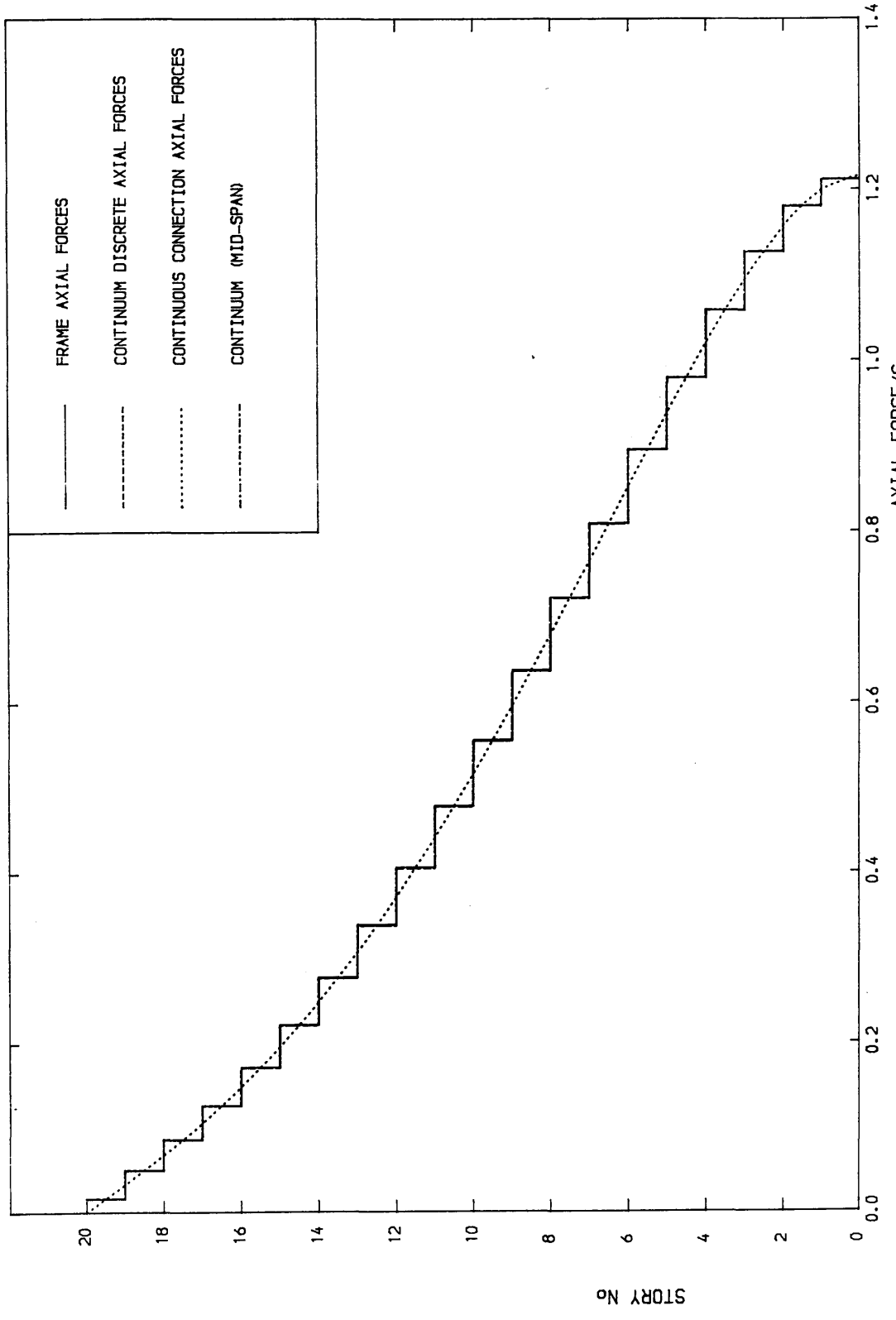

Fig. 3.32. AXIAL FORCES IN WALLS ($\lambda_1 = d_1 / d_2 = 3$)
$Sm = 0.5$

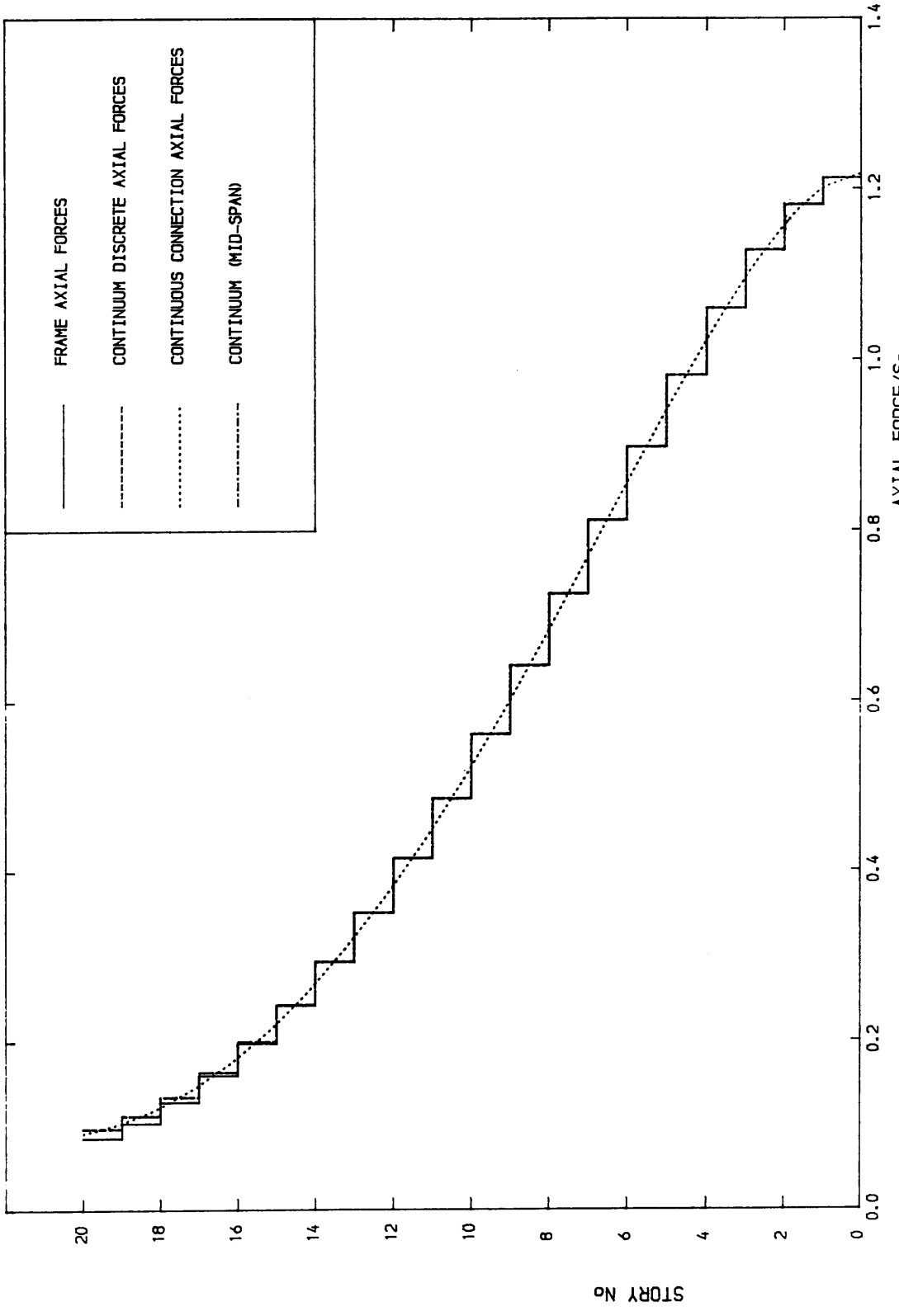

Fig. 3.33. AXIAL FORCES IN WALLS ($\lambda_1 = d_1 / d_2 = 3$)
Sm = 10.0

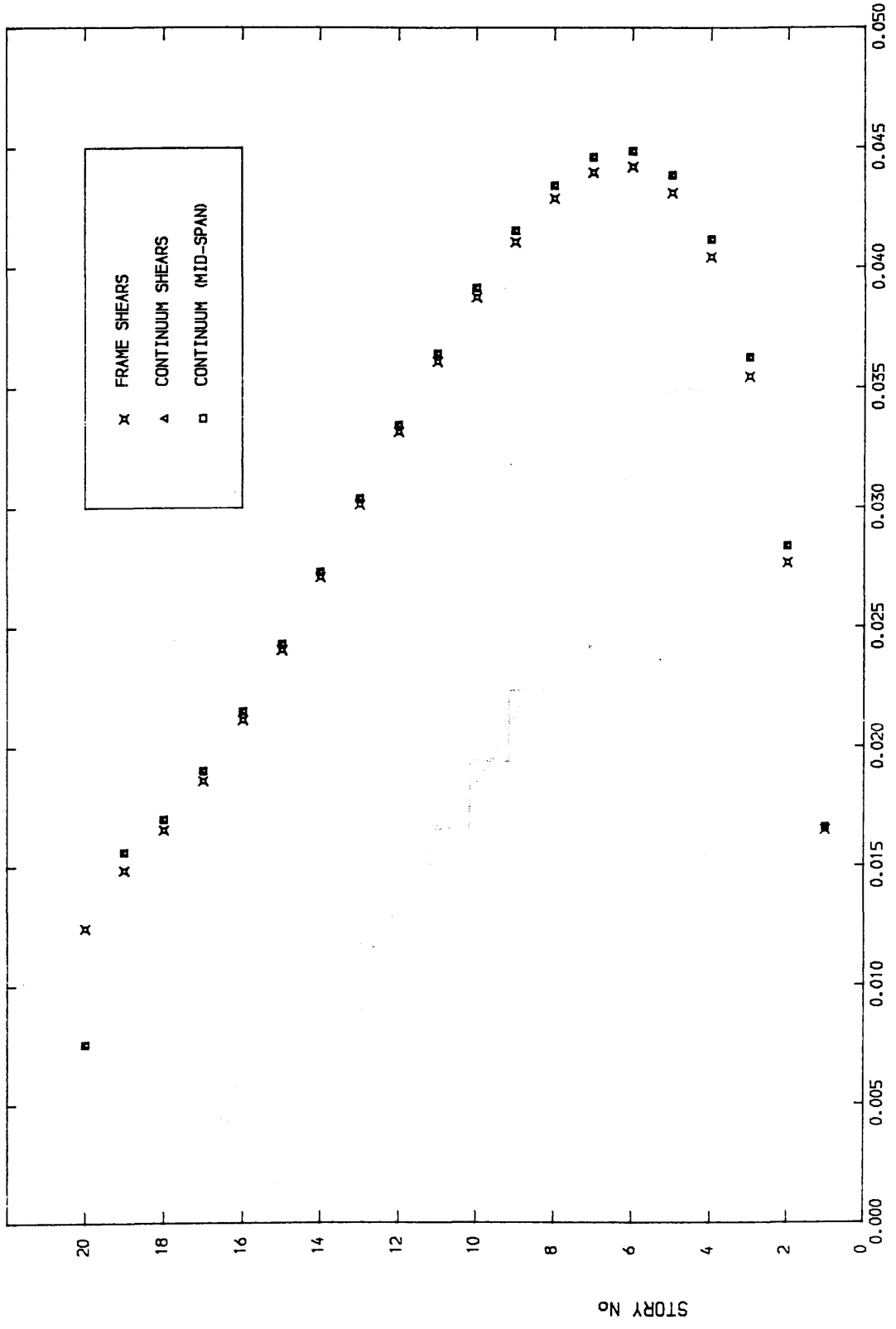

Fig. 3.34. SHEARS IN BEAMS ($\lambda_1 = d_1 / d_2 = 10$)
Sm = 1.0

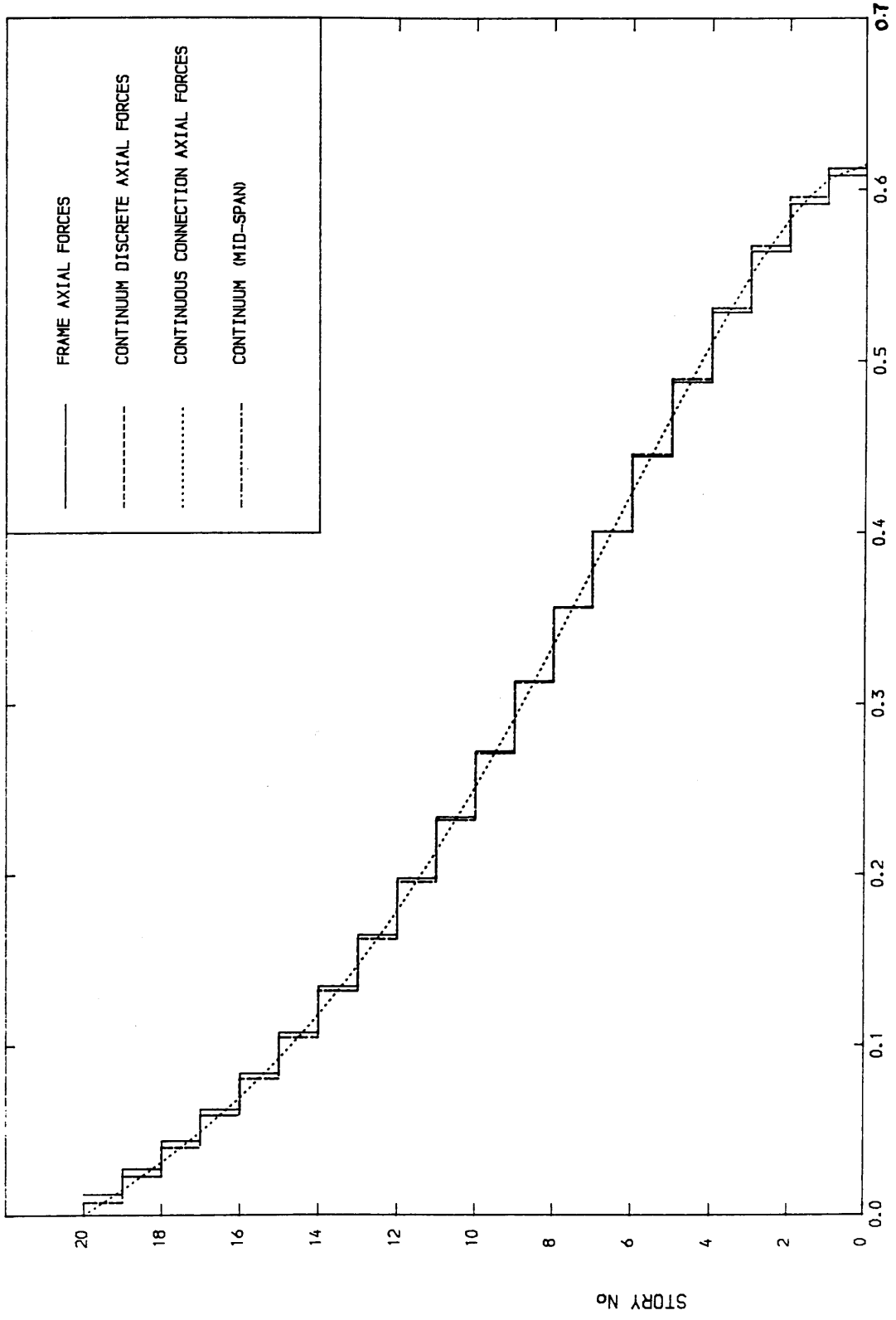

Fig. 3.35. AXIAL FORCES IN WALLS ($\lambda_1 = d_1/d_2 = 10$)
Sm = 1.0

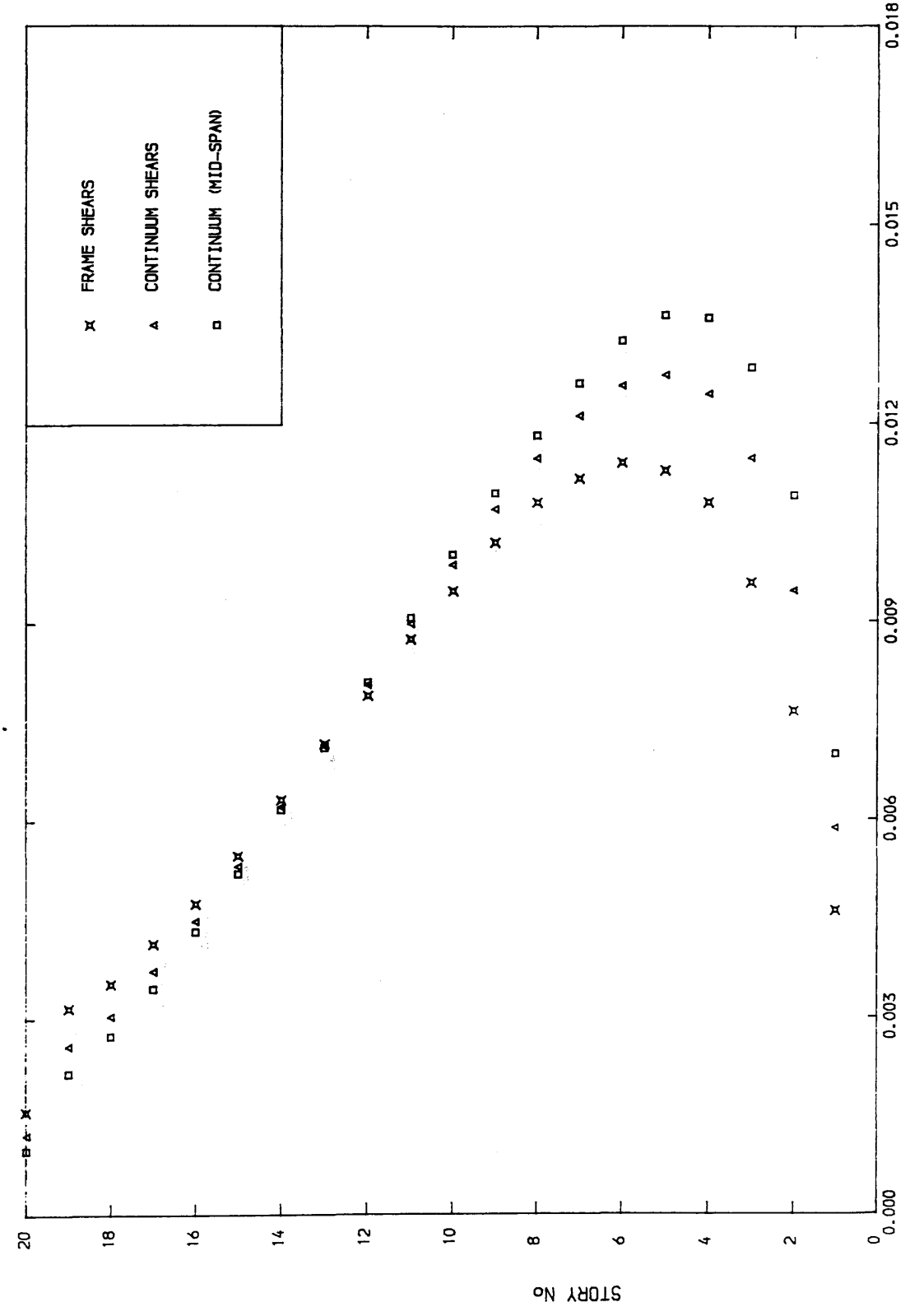

Fig. 3.36. SHEARS IN BEAMS ($\lambda_1 = d_1 / d_2 = 54$)
$S_m = 0.5$

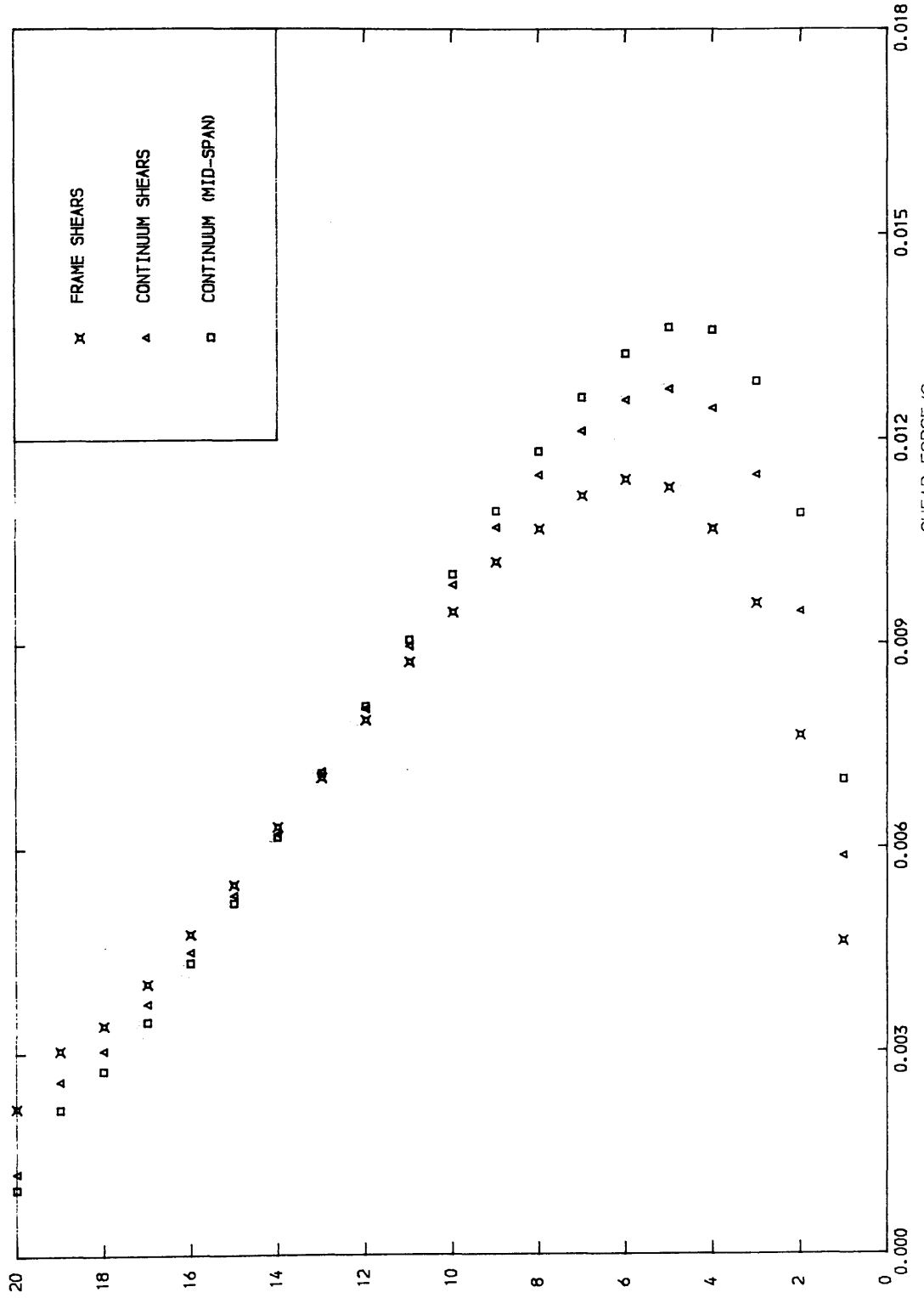

Fig. 3.37. SHEARS IN BEAMS ($\lambda_1 = d_1 / d_2 = 54$)
Sm = 1.0

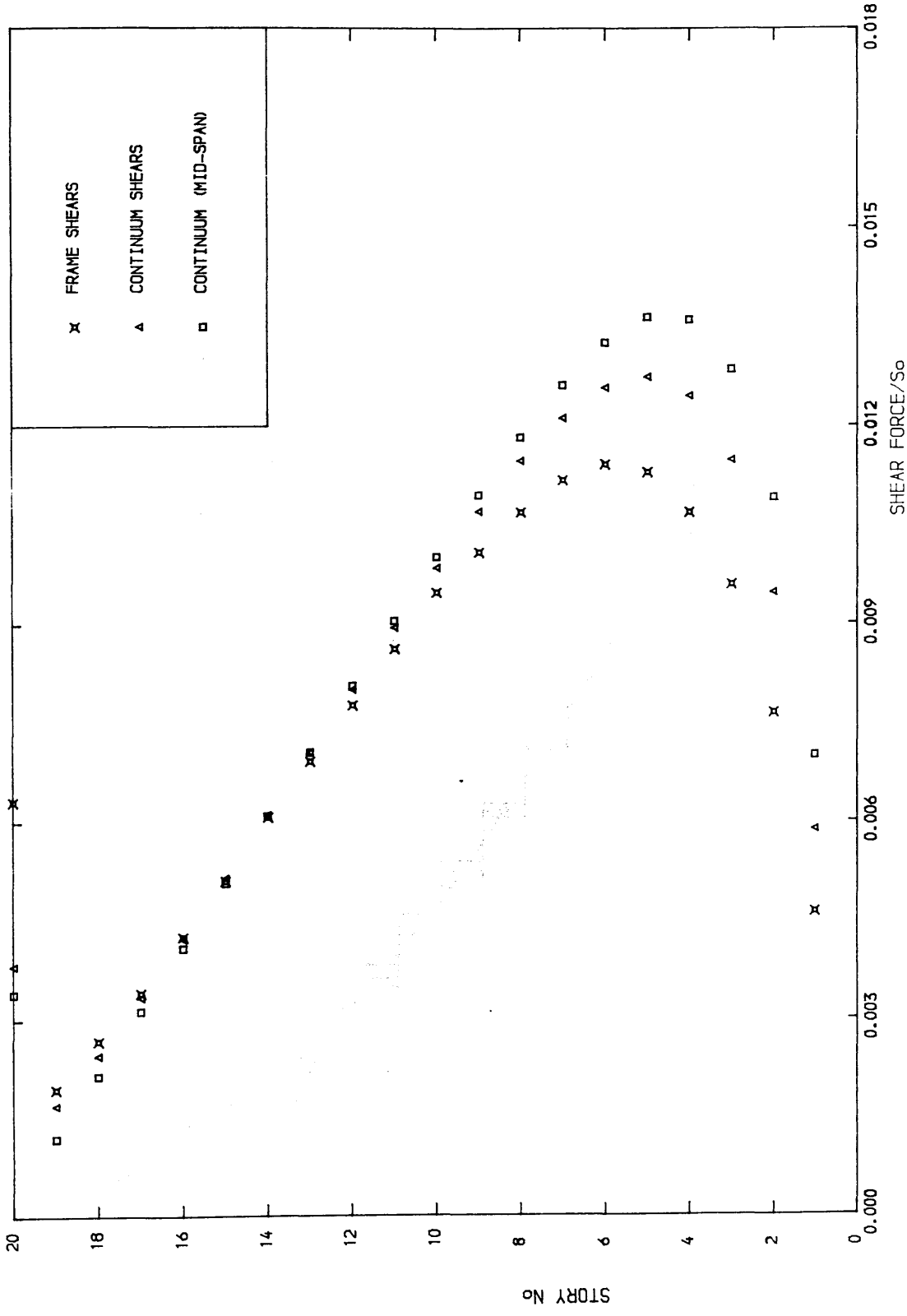

Fig. 3.38. SHEARS IN BEAMS ($\lambda_1 = d_1 / d_2 = 5.1$)
Sm = 10.0

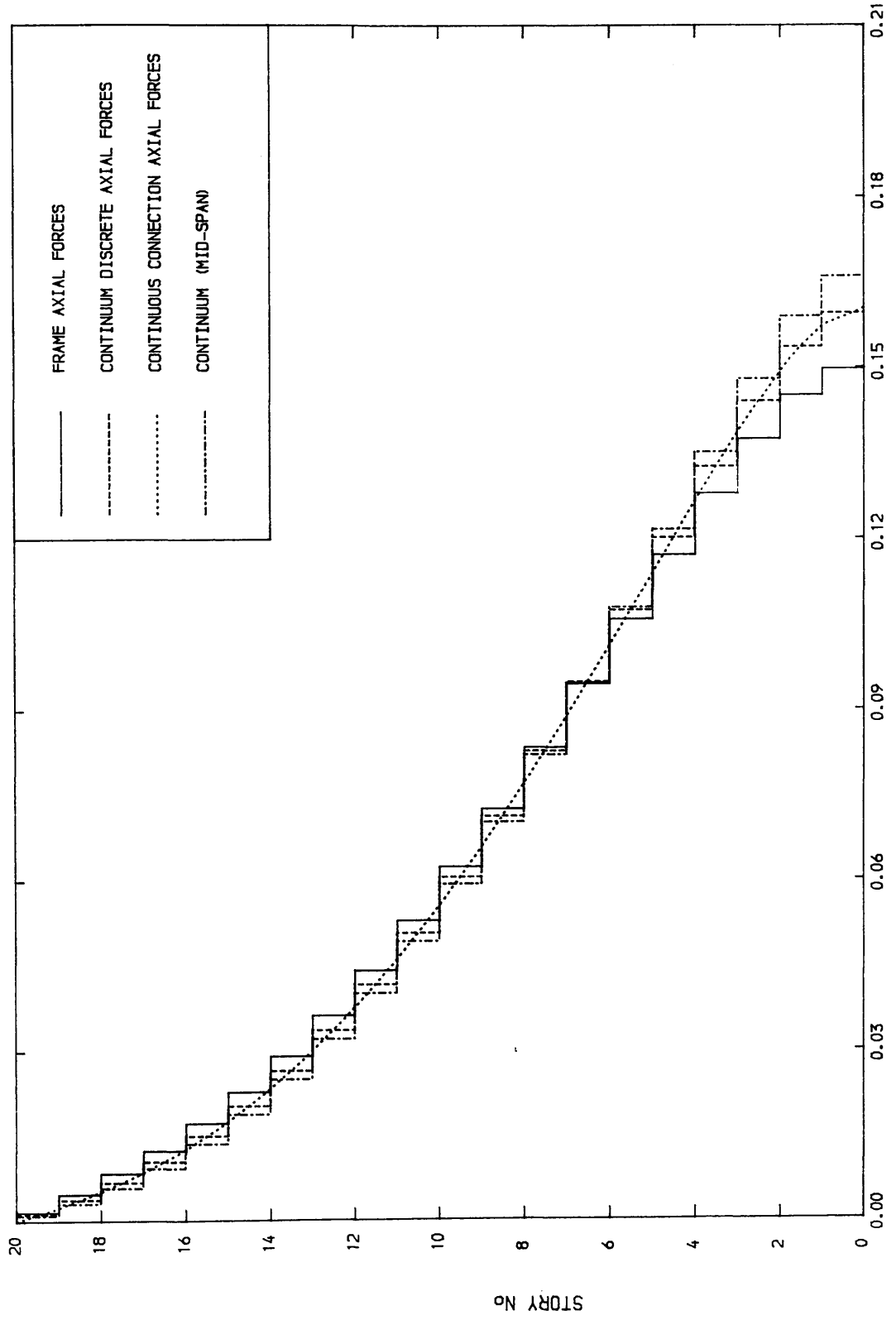

Fig. 3.39. AXIAL FORCES IN WALLS ($\lambda_1 = d_1 / d_2 = 54$)
Sm = 0.5

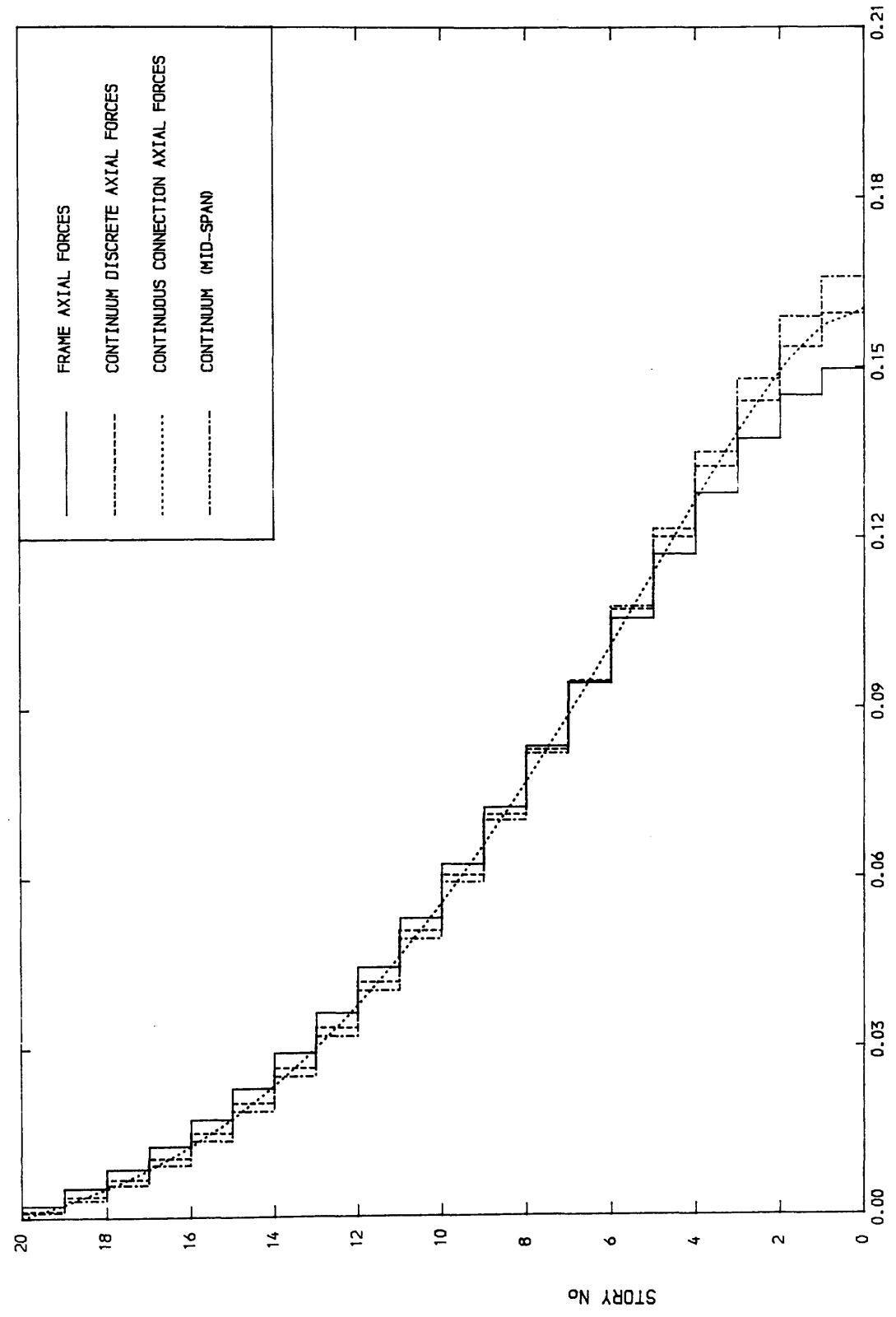

Fig. 3.40. AXIAL FORCES IN WALLS ($\lambda_1 = d_1 / d_2 = 54$)
Sm = 1.0

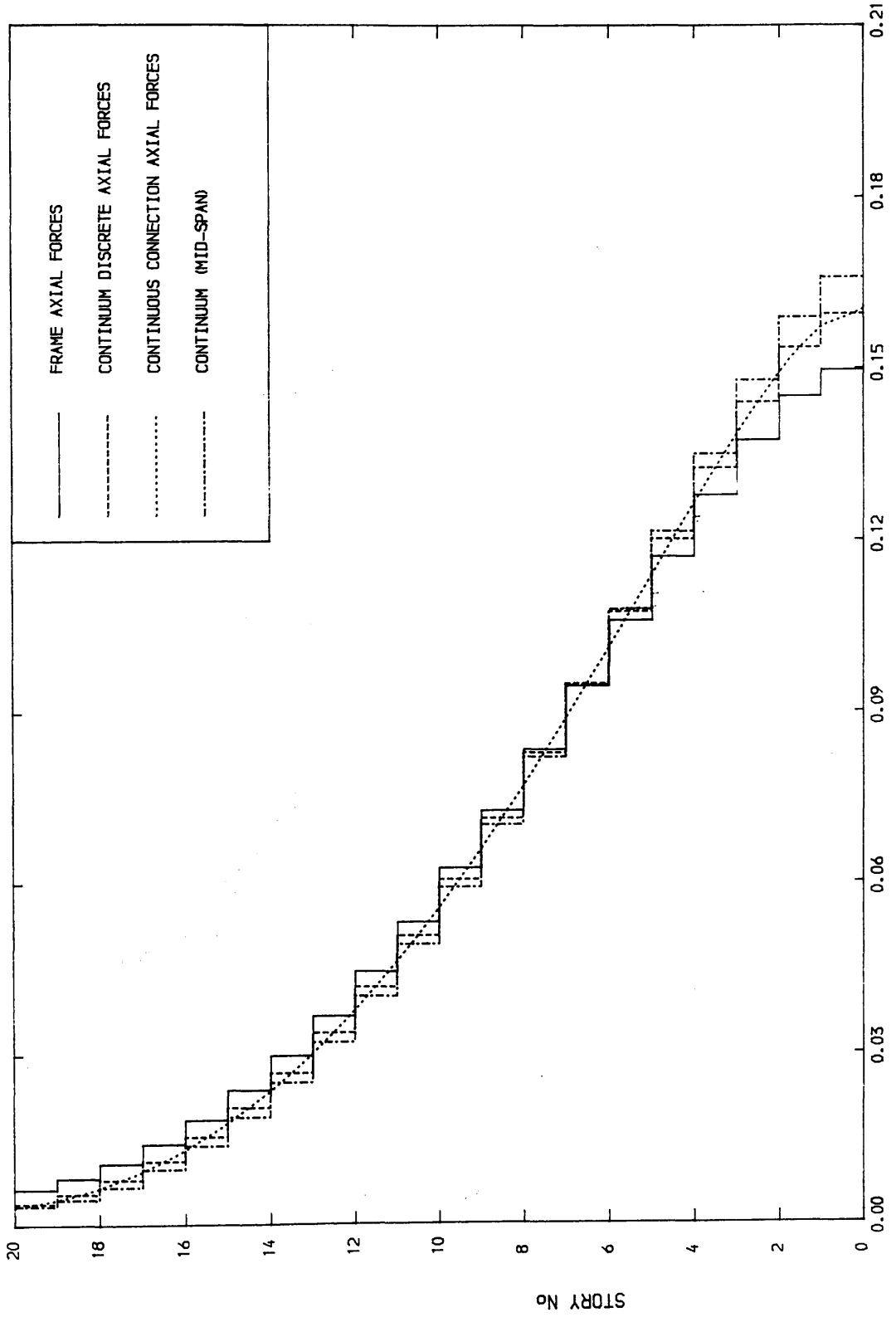

Fig. 3.41. AXIAL FORCES IN WALLS ($\lambda_1 = d_1 / d_2 = 54$)
Sm = 10.0

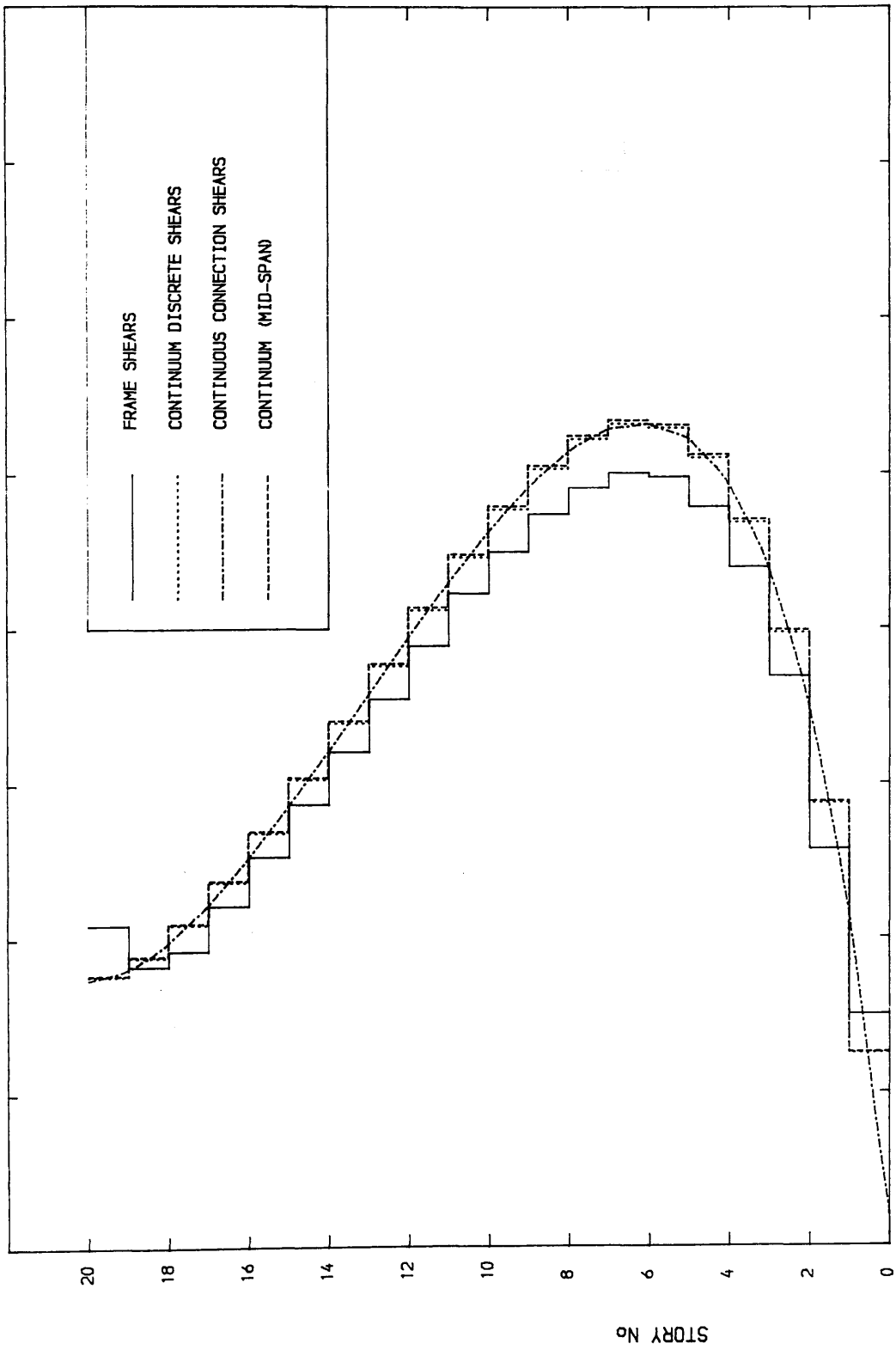

Fig. 3.42. SHEARS IN WALL2 ($\lambda_1 = d_1 / d_2 = 10$)
Sm = 1.0

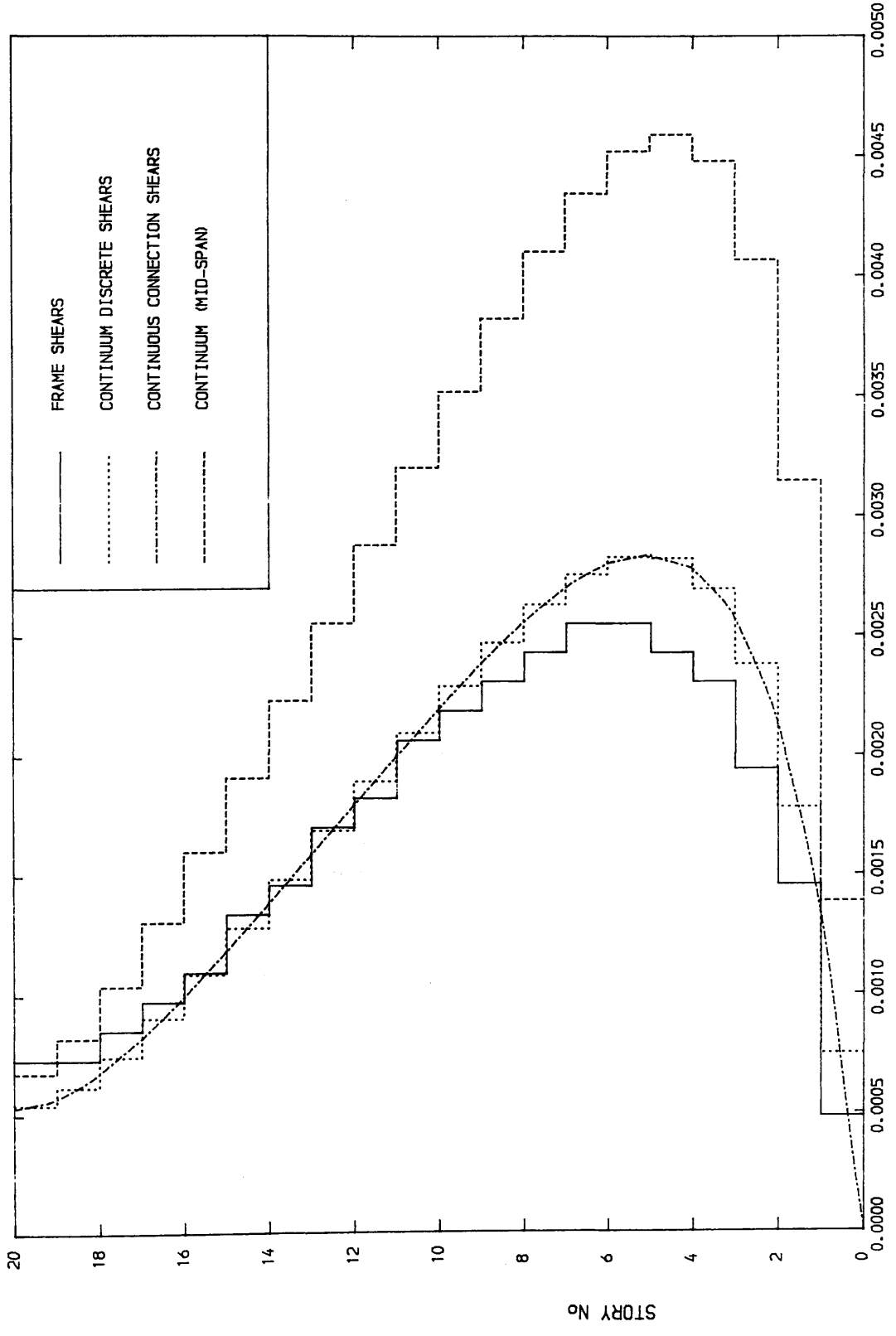

Fig. 3.43. SHEARS IN WALL2 ($\lambda_1 = d_1 / d_2 = 54$)
Sm = 1.0

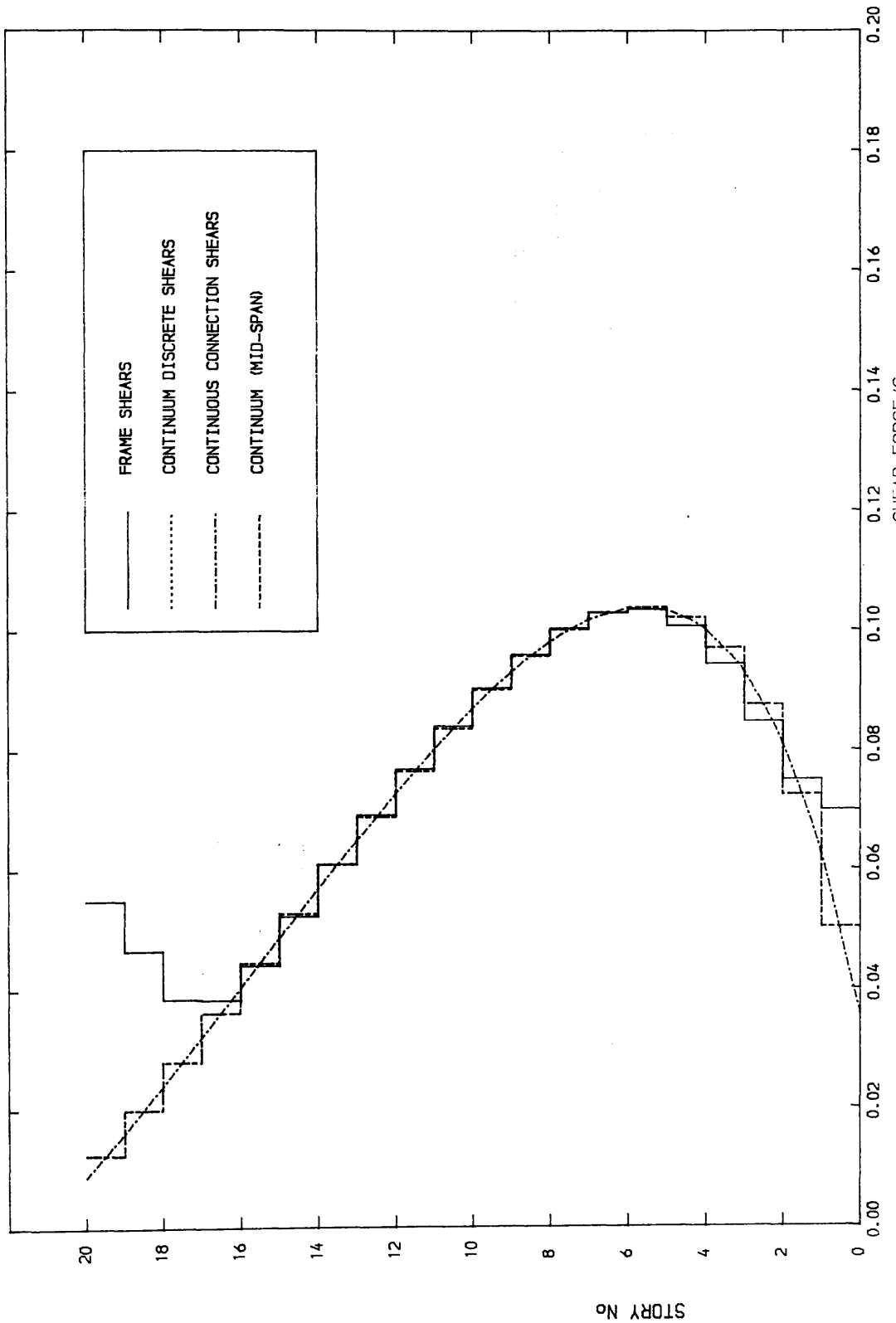

Fig. 3.44. SHEARS IN WALL2 ($\lambda_1 = d_1/d_2 = 3$)

Sm = 10.0

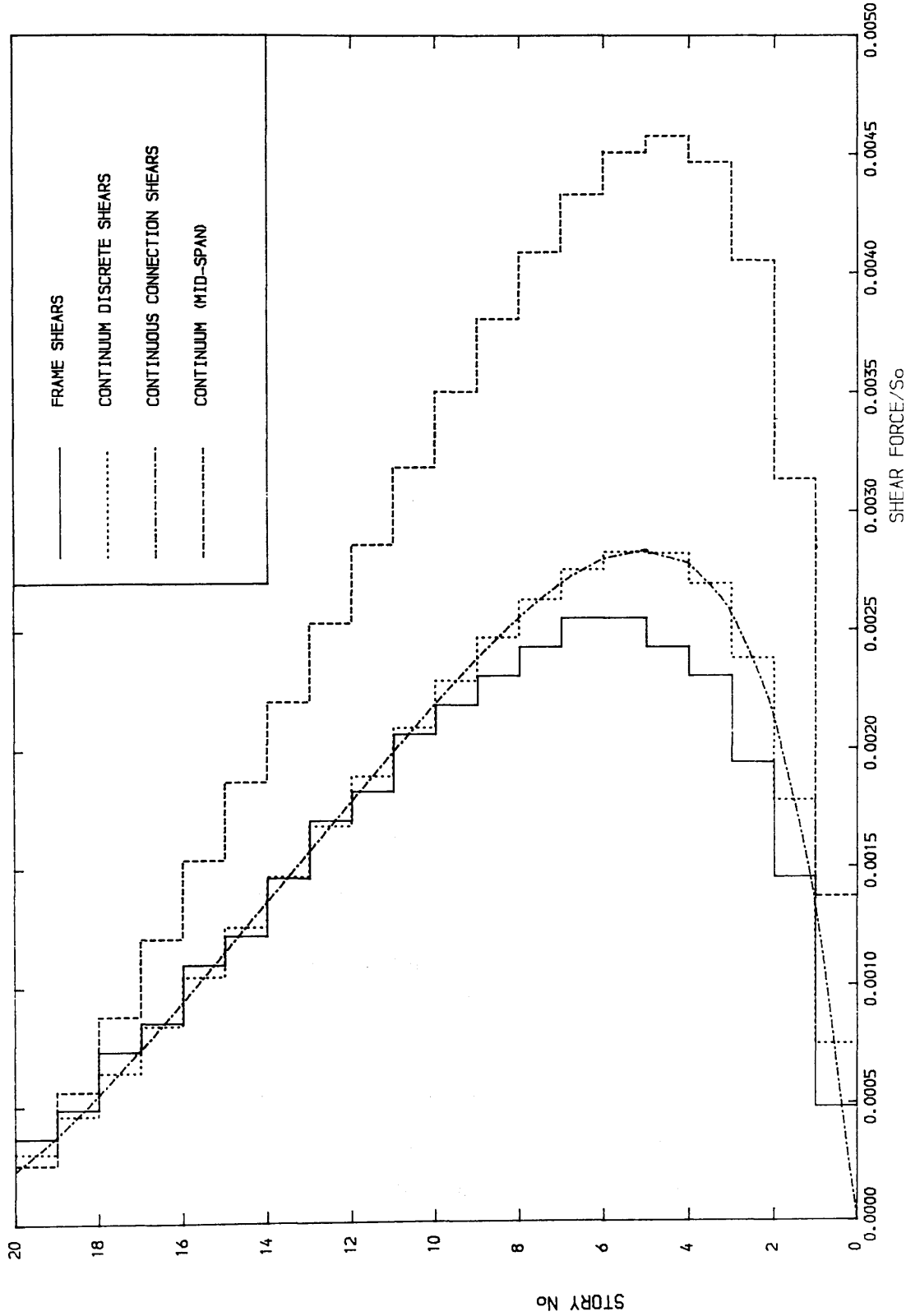

Fig. 3.45. SHEARS IN WALL2 ($\lambda_1 = d_1 / d_2 = 54$)

Sm = 10.0

CHAPTER FOUR

EFFECT OF TWO STIFFENING BEAMS ON COUPLED SHEAR WALLS

4. 1 Introduction

In a residential building, the depth of a lintel beam connecting two coupled shear walls will usually be limited by the difference between the floor to floor height and the floor clear height; hence the lintel beams cannot be very stiff and the coupling effect of the lintel beams on shear walls may not be able to provide the required lateral stiffness. This can be overcome by introducing additional stiffening beams at one or more levels along the height of the structure, which will enhance the coupling effect of the normal lintel beams. Nearly all papers published on the behaviour of coupled shear walls assume that the lintel beams connecting the walls are taken to be of uniform section.

This chapter describes the general continuum analysis of coupled shear walls, on rigid or flexible foundations, with one or two stiffening beams. The influence of the rigidities of the stiffening beams and their locations on the internal forces and lateral deflections of the structure are also investigated.

4. 2 Analysis of forces in the continuous medium

Consider a coupled shear wall system with two stiffening beams 1 and 2 at levels x_1, and x_2 ($x_1 > x_2$) respectively between two walls resting on a flexible foundation. As shown in Fig. 4.1 (a), the continuum structure is divided into 3 zones. Let i denote the zone numbers (i = 1, 2, 3), from top to bottom delimited by the top of the structure, the stiffening beams and the base and s denotes the stiff beam number (s = 1, 2). The structure is

assumed to be subjected to the same three kinds of typical lateral loads as before, namely a uniformly distributed load of intensity w, an upper triangularly distributed load of intensity w_1 at the top, and a concentrated load P acting at the top of the structure.

In addition to the assumptions made in chapter 2, the following further assumptions are also made

(1) To form the continuous model, it is necessary to assume that part of the flexural rigidity and cross sectional area of the discrete stiffening beams is smeared over half a storey height above and below the level concerned. The remaining flexural rigidities I_{ns} and cross sectional areas A_{ns} are assumed to act at the discrete levels (Fig. 4.1 (b)). I_{ns} and A_{ns} are related to the true inertias I_{fs} and cross sectional areas A_{bs} by the relations,

$$I_{ns} = I_{fs} - I_b$$

and

$$A_{ns} = A_{bs} - A_b$$

(2) The stiffening beams are assumed to deform with a different point of contraflexure at distance Δ_s from the mid-span position of the stiffening beams towards the less stiff wall. The value of the distance Δ_s will be considered later.

(3) A shear force $(V_m)_s$, and as will be shown, later, a bending moment $(M_d)_s$, is assumed to exist in each stiffening beam s at the cut position Δ from the centre line of the lamina towards the less stiff wall. (Fig. 4.2 (b)).

For the three types of loading considered, the external moment, M_e is given by equation (2.1)

The moment-curvature relationship for each wall is

$$EI_1 \frac{d^2y_i}{dx^2} = (M_1)_i = M_e - (M_{t1})_i - (M_A)_i \quad \ldots\ldots\ldots\ldots\ldots \quad (4.1)$$

$$EI_2 \frac{d^2y_i}{dx^2} = (M_2)_i = -(M_{t2})i + (M_A)_i \quad \ldots\ldots\ldots\ldots\ldots \quad (4.2)$$

where M_{t1} and M_{t2} are the moments due to shear forces in the continuous medium, given by

$$(M_{t1})_1 = (L_1+\Delta)T_1 + M_p \quad , \qquad (M_{t2})_1 = (L_2-\Delta)T_1 - M_p$$

$$(M_{t1})_2 = (L_1+\Delta)T_2 + (M_d)_1 + M_p, \quad (M_{t2})_2 = (L_2-\Delta)T_2 - (M_d)_2 - M_p$$

$$(M_{t1})_3 = (L_1+\Delta)T_3 + (M_d)_1 + (M_d)_2 + M_p$$

$$(M_{t2})_3 = (L_2-\Delta)T_3 - (M_d)_1 - (M_d)_2 - M_p$$

where

$$T_1 = \int_x^H q_1 \, dx$$

$$T_2 = \int_{x_1}^H q_1 \, dx + (V_m)_1 + \int_x^{x_1} q_2 \, dx \quad \ldots\ldots\ldots\ldots\ldots\ldots \quad (4.3)$$

$$T_3 = \int_{x_1}^H q_1 \, dx + (V_m)_1 + \int_{x_2}^{x_1} q_2 \, dx + (V_m)_2 + \int_x^{x_2} q_3 \, dx$$

and

$$(M_d)_s = (V_m)_s \, (\Delta_s - \Delta) \qquad (s = 1, 2)$$

in which Δ_s is the shift in the point of contraflexure in the stiffening beam s from the mid-span position towards the less stiff wall, and $(V_m)_s$ is the concentrated shear force in the stiffening beam s

The moment, M_A due to the axial forces n in the connecting medium is given by,

$$(M_A)_1 = \int_x^H n_1(\lambda)\ (\lambda-x)\ d\lambda + Q_t\ (H-x)$$

$$(M_A)_2 = \int_{x_1}^H n_1(\lambda)\ (\lambda-x)\ d\lambda + \int_x^{x_1} n_2(\lambda)\ (\lambda-x)\ d\lambda + Q_t\ (H-x) \quad .. \quad (4.4)$$

$$= (M_A)_1\ (x_1) + Q_t\ (x_1-x) + \int_x^{x_1} n_2(\lambda)\ (\lambda-x)\ d\lambda$$

$$(M_A)_3 = \int_{x_1}^H n_1(\lambda)\ (\lambda-x)\ d\lambda + \int_{x_2}^{x_1} n_2(\lambda)\ (\lambda-x)\ d\lambda +$$

$$\int_x^{x_2} n_3(\lambda)\ (\lambda-x)\ d\lambda + Q_t\ (H-x)$$

$$= (M_A)_2\ (x_2) + Q_t\ (x_2-x) + \int_x^{x_2} n_3(\lambda)\ (\lambda-x)\ d\lambda$$

in which λ, is a dummy variable of integration, and Q_t is the top concentrated interactive force given by equation (2.23).

The addition of equations (4.1) and (4.2) yields the overall moment– curvature relationships for the three zones,

$$EI\ \frac{d^2y_i}{dx^2} = (M_t)_i = M_e - L\ T_i \quad \ldots\ldots\ldots\ldots\ldots\ldots\ldots \quad (4.5)$$

Since the curvatures in the two walls are equal at all levels, it follows from equation (4.5) that

$$(M_1)_i = \frac{I_1}{I} (M_e - T_i.L)$$

$$(M_2)_i = \frac{I_2}{I} (M_e - T_i.L) \quad \ldots\ldots\ldots\ldots\ldots\ldots \quad (4.6)$$

where M_1 and M_2 are the bending moments in walls 1 and 2 respectively

and $I = I_1 + I_2$

From equations (4.1) and (4.2),

$$(M_A)_i = \frac{I_2}{I} M_e + \frac{I_1}{I} L\, T_i - (M_{t_1})_i \quad \ldots\ldots\ldots\ldots\ldots\ldots \quad (4.7)$$

and hence, from equations (4.4)

$$n_i = \frac{d^2(M_A)_i}{dx^2} = \frac{I_2}{I} \frac{d^2M_e}{dx^2} + \left(\frac{I_1}{I} L - \Delta - L_1\right) \frac{d^2T_i}{dx^2} \quad \ldots\ldots\ldots \quad (4.8)$$

where

$$\frac{d^2M_e}{dx^2} = \frac{1}{H} (U + 2W.\xi) \quad \ldots\ldots\ldots\ldots\ldots\ldots\ldots\ldots\ldots\ldots \quad (4.9)$$

Following the same procedure as, in chapter 2, the expressions of the shears in the walls will be given by,

$$(S_1)_i = \left(\frac{I_1}{I} L - \Delta - L_1\right) \frac{dT_i}{dx} - \frac{I_1}{I} \frac{dM_e}{dx}$$

$$(S_2)_i = \left(\frac{I_2}{I} L + \Delta - L_2\right) \frac{dT_i}{dx} - \frac{I_2}{I} \frac{dM_e}{dx} \quad \ldots\ldots\ldots\ldots \quad (4.10)$$

For the two walls, the percentage of composite cantilever action and the

percentage of individual cantilever action will be respectively given by,

$$(K_2)_i = 100 \frac{\alpha^2}{\beta^2} \frac{T_i}{M_e} \quad \ldots\ldots\ldots\ldots\ldots\ldots\ldots\ldots\ldots\ldots \quad (4.11)$$

and

$$(K_1)_i = 100 - (K_2)_i \quad \ldots\ldots\ldots\ldots\ldots\ldots\ldots\ldots\ldots\ldots \quad (4.12)$$

The compatibility of the vertical displacements in the three zones requires that

$$L \frac{dy_1}{dx} - \frac{hb^3}{12EI_d} q_1 - \frac{1}{E} \left(\frac{1}{A_1} + \frac{1}{A_2} \right) \left[\int_{x_1}^{x} T_1 \, dx + \int_{x_2}^{x_1} T_2 \, dx + \int_{0}^{x_2} T_3 \, dx \right] - \delta = 0 \quad .. \quad (4.13)$$

$$L \frac{dy_2}{dx} - \frac{hb^3}{12EI_d} q_2 - \frac{1}{E} \left(\frac{1}{A_1} + \frac{1}{A_2} \right) \left[\int_{x_2}^{x} T_2 \, dx + \int_{0}^{x_2} T_3 \, dx \right] - \delta = 0 \quad . \quad (4.14)$$

$$L \frac{dy_3}{dx} - \frac{hb^3}{12EI_d} q_3 - \frac{1}{E} \left(\frac{1}{A_1} + \frac{1}{A_2} \right) \int_{0}^{x} T_3 \, dx - \delta = 0 \quad \ldots\ldots\ldots \quad (4.15)$$

where y_i, q_i and T_i are respectively the lateral deflection, the laminar shear and the axial force in the walls in zone i, A_1 and A_2 are the cross sectional areas of walls 1 and 2 respectively, E is the modulus of elasticity and h is the storey height.

The four successive terms in the compatibility equations again denote the relative displacement at the cut due to bending of the walls, deformation of the laminae due to both bending and shear deformations in the connecting medium, axial deformation of the walls and the relative vertical foundation settlement.

The effect of shearing deformation in the lintel connecting beams may be included by replacing the true second moment of area I_b by the reduced second moment of area I_d, given by equation (2.34)

The compatibility conditions at the point of contraflexure of the stiffening

beams are,

$$L\frac{dy}{dx} - \frac{V_{m1}.b^3}{12E_{m1}I_{m1}} - \frac{1}{E}\left(\frac{1}{A_1}+\frac{1}{A_2}\right)\left[\int_{x_2}^{x_1} T_2\,dx + \int_{0}^{x_2} T_3\,dx\right] - \delta = 0 \quad \ldots\ldots (4.16)$$

$$L\frac{dy}{dx} - \frac{V_{m2}\,b^3}{12E_{m2}I_{m2}} - \frac{1}{E}\left(\frac{1}{A_1}+\frac{1}{A_2}\right)\int_{0}^{x_2} T_3\,dx - \delta = 0 \quad \ldots\ldots\ldots (4.17)$$

where

$$I_{m1} = R_1.I_{n1}$$

$$\ldots\ldots\ldots\ldots\ldots (4.18)$$

$$I_{m2} = R_2.I_{n2}$$

$$R_1 = \left[\,1 - S_{f_1} / (1 + S_{f_1})\,\right].C_{f_1}$$

$$\ldots\ldots\ldots\ldots\ldots (4.19)$$

$$R_2 = \left[\,1 - S_{f_2} / (1 + S_{f_2})\,\right].C_{f_2}$$

$$S_{f_1} = 24f\,\frac{I_{n1}}{A_{n1}}\,\frac{1+\nu}{b^2}\,C_{f_1} \quad (= 2.4\,(D_1/b)^2\,(1+\nu)\,C_{f_1})$$

$$\ldots\ldots\ldots\ldots (4.20)$$

$$S_{f_2} = 24f\,\frac{I_{n2}}{A_{n2}}\,\frac{1+\nu}{b^2}\,C_{f_2} \quad (= 2.4\,(D_2/b)^2\,(1+\nu)\,C_{f_2})$$

The terms in brackets refer to the specific case of a beam of rectangular cross section.

$$C_{f_1} = 1 - \frac{12(\Delta_1/b)^2}{1 + 12(\Delta_1/b)^2}\,, \qquad C_{f_2} = \frac{12(\Delta_2/b)^2}{1 + 12(\Delta_2/b)^2} \quad \ldots\ldots (4.21)$$

By equating corresponding terms of equations (4.13) at $x = x_1$ and $x = x_2$, the shear forces in the stiffening beams will be respectively given by

$$V_{m1} = \gamma_1 H\, q_1(x_1) - \gamma_1 H\, q_2(x_1)$$

$$V_{m2} = \gamma_2 H\, q_2(x_2) = \gamma_2 H\, q_3(x_2) \qquad \ldots\ldots\ldots\ldots\ldots\ldots\ldots\ldots \quad (4.22)$$

where $q_1(x_1)$, $q_2(x_1)$ and $q_2(x_2)$, $q_3(x_2)$ are the laminar shear flows at $x = x_1$ and $x = x_2$ respectively, and γ_1 and γ_2 are the relative flexural rigidities of the stiffening beams given by

$$\gamma_1 = \frac{1}{J}\,\frac{E_{m1} I_{m1}}{EI_d} = \frac{S_{m1}}{J}\,\frac{E_{m1}}{E}\,\frac{R_1}{R_f} = \frac{S_{m1}}{J}\,\frac{E_{m1}}{E}\,\frac{1 + S_f}{1 + S_{f_1}}\,\frac{C_{f_1}}{C_f}$$

$$\gamma_2 = \frac{1}{J}\,\frac{E_{m2} I_{m2}}{EI_d} = \frac{Sm2}{J}\,\frac{E_{m2}}{E}\,\frac{R_2}{R_f} = \frac{S_{m2}}{J}\,\frac{E_{m2}}{E}\,\frac{1 + S_f}{1 + S_{f_2}}\,\frac{C_{f_2}}{C_f} \qquad \ldots\ldots \quad (4.23)$$

in which S_{m1} and S_{m2} are the relative flexural second moments of area of the stiffening beams given by

$$S_{m1} = \frac{I_{n1}}{I_b}$$

$$S_{m2} = \frac{I_{n2}}{I_b} \qquad \ldots\ldots\ldots\ldots\ldots\ldots\ldots \quad (4.24)$$

Differentiating equations (4.13), (4.14) and (4.15) and combining equations (2.4) and (4.5) to eliminate the variables y and q yields the governing differential equations for the axial force T in each zone i,

$$\frac{d^2 T_i}{dx^2} - \alpha^2 T_i = - \beta^2 M_e \qquad \ldots\ldots\ldots\ldots\ldots\ldots\ldots\ldots\ldots\ldots\ldots \quad (4.25)$$

where

$$\beta^2 = \frac{12\ I_d.L}{hb^3 I} \qquad \text{(4.26)}$$

$$\alpha^2 = \beta^2 \frac{I'}{m} \qquad \text{(4.27)}$$

in which

$I' = (I + mL)$, which is the second moment of area of the structure acting as a composite cantilever. (4.28)

$m = \frac{A_1 A_2 L}{A}$, which is the sum of the static moments of area of the walls. .... (4.29)

$A = A_1 + A_2$

The complete solution to equation (4.25) is as follows

$$T_i = B_i.\cosh k\xi + C_i.\sinh k\xi + \frac{\beta^2}{\alpha^2} H \left(M(\xi) + \frac{U + 2W\xi}{k^2} \right) \qquad \text{... (4.30)}$$

where k is the relative flexural rigidity of lintel beams, (αH).

The corresponding expressions for the laminar shear can then be derived by using equation (2.4), and are given in each zone i as follows

$$q_i = - \frac{1}{H} \left[k (B_i.\sinh k\xi + C_i.\cosh k\xi) + \frac{\beta^2}{\alpha^2} H \left(\frac{dMe}{dx} + \frac{2W}{k^2} \right) \right] \qquad \text{... (4.31)}$$

The axial force in the walls and the laminar shear at the base level can be obtained respectively as, at x = 0,

$$T_0 = B_3 + \frac{\beta^2}{\alpha^2} H \left[U \left(\frac{1}{2} + \frac{1}{k^2} \right) + \frac{2}{3} W + P \right] \qquad \text{(4.32)}$$

$$q_0 = -\left[C_3.\alpha - \frac{\beta^2}{\alpha^2} \left\{ U + P + W \left(1 - \frac{2}{k^2} \right) \right\} \right] \quad \ldots\ldots\ldots \quad (4.33)$$

The expression for the axial flow becomes,

$$n_i = \frac{d^2(M_A)_i}{dx^2} = \frac{I_2}{I} \frac{d^2M_e}{dx^2} + \left(\frac{I_1}{I} L - \Delta - L_1 \right) \frac{d^2T_i}{dx^2} \quad \ldots\ldots\ldots \quad (4.34)$$

where

$$\frac{d^2T_i}{dx^2} = -\frac{dq_i}{dx}$$

$$= \frac{1}{H^2} k^2 \left[B_i \cosh k\xi + C_i \sinh k\xi \right] + \frac{\beta^2}{\alpha^2} \frac{1}{H} \left[U + 2W.\xi \right]$$

The values of the integration constants B_1, B_2, B_3, C_1, C_2 and C_3 can be determined by considering the boundary conditions for the problem.

Boundary conditions

(1) At the top of the structure, $x = H$, the axial force in each wall is equal to zero, that is

$$Ta\ (H) = 0 \quad \ldots\ldots\ldots\ldots\ldots\ldots\ldots\ldots\ldots\ldots\ldots\ldots\ldots \quad (4.35)$$

Therefore, equation (4.31) results in

$$B_1 = -C_1 \tanh k + \mu_1 \quad \ldots\ldots\ldots\ldots\ldots\ldots\ldots\ldots\ldots\ldots \quad (4.36)$$

where

$$\mu_1 = -\frac{\beta^2}{\alpha^2} H \frac{(U + 2W)}{k^2 \cosh k}$$

(2) From equations (4.3), the boundary condition for the axial forces of the walls at levels x_1 and x_2 is respectively

$$T_1 (x_1) + V_{m1} = T_2(x_1)$$

$$T_2 (x_2) + V_{m2} = T_3(x_2) \qquad \ldots\ldots\ldots\ldots\ldots\ldots\ldots\ldots\ldots\ldots \quad (4.37)$$

and hence

$$B_1 \mu_{21} + C_1 \mu_{31} = \mu_{41} + B_2.\cosh k\xi_1 + C_2.\sinh k\xi_1$$

$$B_2 \mu_{22} + C_2 \mu_{32} = \mu_{42} + B_3.\cosh k\xi_2 + C_3.\sinh k\xi_2 \qquad \ldots\ldots \quad (4.38)$$

where

$$\mu_{21} = \cosh k\xi_1 - \gamma_1 k.\sinh k\xi_1$$

$$\mu_{22} = \cosh k\xi_2 - \gamma_2 k.\sinh k\xi_2$$

$$\mu_{31} = \sinh k\xi_1 - \gamma_1 k.\cosh k\xi_1$$

$$\mu_{32} = \sinh k\xi_2 - \gamma_2 k.\cosh k\xi_2$$

$$\mu_{41} = -\gamma_1 \frac{\beta^2}{\alpha^2} H \left[U (1-\xi_1) + P + W \left\{ (1 - (\xi_1)^2) - \frac{2}{k^2} \right\} \right]$$

$$\mu_{42} = -\gamma_2 \frac{\beta^2}{\alpha^2} H \left[U (1-\xi_2) + P + W \left\{ (1 - (\xi_2)^2) - \frac{2}{k^2} \right\} \right]$$

where ξ_1 and ξ_2 are the height ratios x_1/H and x_2/H respectively

(3) Equations (4.22) give respectively

$$q_1 (x_1) = q_2 (x_1)$$

$$q_2 (x_2) = q_3 (x_2) \qquad \ldots\ldots\ldots\ldots\ldots\ldots\ldots\ldots\ldots\ldots \quad (4.39)$$

Substituting for x by x_1 and x_2 in equations (4.31) for i = 1 and 2 respectively, the following relationships are obtained, respectively,

$$(B_1 - B_2).\tanh k\xi_1 = C_2 - C_1$$

$$(B_2 - B_3).\tanh k\xi_2 = C_3 - C_2 \quad \ldots\ldots\ldots\ldots\ldots\ldots\ldots\ldots \quad (4.40)$$

(4) Considering the the compatibility equation (4.15) at the base level, x = 0, where the separate wall bases rest on elastic foundations, both vertical and rotational deformations of the separate bases will be considered and the base compatibility equation can be expressed as

$$L\theta - \frac{h\, b^3}{12EI_d} q_0 - \delta = 0 \quad \ldots\ldots\ldots\ldots\ldots\ldots\ldots\ldots \quad (4.41)$$

where the rotation θ and the relative settlement δ of the walls at the foundation are given by

$$\theta = \frac{M_0}{K_r} \quad \ldots\ldots\ldots\ldots\ldots\ldots\ldots\ldots\ldots\ldots\ldots\ldots\ldots\ldots \quad (4.42)$$

$$\delta = \frac{T_0}{K_\delta} \quad \ldots\ldots\ldots\ldots\ldots\ldots\ldots\ldots\ldots\ldots\ldots\ldots\ldots\ldots \quad (4.43)$$

where

$$M_0 = M_{e0} - T_0.L = (M_1)_{3(0)} + (M_2)_{3(0)} \quad \ldots\ldots\ldots\ldots\ldots\ldots \quad (4.44)$$

K_r and K_δ are the rotational and translational elastic stiffnes of the soil foundation as defined in chapter 2 and M_{e0} is the moment at the base level due to external load.

Substituting equations (4.42) and (4.43) into equation (4.41) and using equation (4.44) yields

$$\lambda r/L\ Me_0 - q_0 - \mu_f\ T_0 = 0 \quad \ldots\ldots\ldots\ldots\ldots\ldots\ldots\ldots \quad (4.45)$$

in which

$$\mu_f = \lambda_\delta + \lambda_r = \frac{\beta^2 EI}{L}\left[\frac{L^2}{K_r} + \frac{1}{K_\delta}\right] = \frac{12\,EI_d}{hb^3}\left[\frac{L^2}{K_r} + \frac{1}{K_\delta}\right]$$

$$\lambda_\delta = \frac{\beta^2 EI}{L}\,\frac{1}{K_\delta} = \frac{12\,EI_d}{K_\delta\, hb^3}$$

$$\lambda_r = \frac{\beta^2 EI\, L}{K_r} = \frac{12\,EI_d\, L^2}{K_r\, hb^3}$$

and λ_δ and λ_r can be interpreted as the settlement and rotation flexibility of the soil foundations.

Substituting equations (4.32) and (4.33) into equation (4.45) and simplifying yields

$$C_3 = H/k\,[\,B_3.\mu_f - \mu_5\,] \qquad \ldots\ldots (4.46)$$

where

$$\mu_5 = -\frac{\beta^2}{\alpha^2}\left[U+P+W\left(1-\frac{2}{k^2}\right) + \mu_f H\left(M(0)+\frac{U}{k^2}\right)\right]+\frac{\lambda_r}{L} H M(0)$$

The solutions of the simultaneous equations (4.36), (4.38), (4.40) and (4.46) give the expressions of the integration constants as follows

$$B_1 = -C_1.\tanh k + \mu_1$$

$$C_1 = \frac{C_2 - \mu_1.\tanh k\xi_1 + B_2.\tanh k\xi_1}{\varepsilon_1}$$

$$B_2 = \frac{\varepsilon_1(\mu_1\mu_{21} - \mu_{41}) + \varepsilon_2.\mu_1.\tanh k\xi_1 - C_2(\varepsilon_1.\sinh k\xi_1 + \varepsilon_2)}{\varepsilon_1.\cosh k\xi_1 + \varepsilon_2.\tanh k\xi_1}$$

$$\ldots\ldots (4.47)$$

$$C_2 = \frac{\varepsilon_1[D_{12}(\mu_1.\mu_{21}-\mu_{41}) - D_{32}.\cosh k\xi_1] + \varepsilon_2 \tanh k\xi_1(\mu_1 D_{12} - D_{32})}{\varepsilon_1\,[D_{22}.\cosh k\xi_1 + D_{12}.\sinh k\xi_1] + \varepsilon_2\,[D_{22}.\tanh k\xi_1 + D_{12}]}$$

$$B_3 = \frac{B_2.\mu_{22} - \mu_{42} + \frac{\mu_5 H}{k} \sinh k\xi_2 + C_2.\mu_{32}}{\cosh k\xi_2 + \frac{\mu_f H}{k} \sinh k\xi_2}$$

$$C_3 = H/k \left[B_3.\mu_f - \mu_5 \right]$$

where

$$\varepsilon_1 = 1 - \tanh k.\tanh k\xi_1$$

$$\varepsilon_2 = \mu_{21}.\tanh k - \mu_{31}$$

$$D_{12} = \mu_{22} (\tanh k\xi_2 + \mu_f H/k) - \tanh k\xi_2 (\cosh k\xi_2 + \mu_f H/k.\sinh k\xi_2)$$

$$D_{22} = \cosh k\xi_2 + \mu_f H/k.\sinh k\xi_2 - \mu_{32}.(\tanh k\xi_2 + \mu_f H/k)$$

$$D_{32} = \mu_5 H/k \left[(\cosh k\xi_2 + \mu_f H/k.\sinh k\xi_2) - \sinh k\xi_2 (\tanh k\xi_2 + \mu_f H/k) \right] + \mu_{42} (\tanh k\xi_2 + \mu_f H/k)$$

4. 3 Analysis of lateral deflection

By integrating equations (4.5) twice and using the boundary conditions

$$y_3 (0) = 0$$

$$\frac{dy_3}{dx} (0) = \theta$$

$$y_1 (x_1) = y_2 (x_1)$$

$$\frac{dy_1}{dx} (x_1) = \frac{dy_2}{dx} (x_1) \qquad \ldots\ldots\ldots\ldots\ldots\ldots \quad (4.48)$$

$$y_2 (x_2) = y_3 (x_2)$$

$$\frac{dy_2}{dx}(x_2) = \frac{dy_3}{dx}(x_2)$$

the lateral deflections of the structure can be found as

$$y_1 = \frac{1}{EI} H^2 \left[(1 - S_d) \Pi (\xi) H + \frac{L}{k} F_1 (\xi) + \frac{L}{k^2} F_2 (\xi) - S_d H \left(\frac{U \xi^2}{2 k^2} + \frac{W \xi^3}{3 k^2} \right) \right] + \theta H . \xi \quad \ldots\ldots\ldots\ldots\ldots\ldots \quad (4.49)$$

$$y_2 = \frac{1}{EI} H^2 \left[(1 - S_d) \Pi (\xi) H + \frac{L}{k} F_3 (\xi) + \frac{L}{k^2} F_4 (\xi) - S_d H \left(\frac{U \xi^2}{2 k^2} + \frac{W \xi^3}{3 k^2} \right) \right] + \theta H . \xi \quad \ldots\ldots\ldots\ldots\ldots\ldots \quad (4.50)$$

$$y_3 = \frac{1}{EI} H^2 \left[(1 - S_d) \Pi (\xi) H + \frac{L}{k^2} F_5 (\xi) - S_d H \left(\frac{U \xi^2}{2 k^2} + \frac{W \xi^3}{3 k^2} \right) \right] + \theta H . \xi \quad \ldots\ldots\ldots\ldots\ldots\ldots \quad (4.51)$$

where

$$S_d = \frac{\beta^2}{\alpha^2} L = \frac{m L}{I'}$$

$$\Pi (\xi) = 1/120 . \xi^2 \left[5 U (\xi^2 - 4 \xi + 6) + 2 W (\xi^3 - 10 \xi + 20) + 20 P (3 - \xi) \right]$$

$$F_1 (\xi) = (\xi - \xi_1) \left[(B_1 - B_2) . \sinh k\xi_1 + (C_1 - C_2) . \cosh k\xi_1 \right] + (\xi - \xi_2) \left[(B_2 - B_3) . \sinh k\xi_2 + (C_2 - C_3) . \cosh k\xi_2 \right]$$

$$F_2 (\xi) = B_1 (\cosh k\xi_1 - \cosh k\xi) + B_2 (\cosh k\xi_2 - \cosh k\xi_1) + C_1 (\sinh k\xi_1 - \sinh k\xi) + C_2 (\sinh k\xi_2 - \sinh k\xi_1) + B_3 (1 - \cosh k\xi_2) + C_3 (k\xi - \sinh k\xi_2) .$$

$$F_3(\xi) = (\xi - \xi_2)\,[\,(B_2 - B_3).\sinh k\xi_2 + (C_2 - C_3).\cosh k\xi_2\,]$$

$$F_4(\xi) = B_2(\cosh k\xi_2 - \cosh k\xi) + B_3(1 - \cosh k\xi_2) + C_2(\sinh k\xi_2 - \sinh k\xi) + C_3(k\xi - \sinh k\xi_2)$$

$$F_5(\xi) = B_3(1 - \cosh k\xi) + C_3(k\xi - \sinh k\xi).$$

For the case of a coupled shear wall on rigid foundation, $\mu_f = \lambda_\delta = \lambda_r = 0$, $\delta = \theta = 0$ and the boundary condition represented in equation (4.45) can be reduced to the condition $q_0 = 0$. The expressions of the integration constants can then be expressed as follows

$$B_1 = -C_1.\tanh k + \mu_1$$

$$C_1 = \frac{C_2 - \mu_1.\tanh k\xi_1 + B_2.\tanh k\xi_1}{\varepsilon_1}$$

$$B_2 = \frac{\varepsilon_1(\mu_1\mu_{21} - \mu_{41}) + \varepsilon_2.\mu_1.\tanh k\xi_1 - C_2(\varepsilon_1.\sinh k\xi_1 + \varepsilon_2)}{\varepsilon_1.\cosh k\xi_1 + \varepsilon_2.\tanh k\xi_1} \qquad \ldots\ldots\ldots (4.52)$$

$$C_2 = \frac{\varepsilon_1[D_{12}(\mu_1.\mu_{21} - \mu_{41}) - D_{32}.\cosh k\xi_1] + \varepsilon_2\tanh k\xi_1(\mu_1.D_{12} - D_{32})}{\varepsilon_1\,[D_{22}.\cosh k\xi_1 + D_{12}.\sinh k\xi_1] + \varepsilon_2\,[D_{22}.\tanh k\xi_1 + D_{12}]}$$

$$B_3 = \frac{B_2.\mu_{22} - \mu_{42} + \mu_5 H/k \sinh k\xi_2 + C_2.\mu_{32}}{\cosh k\xi_2}$$

$$C_3 = -\mu_5 H/k$$

where the expressions of μ_5, D_{12}, D_{22} and D_{32} become respectively

$$\mu_5 = -\frac{\beta^2}{\alpha^2}\left[\,U + P + W\left(1 - \frac{2}{k^2}\right)\,\right]$$

$$D_{12} = (\,\mu_{22} - \cosh k\xi_2\,).\tanh k\xi_2 = \gamma_2 k.\sinh k\xi_2.\tanh k\xi_2$$

$$D_{22} = \cosh k\xi_2 - \mu_{32}.\tanh k\xi_2 = \cosh k\xi_2 + \gamma_2 k.\sinh k\xi_2 - \sinh k\xi_2.\tanh k\xi_2$$

$$D_{32} = \mu_5 H/k \left[\cosh k\xi_2 - \sinh k\xi_2.\tanh k\xi_2 \right] + \mu_{42}.\tanh k\xi_2$$

The base shears in equations (4.8) become proportional to their inertias and reduce to

$$(S_1)_3\ (0) = -\frac{I_1}{I}\frac{dM_e}{dx}(0)$$

$$(S_2)_3\ (0) = -\frac{I_2}{I}\frac{dM_e}{dx}(0) \qquad \ldots\ldots\ldots\ldots\ldots\ldots\ldots\ldots\ldots\ldots\ldots\ldots\ (4.53)$$

4. 4 Discretisation

The expressions of the discrete shear force, Q_f and the axial force, N_f in any internal lintel beam, f, may be obtained respectively in each zone from the corresponding continuous distributed forces, once the laminar shears q_i and the axial distributions n_i are determined as,

$$(Q_f)_i = \int_{x-h/2}^{x+h/2} q_i.dx$$

$$= -\left[B_i \{ \cosh k\mu - \cosh k\varphi \} + C_i \{ \sinh k\mu - \sinh k\varphi \} \right] + \frac{\beta^2}{\alpha^2} H.N(\xi). \qquad \ldots\ (4.54)$$

$$(N_f)_i = \int_{x-h/2}^{x+h/2} n_i.dx$$

$$= -\frac{I_2}{I} Z_f(\xi) +$$

$$\left(\frac{I_1}{I} L - \Delta - L_1 \right) \left[\frac{k}{H} \right. \left[B_i \{ \sinh k\mu - \sinh k\varphi \} + \right.$$

$$C_i \{ \cosh k\mu - \cosh k\varphi \} \left. \right] +$$

$$\left. \frac{\beta^2}{\alpha^2} Z_f(\xi) \right] \quad \ldots\ldots \quad (4.55)$$

At the stiffening beams, the shear force and the axial force are respectively given by

$$Q(x_1) = \int_{x_1}^{x_1+h/2} q_1 . dx + V_{m1} + \int_{x_1-h/2}^{x_1} q_2 . dx$$

$$= -\left[B_1 \{ \cosh k\tau - \cosh k\xi_1 + \gamma_1 k . \sinh k\xi_1 \} + \right.$$

$$C_1 \{ \sinh k\tau - \sinh k\xi_1 + \gamma_1 k . \cosh k\xi_1 \} +$$

$$B_2 \{ \cosh k\xi_1 - \cosh k\rho \} +$$

$$\left. C_2 \{ \sinh k\xi_1 - \sinh k\rho \} \right] +$$

$$\frac{\beta^2}{\alpha^2} H \left[N(\xi_1) - \gamma_1 \frac{dM_e}{dx}(\xi_1) \right] \quad \ldots\ldots\ldots\ldots \quad (4.56)$$

$$N(x_1) = \int_{x_1}^{x_1+h/2} n_1 . dx + \int_{x_1-h/2}^{x_1} n_2 . dx$$

$$= -\frac{I_2}{I} Z(\xi_1) +$$

$$\left(\frac{I_1}{I} L - \Delta - L_1 \right) \left[\frac{k}{H} \right. \left[B_1 \{ \sinh k\tau - \sinh k\xi_1 \} + \right.$$

$$B_2 \{ \sinh k\xi_1 - \sinh k\rho \} +$$

$$C_1 \{ \cosh k\tau - \cosh k\xi_1 \} +$$

$$\left. C_2 \{ \cosh k\xi_1 - \cosh k\rho \} \right] +$$

$$\frac{\beta^2}{\alpha^2} Z(\xi_1) \Big] \qquad \ldots\ldots \quad (4.57)$$

$$Q(x_2) = \int_{x_2}^{x_2+h/2} q_2.dx + V_{m2} + \int_{x_2-h/2}^{x_2} q_3.dx$$

$$= -\Big[B_2 \{ \cosh k\chi - \cosh k\xi_2 + \gamma_2 k.\sinh k\xi_2 \} +$$

$$C_2 \{ \sinh k\chi - \sinh k\xi_2 + \gamma_2 k.\cosh k\xi_2 \} +$$

$$B_3 \{ \cosh k\xi_2 - \cosh k\upsilon \} +$$

$$C_3 \{ \sinh k\xi_2 - \sinh k\upsilon \} \Big] +$$

$$\frac{\beta^2}{\alpha^2} H \Big[N(\xi_2) - \gamma_2 \frac{dM_e}{dx}(\xi_2) \Big] \qquad \ldots\ldots\ldots \quad (4.58)$$

$$N(x_2) = \int_{x_2}^{x_2+h/2} n_2.dx + \int_{x_2-h/2}^{x_2} n_3.dx$$

$$= -\frac{I_2}{I} Z(\xi_2) +$$

$$\Big(\frac{I_1}{I} L - \Delta - L_1 \Big) \Big[\frac{k}{H} \Big[B_2 \{\sinh k\chi - \sinh k\xi_2\} +$$

$$C_2 \{\cosh k\chi - \cosh k\xi_2\} +$$

$$B_3 \{\sinh k\xi_2 - \sinh k\upsilon\} +$$

$$C_3 \{\cosh k\xi_2 - \cosh k\upsilon\} \Big] +$$

$$\frac{\beta^2}{\alpha^2} Z(\xi_2) \Big] \qquad \ldots \quad (4.59)$$

where

$$\tau = \xi_1 + \frac{1}{2J} \quad , \quad \chi = \xi_2 + \frac{1}{2J}$$

$$\rho = \xi_1 - \frac{1}{2J} \quad , \quad \upsilon = \xi_2 - \frac{1}{2J} \qquad \ldots\ldots \quad (4.60)$$

$$Q(H) = -\left[B_1 \{ \cosh k - \cosh k\varphi \} + C_1 \{ \sinh k - \sinh k\varphi \} \right] + \frac{\beta^2}{\alpha^2} H N_1 \quad \ldots\ldots\ldots \quad (4.61)$$

$$N(H) = \frac{I_2}{I}\left[Z(1) - P \right] + \left(\frac{I_1}{I} L - \Delta - L_1 \right) \left[\frac{k}{H} \left[B_1 \{ \sinh k - \sinh k\varphi \} + C_1 \{ \cosh k - \cosh k\varphi \} \right] + \frac{\beta^2}{\alpha^2}\left[Z(1) - P \right] \right] + Q_t \quad \ldots\ldots\ldots \quad (4.62)$$

The shear forces and the axial forces in the discrete set of walls will be given as shown in chapter 2. However, the moments in walls, are respectively given by

$$(M_1)_{f_1} = h \sum_{f}^{j=1} (S_1^{f_1})_j - (T)_{f_1}(L_1+\Delta) - \bar{M}$$

$$(M_2)_{f_1} = h \sum_{f}^{j=1} (S_2^{f_1})_j - (T)_{f_1}(L_2-\Delta) + \bar{M} \quad \ldots\ldots \quad (4.63)$$

$$(M_1)_{f_2} = (M_1)_{f_1} - Q_f(L_1+\Delta) - M^*$$

$$(M_2)_{f_2} = (M_2)_{f_1} - Q_f(L_2-\Delta) + M^*$$

where

$$\bar{M} = \begin{cases} M_p & \text{for} \quad x_1 \leqslant x \leqslant H \\ (M_m)_1 + M_p & \text{for} \quad x_2 \leqslant x < x_1 \\ (M_m)_1 + (M_m)_2 + M_p & \text{for} \quad 0 \leqslant x < x_2 \end{cases}$$

and

$$M^* = \begin{cases} 0 & \text{for } x_1 < x \leqslant H,\ x_2 < x < x_1, \text{ and } 0 \leqslant x < x_2 \\ (M_m)_1 & \text{for } x = x_1 \\ (M_m)_2 & \text{for } x = x_2 \end{cases}$$

$$(M_m)_s = (\Delta_s - \Delta) Q_f(x_s), \qquad (s = 1, 2) \qquad \ldots\ldots \quad (4.64)$$

where Δ_s is the amount by which the point of contraflexure in the stiffening beam s is shifted from the mid-span position towards the less stiff wall obtained by a procedure similar to that followed in Chapter 2 for the determination of the shift of the point of contraflexure Δ. The shift Δ_s, in each stiffening beam, s, will be given by,

$$\Delta_s = L_2 \frac{\frac{I_1}{I_2} - \frac{L_1}{L_2}}{1 + \frac{I_1}{I_2} + 12\frac{bI_1}{hI_{fs}}} \qquad (s = 1, 2) \qquad \ldots\ldots \quad (4.65)$$

In the case of one stiff beam being at the top of the structure, that is when $x_1 = H$, Δ_1, becomes

$$\Delta_1 = \Delta_t = L_2 \frac{\frac{I_1}{I_2} - \frac{L_1}{L_2}}{1 + \frac{I_1}{I_2} + 6\frac{bI_1}{hI_{f1}}} \qquad \ldots\ldots\ldots\ldots\ldots\ldots\ldots \quad (4.66)$$

Again, as stated in Chapter 2 for Δ and Δ_t, equations (4.65) and (4.66) show that, whenever the second moments of inertias of the walls are proportional to the distances from the mid-span position of the connecting beams to the centroidal axes of the walls, the value of the shift Δ_s, will be equal to zero, that is the line of contraflexure will pass through the continuous lamina at mid-span position of the stiffening beams.

Note that in the special case of equal walls, $\Delta_s = 0$, and the moments $(M_m)_s$ will be equal to zero.

Alternative calculation of moments

As before, in chapter 2, section 2.3, the bending moments in the discrete set of walls can alternatively be calculated from

$$(M_1)_{f1} = M_1 + 0.5\,[Q_f(L_1+\Delta) + \bar{M}]$$

$$(M_2)_{f1} = M_2 + 0.5\,[Q_f(L_2-\Delta) - \bar{M}] \qquad \ldots\ldots \quad (4.67)$$

$$(M_1)_{f2} = M_1 - 0.5\,[Q_f(L_1+\Delta) + \bar{M}]$$

$$(M_2)_{f2} = M_2 - 0.5\,[Q_f(L_2-\Delta) - \bar{M}] \qquad \ldots\ldots\ldots \quad (4.68)$$

where

$\bar{M} = M_p$ for $X = H$

$\bar{M} = (M_m)_s$ for $X = X_s$, $s = 1, 2$

$\bar{M} = 0$ for $X \neq X_s$ and $X \neq H$

4. 5 Particular cases

Case 1: One stiffening beam.

For the particular case where there is only one stiffening beam, γ_2 is equal to zero and for an arbitrary value of the height ratio, ξ_2 equal to zero, it follows that

$$\mu_{22} = 1$$

$$\mu_{32} = \mu_{42} = 0$$

The expressions of the integration constants, B_1 and C_1 remain the same and the other constants will have the following expressions

(a) Shear wall on flexible foundation

$$C_2 = \frac{\varepsilon_1 H/K \left[\mu_f(\mu_1.\mu_{21}-\mu_{41})-\mu_5.\cosh k\xi_1\right]+\varepsilon_2 H/k \tanh k\xi_1(\mu_1\mu_f-\mu_5)}{\varepsilon_1 \left[\cosh k\xi_1+ \mu_f H/k.\sinh k\xi_1\right] + \varepsilon_2 \left[\tanh k\xi_1+ \mu_f H/k\right]}$$

$$= C_3 \qquad \ldots\ldots\ldots\ldots \quad (4.69)$$

$$B_2 = B_3 = \frac{\varepsilon_1(\mu_1\mu_{21}-\mu_{41})+\varepsilon_2.\mu_1.\tanh k\xi_1-C_2\ (\varepsilon_1.\sinh k\xi_1+ \varepsilon_2)}{\varepsilon_1.\cosh k\xi_1 + \varepsilon_2.\tanh k\xi_1}$$

and the fonctions $F_1(\xi)$ to $F_5(\xi)$ become, respectively,

$$F_1(\xi) = (\xi - \xi_1)\left[(B_1 - B_2).\sinh k\xi_1 + (C_1 - C_2).\cosh k\xi_1\right]$$

$$F_2(\xi) = B_1(\cosh k\xi_1 - \cosh k\xi) + B_2(1 - \cosh k\xi_1) + C_1(\sinh k\xi_1 - \sinh k\xi) + C_2(k\xi - \sinh k\xi_1)$$

$$F_3(\xi) = 0$$

$$F_4(\xi) = F_5(\xi) = B_2(1 - \cosh k\xi) + C_2(k\xi - \sinh k\xi)$$

(b) Shear wall on rigid foundation

$$B_2 = B_3 = \frac{\varepsilon_1(\mu_1\mu_{21}-\mu_{41}) + \varepsilon_2.\mu_1.\tanh k\xi_1 - C_2(\varepsilon_1.\sinh k\xi_1+\varepsilon_2)}{\varepsilon_1.\cosh k\xi_1 + \varepsilon_2.\tanh k\xi_1} \qquad \ldots\ldots\ldots \quad (4.70)$$

$$C_2 = C_3 = -\mu_5 H/k$$

Case 2: Unstiffened coupled shear walls.

The case of an unstiffened shear wall is obtained by puting $\gamma_1 = \gamma_2 = 0$ and $x_1 = x_2 = 0$. The integration constants reduce to

(a) Shear wall on a flexible foundation

$$C_1 = C_2 = C_3 = C = \frac{H/k\ (\mu_1\mu_f - \mu_5)}{1 + \mu_f H/k \tanh k} \qquad \ldots\ldots\ldots\ldots \quad (4.71)$$

$$B_1 = B_2 = B_3 = B = \mu_1 - C_2.\tanh k$$

and the expressions of $F_1(\xi)$ to $F_5(\xi)$ become, respectively,

$$F_1(\xi) = F_3(\xi) = 0$$

$$F_2(\xi) = F_4(\xi) = F_5(\xi) = B\ (1 - \cosh k\xi) + C\ (k\xi - \sinh k\xi)$$

(b) Shear wall on a rigid foundation.

For the case of rigid foundations, equations (4.71), reduce to

$$C_1 = C_2 = C_3 = C = H/k\ [\ U+P+W\ (1-2/k^2)\ ] \qquad \ldots\ldots\ldots \quad (4.72)$$

$$B_1 = B_2 = B_3 = B = \mu_1 - C_2.\tanh k$$

<u>Case 3: Coupled shear walls with a top and a bottom stiff beams</u>.

For the particular case of a shear coupled shear wall with a top and a bottom stiff beams, $\xi_1 = 1$ and $\xi_2 = 0$, it follows from equations (4.47) that

$$B = B_1 = B_2 = B_3 = -\bar{B} - \bar{C}.C_1 \qquad \ldots\ldots\ldots\ldots\ldots\ldots \quad (4.73)$$

where

$$\bar{B} = -\frac{\beta^2}{\alpha^2} H \frac{U + 2W + k^2\gamma\ (\ 2W/k^2 - P\ )}{k^2 \cosh k}$$

$$\bar{C} = \frac{\sinh k + k\gamma.\cosh k}{\cosh k + k\gamma.\sinh k}$$

$$C = C_1 = C_2 = C_3 = \frac{\frac{\beta^2}{\alpha^2} H\,(S_k/H + S_k\mu_f\gamma_2 + \mu_f.R_k) - L\,\lambda_r M_{e0}}{k\,(1/H + \mu_f\gamma_2) + \mu_f\bar{C}} \qquad (4.74)$$

and

$$S_k = P + U + W\left[1 - 2/k^2\right]$$

$$M(0) = M(\xi) \qquad \text{for } \xi = 0$$

$$R_k = M(0) + \frac{U}{k^2} - B\,\frac{-\alpha^2}{\beta^2 H}$$

The expressions of $F_1(\xi)$ to $F_5(\xi)$ become,

$$F_1(\xi) = F_3(\xi) = 0$$

$$F_2(\xi) = F_4(\xi) = F_5(\xi) = B\,(1 - \cosh k\xi) + C\,(k\xi - \sinh k\xi)$$

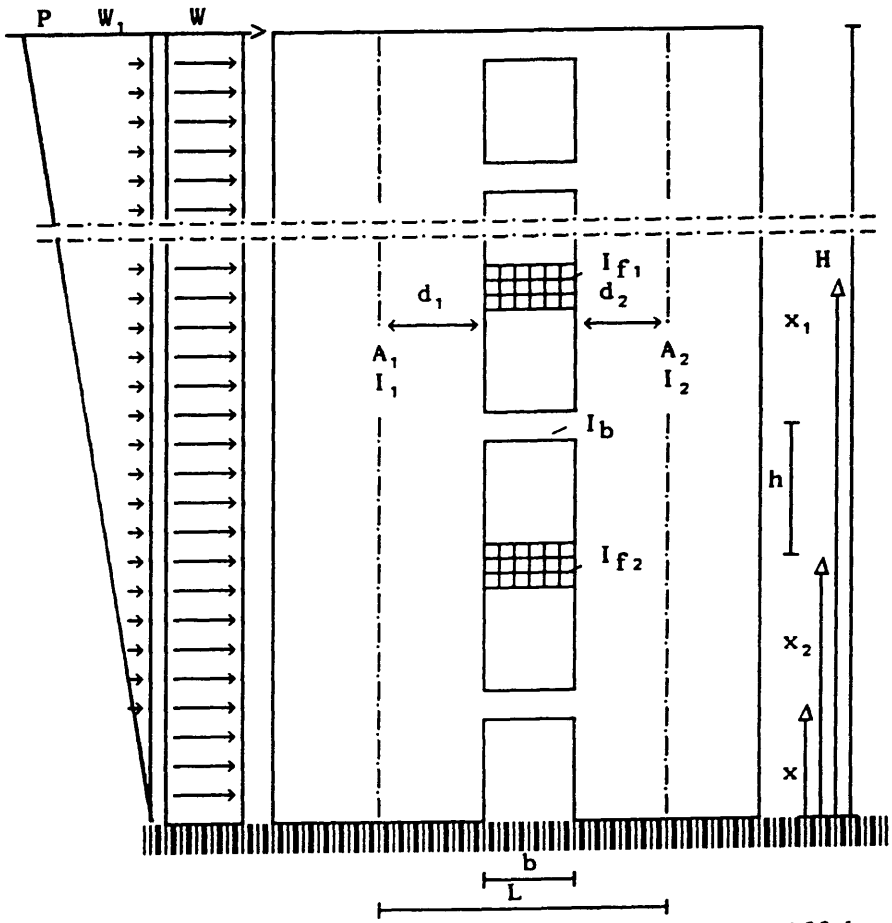

Fig. 4.1 (a) Coupled shear wall with two stiff beams.

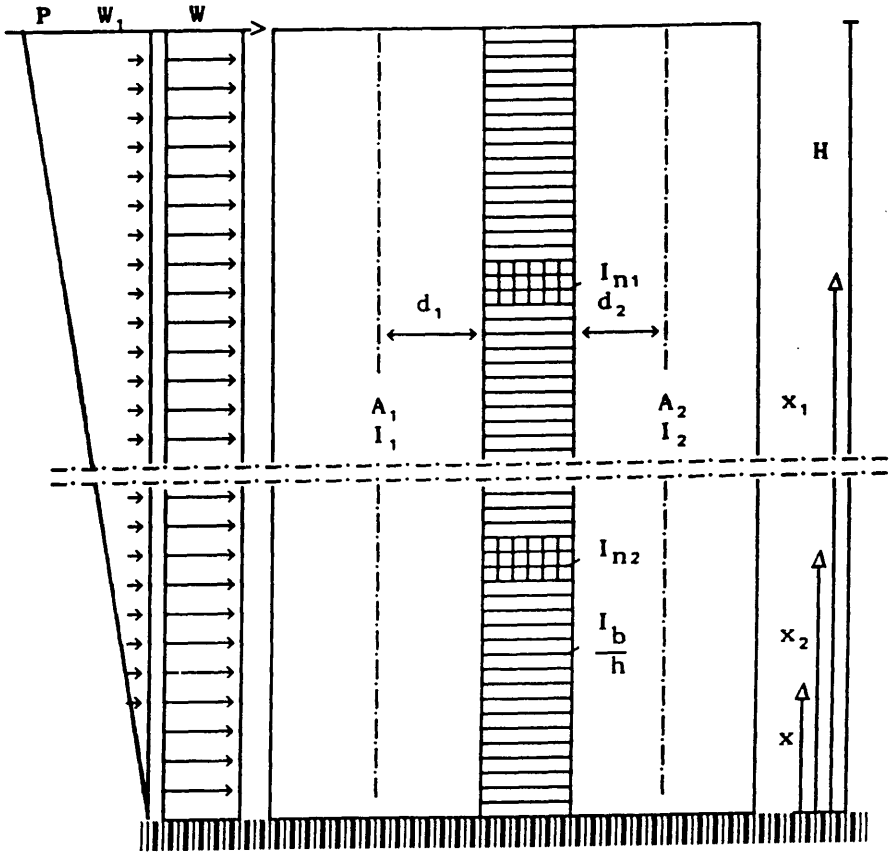

Fig. 4.1 (b) Equivalent substitute system.

Fig. 4.1

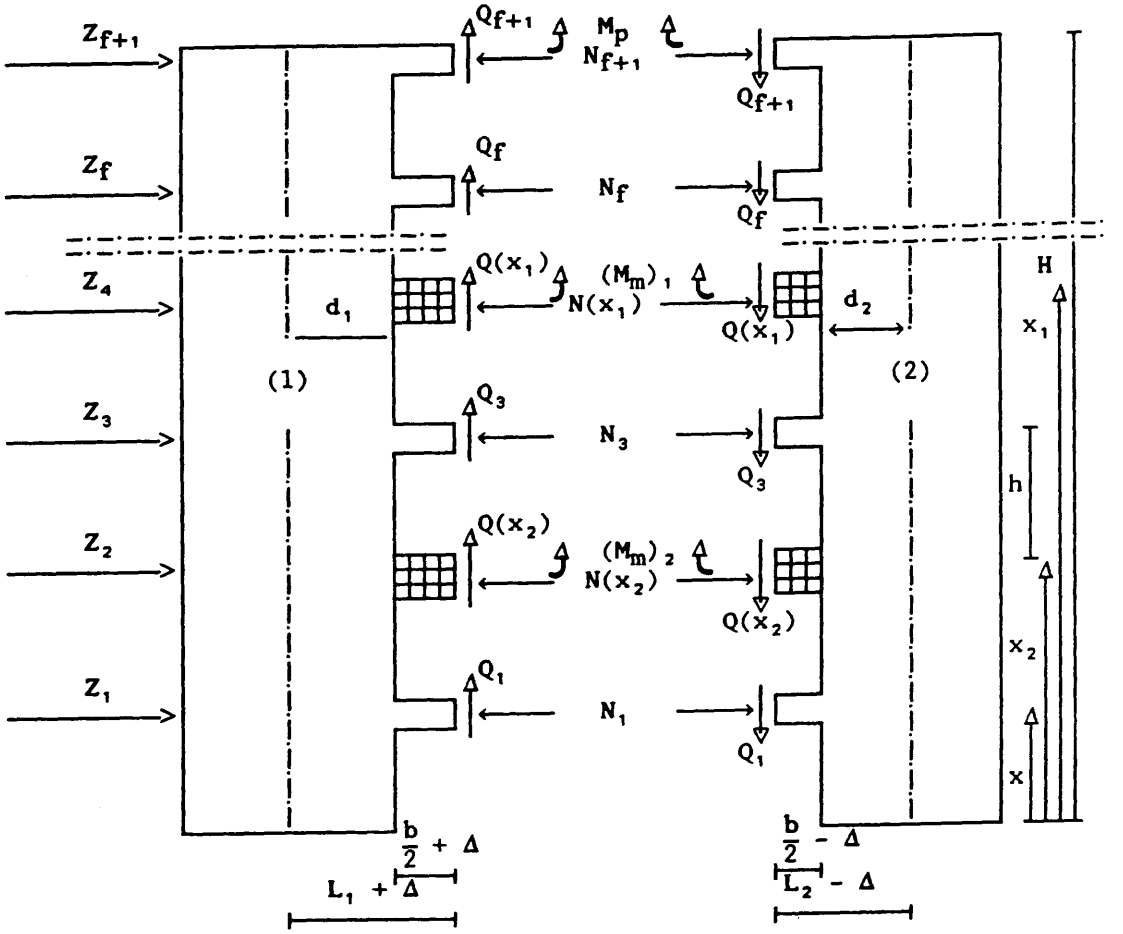

(a) Discrete System

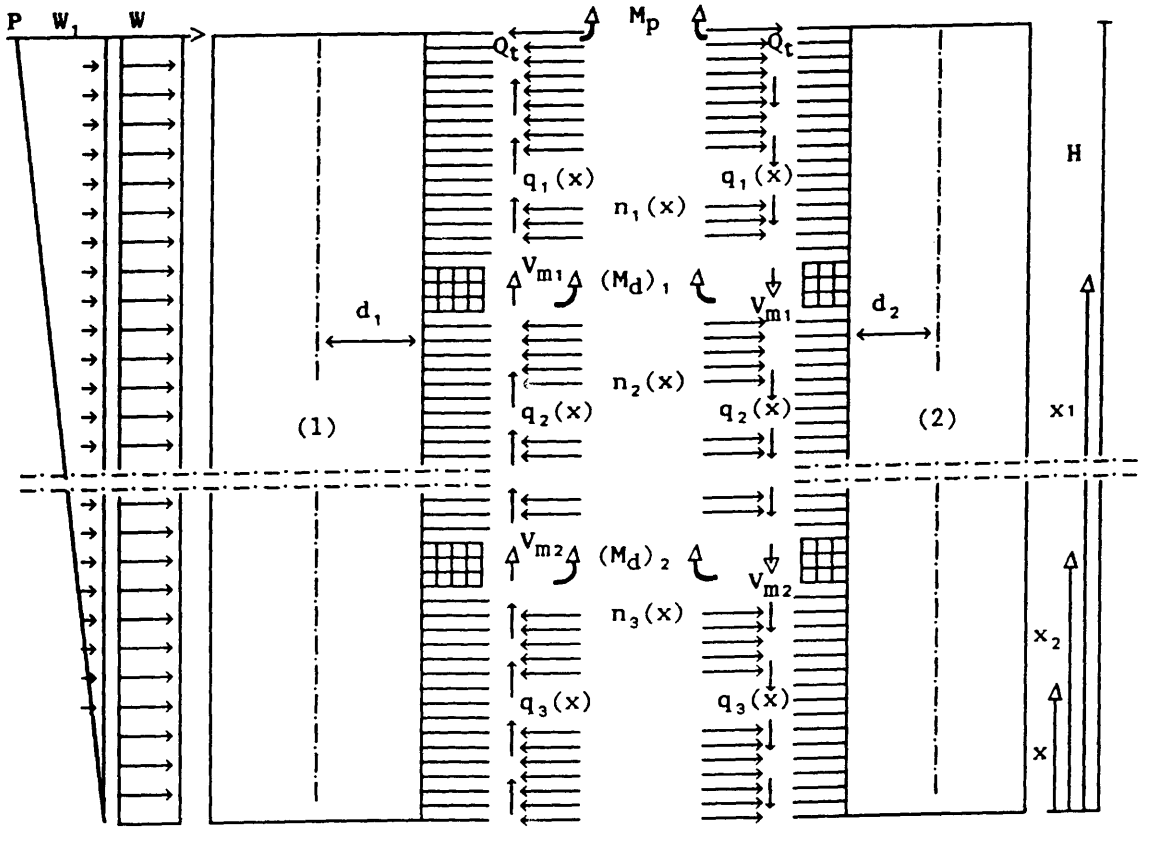

(b) Substitute system

Fig. 4.2

CHAPTER FIVE

NUMERICAL INVESTIGATIONS OF STIFFENED COUPLED SHEAR WALLS.

5. 1 Introduction

As stated in Chapter 4, the lintel beams connecting two coupled shear walls may not be very stiff and their coupling effect can not provide the required lateral stiffness of the structure. This can be overcome by introducing additional stiffening beams at one or more levels along the height of the structure, which will enhance the coupling effect of the normal lintel beams

The object of this Chapter is to evaluate the effect of the stiffening beams on the behaviour of coupled shear walls on rigid foundations, the influence of the rigidities of the stiffening beams and their locations on the internal forces and lateral deflections of the structure, and to investigate the accuracy of the continuum theory presented in Chapter 4 by comparison with the frame analogy.

The numerical investigations conducted on the analysis of stiffened coupled shear walls are presented in two sections. Firstly, graphs for laminar shear flow, maximum laminar shear, lateral deflection and maximum deflection, all in dimensionless form, are plotted against the height ratio. The graphs illustrate the influence of the relative flexural rigidity of the stiffening beams and their locations on the behaviour of coupled shear walls resting on rigid foundations. Graphs for the maximum laminar shear and the maximum top deflection are also plotted against the relative flexural rigidity for various stiffening beam locations. The curves take into consideration the three cases of a shear wall with two stiffening beams, one

stiffening beam and unstiffened shear walls, for two values of the relative stiffness parameter αH of 3 and 6. For coupled shear walls on elastic foundations, numerical results are shown in tabular form in Appendix B. Secondly, in order to assess the accuracy of the results given by the continuum method, a comparison of results is made with those obtained from a frame analysis for coupled shear walls on rigid foundations with two stiffening beams at different locations.

5. 2 Design curves

In this section graphs showing the distribution of laminar shear over the height of the structure, the lateral deflection of the structure, the magnitude of the maximum laminar shear and maximum deflection are presented in dimensionless form to illustrate the structural response of unstiffened coupled shear walls and shear walls with one or two stiffening beams subjected to uniformly distributed lateral load and supported on rigid foundations.

Figs. 5.1 to 5.3 show the distribution of the laminar shear over the height for the case of a shear wall with a relative stiffness parameter $\alpha H = 3$ for three different stiffening beam spacings, namely height ratios of 1 and 0.5, 0.67 and 0.33, and 0.75 and 0.25 respectively for a range of flexural rigidities of the beams of 0, 0.20, 0.60 1.0, 2.0 and 5.0. For the same range of flexural rigidities of the stiffening beams, Figs. 5.4 to 5.6 show the lateral deflection profiles of the structure for the same locations of stiffening beams and for a value of geometrical parameter S_d ($\beta^2 L/\alpha^2$) of 0.9.

For a shear wall with one stiffening beam at mid-height level, Figs. 5.7 and 5.8 show the same distribution for two different relative stiffness parameters αH of 3 and 6 respectively, for the same range of flexural rigidities (γ) of the stiffening beam. Figs. 5.9 and 5.10, show the lateral

deflection over the height for the same conditions and for a parameter S_d of 0.9.

Figs. 5.11 and 5.12 show the variation of the maximum laminar shear and maximum top deflection respectively with the relative flexural rigidity of the stiffening beams, for a range of locations of both one and two stiffening beams. Figs. 5.13 and 5.14 show the effect of the stiffening beam location on the maximum laminar shear for a shear wall with one stiffening beam only, for values of αH of 3.0 and 6.0 respectively. Figs. 5.15 and 5.16 show the effect of the same stiffening beam locations for the same stiffness parameter αH on the maximum top deflection for a geometrical parameter S_d of 0.9.

5. 3 Discussion

The curves previously cited show clearly the effect of the flexural rigidities of the stiffening beams in reducing the laminar shear in the continuous medium and the lateral deflection over the height of the structure. The greater the flexural rigidity of the stiffening beams, the greater the reduction in laminar shear and lateral deflections. The provision of two stiffening beams has more effect in reducing the maximum laminar shear and maximum top lateral deflections. However, the best reduction in terms of both laminar shear and lateral deflections is achieved with two stiffening beams positioned at two thirds and one third of the height of the structure. It is also important to notice the greater effect of the stiffening beams which is achieved with coupled shear wall structures with a relatively low stiffness parameter αH than with a stiffer structure.

5. 4 Example structures

In this section two example structures have been chosen in order to assess the accuracy of the results obtained from the continuum theory of

coupled shear walls with two stiffening beams, presented in Chapter 4, by comparison with the results obtained from a frame analysis. The dimensions and structural properties of the 24-storey coupled shear wall structures are shown in Fig. 5.17. The two examples have the same geometrical dimensions and properties apart from the widths of the walls which are taken to be

(a) $2\,d_1 = 2\,d_2 = 8.0$ m

(b) $2\,d_1 = 12$m, $2d_2 = 4.0$ m

The results are presented as a set of non-dimensional curves for two cases, namely:

Case (1) Shear wall with two stiffening beams, one at the top and one at mid-height of the structure.

Case (2) Shear wall with two stiffening beams, one at two thirds of the height and one at one third of the height.

It has been shown in Chapter 3 that for the case of symmetrical structures with two equal walls that the results from the continuum and analogous frame analysis are always in close agreement. As a consequence, only a few curves are shown here to demonstrate the results for stiffened walls. Figs. 5.18 to 5.21 show the discrete shears in the connecting beams and the discrete axial forces in the walls for the two different spacings of the stiffening beams. The four figures show good agreement between the continuum method discretisation and the frame results.

For the case of the unsymmetrical shear wall with a wall-width ratio of 3, more results are shown. Fig. 5.22 shows the lateral deflection of the structure over the height for Case (2). The figure shows a very small difference between the continuum method curve and the curve given by the frame method. For the same case, Fig. 5.23 shows the discrete shears in the beams. The stiffening beams shears are shown in Figs. 5.18, 5.20, and

5.23. The two first figures show very close agreement between the continuum shears and the frame analogy shears, whereas the stiffening beams shears given by the frame method shown in the last figure are slightly less than those given by the continuum method. For the same case, Fig. 5.24 shows the moments in the smaller wall and demonstrates good agreement between the continuum method, the alternative method and the frame method. Fig. 5.25 shows the axial forces in the walls for case 2. The results are again very satisfactory in terms of comparison with the frame analogy results.

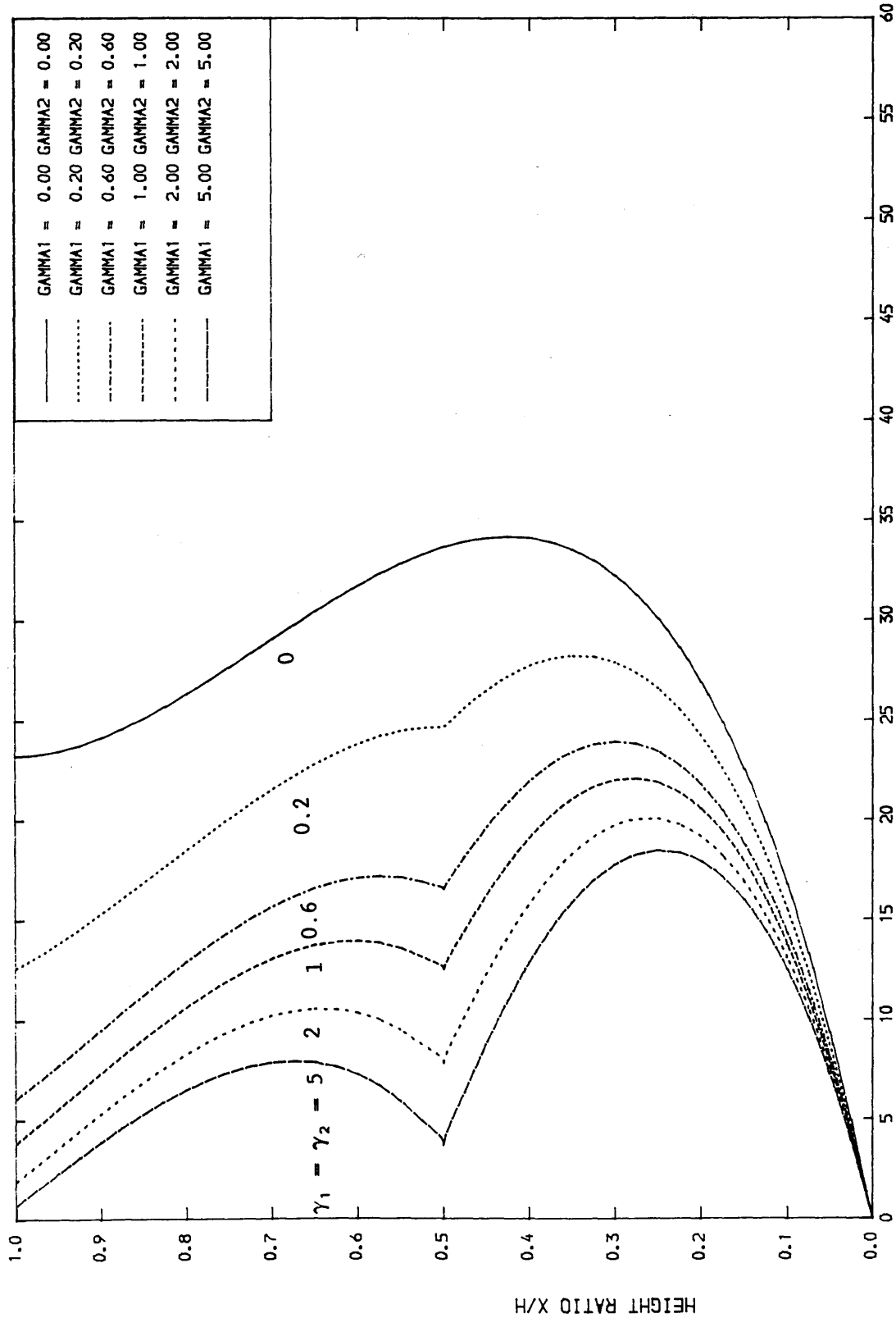

Fig.5.1. VARIATION OF LAMINAR SHEAR WITH HEIGHT RATIO FOR DIFFERENT RELATIVE FLEXURAL RIGIDITY OF STIFFENING BEAMS. (X1/H=1.0, X2/H=0.5, K=3)

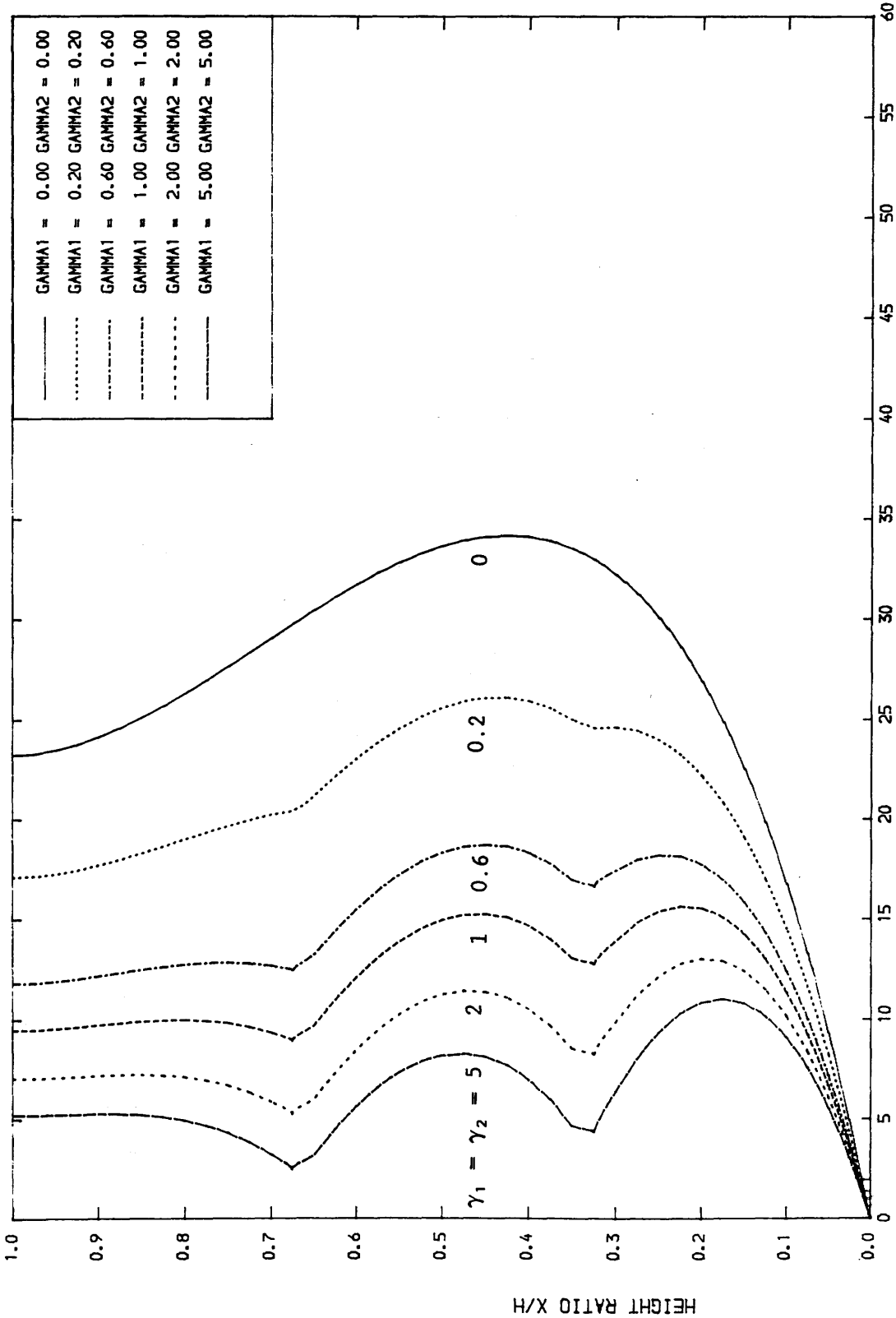

Fig.5.2. VARIATION OF LAMINAR SHEAR WITH HEIGHT RATIO FOR DIFFERENT RELATIVE FLEXURAL RIGIDITY OF STIFFENING BEAMS. (X1/H=0.67, X2/H=0.33, K=3)

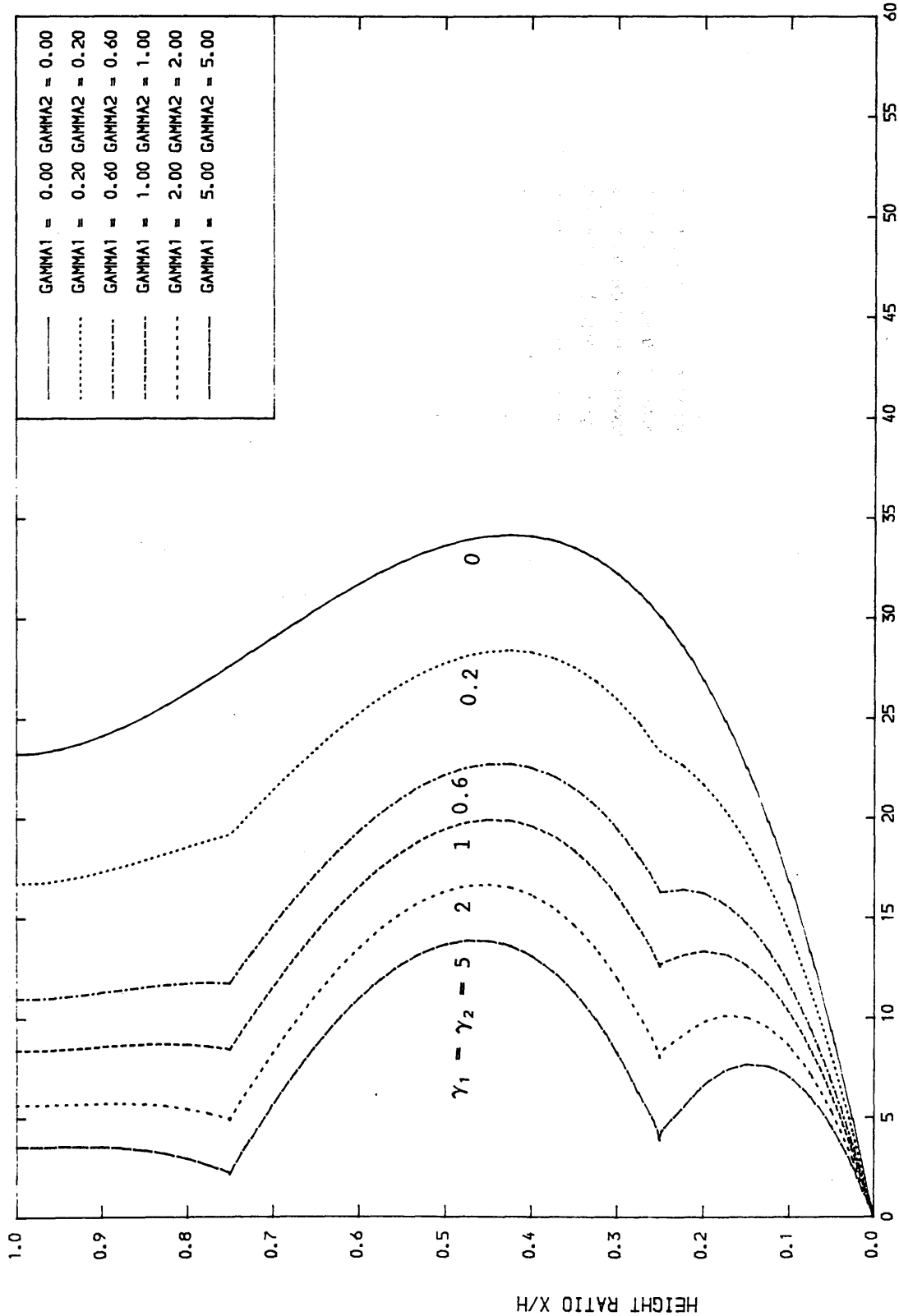

Fig.5.3. VARIATION OF LAMINAR SHEAR WITH HEIGHT RATIO FOR DIFFERENT RELATIVE FLEXURAL RIGIDITY OF STIFFENING BEAMS. (X1/H=0.75, X2/H=0.25, K=3)

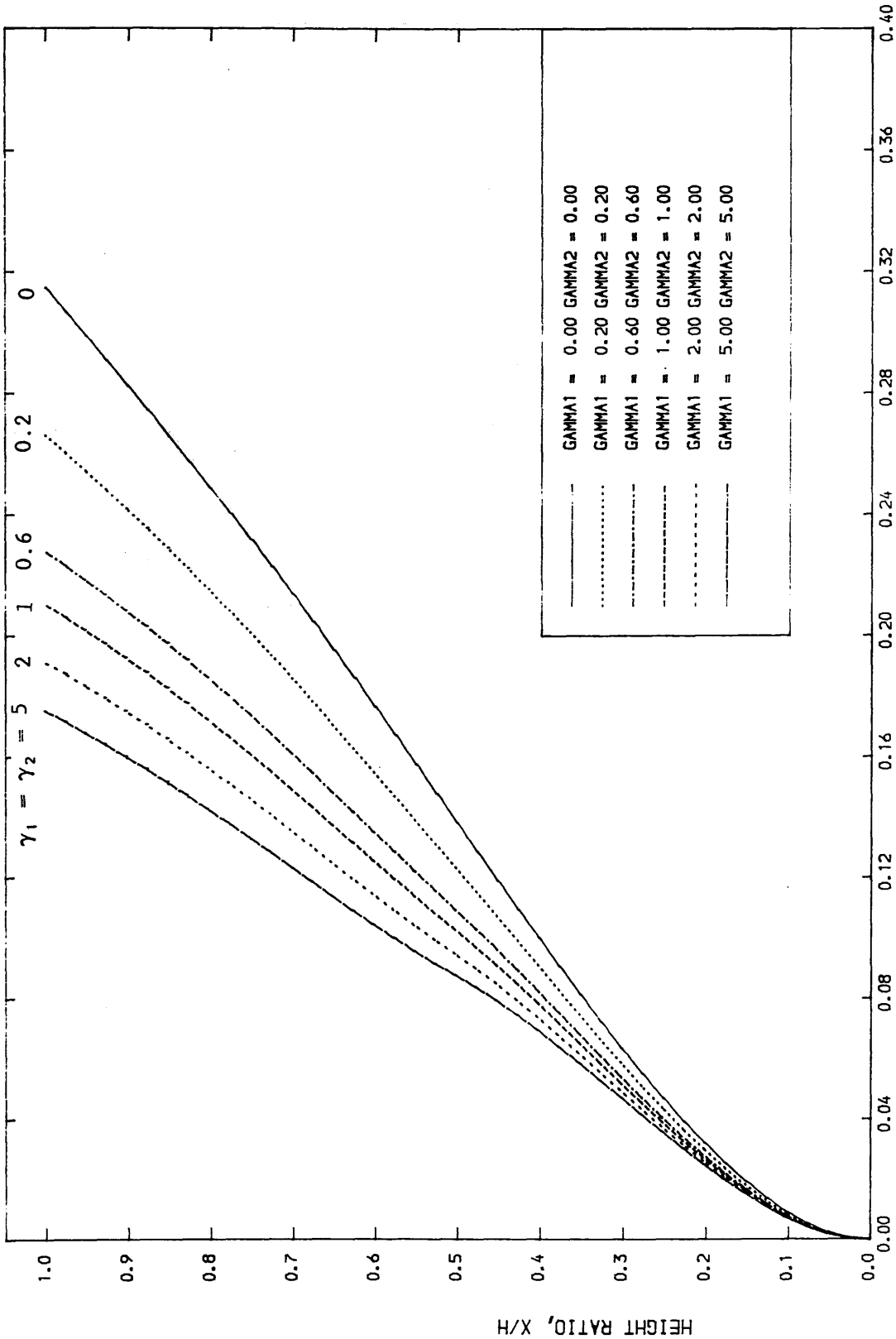

Fig.5.4. VARIATION OF LATERAL DEFLECTION WITH HEIGHT RATIO FOR DIFFERENT RELATIVE FLEXURAL RIGIDITY OF STIFFENING BEAMS. (X1/H=1.0, X2/H=0.5, K=3, Sd=0.9)

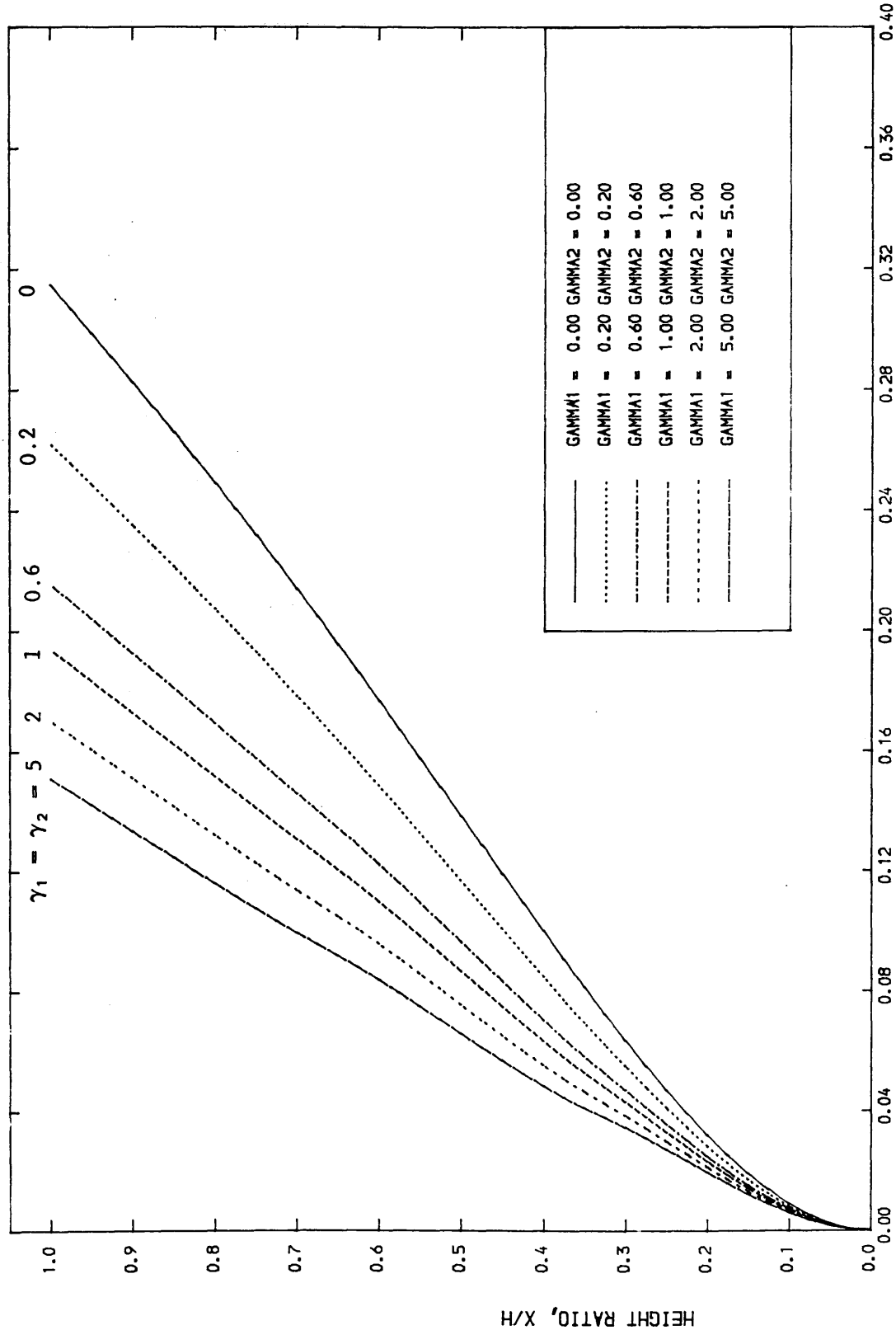

Fig.5.5. VARIATION OF LATERAL DEFLECTION WITH HEIGHT RATIO FOR DIFFERENT RELATIVE FLEXURAL RIGIDITY OF STIFFENING BEAMS. (X1/H=0.67, X2/H=0.33, K=3, Sd=0.9)

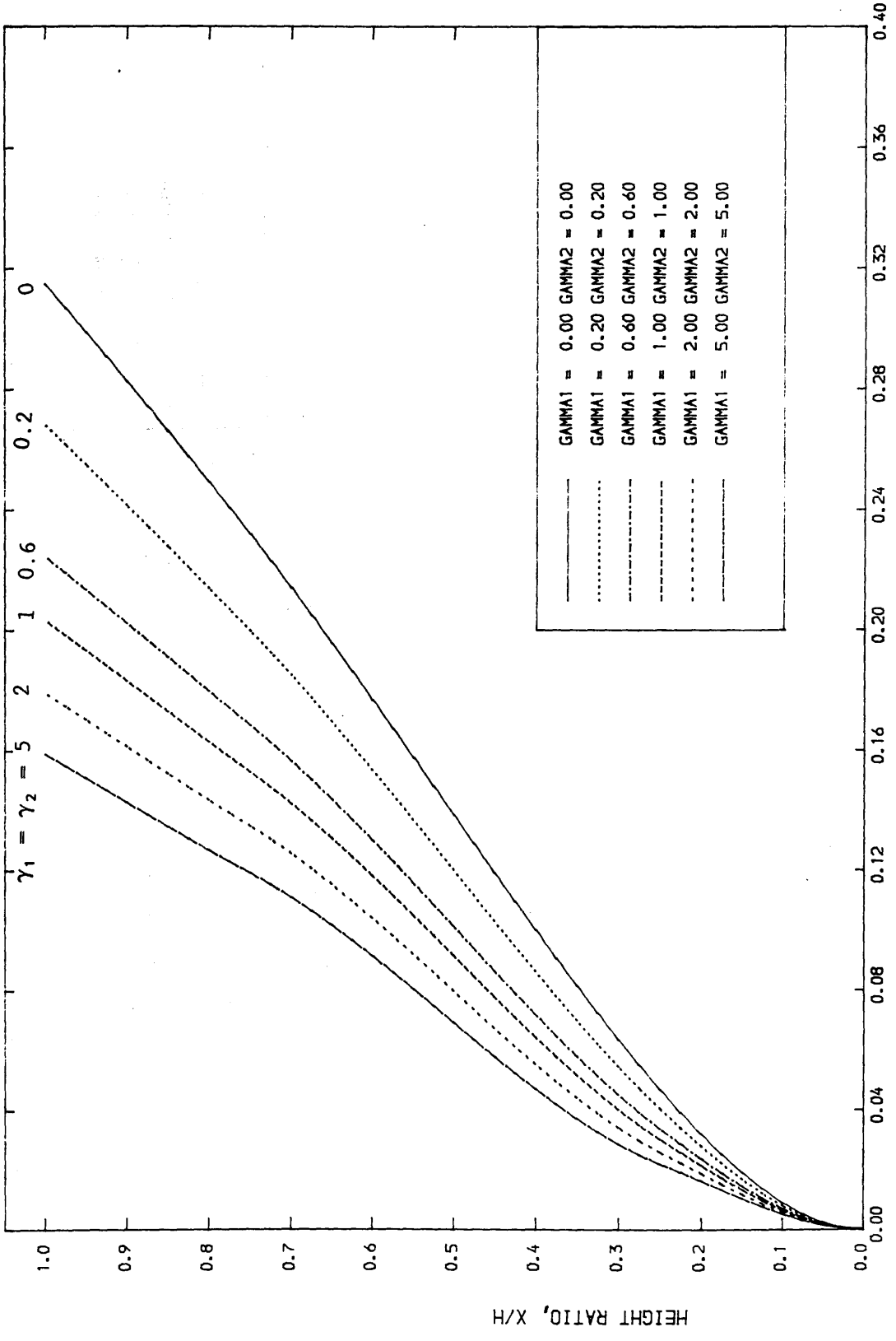

Fig.5.6. VARIATION OF LATERAL DEFLECTION WITH HEIGHT RATIO FOR DIFFERENT RELATIVE FLEXURAL RIGIDITY OF STIFFENING BEAMS. (X1/H=0.75, X2/H=0.25, K=3, Sd=0.9)

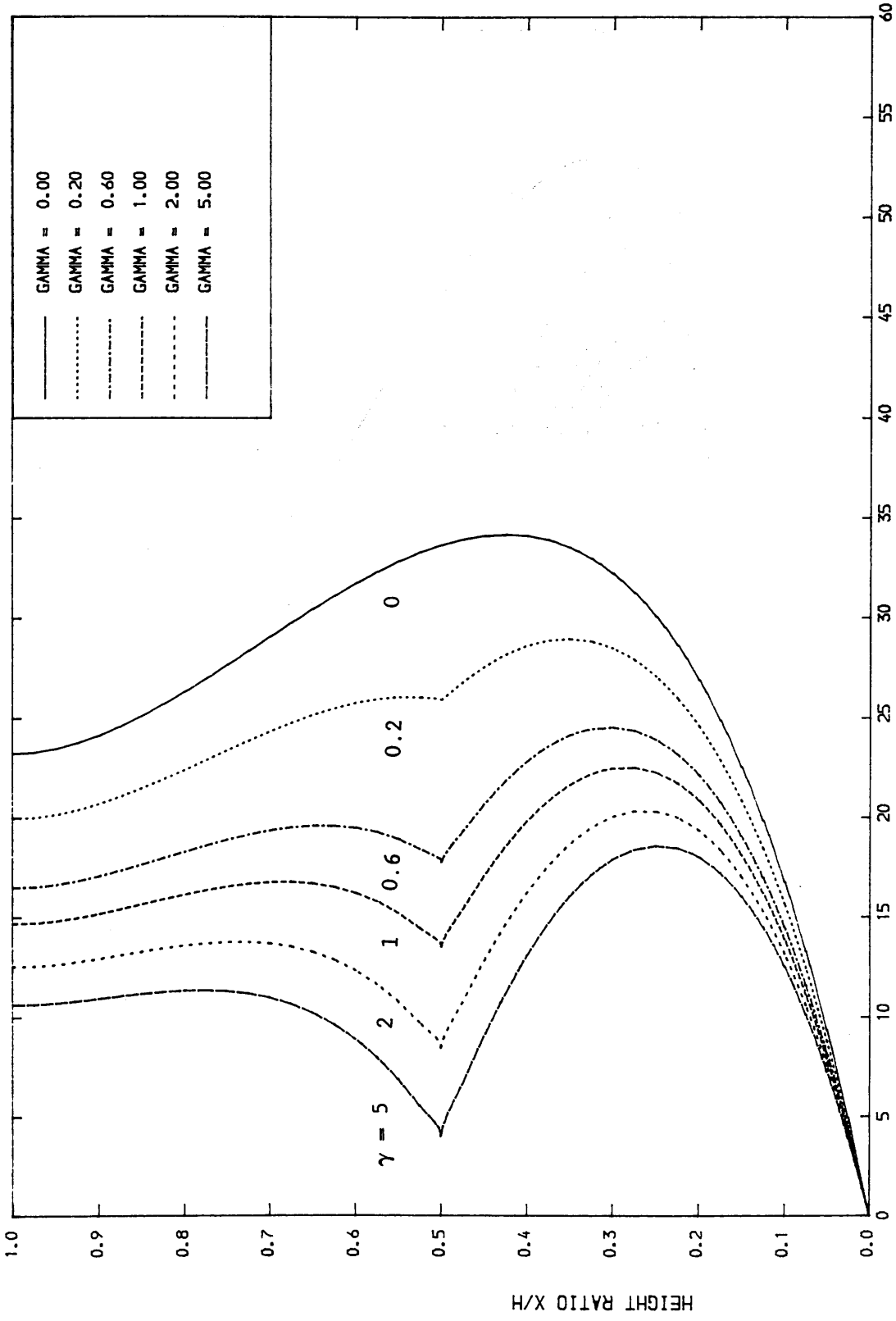

Fig.5.7. VARIATION OF LAMINAR SHEAR WITH HEIGHT RATIO FOR DIFFERENT RELATIVE FLEXURAL RIGIDITY OF STIFFENING BEAM. (X1/H=0.5, K=3.0)

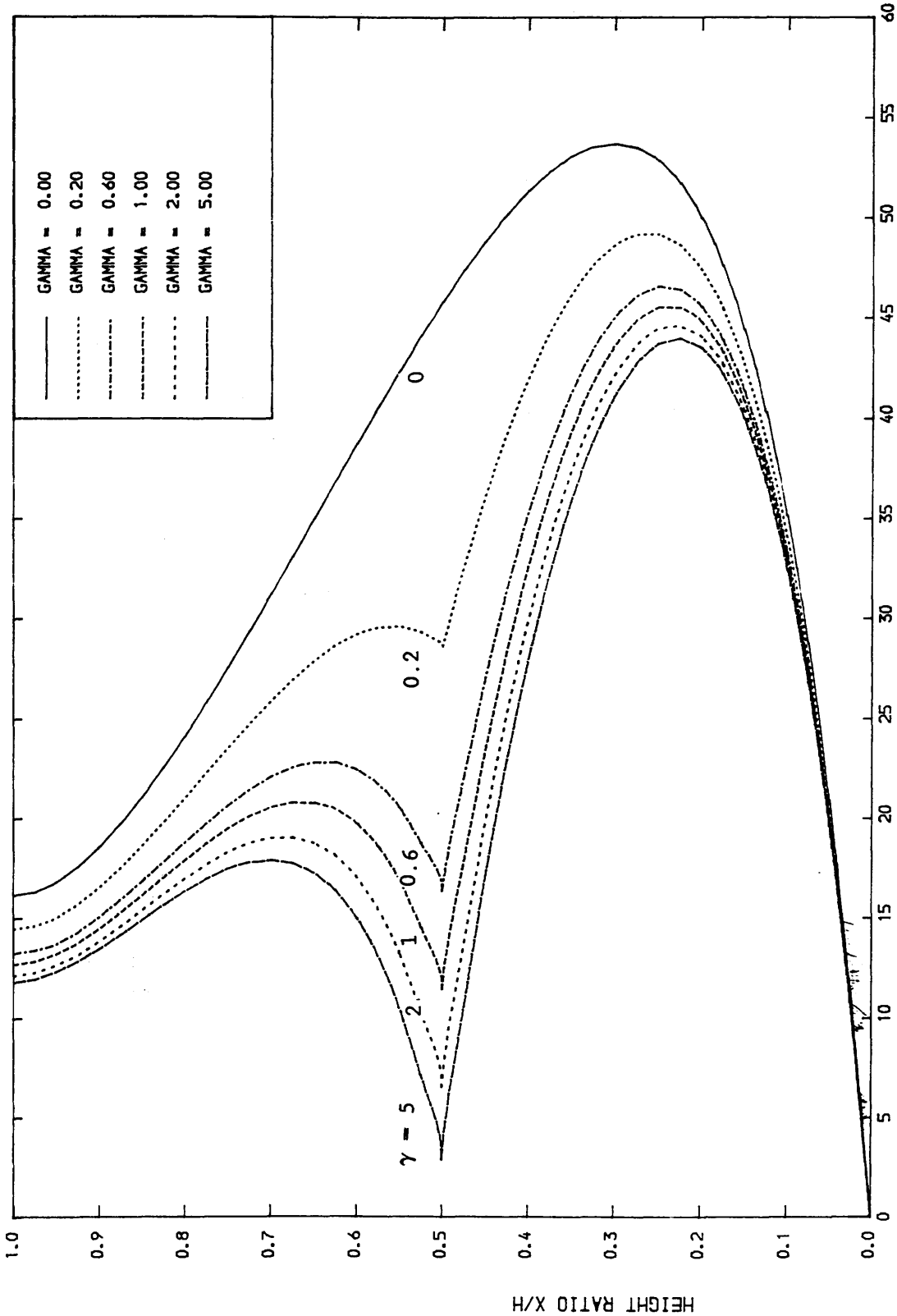

Fig.5.8. VARIATION OF LAMINAR SHEAR WITH HEIGHT RATIO FOR DIFFERENT RELATIVE FLEXURAL RIGIDITY OF STIFFENING BEAM. (X1/H=0.5, K=6.0)

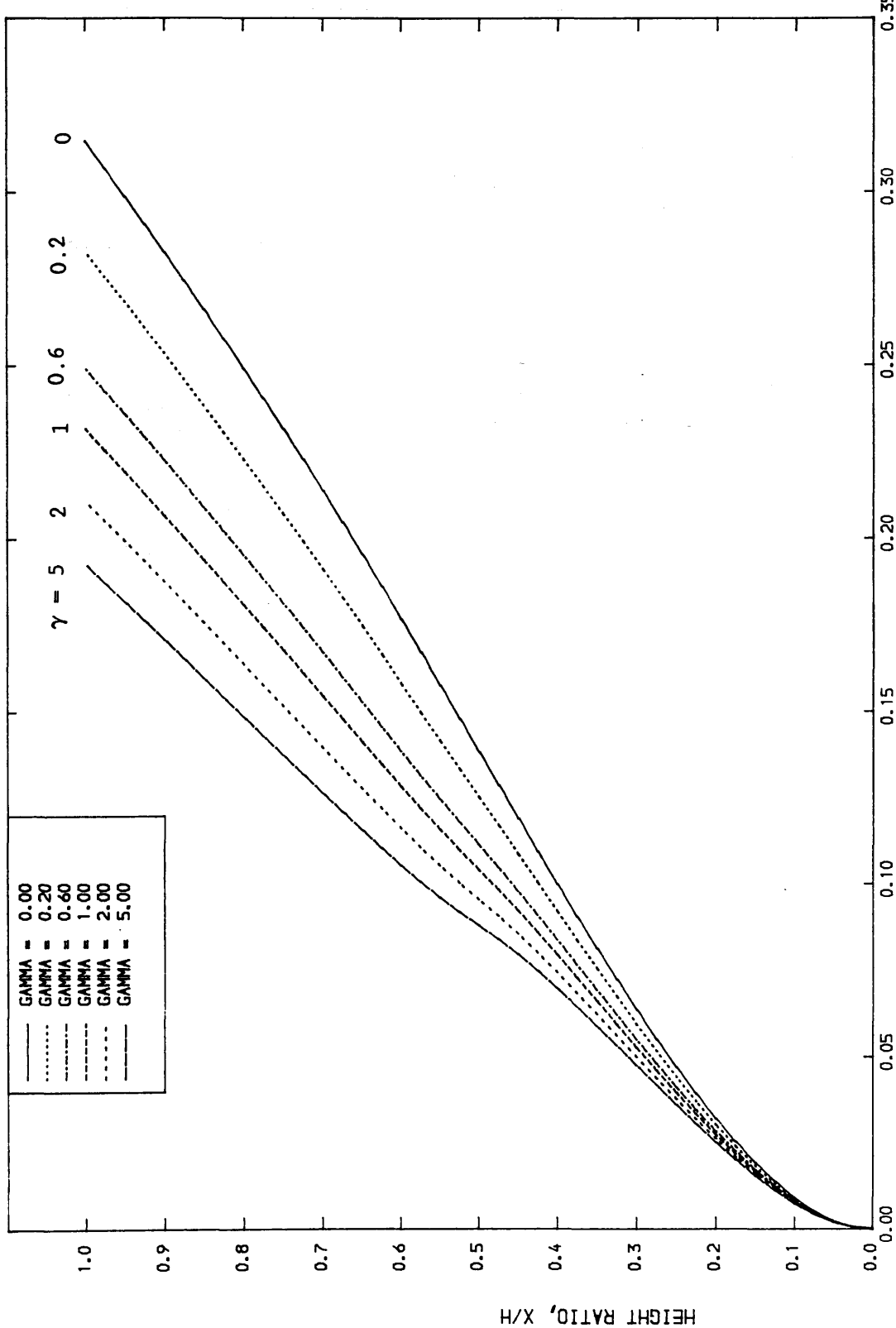

Fig.5.9. VARIATION OF LATERAL DEFLECTION WITH HEIGHT RATIO FOR DIFFERENT RELATIVE FLEXURAL RIGIDITY OF STIFFENING BEAM. (X1/H=0.5, K=3, Sd=0.9)

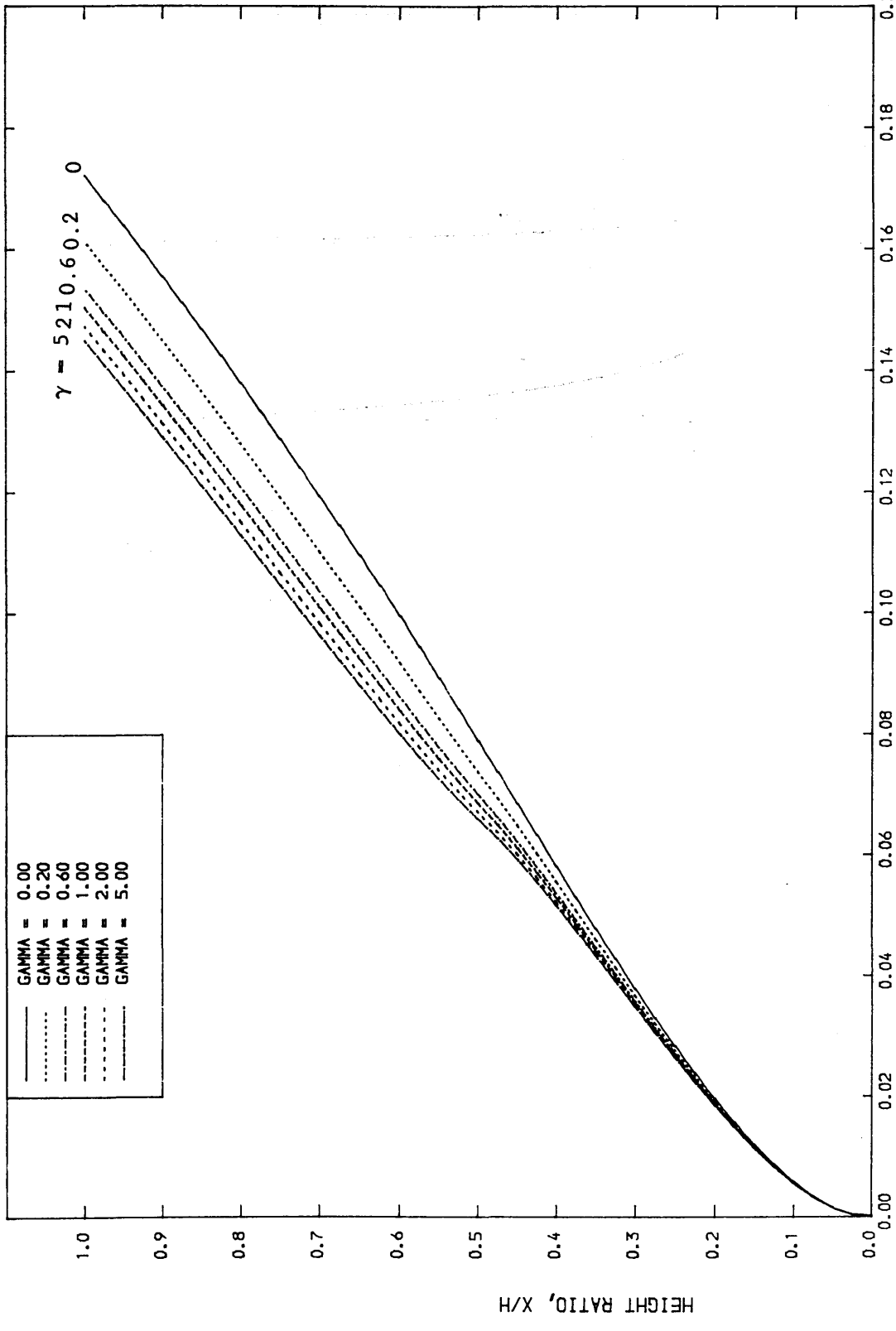

Fig.5.10. VARIATION OF LATERAL DEFLECTION WITH HEIGHT RATIO FOR DIFFERENT RELATIVE FLEXURAL RIGIDITY OF STIFFENING BEAM. (X1/H=0.5, K=6, Sd=0.9)

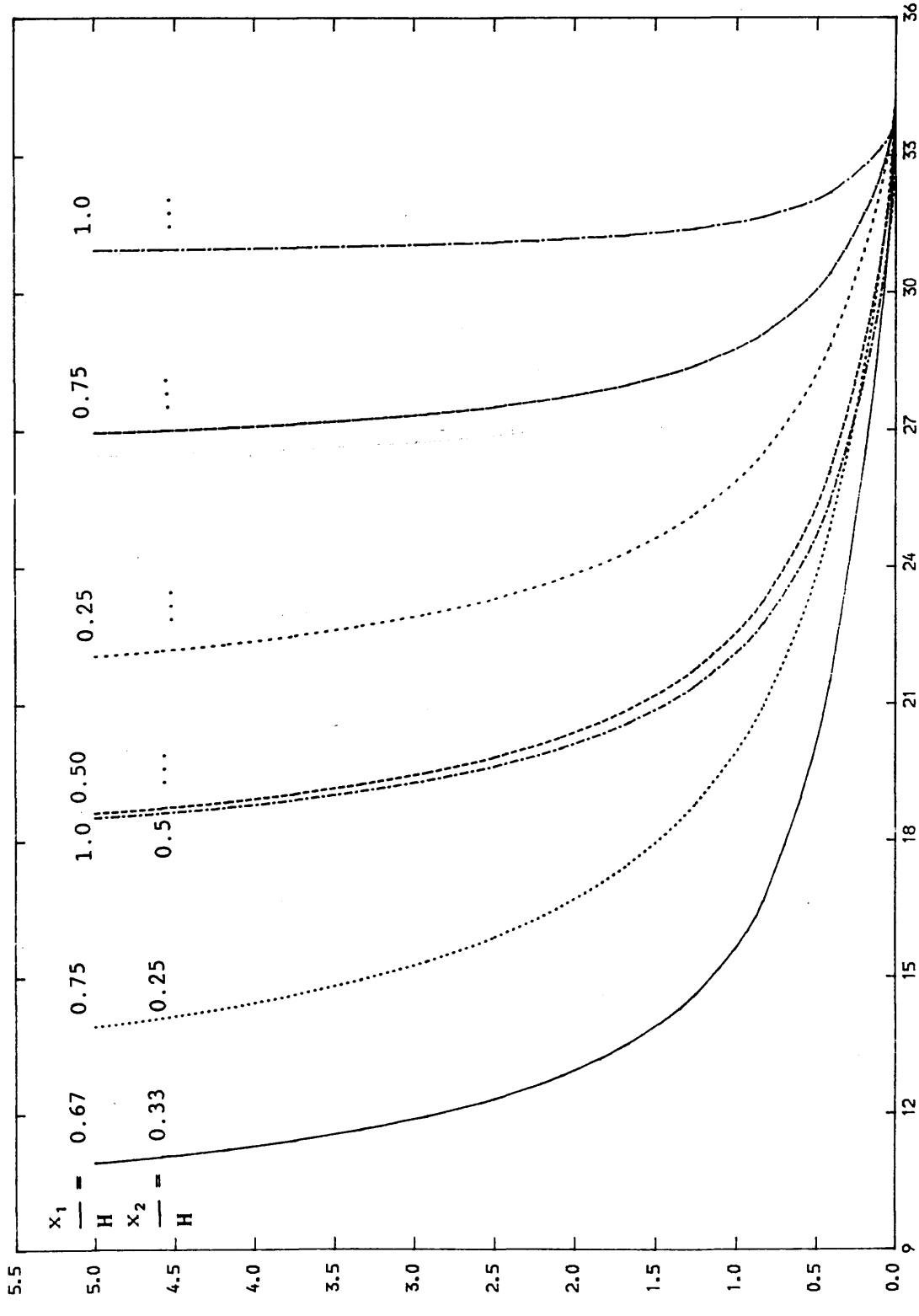

Fig.5.11. VARIATION OF MAXIMUM LAMINAR SHEAR WITH RELATIVE FLEXURAL RIGIDITY OF STIFFENING BEAMS FOR DIFFERENT STIFFENING BEAM LOCATIONS (K=3)

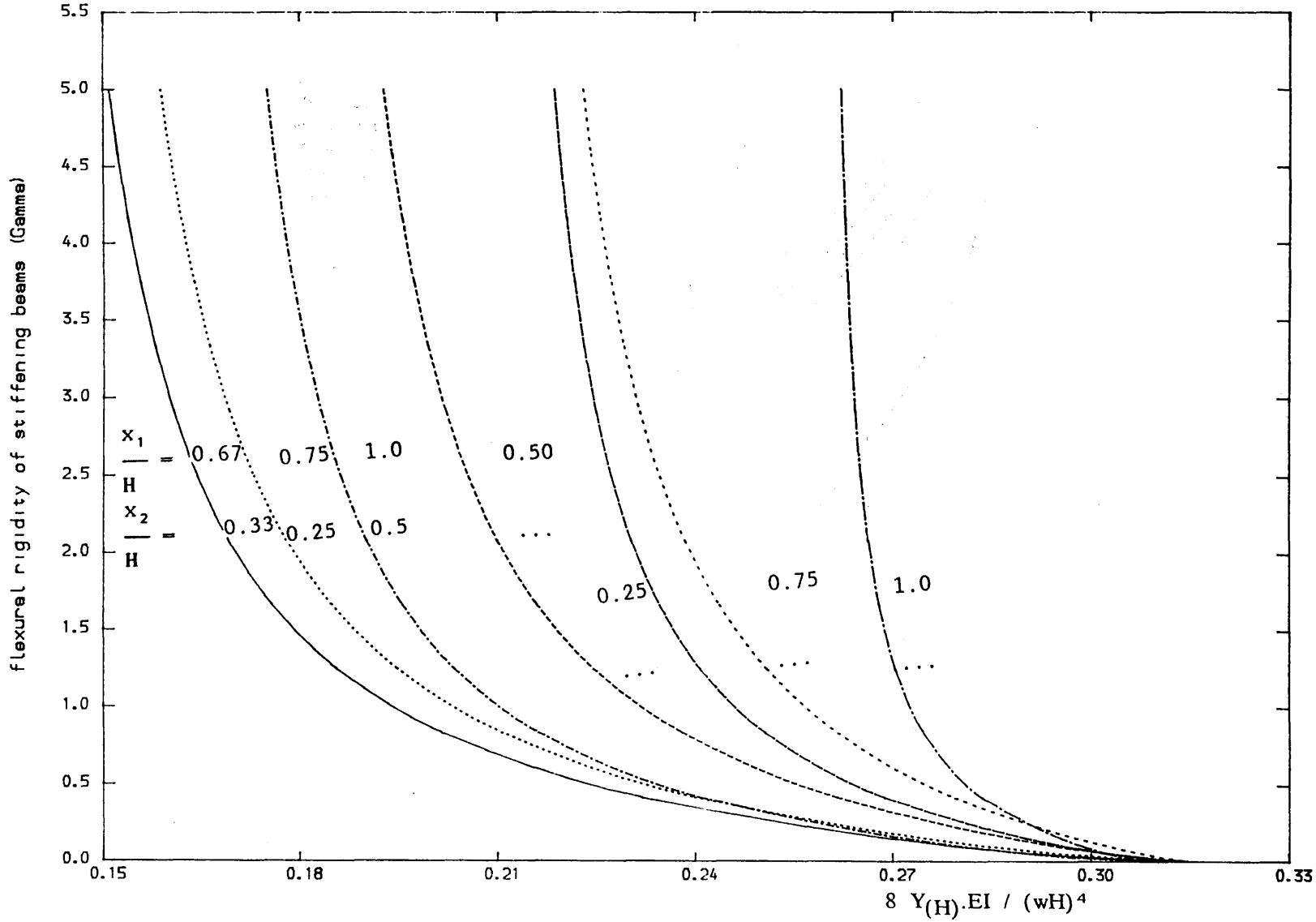

Fig. 5.12. VARIATION OF TOP DEFLECTION WITH RELATIVE FLEXURAL RIGIDITY OF STIFFENING BEAMS FOR DIFFERENT STIFFENING BEAM LOCATIONS (K=3, Sd=0.9)

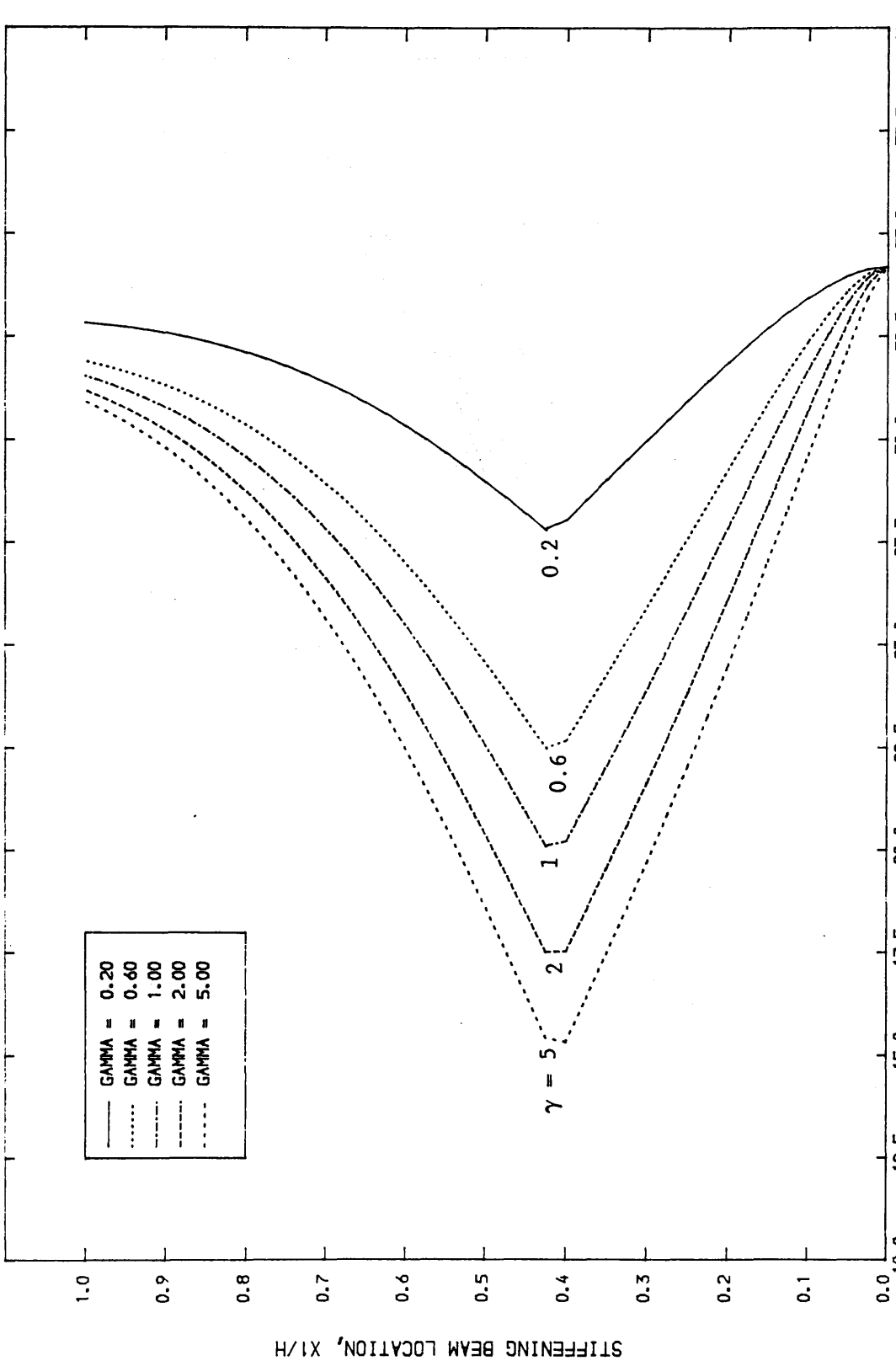

Fig.5.13. EFFECT OF STIFFENING BEAM LOCATION ON MAXIMUM LAMINAR SHEAR K=3.0

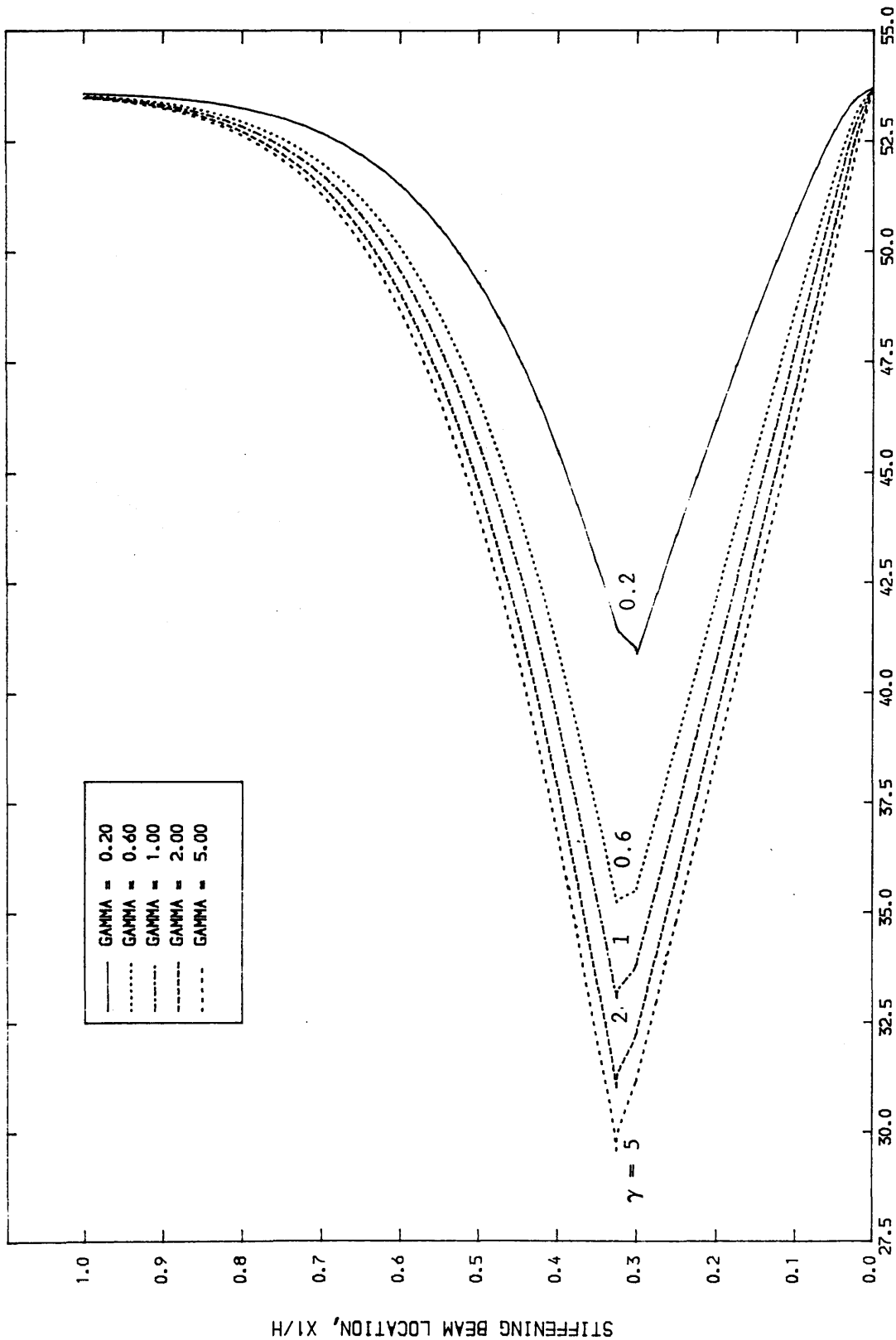

Fig.5.14. EFFECT OF STIFFENING BEAM LOCATION ON MAXIMUM LAMINAR SHEAR K=6.0

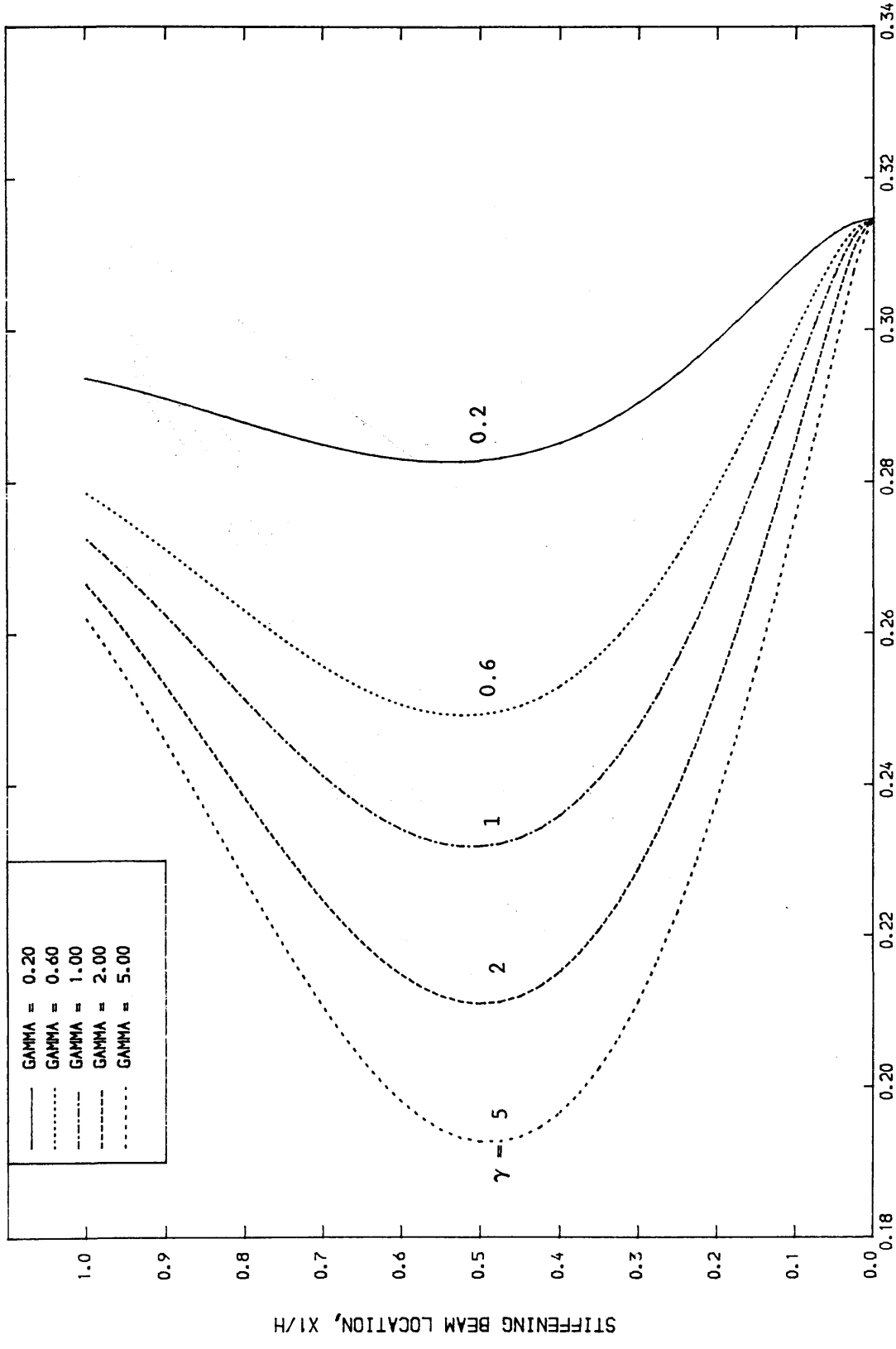

Fig.5.15. EFFECT OF STIFFENING BEAM LOCATION ON TOP DEFLECTION
K=3.0, Sd = 0.9

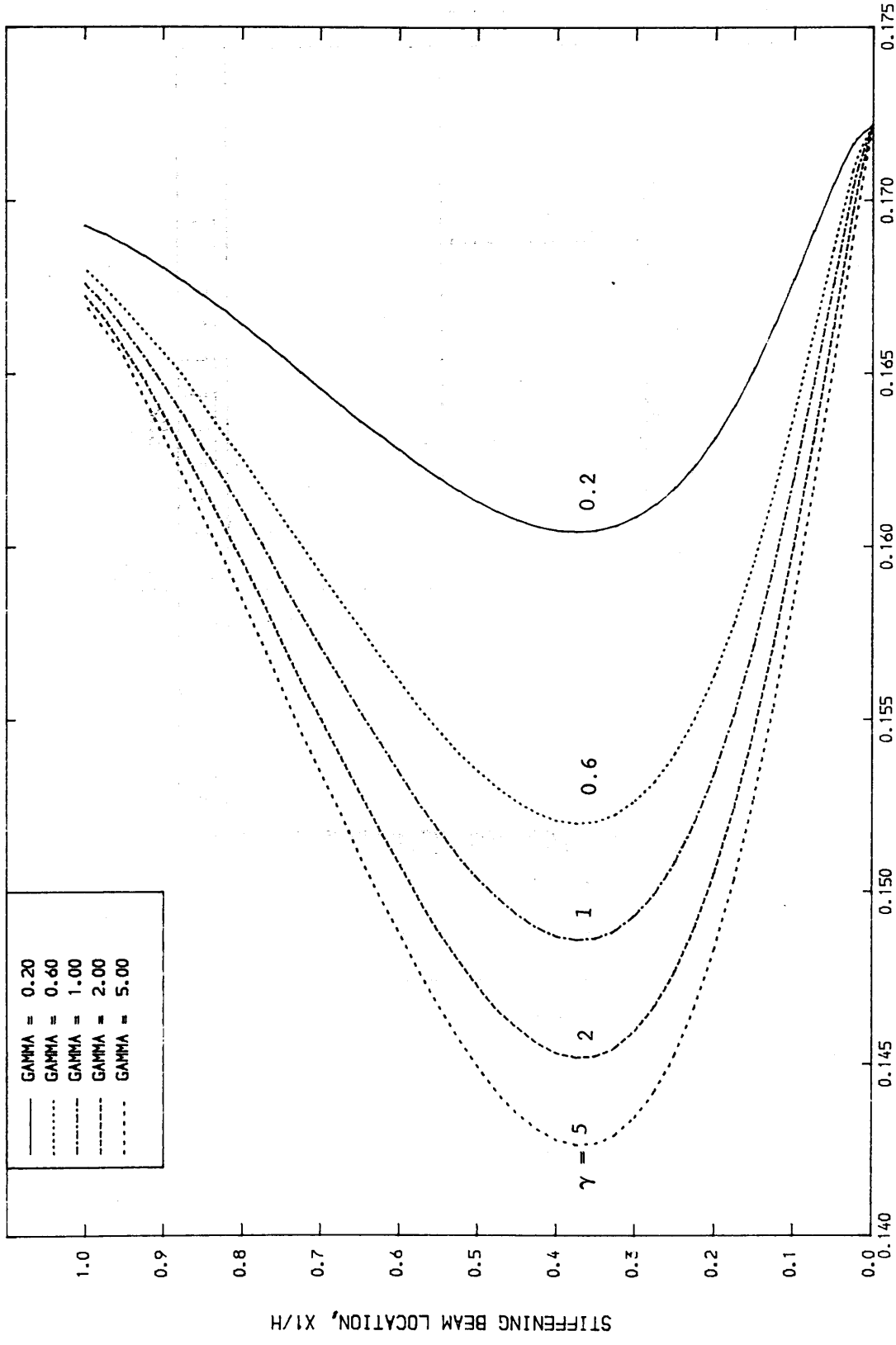

Fig.5.16. EFFECT OF STIFFENING BEAM LOCATION ON TOP DEFLECTION
K=6.0, Sd = 0.9

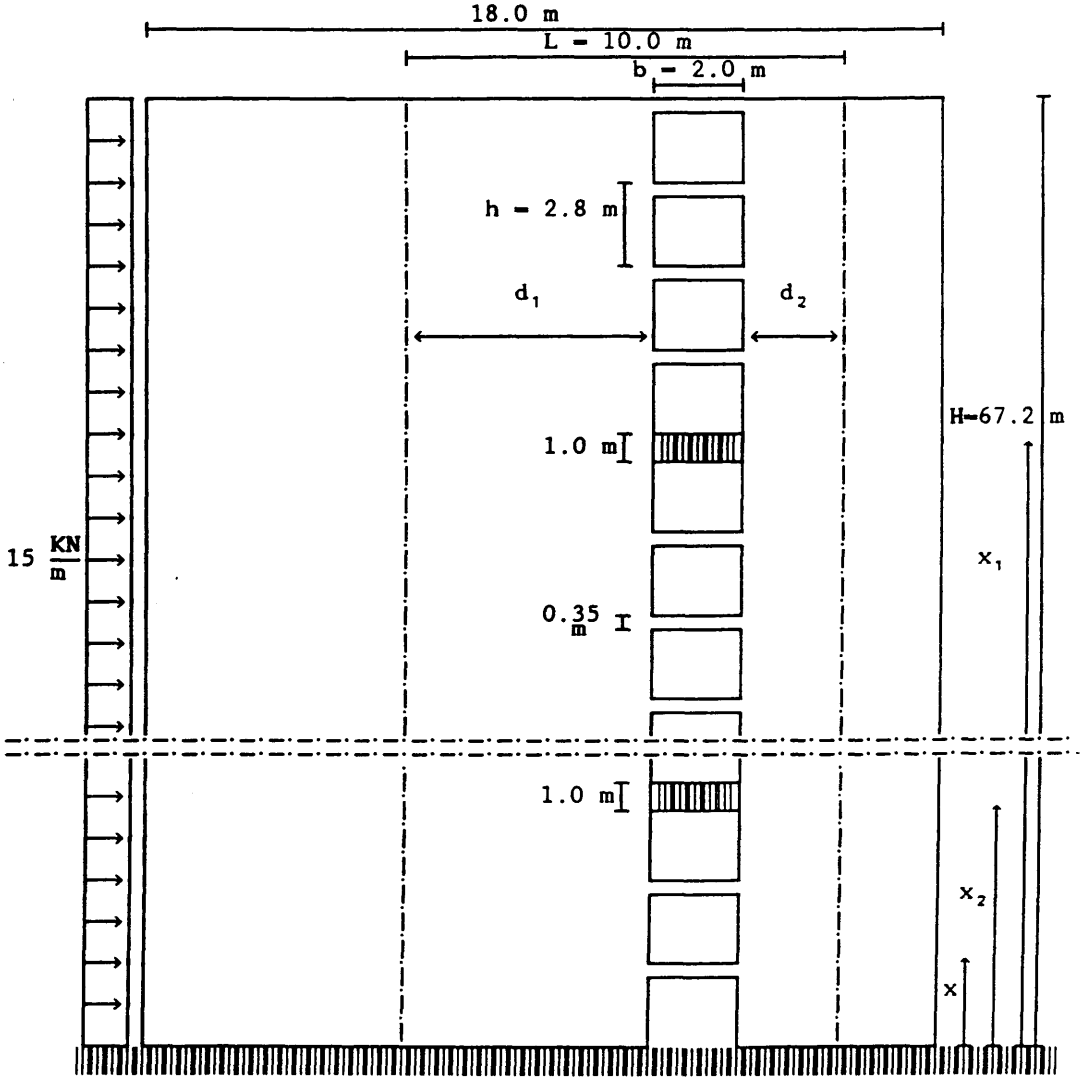

Elevation

Shear wall cross section

Coupling beam section (0.35 × 0.20 m)
Stiffening beam section (1.0 × 0.20 m)
Inertia of main beams $I_b = 7.14\ 10^{-4}\ m^4$
Inertia of the stiffening beams $I_{f_1} = I_{f_2} = 16.67\ 10^{-2}\ m^4$
$\gamma_1 = \gamma_2 = 0.93$
$E = E_{m1} = E_{m2} = 2.0\ 10^7\ KN/m$
$d_1 + d_2 = 8.4\ m$
(a) $d_1 = d_2 = 4.0\ m$, $\alpha H = 3.51$
(b) $d_1 = 6.0\ m$, $\alpha H = 2.94 \simeq 3.0$
$d_2 = 2.0\ m$

Fig. 5.17

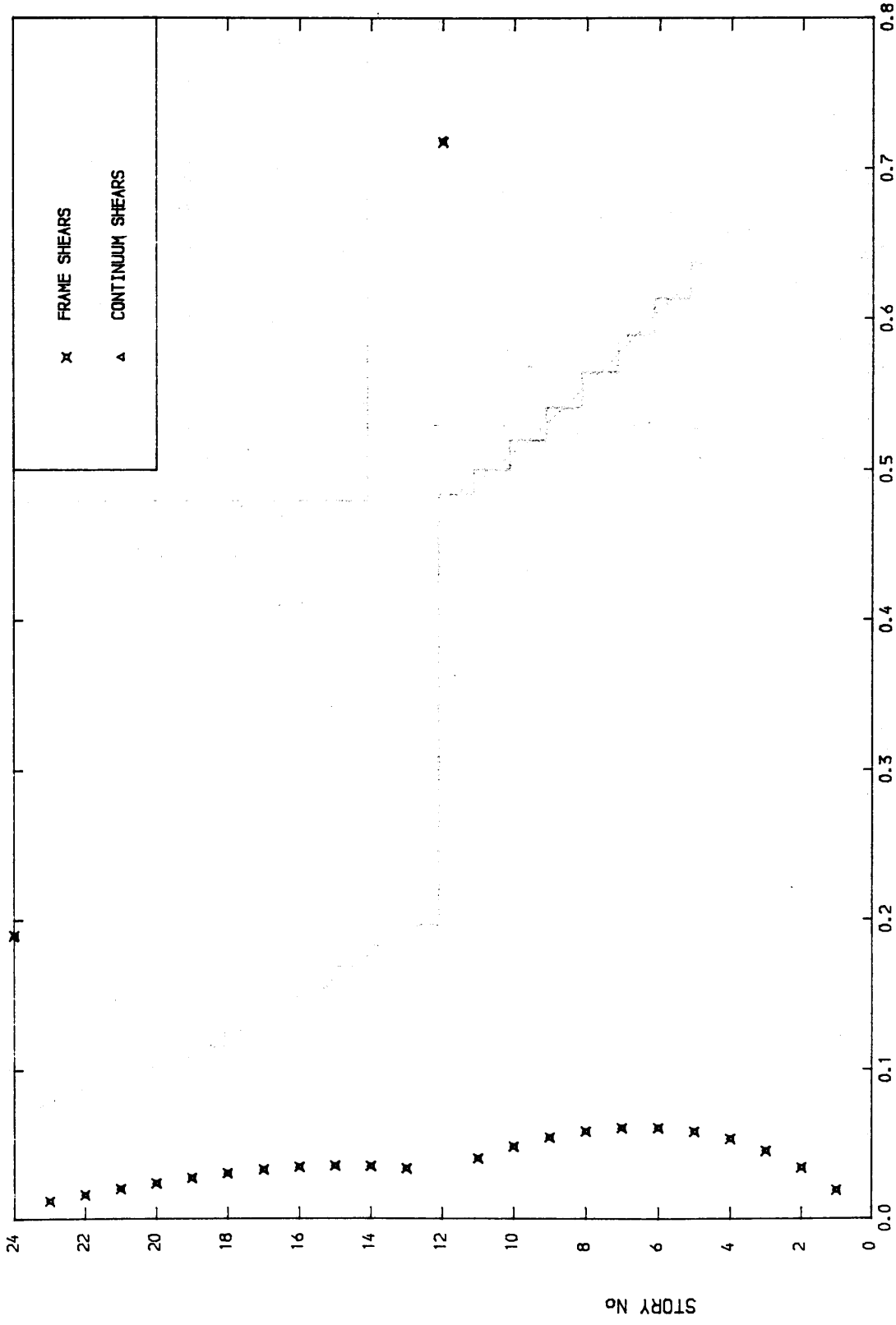

Fig.5.18. SHEARS IN BEAMS ($\lambda_1 = d_1/d_2 = 1$)
X1/H=1.0, X2/H=0.5

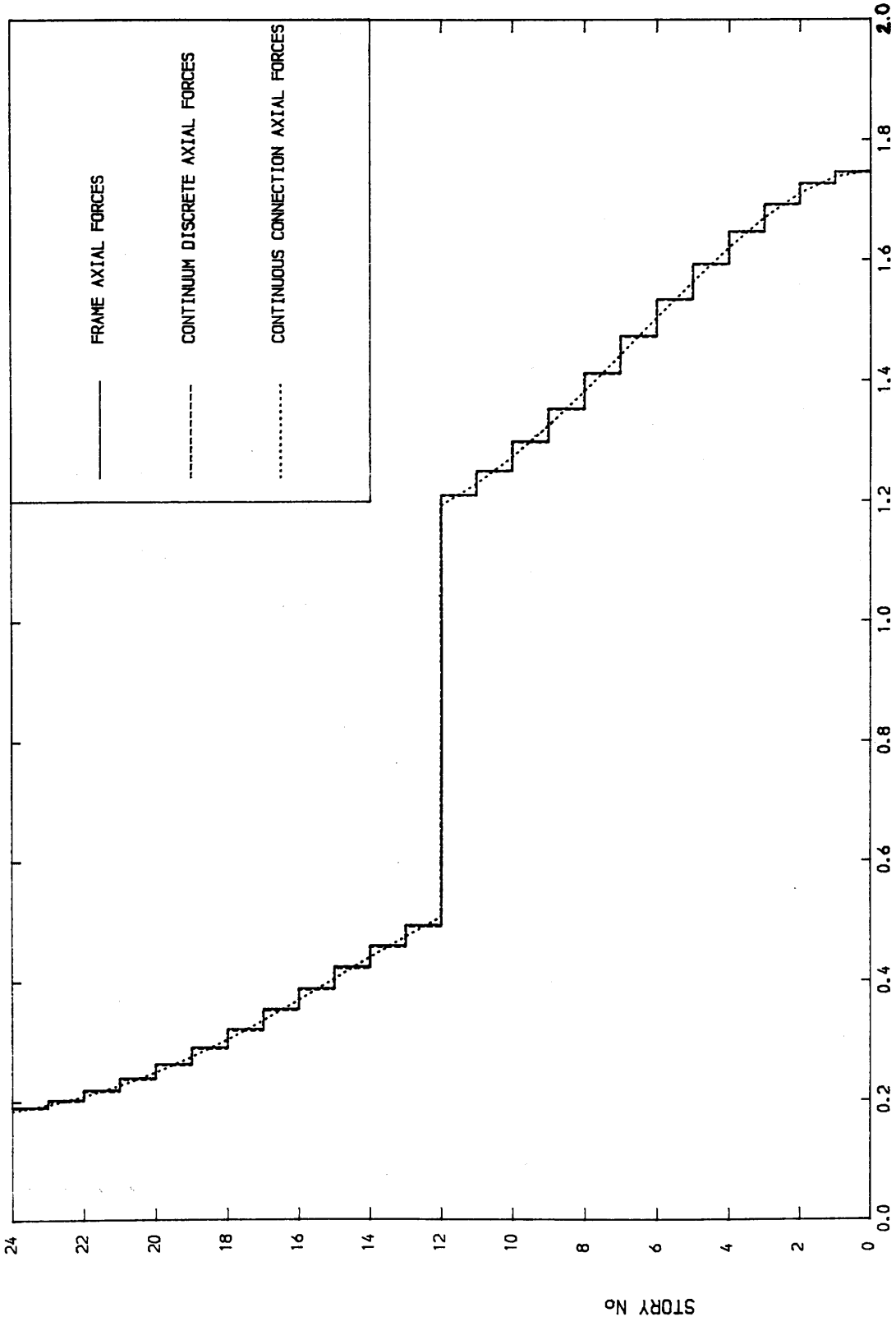

Fig.5.19. AXIAL FORCES IN WALLS ($\lambda_1 = d_1 / d_2 = 1$)
X1/H=1.0, X2/H=0.5

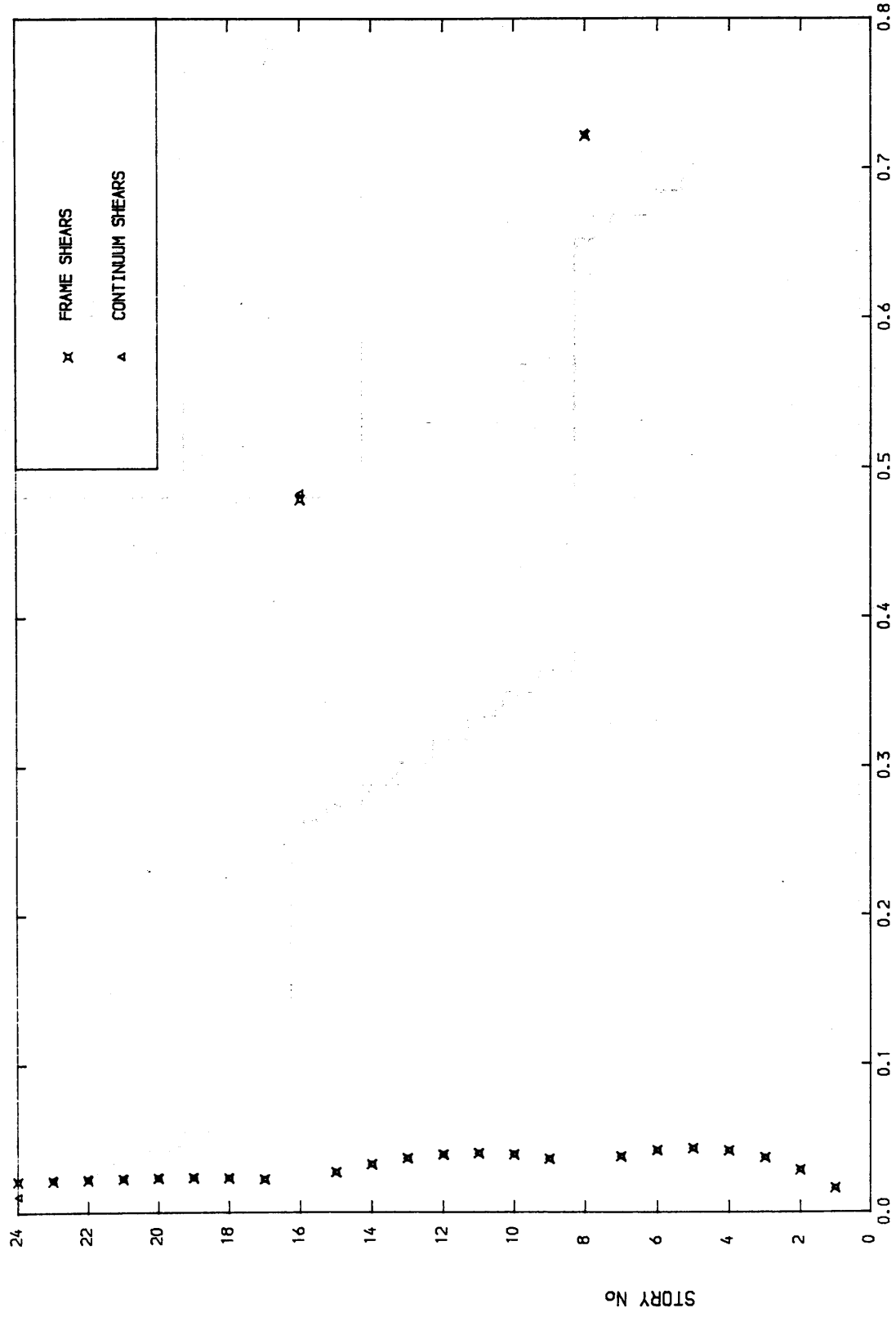

Fig. 5.20. SHEARS IN BEAMS ($\lambda_1 = d_1 / d_2 = 1$) X1/H=2/3, X2/H=1/3

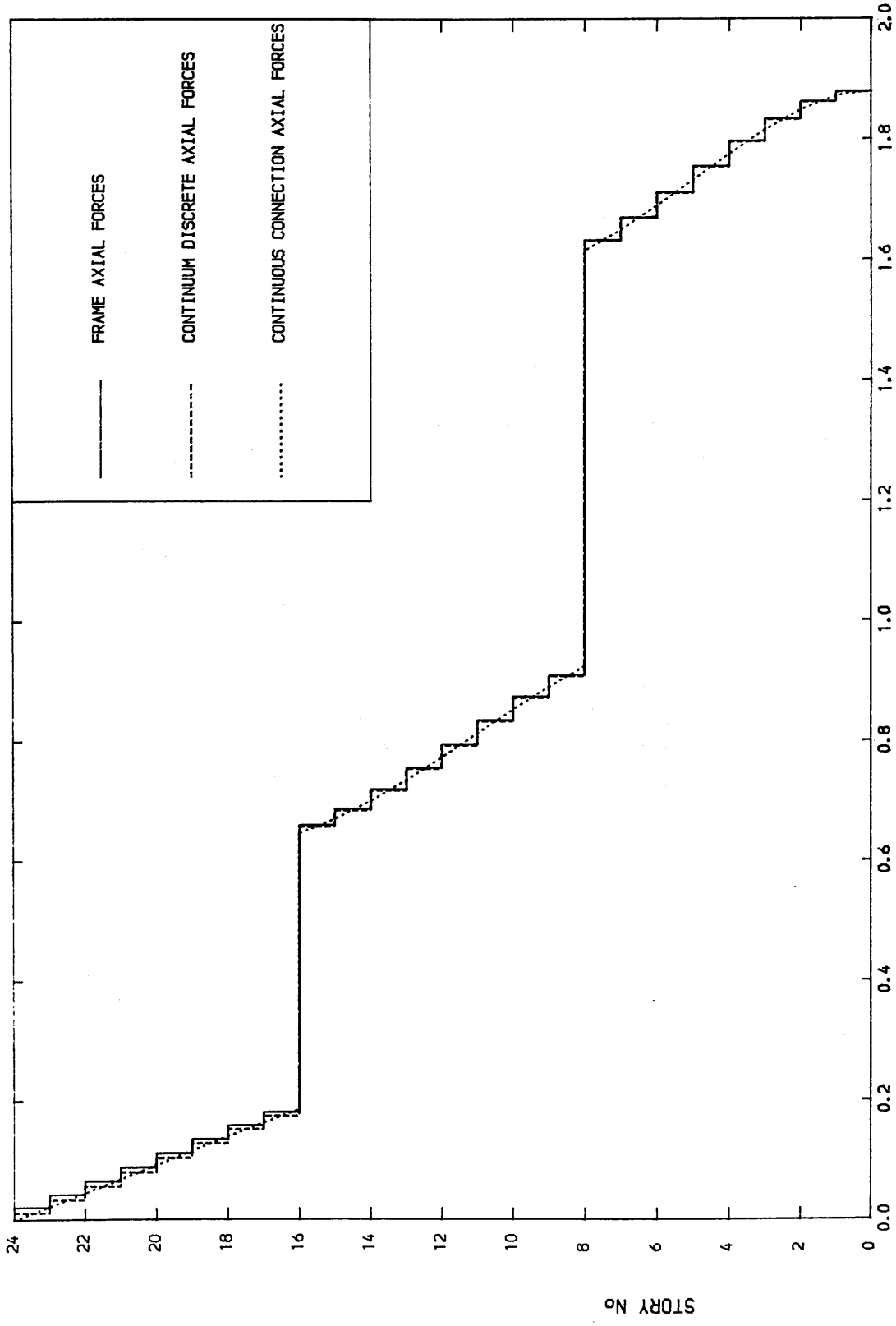

Fig.5.21. AXIAL FORCES IN WALLS ($\lambda_1 = d_1 / d_2 = 1$)
X1/H=2/3, X2/H=1/3

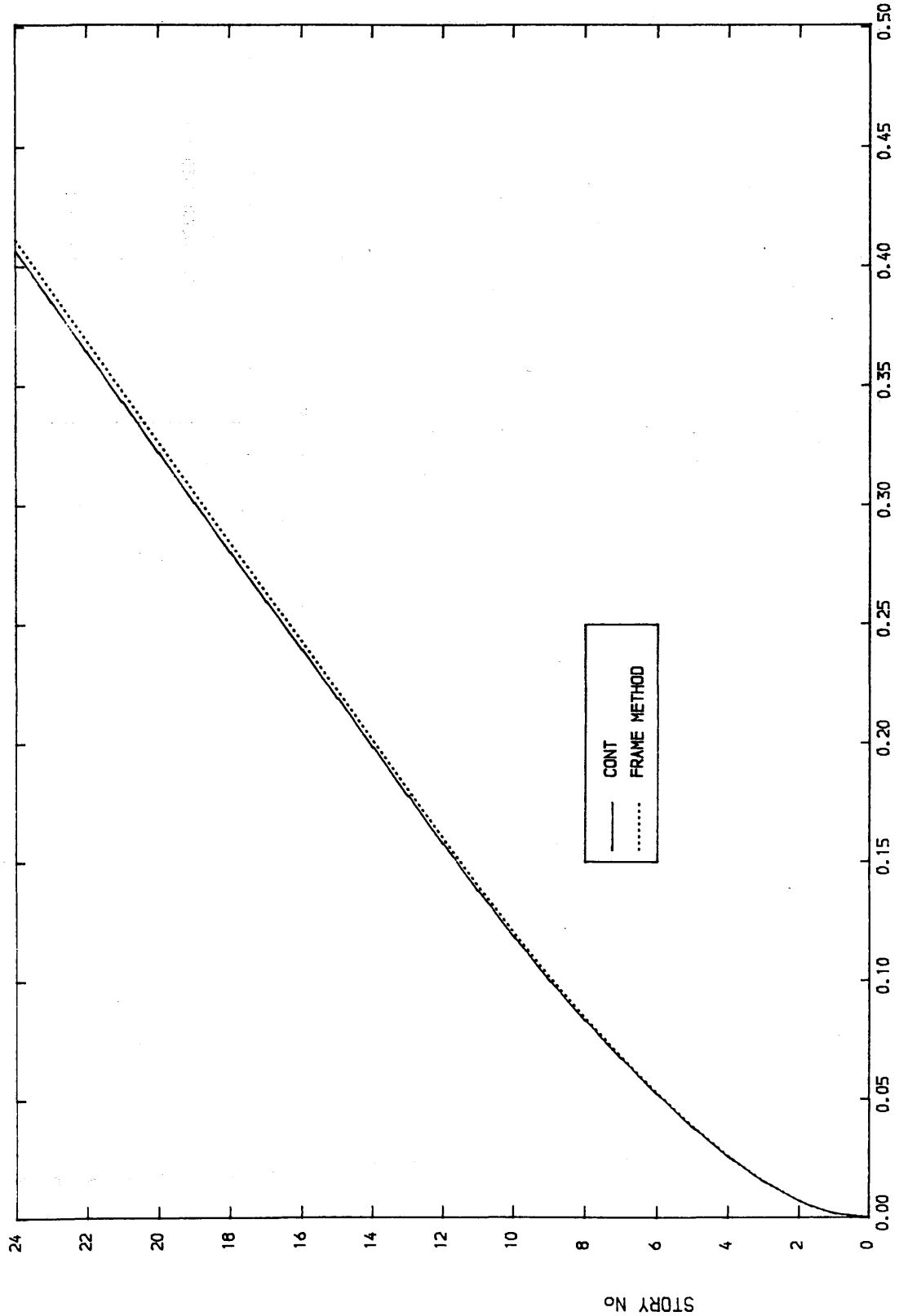

Fig.5.22. LATERAL DEFLECTION ($\lambda_1 = d_1/d_2 = 3$)
X1/H=2/3, X2/H=1/3

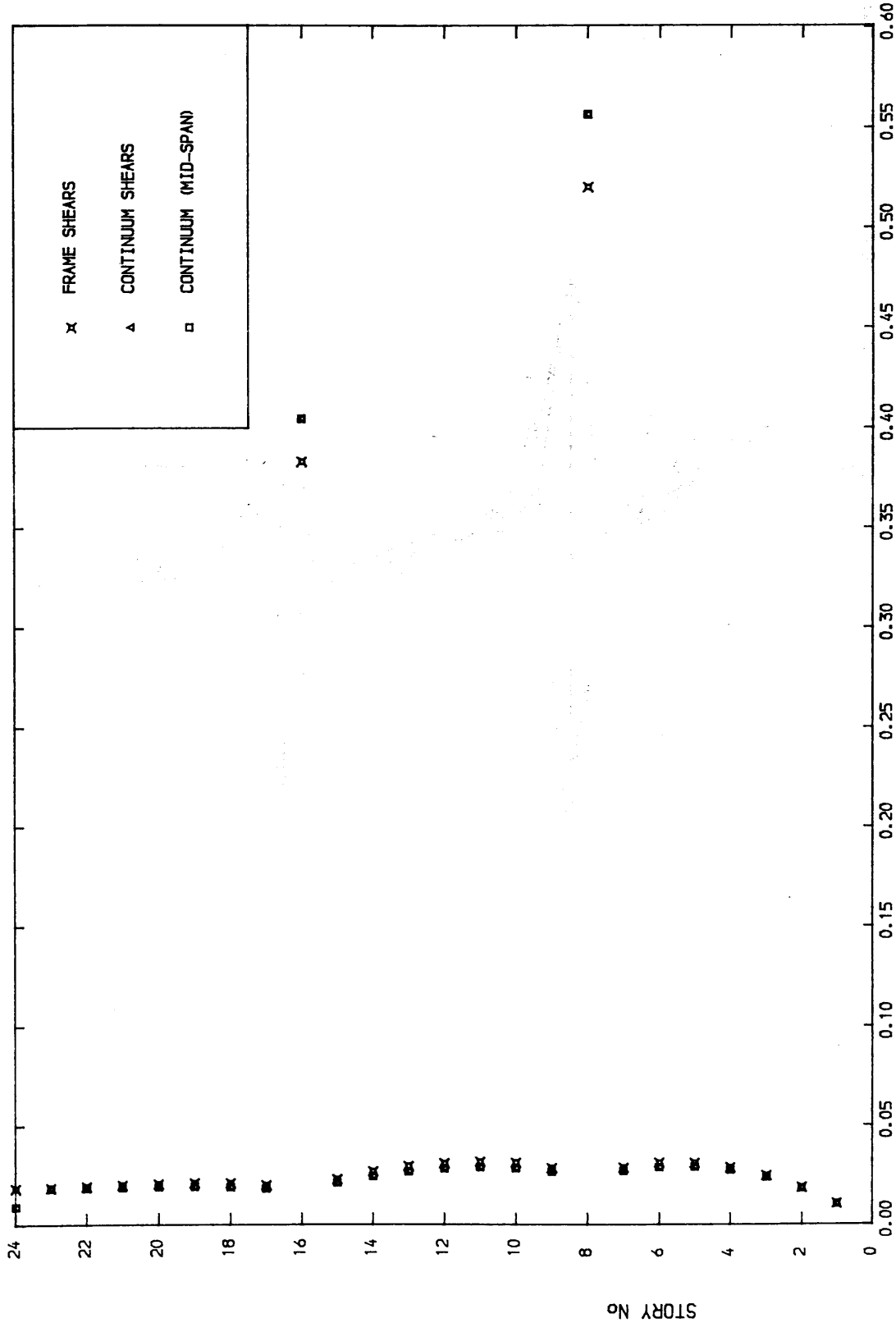

Fig. 5.23. SHEARS IN BEAMS ($\lambda_1 = d_1 / d_2 = 3$) X1/H=2/3, X2/H=1/3

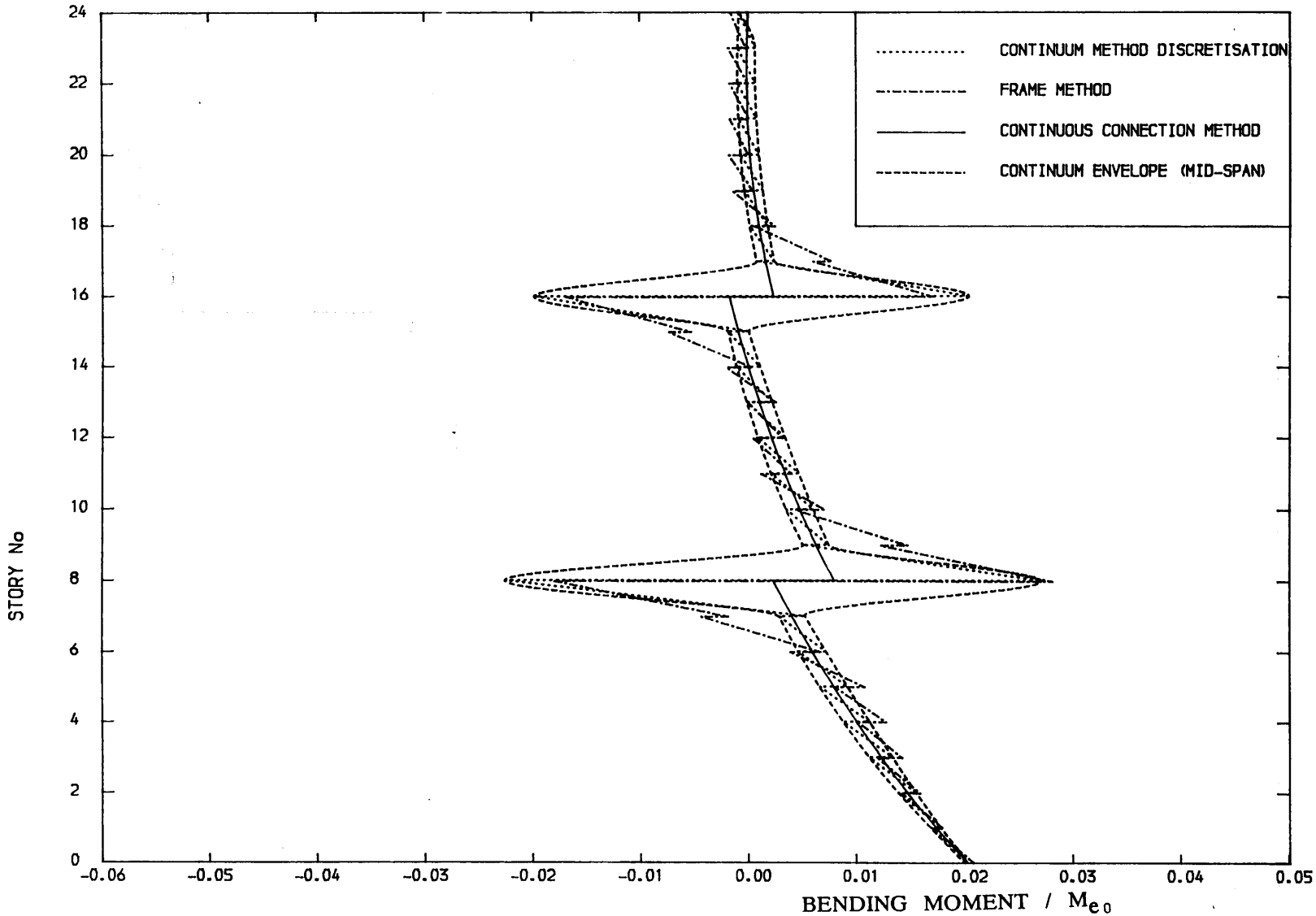

Fig. 5.24. MOMENTS IN WALL2 ($\lambda_1 = d_1/d_2 = 3$)
X1/H=2/3, X2/H=1/3 ALTERNATIVE CALCULATION

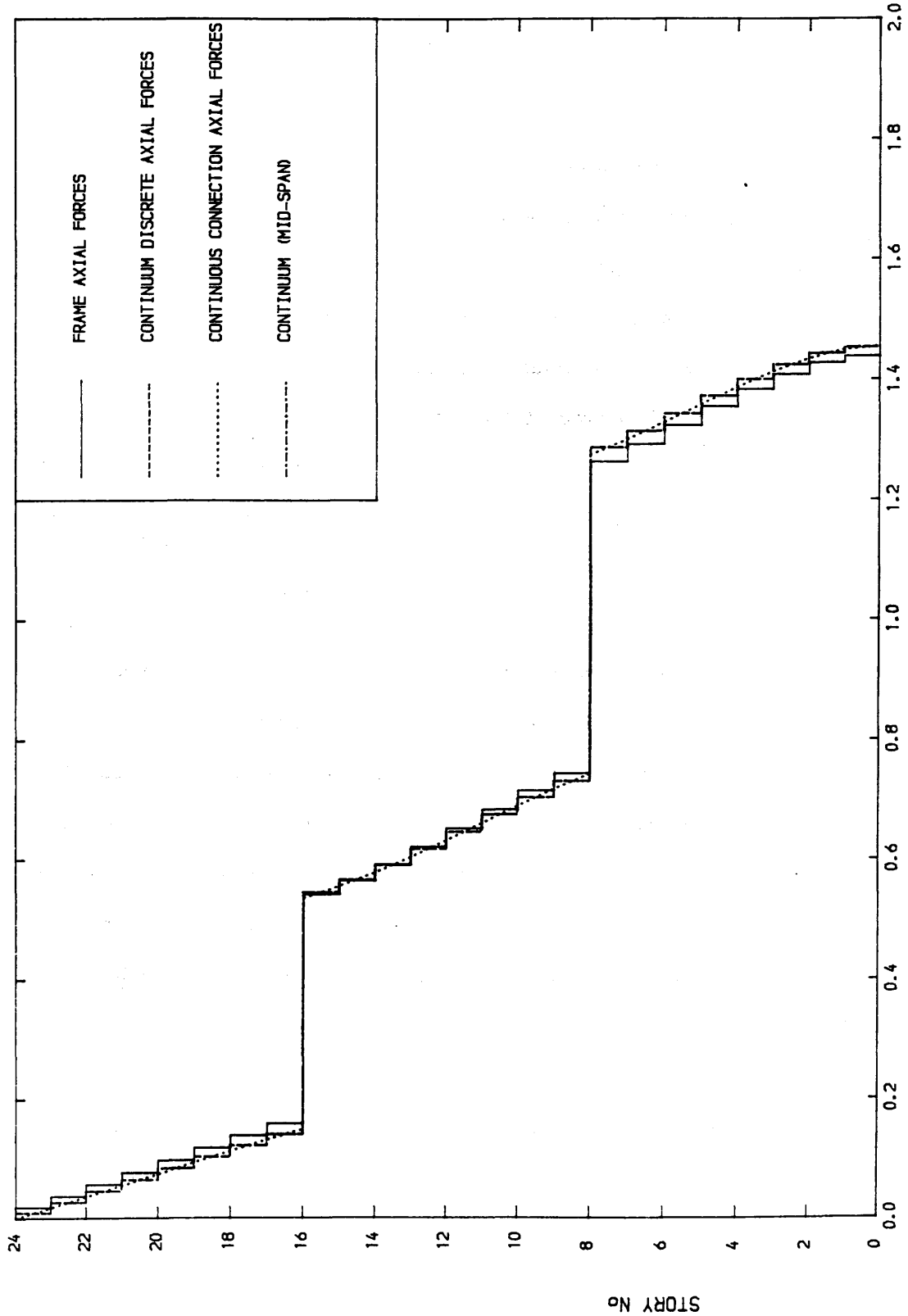

Fig. 5.25. AXIAL FORCES IN WALLS ($\lambda_1 = d_1/d_2 = 3$)
X1/H=2/3, X2/H=1/3

CHAPTER SIX

CONCLUSIONS

Based on the continuous connection method, revised continuum analyses have been presented for unstiffened coupled shear walls, coupled shear walls with a top stiff beam and shear walls with stiffening beams at one or more levels at any position along the height of the structure, supported on rigid or elastically deformable foundations and subjected to lateral loads. The revised analysis uses a modification to the assumed line of contraflexure, and gives formulas by which its position may be calculated. The method of including the top boundary condition has also been considered in the analysis so that a better modelling of the structure is achieved, and an alternative discrete calculation of the wall moments is shown to be necessary.

These analyses have enabled an examination to be carried out of the effects of the unsymmetry of the structure, especially when one wall is much smaller compared to the other wall, and the introduction of stiffening beams and their locations on the behaviour of a number of example structures. For coupled shear wall structures with unequal walls, and using the revised line of contraflexure, the relative flexural rigidity of lintel beams is reduced by up to 50% compared to the relative flexural rigidity of lintel beams using the conventional mid-span position of the line of contraflexure for the extreme case of a wall connected to a column by beams. This means that the assumption of the conventional mid-span position of the line of contraflexure overestimates the relative flexural rigidity of the lintel beams.

Inconsistencies occur when using the conventional mid-span position

of the line of contraflexure. In particular, a fictitious concentrated interactive force is found to exist in the connecting medium at the top of the structure. The magnitude of this force can reach up to 10% of the total applied lateral load, for certain geometrical situations. However, this force may be reduced by up to 90% by using the revised line of contraflexure. It has been shown that for the case of a wall connected to a column, the shift of the line of contraflexure is of interest only when the relative bending stiffness of the smaller wall λ_3 (= $I_2 b/I_b h$) is less than about 5. When the relative bending stiffness λ_3 is greater than about 5, the results are not substantially altered by the revised line of contraflexure. Also, the most important move of the line of contraflexure in this case is accompanied by values of the relative bending stiffness λ_3 less than 1.0. Therefore, for λ_3 below 5, the accuracy of the continuum method using the conventional mid-span assumption falls off sharply and may not be acceptable. However, the position of the point of contraflexure at the top beam to that of the main beams Δ_t/Δ is shown to depend on the width ratio λ_1 and the relative bending stiffness λ_3, for λ_1 and λ_3 less than about 3 and 5 respectively. For a width ratio more than about 3, the ratio Δ_t/Δ depends only on the relative bending stiffness λ_3. However, for values of the relative bending stiffness λ_3 over 5, Δ_t/Δ is constant and is equal approximately to 2, which means that for values of λ_3 greater than about 5, the shift in the point of contraflexure in the top beam can be twice the shift in the line of contraflexure in the other beams.

The introduction of stiffening beams induces higher wall axial forces and consequently reduces the bending moments in the walls. The wall lateral deflections and beam laminar shears are also reduced. The provision of two stiffening beams of the same stiffness has a greater effect on the overall behaviour of the structure than one stiffening beam only. However, the locations of the stiffening beams are also very important and smaller

deflections and laminar shears are obtained with two stiffening beams located at one third and two thirds of the height of the structure compared to locations at the top and mid-height or at one quarter and three quarters of the height. The effect of one stiffening beam only however, is greatest when the location is around the mid-height position for the maximum top deflection and between 0.4 and 0.5 for the maximum laminar shear.

A number of non-dimensional curves showing the magnitude of the top concentrated interactive shear force, the beam relative stiffness reduction factors, the position of the line of contraflexure for the extreme case of a wall connected to a column, and the point of contraflexure ratio (Δ_t/Δ) have been presented. For the case of a shear wall with stiffening beams at one or more levels, resting on rigid foundations, and subjected to uniformly distributed lateral loads, design curves have been presented to illustrate the effects of the stiffening beams and their locations on the distribution of the laminar shear over the height of the structure, the lateral deflections of the structure, the magnitude of the maximum laminar shear and the maximum deflection. These curves show that the stiffening beams are more effective in improving the behaviour of the structure only when the stiffness parameter k is relatively small, say, less than about 4 or 5.

From an investigation of the behaviour of representative model structures supported on rigid foundations and subjected to a uniformly distributed lateral load, comparative study has been carried out to test the continuum results with those obtained from the frame method. The results are given in a non-dimensional graphic form.

These curves show that the revised position of the line of contraflexure is in good agreement with the one given by the frame method in all cases. Also the lateral deflections of the structure have shown very good accuracy. For the case of an unstiffened shear wall structure, the

shears and moments in the smaller wall are generally not altered by the revised line of contraflexure for small width ratios λ_1 provided that the structure is not stiffened. However, for bigger wall ratios, especially for the extreme case of a wall connected to a column, the accuracy of the continuum method using the conventional mid-span assumption falls off sharply. But the results using the revised line of contraflexure are accurate enough for practical purposes.

For the case of coupled shear walls stiffened at the top of the structure or at one or more levels along the height, the shears and moments in the smaller wall obtained after discretisation show very poor accuracy when the original calculation is used. the accuracy in the moments is greatly improved by the alternative calculation presented in Chapters 2 and 4, (sections 2.3 and 4.3.3 respectively), which assumes that the beam moment is distributed equally between the stories above and below the level concerned. These alternative moments have shown good accuracy in all circumstances. The discrete shears in the beams have been satisfactory in general apart from some small discrepancies which arise at the stiffening beam levels with the increase of the stiffness of these beams. The wall axial forces increase with the increase in the stiffness of the stiffening beams and are of acceptable accuracy.

Conclusions based on numerical investigations on a representative structure and their generality might be questioned. However, the range of structures investigated included a fairly extensive range of the parameters which govern the behaviour of coupled shear walls, (especially k, H, and $\beta^2/\alpha^2.L$) and it is expected that the conclusions should be of general application.

APPENDIX A.

Expression of the continuum method theory equations in dimensionless form for stiffened walls.

It is useful to express the equations for q, T and y in dimensionless form to enable design curves to be drawn.

Consider the special case of coupled shear walls on rigid foundations. By substituting for B_1, B_2, B_3, C_1, C_2 and C_3 from equations (4.52) into equations (4.30), (4.31), (4.49), (4.50) and (4.51) the axial force in the walls T_i, the laminar shear q_i, and the lateral deflection y_i, and also the percentage of individual and composite cantilever action $(K_1)_i$ and $(K_2)_i$ in the three zones, and the shear forces V_{m1} and V_{m2} in the stiffening beams for a coupled shear wall supported on rigid foundations and subjected to the load patterns shown in fig. 1 are given by

$$T_i = \frac{\beta^2}{\alpha^2} H T_i^* \quad \ldots\ldots\ldots\ldots\ldots\ldots\ldots\ldots\ldots\ldots\ldots\ldots \quad (A.1)$$

$$q_i = \frac{\beta^2}{\alpha^2} q_i^* \quad \ldots\ldots\ldots\ldots\ldots\ldots\ldots\ldots\ldots\ldots\ldots\ldots \quad (A.2)$$

$$y_i = \frac{H^3}{EI} y_i^* \quad \ldots\ldots\ldots\ldots\ldots\ldots\ldots\ldots\ldots\ldots\ldots\ldots \quad (A.3)$$

$$V_{m1} = \frac{\beta_2}{\alpha_2} H V_{m1}^*$$

$$\ldots\ldots\ldots\ldots\ldots\ldots\ldots\ldots\ldots\ldots\ldots\ldots \quad (A.4)$$

$$V_{m2} = \frac{\beta^2}{\alpha^2} H V_{m2}^*$$

$$(K_2)_i = \frac{T_i^*}{M(\xi)} \quad \text{..... (A.5)}$$

$$(K_1)_i = 100 - \frac{T_i^*}{M(\xi)} \quad \text{..... (A.6)}$$

where

$$V_{m1}^* = \gamma_1 \, q_1^*(\xi_1) = \gamma_1 \, q_2^*(\xi_1)$$

$$V_{m2}^* = \gamma_2 \, q_2^*(\xi_2) = \gamma_2 \, q_3^*(\xi_2) \quad \text{..... (A.7)}$$

$$q_i^* = - B_i^*.k \sinh k\xi - C_i^*.k \cosh k\xi + U(1-\xi) + W\left((1-\xi^2) - \frac{2}{k^2}\right) + P \quad \text{..... (A.8)}$$

$$T_i^* = B_i^*.\cosh k\xi + C_i^*.\sinh k\xi + M(\xi) + \frac{U + 2W\xi}{k^2} \quad \text{... (A.9)}$$

$$y_1^* = (1 - S_d)\,\Pi(\xi) + \frac{S_d}{k} F_1^*(\xi) + \frac{S_d}{k^2} F_2^*(\xi) - S_d \xi^2 \left(\frac{U}{2k^2} + \frac{W\xi}{3k^2}\right)$$

$$y_2^* = (1 - S_d)\,\Pi(\xi) + \frac{S_d}{k} F_3^*(\xi) + \frac{S_d}{k^2} F_4^*(\xi) - S_d \xi^2 \left(\frac{U}{2k^2} + \frac{W\xi}{3k^2}\right) \quad \text{..... (A.10)}$$

$$y_3^* = (1 - S_d)\,\Pi(\xi) + \frac{S_d}{k^2} F_5^*(\xi) - S_d \xi^2 \left(\frac{U}{2k^2} + \frac{W\xi}{3k^2}\right). \quad \text{(A.11)}$$

and

$$F_1^*(\xi) = (\xi-\xi_1)\,[(B_1^*-B_2^*).\sinh k\xi_1 + (C_1^*-C_2^*).\cosh k\xi_1] + (\xi-\xi_2)\,[(B_2^*-B_3^*).\sinh k\xi_2 + (C_2^*-C_3^*).\cosh k\xi_2]$$

$$F_2^*(\xi) = B_1^*(\cosh k\xi_1-\cosh k\xi) + B_2^*(\cosh k\xi_2-\cosh k\xi_1) + C_1^*(\sinh k\xi_1-\sinh k\xi) + C_2^*(\sinh k\xi_2-\sinh k\xi_1) + B_3^*(1-\cosh k\xi) + C_3^*(k\xi-\sinh k\xi_2).$$

$$F_3^*(\xi) = (\xi-\xi_2)\,[(B_2^*-B_3^*).\sinh k\xi_2+(C_2^*-C_3^*).\cosh k\xi_2]$$

$$\Delta_4^*(\xi) = B_2^*(\cosh k\xi_2-\cosh k\xi) + B_3^*(1-\cosh k\xi_2) + C_2^*(\sinh k\xi_2-\sinh k\xi) + C_3^*(k\xi-\sinh k\xi_2)$$

$$F_5^*(\xi) = B_3^*(1-\cosh k\xi) + C_3^*(k\xi-\sinh k\xi).$$

$$B_1^* = -C_1^*.\tanh k + \mu_1^*$$

$$C_1^* = \frac{C_2^* - \mu_1^*.\tanh k\xi_1 + B_2^*.\tanh k\xi_2}{\varepsilon_1}$$

$$B_2^* = \frac{\varepsilon_1(\mu_1^*\mu_{21}-\mu_{41}^*) + \varepsilon_2.\mu_1^*.\tanh k\xi_1 - C_2^*(\varepsilon_1.\sinh k\xi_1+\varepsilon_2)}{\varepsilon_1.\cosh k\xi_1 + \varepsilon_2.\tanh k\xi_1}$$

$$C_2^* = \frac{\varepsilon_1[D_{12}(\mu_1^*\mu_{21}-\mu_{41}^*)-D_{32}^*\cosh k\xi_1]+\varepsilon_2\tanh k\xi_1(\mu_1^*D_{12}-D_{32}^*)}{\varepsilon_1\,[D_{22}.\cosh k\xi_1+D_{12}.\sinh k\xi_1] + \varepsilon_2\,[D_{22}.\tanh k\xi_1+D_{12}]}$$

... (A.12)

$$B_3^* = \frac{B_2^*.\mu_{22} - \mu_{42}^* - \left(\dfrac{U+P+W\left(1-\dfrac{2}{k^2}\right)}{k}\right).\sinh k\xi_2 + C_2^*.\mu_{32}}{\cosh k\xi_2}$$

$$C_3^* = -\frac{1}{k}\left[\,U + P + W\left(1-\frac{2}{k^2}\right)\,\right]$$

$$D_{32}^* = -\frac{1}{k}\left(U + P + W\left(1 - \frac{2}{k^2} \right) \right)\left[\cosh k\xi_2 - \sinh k\xi_2 . \tanh k\xi_2 \right] + \mu_{42}^* . \tanh k\xi_2$$

$$\mu_1^* = -\frac{U + 2W}{k^2 \cosh k}$$

$$\mu_{41}^* = -\gamma_1 \left[U(1-\xi_1) + P + W\left\{ (1 - (\xi_1)^2) - \frac{2}{k^2} \right\} \right]$$

$$\mu_{42}^* = -\gamma_2 \left[U(1-\xi_2) + P + W\left\{ (1 - (\xi_2)^2) - \frac{2}{k^2} \right\} \right]$$

Thus the expressions of q_i^*, T_i^*, $V_{m_1}^*$, $V_{m_2}^*$, K_1 and K_2 are functions of the geometrical parameter α, the height ratios ξ, ξ_1 and ξ_2, the relative flexural rigidities of the stiffening beams γ_1 and γ_2, and the type of lateral loading. In addition to these parameters, the term y_i^* is also dependent on the parameter S_d.

1. <u>Case of a uniformly distributed wind loading, U</u>

For the special case of uniformly distributed wind loading, P = W = 0, and the previous expressions become

$$q_i^* = U\, q_i' \qquad \text{(A.13)}$$

$$T_i^* = \frac{1}{2} U\, T_i' \qquad \text{(A.14)}$$

$$y_i^* = \frac{1}{8} U\, \bar{y}_i \qquad \text{(A.15)}$$

$$(K_2)_i = \frac{T_i'}{(1-\xi)^2} \qquad \text{(A.16)}$$

$$(K_1)_i = 100 - \frac{T_i'}{(1-\xi)^2} \qquad \text{(A.17)}$$

$$V_{m_1}' = \gamma_1 \, q_1'(\xi_1) = \gamma_1 \, q_2'(\xi_1)$$

$$V_{m_2}' = \gamma_2 \, q_2'(\xi_2) = \gamma_2 \, q_3'(\xi_2) \qquad \text{(A.18)}$$

where

$$q_i' = - B_i' k . \sinh k\xi - C_i' k . \cosh k\xi + 1 - \xi \qquad \text{(A.19)}$$

$$T_i' = B_i' . \cosh k\xi + C_i' . \sinh k\xi + \frac{1}{2} (1 - \xi)^2 + \frac{1}{k^2} \qquad \text{(A.20)}$$

$$\bar{y}_1 = (1 - S_d) \bar{\Pi} (\xi) + \frac{S_d}{k} F_1'(\xi) + \frac{S_d}{k^2} F_2'(\xi) - \frac{1}{2 k^2} S_d \xi^2 \qquad \text{(A.21)}$$

$$\bar{y}_2 = (1 - S_d) \bar{\Pi} (\xi) + \frac{S_d}{k} F_3'(\xi) + \frac{S_d}{k^2} F_4'(\xi) - \frac{1}{2 k^2} S_d \xi^2 \qquad \text{(A.22)}$$

$$\bar{y}_3 = (1 - S_d) \bar{\Pi} (\xi) + \frac{S_d}{k^2} F_5'(\xi) - \frac{1}{2 k^2} S_d \xi^2 \qquad \text{(A.23)}$$

and

$$\bar{\Pi} (\xi) = \frac{1}{24} [\xi^2 - 4 \xi + 6]$$

$$F_1'(\xi) = (\xi - \xi_1) [(B_1' - B_2') . \sinh k\xi_1 + (C_1' - C_2') . \cosh k\xi_1] + (\xi - \xi_2) [(B_2' - B_3') . \sinh k\xi_2 + (C_2' - C_3') . \cosh k\xi_2]$$

$$F_2'(\xi) = B_1'(\cosh k\xi_1-\cosh k\xi) + B_2'(\cosh k\xi_2-\cosh k\xi_1) + C_1'(\sinh k\xi_1-\sinh k\xi) + C_2'(\sinh k\xi_2-\sinh k\xi_1) + B_3'(1 - \cosh k\xi) + C_3'(k\xi - \sinh k\xi_2).$$

$$F_3'(\xi) = (\xi - \xi_2)\,[(B_2'-B_3').\sinh k\xi_2+(C_2'-C_3').\cosh k\xi_2]$$

$$F_4'(\xi) = B_2'(\cosh k\xi_2 - \cosh k\xi) + B_3'(1 - \cosh k\xi_2) + C_2'(\sinh k\xi_2 - \sinh k\xi) + C_3'(k\xi - \sinh k\xi_2)$$

$$F_5'(\xi) = B_3'(1 - \cosh k\xi) + C_3'\,(k\xi - \sinh k\xi).$$

$$B_1' = - C_1'.\tanh k + \mu_1'$$

$$C_1' = \frac{C_2' - \mu_1'.\tanh k\xi_1 + B_2'.\tanh k\xi_2}{\varepsilon_1}$$

$$B_2' = \frac{\varepsilon_1(\mu_1'\mu_{21}-\mu_{41}') + \varepsilon_2.\mu_1'.\tanh k\xi_1 - C_2'(\varepsilon_1.\sinh k\xi_1+\varepsilon_2)}{\varepsilon_1.\cosh k\xi_1 + \varepsilon_2.\tanh k\xi_1}$$

$$C_2' = \frac{\varepsilon_1[D_{12}(\mu_1'\mu_{21}-\mu_{41}')-D_{32}'\cosh k\xi_1]+\varepsilon_2\tanh k\xi_1(\mu_1'D_{12}-D_{32}')}{\varepsilon_1\,[D_{22}.\cosh k\xi_1+D_{12}.\sinh k\xi_1] + \varepsilon_2\,[D_{22}.\tanh k\xi_1+D_{12}]} \quad \ldots\ldots \text{(A.24)}$$

$$B_3' = \frac{B_2'.\mu_{22} - \mu_{42}' - \frac{1}{k}.\sinh k\xi_2 + C_2'.\mu_{32}}{\cosh k\xi_2}$$

$$C_3' = \frac{1}{k}$$

$$D_{32}' = -\frac{1}{k}[\,\cosh k\xi_2 - \sinh k\xi_2.\tanh k\xi_2\,] + \mu_{42}^*.\tanh k\xi_2$$

$$\mu_1' = -\frac{1}{k^2 \cosh k}$$

$$\mu_{41}' = -\gamma_1 [\, 1-\xi_1 \,]$$

$$\mu_{42}' = -\gamma_2 [\, 1-\xi_2 \,]$$

2. <u>Case of an upper triangularly distributed load, W.</u>

In this case P = U = 0, and the following expressions are derived

$$q_i^* = W\, q_i' \qquad \ldots\ldots\ldots\ldots\ldots\ldots\ldots \quad (A.25)$$

$$T_i^* = \frac{2}{3} W\, T_i' \qquad \ldots\ldots\ldots\ldots\ldots\ldots\ldots \quad (A.26)$$

$$y_i^* = \frac{11}{60} W\, \bar{y}_i \qquad \ldots\ldots\ldots\ldots\ldots\ldots\ldots \quad (A.27)$$

$$(K_2)_i = \frac{2T_i'}{2 - \xi \{ 3 - (\xi)^2 \}} \qquad \ldots\ldots\ldots\ldots \quad (A.28)$$

$$(K_1)_i = 100 - \frac{2T_i'}{2 - \xi \{ 3 - (\xi)^2 \}} \qquad \ldots\ldots\ldots\ldots \quad (A.29)$$

$$V_{m1}' = \gamma_1\, q_1'(\xi_1) = \gamma_1\, q_2'(\xi_1)$$

$$\ldots\ldots\ldots \quad (A.30)$$

$$V_{m2}' = \gamma_2\, q_2'(\xi_2) = \gamma_2\, q_3'(\xi_2)$$

where

$$q_i' = -B_i' k.\sinh k\xi - C_i' k.\cosh k\xi + (1 - \xi^2) - \frac{2}{k^2} \qquad (A.31)$$

$$T_i' = B_i'.\cosh k\xi + C_i'.\sinh k\xi + \frac{1}{3}\left[2 - \xi\left\{3 - (\xi)^2\right\}\right] + \frac{2\xi}{k^2} \qquad (A.32)$$

$$\bar{y}_1 = \frac{60}{11}\left[\left(1 - S_d\right)\bar{\Pi}(\xi) + \frac{S_d}{k}F_1'(\xi) + \frac{S_d}{k^2}F_2'(\xi)\right] - \frac{20}{11k^2}S_d\,\xi^3 \qquad (A.33)$$

$$\bar{y}_2 = \frac{60}{11}\left[\left(1 - S_d\right)\bar{\Pi}(\xi) + \frac{S_d}{k}F_3'(\xi) + \frac{S_d}{k^2}F_4'(\xi)\right] - \frac{20}{11k^2}S_d\,\xi^3 \qquad (A.34)$$

$$\bar{y}_3 = \frac{60}{11}\left[\left(1 - S_d\right)\bar{\Pi}(\xi) + \frac{S_d}{k^2}F_5'(\xi)\right] - \frac{20}{11k^2}S_d\,\xi^3 \qquad (A.35)$$

and

$$\bar{\Pi}(\xi) = \frac{1}{60}\left[\xi^3 - 10\xi + 20\right]$$

$$F_1'(\xi) = (\xi-\xi_1)\left[(B_1'-B_2').\sinh k\xi_1 + (C_1'-C_2').\cosh k\xi_1\right] + (\xi-\xi_2)\left[(B_2'-B_3').\sinh k\xi_2 + (C_2'-C_3').\cosh k\xi_2\right]$$

$$F_2'(\xi) = B_1'(\cosh k\xi_1-\cosh k\xi) + B_2'(\cosh k\xi_2-\cosh k\xi_1) + C_1'(\sinh k\xi_1-\sinh k\xi) + C_2'(\sinh k\xi_2-\sinh k\xi_1) + B_3'(1 - \cosh k\xi) + C_3'(k\xi - \sinh k\xi_2).$$

$$F_3'(\xi) = (\xi - \xi_2)\left[(B_2'-B_3').\sinh k\xi_2+(C_2'-C_3').\cosh k\xi_2\right]$$

$$F_4'(\xi) = B_2'(\cosh k\xi_2 - \cosh k\xi) + B_3'(1 - \cosh k\xi_2) + C_2'(\sinh k\xi_2 - \sinh k\xi) + C_3'(k\xi - \sinh k\xi_2)$$

$$F_5'(\xi) = B_3'(1 - \cosh k\xi) + C_3^{*}\,(k\xi - \sinh k\xi).$$

$$B_1' = - C_1'.\tanh k + \mu_1'$$

$$C_1' = \frac{C_2' - \mu_1'.\tanh k\xi_1 + B_2'.\tanh k\xi_2}{\varepsilon_1}$$

$$B_2' = \frac{\varepsilon_1(\mu_1'\mu_{21}-\mu_{41}') + \varepsilon_2.\mu_1'.\tanh k\xi_1 - C_2'(\varepsilon_1.\sinh k\xi_1+\varepsilon_2)}{\varepsilon_1.\cosh k\xi_1 + \varepsilon_2.\tanh k\xi_1}$$

$$C_2' = \frac{\varepsilon_1[D_{12}(\mu_1'\mu_{21}-\mu_{41}')-D_{32}'\cosh k\xi_1]+\varepsilon_2\tanh k\xi_1(\mu_1'D_{12}-D_{32}')}{\varepsilon_1\,[D_{22}.\cosh k\xi_1+D_{12}.\sinh k\xi_1] + \varepsilon_2\,[D_{22}.\tanh k\xi_1+D_{12}]} \quad \ldots\ldots \text{(A.36)}$$

$$B_3' = \frac{B_2'.\mu_{22} - \mu_{42}' - \left(\frac{1}{k} - \frac{2}{k^3}\right).\sinh k\xi_2 + C_2'.\mu_{32}}{\cosh k\xi_2}$$

$$C_3' = \frac{1}{k}\left[\,1 - \frac{2}{k^2}\,\right]$$

$$D_{32}' = -\frac{1}{k}\left[\,1 - \frac{2}{k^2}\,\right]\left[\,\cosh k\xi_2 - \sinh k\xi_2.\tanh k\xi_2\,\right] + \mu_{42}^{*}.\tanh k\xi_2$$

$$\mu_1' = - \frac{2W}{k^2\cosh k}$$

$$\mu_{41}' = - \gamma_1\left[\,1 - \xi_1^2 - \frac{2}{k^2}\,\right]$$

$$\mu_{42}' = - \gamma_2\left[\,1 - \xi_2^2 - \frac{2}{k^2}\,\right]$$

3. Case of a concentrated top loading, P.

In the particular case of a concentrated top loading, P, both U, and W are equal to zero and the following expressions are derived

$$q_i^* = P\, q_i' \qquad \text{(A.37)}$$

$$T_i^* = P\, T_i' \qquad \text{(A.38)}$$

$$y_i^* = \frac{1}{3} P\, \bar{y}_i \qquad \text{(A.39)}$$

$$(K_2)_i = \frac{T_i'}{1 - \xi} \qquad \text{(A.40)}$$

$$(K_1)_i = 100 - \frac{T_i'}{1 - \xi} \qquad \text{(A.41)}$$

$$V_{m1}' = \gamma_1\, q_1'(\xi_1) = \gamma_1\, q_2'(\xi_1)$$

$$V_{m2}' = \gamma_2\, q_2'(\xi_2) = \gamma_2\, q_3'(\xi_2) \qquad \text{(A.42)}$$

where

$$q_i' = - B_i'k.\sinh k\xi - C_i'k.\cosh k\xi + 1 \qquad \text{(A.43)}$$

$$T_i' = B_i'.\cosh k\xi + C_i'.\sinh k\xi + 1 - \xi \qquad \text{(A.44)}$$

$$\bar{y}_1 = 3 \left[(1 - S_d) \bar{\Pi} (\xi) + \frac{S_d}{k} F_1'(\xi) + \frac{S_d}{k^2} F_2'(\xi) \right] \qquad \text{(A.45)}$$

$$\bar{y}_2 = 3 \left[(1 - S_d) \bar{\Pi} (\xi) + \frac{S_d}{k} F_3'(\xi) + \frac{S_d}{k^2} F_4'(\xi) \right] \qquad \text{(A.46)}$$

$$\bar{y}_3 = 3 \left[(1 - S_d) \bar{\Pi} (\xi) + \frac{S_d}{k^2} F_5'(\xi) \right] \qquad \text{(A.47)}$$

and

$$\bar{\Pi}(\xi) = \frac{1}{6}\left[\, 3 - \xi \,\right]$$

$$F_1'(\xi) = (\xi-\xi_1)\left[(B_1'-B_2').\sinh k\xi_1 + (C_1'-C_2').\cosh k\xi_1\right] +$$
$$(\xi-\xi_2)\left[(B_2'-B_3').\sinh k\xi_2 + (C_2'-C_3').\cosh k\xi_2\right]$$

$$F_2'(\xi) = B_1'(\cosh k\xi_1-\cosh k\xi) + B_2'(\cosh k\xi_2-\cosh k\xi_1) +$$
$$C_1'(\sinh k\xi_1-\sinh k\xi) + C_2'(\sinh k\xi_2-\sinh k\xi_1) +$$
$$B_3'(1 - \cosh k\xi) + C_3'(k\xi - \sinh k\xi_2).$$

$$F_3'(\xi) = (\xi - \xi_2)\left[(B_2'-B_3').\sinh k\xi_2+(C_2'-C_3').\cosh k\xi_2\right]$$

$$F_4'(\xi) = B_2'(\cosh k\xi_2 - \cosh k\xi) + B_3'(1 - \cosh k\xi_2) +$$
$$C_2'(\sinh k\xi_2 - \sinh k\xi) + C_3'(k\xi - \sinh k\xi_2)$$

$$F_5'(\xi) = B_3'(1 - \cosh k\xi) + C_3^{*}\,(k\xi - \sinh k\xi).$$

$$B_1' = - C_1'.\tanh k$$

$$C_1' = \frac{C_2' + B_2'.\tanh k\xi_2}{\varepsilon_1}$$

$$B_2' = \frac{- \varepsilon_1\mu_{41}' - C_2'(\varepsilon_1.\sinh k\xi_1+\varepsilon_2)}{\varepsilon_1.\cosh k\xi_1 + \varepsilon_2.\tanh k\xi_1}$$

$$C_2' = \frac{\varepsilon_1\left[- D_{12}\,\mu_{41}' - D_{32}'\cosh k\xi_1 \right] - \varepsilon_2\, D_{32}'\, \tanh k\xi_1}{\varepsilon_1\left[D_{22}.\cosh k\xi_1+D_{12}.\sinh k\xi_1\right] + \varepsilon_2\left[D_{22}.\tanh k\xi_1+D_{12}\right]} \qquad \ldots\ (A.48)$$

$$B_3' = \frac{B_2'.\mu_{22} - \mu_{42}' - \frac{1}{k}.\sinh k\xi_2 + C_2'.\mu_{32}}{\cosh k\xi_2}$$

$$C_3' = \frac{1}{k}$$

$$D_{32}' = -\frac{1}{k}\left[\cosh k\xi_2 - \sinh k\xi_2 . \tanh k\xi_2 \right] + \mu_{42}^* . \tanh k\xi_2$$

$$\mu_{41}' = -\gamma_1$$

$$\mu_{42}' = -\gamma_2$$

In all the cases listed above, the expressions of q_i', T_i', V_{m_1}', V_{m_2}', K_1 and K_2 are functions only of the geometrical parameter α, the height ratios ξ, ξ_1 and ξ_2 and the relative flexural rigidities of the stiffening beams γ_1 and γ_2. In addition the dimensionless parameters, the term $\bar{y}_i$ is also dependant on the parameter S_d

Particular cases.

Case 1: One stiffening beam

in the particular case of only one stiffening beam equations (A.12) become,

$$B_1^* = - C_1^* . \tanh k + \mu_1^*$$

$$C_1^* = \frac{C_2^* - \mu_1^* . \tanh k\xi_1}{\epsilon_1}$$

$$B_2^* = B_3^* = \frac{\epsilon_1(\mu_1^*\mu_{21} - \mu_{41}^*) + \epsilon_2\mu_1^* \tanh k\xi_1 - C_2^*(\epsilon_1 \sinh k\xi_1 + \epsilon_2)}{\epsilon_1 . \cosh k\xi_1 + \epsilon_2 . \tanh k\xi_1} \quad \ldots\ (A.49)$$

$$C_2^* = C_3^* = -\frac{1}{k}\left[U + P + W\left(1 - \frac{2}{k^2} \right) \right]$$

and the functions $F_1(\xi)$ to $F_5(\xi)$ become, respectively,

$$F_1^*(\xi) = (\xi - \xi_1)\,[\,(B_1^* - B_2^*).\sinh k\xi_1 + (C_1^* - C_2^*).\cosh k\xi_1\,]$$

$$F_2^*(\xi) = B_1^*(\cosh k\xi_1 - \cosh k\xi) + B_2^*(1 - \cosh k\xi_1) + C_1^*(\sinh k\xi_1 - \sinh k\xi) + C_2^*(k\xi - \sinh k\xi_1)$$

$$F_3^*(\xi) = 0$$

$$F_4^*(\xi) = F_5^*(\xi) = B_2^*(1 - \cosh k\xi) + C_2^*(k\xi - \text{sink } k\xi)$$

However equations (A.24), become,

$$B_1' = -C_1'.\tanh k + \mu_1'$$

$$C_1' = \frac{C_2' - \mu_1'.\tanh k\xi_1}{\varepsilon_1}$$

$$B_2' = B_3' = \frac{\varepsilon_1(\mu_1'\mu_{21} - \mu_{41}') + \varepsilon_2\mu_1'\tanh k\xi_1 - C_2'(\varepsilon_1\sinh k\xi_1 + \varepsilon_2)}{\varepsilon_1.\cosh k\xi_1 + \varepsilon_2.\tanh k\xi_1} \quad \ldots\ (A.50)$$

$$C_2' = C_3' = \frac{1}{k}$$

and the fonctions $F_1(\xi)$ to $F_5(\xi)$ become, respectively,

$$F_1'(\xi) = (\xi - \xi_1)\,[\,(B_1' - B_2').\sinh k\xi_1 + (C_1' - C_2').\cosh k\xi_1\,]$$

$$F_2'(\xi) = B_1'(\cosh k\xi_1 - \cosh k\xi) + B_2'(1 - \cosh k\xi_1) + C_1'(\sinh k\xi_1 - \sinh k\xi) + C_2'(k\xi - \sinh k\xi_1)$$

$$F_3'(\xi) = 0$$

$$F_4'(\xi) = F_5'(\xi) = B_2'(1 - \cosh k\xi) + C_2'(k\xi - \text{sink } k\xi)$$

Case 2: Unstiffened coupled shear wall

In the case of an unstiffened shear wall equations (A.12), reduce to,

$$C_1^* = C_2^* = C_3^* = C^* = 1/k \left[U+P+W\,(1-2/k^2) \right]$$

..... (A.51)

$$B_1^* = B_2^* = B_3^* = B^* = \mu_1^* - C_2^*.\tanh k$$

and the expressions for $F_1^*(\xi)$ to $F_5^*(\xi)$ become, respectively,

$$F_1^*(\xi) = F_3^*(\xi) = 0$$

$$F_2^*(\xi) = F_4^*(\xi) = F_5^*(\xi) = B^*(1 - \cosh k\xi) + C^*(k\xi - \sinh k\xi)$$

However equations (A.24) reduce to

$$C_1' = C_2' = C_3' = C' = 1/k$$

..... (A.52)

$$B_1' = B_2' = B_3' = B' = \mu_1' - C_2'.\tanh k$$

The expressions for $F_1'(\xi)$ to $F_5'(\xi)$ become, respectively,

$$F_1'(\xi) = F_3'(\xi) = 0$$

$$F_2'(\xi) = F_4'(\xi) = F_5'(\xi) = B'(1 - \cosh k\xi) + C'(k\xi - \sinh k\xi)$$

and the expressions for q', T', $\bar{y}$ and $\bar{y}_{max}$ for the case of a uniformly distributed loading, will be given by

$$q' = 1 - \xi + \frac{1}{k.\cosh k}\left[\sinh k\xi - k \cosh k(1-\xi) \right] \quad ..... \quad (A.53)$$

$$T' = (1 - \xi)^2 + \frac{2}{k^2.\cosh k}\left[\cosh k - \cosh k\xi - k \sinh k(1-\xi) \right]$$

..... (A.54)

$$\bar{y} = \frac{1}{3}\left[\, 1 - \frac{\beta^2}{\alpha^2} L \,\right]\left[\, (1-\xi)^4 + 4\xi - 1 \,\right] + \frac{8}{k^2}\frac{\beta^2}{\alpha^2} L \left[\, \xi\left(1 - \frac{1}{2}\xi\right) - \frac{1}{k^2.\cosh k}\left\{ 1 + k \sinh k - \cosh k\xi - K \sinh k(1-\xi) \right\} \,\right] \quad (A.55)$$

$$\bar{y}_{max} = \left(1 - \frac{\beta^2}{\alpha^2} L \right) + \frac{1}{k^2}\frac{\beta^2}{\alpha^2}\left[\, 4 - \frac{8}{k^2.\cosh k}\left\{ 1 + k \sinh k - \cosh k \right\} \,\right] \quad (A.56)$$

For the case of an upper triangularly distributed load, the expressions for q', T', and $\bar{y}$, and $\bar{y}_{max}$ will be given by

$$q' = -\frac{2}{k.\cosh k}\left\{ \left(\frac{1}{k} - \frac{k}{2}\right) \cosh k(1-\xi) + \sinh k\xi \right\} + \left(1 - \xi^2 \right) - \frac{2}{k^2} \quad \ldots\ldots\ldots\ldots\ldots\ldots\ldots\ldots \quad (A.57)$$

$$T' = -\frac{3}{k^2.\cosh k}\left\{ \left(\frac{1}{k} - \frac{k}{2}\right) \sinh k(1-\xi) - \cosh k\xi \right\} + \frac{1}{2}\left(\xi^3 - 3\xi + 2 \right) + \frac{3\xi}{k^2} \quad \ldots\ldots\ldots\ldots\ldots\ldots\ldots \quad (A.58)$$

$$\bar{y} = \frac{\beta^2}{\alpha^2} L \left[\frac{120}{11}\frac{1}{k^4.\cosh k}\left\{ \left(\frac{1}{k} - \frac{k}{2}\right)\left(\sinh k - k\xi.\cosh k - \sinh k\langle 1 - \xi \rangle \right) - 1 + \cosh k\xi \right\} - \frac{\xi^2}{11}\left(\xi^3 - 10\xi + 20 \right) - \frac{20\xi^3}{11k^2} \right] + \frac{\xi^2}{11}\left(\xi^3 - 10\xi + 20 \right) \quad \ldots\ldots\ldots\ldots\ldots\ldots \quad (A.59)$$

$$\bar{y}_{max} = 1 + \frac{\beta^2}{\alpha^2} L \left[\frac{120}{11} \frac{1}{k^4.\cosh k} \left\{ \left(\frac{1}{k} - \frac{k}{2} \right) (\sinh k - k.\cosh k) - 1 + \cosh k \right\} - 1 - \frac{20}{11k^2} \right] \quad \ldots\ldots\ldots\ldots\ldots\ldots \text{(A.60)}$$

For the case of a concentrated load acting at the top of the structure, the previous expressions, become

$$q' = 1 - \frac{1}{\cosh k} \cosh k(1-\xi) \quad \ldots\ldots\ldots\ldots\ldots\ldots\ldots\ldots \text{(A.61)}$$

$$T' = 1 - \xi - \frac{1}{k.\cosh k} \sinh k(1-\xi) \quad \ldots\ldots\ldots\ldots\ldots\ldots\ldots \text{(A.62)}$$

$$\bar{y} = -3 \frac{\beta^2}{\alpha^2} L \left[- \frac{1}{k^3.\cosh k} \left\{ \sinh k(1-\xi) - \sinh k \right\} - \frac{1}{k^2} \xi \right] + \frac{\xi^2}{2} (3 - \xi) \quad \ldots\ldots\ldots\ldots\ldots\ldots\ldots\ldots \text{(A.63)}$$

$$\bar{y}_{max} = 1 - 3 \frac{\beta^2}{\alpha^2} L \left[\frac{1}{k^3.\cosh k} \sinh k - \frac{1}{k^2} \right] \quad \ldots\ldots\ldots\ldots\ldots\ldots\ldots\ldots \text{(A.64)}$$

APPENDIX B.

Numerical results for stiffened and unstiffened coupled shear walls on rigid or flexible soil foundations

Introduction.

In order to illustrate the behaviour of coupled shear walls on elastic foundations, results based on the theory presented in Chapter 4 have been shown for various cases of unstiffened shear walls, shear walls with only one stiffening beam and shear walls with two stiffening beams. The results are presented in tabular form for various values of the relative flexural rigidities of the stiffening beams and their locations.

Example structures.

Four example structures have been considered. The dimensions and structural properties of the structures are given in Fig. B.1. Three sets of numerical values for the stiffness properties of the soil foundations, the vertical stiffness K_δ and rotational stiffness K_r are considered corresponding to particular limiting cases

(a) Rigid base: for which K_δ and K_r have infinite values

(b) Dense gravel and sand: for which K_δ = 438.7 MN.m and K_r = 13560 MN.m/rad

(c) Dense sand: for which K_δ = 145.9 MN.m and K_r = 5423 MN.m/rad.

	Table 1	Table 2	Table 3	Table 4
Coupling beam section breadth × depth m	0.15 × 0.4	0.4 × 0.4	0.2 × 0.35	0.2 × 0.35
Stiff beams section breadth × depth m	0.15 × 1.454	0.4 × 1.3	0.2 × 1.0	0.2 × 1.0
Young Modulus KN/m^2	$2.0\ 10^7$	$2.4\ 10^5$	$2.0\ 10^7$	$2.0\ 10^7$
I_b m^4	$8.0\ 10^{-4}$	$21.33\ 10^{-4}$	$7.14\ 10^{-4}$	$7.14\ 10^{-4}$
$I_{f_1}=I_{f_2}$ m^4	$3.84\ 10^{-2}$	$7.3233\ 10^{-2}$	$1.667\ 10^{-2}$	$1.667\ 10^{-2}$
h m	3.0	3.0	2.8	2.8
H m	72.0	60.0	67.2	67.2
b m	1.5	1.5	2.0	2.0
d_1 m	4.0	3.25	4.0	6.0
d_2 m	4.0	5.0	4.0	2.0
t_w m	0.15	0.4	0.2	0.2
L m	10.5	9.75	10.0	10.0
αH	6.54	5.11	3.51	2.94
$\gamma_1=\gamma_2$	2.0	1.72	0.93	0.93
K_δ (10^5) KN.m	(a) ∞	(b) 4.387	(c) 1.459	
K_r (10^6) KN.m/rad	(a) ∞	(b) 13.560	(c) 5.423	
Uniform distributed load	15 KN/m			

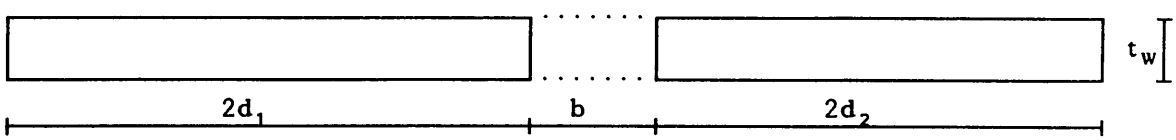

Fig. B.1

	γ_1	γ_2	x_1/H	x_2/H	s:mm	θ $\times 10^{-3}$ rad	Y(H) mm	qmax KN/m	T_0 KN	M_0 KN.m
	0.0	0.0	....	....	0.00	0.00	48.64	51.64	2452.86	15577.85
	2.0	0.0	1.00	....	0.00	0.00	48.04	51.52	2453.25	15574.16
	2.0	0.0	0.75	....	0.00	0.00	46.52	50.64	2456.39	15544.28
	2.0	0.0	0.67	....	0.00	0.00	46.02	49.58	2460.41	15506.10
	2.0	0.0	0.50	....	0.00	0.00	45.08	44.42	2484.01	15281.88
	2.0	0.0	0.33	....	0.00	0.00	44.70	32.43	2564.11	14520.95
(a)	2.0	0.0	0.25	....	0.00	0.00	44.99	34.50	2649.38	13710.92
	2.0	2.0	1.00	0.25	0.00	0.00	44.42	34.13	2649.42	13710.47
	2.0	2.0	1.00	0.50	0.00	0.00	44.65	44.42	2484.00	15282.01
	2.0	2.0	1.00	0.75	0.00	0.00	46.33	50.62	2456.45	15543.73
	2.0	2.0	0.75	0.25	0.00	0.00	43.07	31.52	2649.82	13706.69
	2.0	2.0	0.75	0.50	0.00	0.00	43.79	44.35	2484.38	15278.41
	2.0	2.0	0.67	0.33	0.00	0.00	42.70	32.33	2564.95	14513.02
	2.0	2.0	0.50	0.25	0.00	0.00	42.47	23.36	2652.87	13677.73
	0.0	0.0	....	....	6.47	0.88	102.15	58.38	2840.53	11894.97
	2.0	0.0	1.00	....	6.48	0.88	101.54	58.30	2840.67	11893.66
	2.0	0.0	0.75	....	6.48	0.88	100.01	57.72	2841.78	11883.12
	2.0	0.0	0.67	....	6.48	0.88	99.48	57.00	2843.21	11869.55
	2.0	0.0	0.50	....	6.50	0.87	98.43	53.16	2851.73	11788.58
	2.0	0.0	0.33	....	6.57	0.85	97.79	42.58	2881.80	11502.88
	2.0	0.0	0.25	....	6.64	0.82	97.88	34.63	2915.06	11186.92
(b)	2.0	0.0	0.00	....	6.90	0.75	101.40	52.21	3026.69	10126.41
	2.0	2.0	1.00	0.00	6.90	0.75	100.79	52.10	3026.70	10126.37
	2.0	2.0	0.75	0.00	6.90	0.75	99.28	51.25	3026.81	10125.29
	2.0	2.0	0.50	0.00	6.90	0.75	97.82	45.20	3027.84	10115.53
	2.0	2.0	0.25	0.00	6.92	0.74	97.67	34.51	3033.98	10057.23
	2.0	2.0	1.00	0.25	6.64	0.82	97.31	34.26	2915.08	11186.77
	2.0	2.0	1.00	0.50	6.50	0.87	98.05	53.18	2851.67	11789.12
	2.0	2.0	1.00	0.75	6.48	0.88	99.87	57.72	2841.77	11883.19
	2.0	2.0	0.75	0.25	6.65	0.82	95.96	33.12	2915.21	11185.55
	2.0	2.0	0.75	0.50	6.50	0.87	97.19	53.13	2851.80	11787.87
	2.0	2.0	0.67	0.33	6.57	0.85	95.79	42.50	2882.08	11500.21
	2.0	2.0	0.50	0.25	6.65	0.82	95.36	32.85	2916.23	11175.84
	0.0	0.0	....	....	19.35	2.2	199.53	57.99	2823.21	12059.52
	2.0	0.0	1.00	....	19.35	2.2	198.92	57.92	2823.27	12058.89
	2.0	0.0	0.75	....	19.35	2.2	197.39	57.31	2823.81	12053.78
	2.0	0.0	0.67	....	19.36	2.2	196.87	56.55	2824.50	12047.20
	2.0	0.0	0.50	....	19.39	2.2	195.85	52.50	2828.63	12007.98
	2.0	0.0	0.33	....	19.49	2.2	195.29	41.15	2843.09	11870.62
	2.0	0.0	0.25	....	19.59	2.2	195.48	34.60	2858.77	11721.69
(c)	2.0	0.0	0.00	....	19.82	2.1	199.25	52.07	2892.42	11401.96
	2.0	2.0	1.00	0.00	19.82	2.1	198.64	51.96	2892.43	11401.89
	2.0	2.0	0.75	0.00	19.83	2.1	197.12	51.10	2892.48	11401.41
	2.0	2.0	0.50	0.00	19.83	2.1	195.67	45.00	2892.88	11397.66
	2.0	2.0	0.25	0.00	19.84	2.1	195.56	34.51	2895.25	11375.09
	2.0	2.0	1.00	0.25	19.59	2.2	194.91	34.23	2858.77	11721.65
	2.0	2.0	1.00	0.50	19.39	2.2	195.43	52.51	2828.63	12008.05
	2.0	2.0	1.00	0.75	19.35	2.2	197.25	57.31	2823.81	12053.81
	2.0	2.0	0.75	0.25	19.59	2.2	193.56	31.65	2858.84	11721.01
	2.0	2.0	0.75	0.50	19.39	2.2	194.57	52.45	2828.69	12007.45
	2.0	2.0	0.67	0.33	19.49	2.2	193.29	41.06	2843.23	11869.33
	2.0	2.0	0.50	0.25	19.60	2.2	192.96	30.53	2859.34	11716.30

Table 1

	γ_1	γ_2	x_1/H	x_2/H	s:mm	θ $\times 10^{-3}$ rad	Y(H) mm	qmax KN/m	T_0 KN	M_0 KN.m
	0.00	0.00	....	....	0.00	0.00	7.21	35.31	1476.54	12603.74
	1.72	0.00	1.00	....	0.00	0.00	7.03	34.95	1478.21	12587.41
	1.72	0.00	0.75	....	0.00	0.00	6.74	33.59	1485.01	12521.20
	1.72	0.00	0.67	....	0.00	0.00	6.64	32.35	1491.87	12454.26
	1.72	0.00	0.50	....	0.00	0.00	6.48	27.60	1523.43	12146.54
	1.72	0.00	0.33	....	0.00	0.00	6.46	19.15	1602.70	11373.70
(a)	1.72	0.00	0.25	....	0.00	0.00	6.55	23.75	1670.79	10709.83
	1.72	1.72	1.00	0.25	0.00	0.00	6.39	22.99	1671.10	10706.79
	1.72	1.72	1.00	0.50	0.00	0.00	6.37	27.57	1523.64	12144.51
	1.72	1.72	1.00	0.75	0.00	0.00	6.70	33.58	1485.09	12520.40
	1.72	1.72	0.75	0.25	0.00	0.00	6.15	20.41	1672.28	10695.29
	1.72	1.72	0.75	0.50	0.00	0.00	6.24	27.46	1524.45	12136.61
	1.72	1.72	0.67	0.33	0.00	0.00	6.07	18.95	1605.01	11351.17
	1.72	1.72	0.50	0.25	0.00	0.00	6.07	13.45	1678.15	10637.99
	0.0	0.00	....	....	4.57	0.55	37.07	48.99	2008.04	7421.59
	1.72	0.00	1.00	....	4.57	0.55	36.88	48.82	2008.27	7419.35
	1.72	0.00	0.75	....	4.58	0.54	36.57	48.13	2009.21	7410.16
	1.72	0.00	0.67	....	4.58	0.54	36.45	47.43	2010.19	7400.69
	1.72	0.00	0.50	....	4.59	0.54	36.22	44.21	2014.85	7355.22
	1.72	0.00	0.33	....	4.62	0.53	36.05	36.04	2027.58	7231.06
	1.72	0.00	0.25	....	4.65	0.52	36.03	28.86	2039.37	7116.10
(b)	1.72	0.00	0.00	....	4.74	0.49	36.56	36.34	2079.25	6727.35
	1.72	1.72	1.00	0.00	4.74	0.49	36.37	36.01	2079.28	6727.00
	1.72	1.72	0.75	0.00	4.74	0.49	36.08	34.74	2079.38	6726.09
	1.72	1.72	0.50	0.00	4.74	0.49	35.81	28.99	2079.97	6720.30
	1.72	1.72	0.25	0.00	4.74	0.49	35.85	23.81	2082.30	6697.60
	1.72	1.72	1.00	0.25	4.65	0.52	35.87	28.84	2039.41	7115.74
	1.72	1.72	1.00	0.50	4.59	0.54	36.11	44.19	2014.87	7355.00
	1.72	1.72	1.00	0.75	4.58	0.54	36.53	48.12	2009.23	7410.04
	1.72	1.72	0.75	0.25	4.65	0.52	35.63	28.76	2039.55	7114.39
	1.72	1.72	0.75	0.50	4.59	0.54	35.98	44.12	2014.98	7353.93
	1.72	1.72	0.67	0.33	4.62	0.53	35.65	35.85	2027.88	7228.18
	1.72	1.72	0.50	0.25	4.65	0.52	35.54	28.33	2040.26	7107.50
	0.0	0.00	....	....	13.45	1.4	91.57	47.12	1962.81	7862.56
	1.72	0.00	1.00	....	13.45	1.4	91.38	46.92	1962.91	7861.64
	1.72	0.00	0.75	....	13.46	1.4	91.07	46.15	1963.30	7857.85
	1.72	0.00	0.67	....	13.46	1.4	90.95	45.36	1963.70	7853.96
	1.72	0.00	0.50	....	13.47	1.4	90.73	41.81	1965.61	7835.34
	1.72	0.00	0.33	....	13.51	1.4	90.60	32.99	1970.74	7785.29
	1.72	0.00	0.25	....	13.54	1.4	90.61	25.47	1975.37	7740.18
(c)	1.72	0.00	0.00	....	13.62	1.4	91.22	36.18	1987.82	7618.79
	1.72	1.72	1.00	0.00	13.62	1.4	91.04	35.84	1987.83	7618.67
	1.72	1.72	0.75	0.00	13.62	1.4	90.75	34.55	1987.88	7618.21
	1.72	1.72	0.50	0.00	13.63	1.4	90.48	28.76	1988.11	7615.97
	1.72	1.72	0.25	0.00	13.63	1.4	90.53	23.79	1988.98	7607.40
	1.72	1.72	1.00	0.25	13.54	1.4	90.45	25.45	1975.38	7740.04
	1.72	1.72	1.00	0.50	13.47	1.4	90.62	41.79	1965.62	7835.24
	1.72	1.72	1.00	0.75	13.46	1.4	91.03	46.14	1963.30	7857.80
	1.72	1.72	0.75	0.25	13.54	1.4	90.21	25.36	1975.44	7739.48
	1.72	1.72	0.75	0.50	13.47	1.4	90.49	41.71	1965.66	7834.81
	1.72	1.72	0.67	0.33	13.51	1.4	90.20	32.79	1970.86	7784.11
	1.72	1.72	0.50	0.25	13.54	1.4	90.12	24.90	1975.73	7736.67

Table 2

	γ_1	γ_2	x_1/H	x_2/H	s:mm	θ $\times 10^{-3}$ rad	Y(H) mm	qmax KN/m	T_0 KN	M_0 KN.m
	0.00	0.00	....	....	0.00	0.00	37.24	31.83	1628.45	17584.34
	0.93	0.00	1.00	....	0.00	0.00	34.46	30.32	1644.93	17419.46
	0.93	0.00	0.75	....	0.00	0.00	32.24	28.15	1671.40	17154.80
	0.93	0.00	0.67	....	0.00	0.00	31.57	26.76	1690.13	16967.47
	0.93	0.00	0.50	....	0.00	0.00	30.78	22.35	1758.79	16280.91
	0.93	0.00	0.33	....	0.00	0.00	31.43	20.67	1879.00	15078.76
(a)	0.93	0.00	0.25	....	0.00	0.00	32.42	23.63	1950.36	14365.22
	0.93	0.93	1.00	0.25	0.00	0.00	30.11	21.70	1956.49	14303.88
	0.93	0.93	1.00	0.50	0.00	0.00	29.24	22.11	1763.02	16238.56
	0.93	0.93	1.00	0.75	0.00	0.00	31.50	27.94	1674.16	17127.23
	0.93	0.93	0.75	0.25	0.00	0.00	28.40	19.15	1966.18	14207.04
	0.93	0.93	0.75	0.50	0.00	0.00	28.31	21.73	1769.73	16171.48
	0.93	0.93	0.67	0.33	0.00	0.00	27.62	15.53	1898.66	14882.22
	0.93	0.93	0.50	0.25	0.00	0.00	28.08	13.67	1995.36	13915.24
	0.00	0.00	....	....	4.99	0.88	81.37	41.25	2189.98	11968.99
	0.93	0.00	1.00	....	5.01	0.88	78.25	40.09	2197.44	11894.35
	0.93	0.00	0.75	....	5.04	0.87	75.64	38.31	2209.56	11773.20
	0.93	0.00	0.67	....	5.06	0.86	74.76	37.08	2218.34	11685.42
	0.93	0.00	0.50	....	5.13	0.84	73.27	32.75	2251.76	11351.22
	0.93	0.00	0.33	....	5.28	0.79	72.96	25.55	2314.91	10719.71
	0.93	0.00	0.25	....	5.37	0.76	73.47	24.88	2356.19	10306.92
(b)	0.93	0.00	0.00	....	5.59	0.69	78.41	34.60	2450.80	9360.77
	0.93	0.93	1.00	0.00	5.59	0.69	75.52	33.22	2453.22	9336.59
	0.93	0.93	0.75	0.00	5.60	0.69	73.17	31.19	2457.13	9297.52
	0.93	0.93	0.50	0.00	5.63	0.68	71.40	25.52	2470.28	9166.04
	0.93	0.93	0.25	0.00	5.70	0.65	72.58	24.09	2500.81	8860.65
	0.93	0.93	1.00	0.25	5.38	0.76	71.09	23.06	2358.47	10284.08
	0.93	0.93	1.00	0.50	5.14	0.84	71.65	32.53	2253.55	11333.29
	0.93	0.93	1.00	0.75	5.04	0.87	74.84	38.13	2210.78	11760.99
	0.93	0.93	0.75	0.25	5.38	0.76	69.30	20.70	2362.10	10247.84
	0.93	0.93	0.75	0.50	5.14	0.83	70.63	32.18	2256.43	11304.52
	0.93	0.93	0.67	0.33	5.29	0.78	68.94	24.72	2322.78	10641.00
	0.93	0.93	0.50	0.25	5.41	0.75	68.81	19.59	2373.34	10135.41
	0.00	0.00	....	....	15.70	2.0	155.21	43.51	2290.41	10964.73
	0.93	0.00	1.00	....	15.73	2.0	152.03	42.35	2294.29	10925.87
	0.93	0.00	0.75	....	15.77	2.0	149.37	40.53	2300.61	10862.71
	0.93	0.00	0.67	....	15.80	2.0	148.46	39.26	2305.19	10816.85
	0.93	0.00	0.50	....	15.92	2.0	146.91	34.65	2322.68	10641.98
	0.93	0.00	0.33	....	16.14	1.9	146.56	26.64	2355.52	10313.59
	0.93	0.00	0.25	....	16.29	1.9	147.09	24.95	2376.54	10103.44
(c)	0.93	0.00	0.00	....	16.58	1.8	152.15	34.49	2419.08	9678.03
	0.93	0.93	1.00	0.00	16.59	1.8	149.26	33.09	2420.09	9667.87
	0.93	0.93	0.75	0.00	16.60	1.8	146.92	31.05	2421.72	9651.62
	0.93	0.93	0.50	0.00	16.64	1.8	145.19	25.31	2427.21	9596.70
	0.93	0.93	0.25	0.00	16.72	1.7	146.44	24.03	2439.81	9470.65
	0.93	0.93	1.00	0.25	16.30	1.9	144.71	23.12	2377.66	10092.19
	0.93	0.93	1.00	0.50	15.93	2.0	145.28	34.41	2323.60	10632.80
	0.93	0.93	1.00	0.75	15.77	2.0	148.56	40.35	2301.24	10856.38
	0.93	0.93	0.75	0.25	16.31	1.9	142.92	21.14	2379.45	10074.34
	0.93	0.93	0.75	0.50	15.94	2.0	144.25	34.04	2325.08	10618.04
	0.93	0.93	0.67	0.33	16.17	1.9	142.53	25.72	2359.47	10274.06
	0.93	0.93	0.50	0.25	16.35	1.8	142.44	19.89	2384.99	10018.93

Table 3

	γ_1	γ_2	x_1/H	x_2/H	s:mm	θ $\times 10^{-3}$ rad	Y(H) mm	qmax KN/m	T_0 KN	M_0 KN.m
	0.00	0.00	....	....	0.00	0.00	31.75	22.69	1200.38	21864.97
	0.93	0.00	1.00	....	0.00	0.00	29.70	20.86	1228.03	21588.48
	0.93	0.00	0.75	....	0.00	0.00	28.46	19.06	1259.18	21276.95
	0.93	0.00	0.67	....	0.00	0.00	28.12	18.03	1278.76	21081.18
	0.93	0.00	0.50	....	0.00	0.00	27.82	15.06	1343.21	20436.68
	0.93	0.00	0.33	....	0.00	0.00	28.40	15.40	1440.80	19460.77
(a)	0.93	0.00	0.25	....	0.00	0.00	29.04	17.40	1491.19	18956.94
	0.93	0.93	1.00	0.25	0.00	0.00	27.38	15.36	1502.76	18841.21
	0.93	0.93	1.00	0.50	0.00	0.00	26.75	14.73	1351.03	20358.52
	0.93	0.93	1.00	0.75	0.00	0.00	27.90	18.77	1264.50	21223.82
	0.93	0.93	0.75	0.25	0.00	0.00	26.45	13.49	1515.68	18712.00
	0.93	0.93	0.75	0.50	0.00	0.00	26.24	14.37	1359.96	20269.16
	0.93	0.93	0.67	0.33	0.00	0.00	26.01	10.60	1469.01	19178.71
	0.93	0.93	0.50	0.25	0.00	0.00	26.39	10.43	1547.88	18390.02
	0.00	0.00	....	....	4.72	0.97	82.20	39.63	2069.13	13177.48
	0.93	0.00	1.00	....	4.75	0.96	79.36	38.44	2082.05	13048.34
	0.93	0.00	0.75	....	4.78	0.95	77.46	37.11	2096.88	12899.96
	0.93	0.00	0.67	....	4.80	0.94	76.77	36.26	2106.66	12802.21
	0.93	0.00	0.50	....	4.88	0.92	75.37	33.34	2141.39	12454.85
	0.93	0.00	0.33	....	5.02	0.87	74.37	28.41	2203.64	11832.40
	0.93	0.00	0.25	....	5.12	0.84	74.15	25.30	2244.67	11422.09
(b)	0.93	0.00	0.00	....	5.46	0.73	75.35	27.32	2397.02	9898.55
	0.93	0.93	1.00	0.00	5.47	0.73	73.02	25.75	2401.17	9857.14
	0.93	0.93	0.75	0.00	5.48	0.72	71.55	24.15	2405.88	9810.03
	0.93	0.93	0.50	0.00	5.51	0.71	70.44	20.30	2419.23	9676.52
	0.93	0.93	0.25	0.00	5.58	0.69	70.91	18.51	2446.96	9399.21
	0.93	0.93	1.00	0.25	5.13	0.84	72.27	25.01	2248.63	11382.50
	0.93	0.93	1.00	0.50	4.89	0.92	74.08	33.08	2144.60	12422.80
	0.93	0.93	1.00	0.75	4.79	0.95	76.74	36.91	2099.26	12876.14
	0.93	0.93	0.75	0.25	5.14	0.84	71.16	24.67	2253.11	11337.68
	0.93	0.93	0.75	0.50	4.90	0.91	73.40	32.77	2148.38	12385.02
	0.93	0.93	0.67	0.33	5.05	0.86	71.48	27.59	2214.32	11725.56
	0.93	0.93	0.50	0.25	5.16	0.83	70.74	23.78	2265.24	11216.44
	0.00	0.00	....	....	15.31	2.1	156.95	45.55	2233.89	11529.86
	0.93	0.00	1.00	....	15.36	2.1	153.96	44.25	2240.54	11463.38
	0.93	0.00	0.75	....	15.41	2.1	151.94	42.76	2248.19	11386.93
	0.93	0.00	0.67	....	15.44	2.1	151.18	41.78	2253.24	11336.36
	0.93	0.00	0.50	....	15.57	2.1	149.58	38.28	2271.29	11155.94
	0.93	0.00	0.33	....	15.79	2.0	148.31	32.04	2303.56	10833.22
	0.93	0.00	0.25	....	15.93	2.0	147.97	27.98	2324.54	10623.43
(c)	0.93	0.00	0.00	....	16.43	1.8	149.02	27.32	2396.56	9903.16
	0.93	0.93	1.00	0.00	16.44	1.8	146.69	25.74	2398.30	9885.81
	0.93	0.93	0.75	0.00	16.45	1.8	145.22	24.12	2400.26	9866.16
	0.93	0.93	0.50	0.00	16.49	1.8	144.12	20.23	2405.81	9810.66
	0.93	0.93	0.25	0.00	16.57	1.8	144.63	18.48	2417.26	9696.16
	0.93	0.93	1.00	0.25	15.95	2.0	146.07	27.61	2326.43	10604.54
	0.93	0.93	1.00	0.50	15.58	2.1	148.26	37.97	2272.89	11139.89
	0.93	0.93	1.00	0.75	15.42	2.1	151.19	42.52	2249.40	11374.79
	0.93	0.93	0.75	0.25	15.96	2.0	144.95	27.20	2328.57	10583.12
	0.93	0.93	0.75	0.50	15.59	2.1	147.55	37.60	2274.79	11120.91
	0.93	0.93	0.67	0.33	15.82	2.0	145.37	31.03	2308.77	10781.05
	0.93	0.93	0.50	0.25	16.00	1.9	144.49	26.07	2334.39	10524.85

Table 4

APPENDIX C

COMPUTER PROGRAM

C. 1 Introduction

The numerical investigations carried out in Chapters 3 and 5, based on the continuu method theory presented in Chapter 2 for unequal coupled shear walls and in Chapter 4 fo stiffened coupled shear walls have been carried out using a computer program written i Fortran 77 on an "ICL 3980" machine.

C. 2 Program listing

```
      PROGRAM STIFF
C@@@@@@@@@@@@@@@@@@@@@@@@@@@@@@@@@@@@@@@@@@@@@@@@@@@@@@@@@@@@@@@@@@@@@@
C THIS PROGRAM CALCULATES FORCES AND DEFLECTION IN A SHEAR WALL WITH  @
C A ROW OF OPENINGS AND TWO STIFFENING BEAMS ALONG THE HEIGHT BY THE   @
C SHEAR CONNECTION METHOD FOR RIGID AND FLEXIBLE BASES.                @
C THIS PROGRAM ALSO GIVES THE DISCRETE VALUES OF THE FORCES            @
C AT EACH STOREY LEVEL.                                                @
C@@@@@@@@@@@@@@@@@@@@@@@@@@@@@@@@@@@@@@@@@@@@@@@@@@@@@@@@@@@@@@@@@@@@@@
C
      REAL K,I,L,I1,I2,MOM1,MOM11,MOM2,L1,L2,MOM22,IB,IC,IB1,KR,KV,IB2,
     @K1,K2,M1,M2,M,MOM3,MOM4,MOM33,MOM44
C
      DIMENSION W6(110),W7(110),SS5(110),SS6(110),G(110),FMD1(110),
     @FMD2(110),FMI1(110),SS7(110),SS8(110),FMI2(110),FM(110),
     @DELTA3(110),BOR1(110),BOR2(110),SGMAA(110),SGMAB(110),SGMAC(110),
     @SGMAD(110),BOR4(110)
C
      COMMON/INPUT/YM,SM,CL,UL,TL,B,H,D1,D2,C1,C2,I1,AREA1,I2,AREA2,
     @IB,AB,J,IB1,AB1,IB2,AB2,X1,X2,ISF,KV,KR
      COMMON/OUTPUT/NSTEPS,X(110),T(110),R(110),M1(110),M2(110),THEI2,
     @T22,Z22,THEI4,T44,Z44,S1(110),R1(110),T1(110),Z1(110),Y(110),
     @Y1(110),SZ2(110),SW2(110),QX210,SZ1(110),SW1(110),QX220,SZ(110),
     @SW(110),QX(110),SLO(110),MOM1(110),MOM2(110),MOM11(110),
     @MOM22(110),LEV(110),W(110),SS4(110),SS2(110),W1(110),W3(110),
     @SS3(110),W2(110),W4(110),MOM3(110),MOM33(110),MOM4(110),
     @MOM44(110),K1(110),K2(110),QX1(110),DELTA,GAMA1,GAMA2,RMAX,XMAX1,
     @RMIN,K,S,THETA,V0,LEV1,LEV2,SSMAX,XMAX2
```

```
C
C *** NOMENCLATURE
C
C** YM and SM = Young modulus (E) and Shear modulus (G) respectively.
C** CL, UL, and TL = P, U, and W
C** B and H = Span of the connecting beams (b) and storey height (h)
C** J = Nb of stories (J)
C** HT = Total height of the structure (H)
C** D1 and D2 = Distances from the centroidal axes of the walls to the inner
C                edges of the walls (d1 and d2)
C** C1 and C2 = Whidths of the walls (c1+d1 and c2+d2)
C** I1,I2,AREA1, and AREA2 = I1,I2,A1, and A2
C** IB and AB = Ib and Ab
C** IB1,IB2,AB1, and AB2 = If1,If2,Ab1, and Ab2
C** X1 and X2 = x1 and x2
C** T = Axial forces in walls (T)
C** R = Laminar shear (q)
C** M1 and M2 = Bending moments (M1,M2) in the walls 1 and 2 respectively
C** W = Axial force (N) at beam level in the discrete system
C** KV and KR = Combined vertical and rotational stiffnesses (Kδ,Kr) of
C                the foundation system, respectively.
C** SZ and SW = Shears (S1,S2) in walls 1 and 2 respectively
C** SS2 = Concentrated shear force (Q) at beam level for the discrete system
C** SS3 and SS4 = Axial forces above and below [(T)f1,(T)f2] in the discrete
C                 system of walls at beam levels.
C** W1 and W2 = Shears above and below [(S1)f1,(S1)f2] in the discrete system
C                of wall 1.
C** W3 and W4 = Shears above and below [(S2)f1,(S2)f2] in the discrete system
C                of wall 2.
C** FM = Applied exterior moment (Me).
C** QX = Axial flow in the continuous medium (n)
C** S and theta = Base vertical displacement (s) and base rotation (θ)
C

      CALL DATA
C
      L1=D1+B/2.0
      L2=D2+B/2.0
C
C *** calculation of the shifts of the points of contraflexure from the
C     mid-span position of the corresponding beams.
C
C main lintel beams
C
      DELTA=L2*(I1-L1/L2*I2)/(I1+I2+12.0*B/H*I1*I2/IB)
C
C top lintel beam
C
      DELT=L2*(I1-L1/L2*I2)/(I1+I2+6.0*B/H*I1*I2/IB)
C
C stiffening beams 1 and 2
C
      DELTA1=L2*(I1-L1/L2*I2)/(I1+I2+12.0*B/H*I1*I2/IB1)
      DELTA2=L2*(I1-L1/L2*I2)/(I1+I2+12.0*B/H*I1*I2/IB2)
      IF(X1.EQ.1.0)DELTA1=L2*(I1-L1/L2*I2)/(I1+I2+6.0*B/H*I1*I2/IB1)
      IF(X1.EQ.1.0)DELT=DELTA1
```

```
C
C *** calculation of the reduction factors
C
      CF=1.0-12.0*(DELTA/B)**2/(1.0+12.0*(DELTA/B)**2)
      CF1=1.0-12.0*(DELTA1/B)**2/(1.0+12.0*(DELTA1/B)**2)
      CF2=1.0-12.0*(DELTA2/B)**2/(1.0+12.0*(DELTA2/B)**2)
      RNU=YM/(2.0*SM)-1.0
      RF=1.2
      SF=24*RF*IB/AB*(1.0+RNU)/B**2*CF
      IF(IB1.EQ.IB)SF1=0.0
      IF(IB2.EQ.IB)SF2=0.0
      SF1=24*RF*(IB1-IB)/(AB1-AB)*(1.0+RNU)/B**2*CF1
      SF2=24*RF*(IB2-IB)/(AB2-AB)*(1.0+RNU)/B**2*CF2
      GF=1.0-SF/(1.0+SF)
      GF1=1.0-SF1/(1.0+SF1)
      GF2=1.0-SF2/(1.0+SF2)
C
      SM1=(IB1-IB)/IB
      SM2=(IB2-IB)/IB
      YM1=YM
      YM2=YM
      GAMA1=SM1/J*YM1/YM*GF1/GF*CF1/CF
      GAMA2=SM2/J*YM2/YM*GF2/GF*CF2/CF
      HT=J*H
      L=L1+L2
      AREA=AREA1+AREA2
      I=I1+I2
      IC=IB*GF*CF
      A=12.0*IC*L/(H*B**3*I)
      M=(AREA1*AREA2*L)/AREA
      SI=I+M*L
      E=A*SI/M
      K=SQRT(E)*HT
      G1=K*X1
      G2=K*X2
      FM0=HT*(CL+UL/2.0+TL*2.0/3.0)
C
C *** CALCULATION OF THE CONSTANTS OF INTEGRATION
C
      IF(ISF.EQ.1)THEN
      STW1=0.0
      STW2=0.0
      WRITE(6,*)'RIGID FOUNDATIONS'
      ENDIF
      IF(ISF.EQ.2)THEN
      STW1=12.0*YM*IC/(KV*H*B**3)
      STW2=12.0*YM*IC*L/(KR*H*B**3)
      ENDIF
      STW=STW1+L*STW2
      U1=-A/E*HT*(UL+2.0*TL)/(K**2*COSH(K))
      U21=COSH(G1)-GAMA1*K*SINH(G1)
      U31=SINH(G1)-GAMA1*K*COSH(G1)
      U41=-GAMA1*A/E*HT*((UL*(1.0-X1)+TL*(1.0-X1**2-
     @2.0/K**2)+CL))
      U5=-A/E*((CL+UL)+TL*(1.0-2.0/K**2)+STW*(FM0+UL*HT/K**2))
     @+STW2*FM0
      PSI1=1.0-TANH(K)*TANH(G1)
      PSI2=TANH(K)*U21-U31
```

```
      U22=COSH(G2)-GAMA2*K*SINH(G2)
      U32=SINH(G2)-GAMA2*K*COSH(G2)
      U42=-GAMA2*A/E*HT*((UL*(1.0-X2)+TL*(1.0-X2**2-2.0/K**2)+CL))
      DD=(COSH(G2)+STW*HT/K*SINH(G2))
      DDD=TANH(G2)+STW*HT/K
      D11=PSI1*COSH(G1)+PSI2*TANH(G1)
      D21=-PSI1*SINH(G1)-PSI2
      D31=PSI1*(U1*U21-U41)+PSI2*U1*TANH(G1)
      D12=U22*DDD-TANH(G2)*DD
      D22=DD-U32*DDD
      D32=U5*HT/K*DD+DDD*(U42-U5*HT/K*SINH(G2))
      DD1=(U1*U21-U41)*D12-COSH(G1)*D32
      DD2=TANH(G1)*(U1*D12-D32)
      DD3=D22*COSH(G1)+D12*SINH(G1)
      DD4=D22*TANH(G1)+D12
      CONSB2=(PSI1*DD1+PSI2*DD2)/(PSI1*DD3+PSI2*DD4)
      CONST2=(CONSB2*D21+D31)/D11
      STDA2=(D31*D22-D32*D21)/(D22*D11-D21*D12)
      CONS=CONST2*U22+CONSB2*U32-U42+U5*HT/K*SINH(G2)
      CONST3=CONS/DD
      CONSB3=HT*(CONST3*STW/K-U5/K)
      CONSB1=(CONSB2-(U1-CONST2)*TANH(G1))/PSI1
      CONST1=-CONSB1*TANH(K)+U1
C
      STEP=1.0/J
      NSTEPS=J+1
C
      DO 1 IJ=1,NSTEPS
C
      X(IJ)=1.0-(IJ-1)*STEP
      LEV(IJ)=J*X(IJ)
      LEV1=J*X1
      LEV2=J*X2
      G(IJ)=K*X(IJ)
      IF(IJ.EQ.1)THEN
      BOR1(IJ)=K
      BOR2(IJ)=K*(1.0-1.0/(2.0*J))
      BOR4(IJ)=BOR2(IJ)
      CONST=CONST1
      CONSB=CONSB1
      DELTA3(IJ)=DELT
      IF(X1.EQ.1.0)CONST=CONST2
      IF(X1.EQ.1.0)CONSB=CONSB2
      ENDIF
      IF(IJ.LT.NSTEPS.AND.IJ.GT.1)THEN
      BOR1(IJ)=K*(X(IJ)+1.0/(2.0*J))
      BOR2(IJ)=K*(X(IJ)-1.0/(2.0*J))
      BOR4(IJ)=BOR2(IJ)
      DELTA3(IJ)=DELTA
      IF(X(IJ).GT.X1)THEN
      CONST=CONST1
      CONSB=CONSB1
      ENDIF
      IF(LEV1.EQ.LEV(IJ))THEN
      BOR1(IJ)=K*(X1+1.0/(2.0*J))
      BOR2(IJ)=G1
      CONST=CONST1
      CONSB=CONSB1
```

```
      DELTA3(IJ)=DELTA1
      ENDIF
      IF(X(IJ).GT.X2.AND.X(IJ).LT.X1)THEN
      CONST=CONST2
      CONSB=CONSB2
      ENDIF
      IF(LEV2.EQ.LEV(IJ))THEN
      BOR1(IJ)=K*(X2+1.0/(2.0*J))
      BOR2(IJ)=G2
      CONST=CONST2
      CONSB=CONSB2
      DELTA3(IJ)=DELTA2
      ENDIF
      IF(X(IJ).LT.X2)THEN
      CONST=CONST3
      CONSB=CONSB3
      ENDIF
      ENDIF
      IF(IJ.EQ.NSTEPS)THEN
      BOR1(IJ)=0.0
      BOR2(IJ)=0.0
      BOR4(IJ)=0.0
      CONST=CONST3
      CONSB=CONSB3
      DELTA3(IJ)=DELTA
      ENDIF
      BOR3=K*(X1-1.0/(2.0*J))
      BOR5=K*(X2-1.0/(2.0*J))
      IF(X2.EQ.0.0)BOR5=0.0
C
      FM(IJ)=HT*(CL*(1.0-X(IJ))+UL*(1.0-X(IJ))**2/2.0+TL*(1.0-X(IJ))
     @**2*(2.0+X(IJ))/3.0)
      FM10=HT*(CL*(1.0-X1)+UL*(1.0-X1)**2/2.0+TL*(1.0-X1)
     @**2*(2.0+X1)/3.0)
      FM20=HT*(CL*(1.0-X2)+UL*(1.0-X2)**2/2.0+TL*(1.0-X2)
     @**2*(2.0+X2)/3.0)
      FMD1(IJ)=-CL-UL*(1.0-X(IJ))-TL*(1.0-X(IJ)**2)
      FMD2(IJ)=(UL+2.0*TL*X(IJ))/HT
      FMD110=(UL+2.0*TL*X1)/HT
      FMD120=(UL+2.0*TL*X2)/HT
      FMI1(IJ)=HT**2*(1.0/2.0*CL*X(IJ)*(2.0-X(IJ))-UL/6.0*((1.0-X
     @(IJ))**3-1.0)+TL*X(IJ)/(12.0)*(8.0-6.0*X(IJ)+X(IJ)**3))
      FMI2(IJ)=HT**3*(1.0/6.0*CL*X(IJ)**2*(3.0-X(IJ))+UL/24.0*((1.0-
     @X(IJ))**4+4.0*X(IJ)-1.0)+TL/60.0*X(IJ)**2*(20.0-10.0*X(IJ)+
     @X(IJ)**3))
C
C *** CONTINUOUS SYSTEM
C
C *** CALCULATION OF FORCES
C
      T(IJ)=CONST*COSH(G(IJ))+CONSB*SINH(G(IJ))+A/E*(FM(IJ)+2.0*TL*HT*
     @X(IJ)/K**2+UL*HT/(K**2))
      T(NSTEPS)=CONST3+A/E*(FM0+UL*HT/(K**2))
      IF(ISF.EQ.1)S=0.0
      IF(ISF.EQ.2)S=T(NSTEPS)/KV
      M1(IJ)=I1/I*(FM(IJ)-T(IJ)*L)
      M2(IJ)=I2/I*(FM(IJ)-T(IJ)*L)
      R(IJ)=-K/HT*CONST*SINH(G(IJ))-K/HT*CONSB*COSH(G(IJ))-A/E*
```

```
     @(FMD1(IJ)+2.0*TL/K**2)
      THEI1=CONST1*COSH(G1)+CONSB1*SINH(G1)+A/E*(FM10+2.0*TL*HT/
     @K**2*X1+UL*HT/(K**2))
      THEI2=CONST2*COSH(G1)+CONSB2*SINH(G1)+A/E*(FM10+2.0*TL*HT/
     @K**2*X1+UL*HT/(K**2))
      THEI3=CONST2*COSH(G2)+CONSB2*SINH(G2)+A/E*(FM20+2.0*TL*HT/
     @K**2*X2+UL*HT/(K**2))
      THEI4=CONST3*COSH(G2)+CONSB3*SINH(G2)+A/E*(FM20+2.0*TL*HT/
     @K**2*X2+UL*HT/(K**2))
      VM1=THEI2-THEI1
      VM2=THEI4-THEI3
      M1(NSTEPS)=I1/I*(FM0-T(NSTEPS)*L)
      M2(NSTEPS)=I2/I*(FM0-T(NSTEPS)*L)
      V0=M1(NSTEPS)+M2(NSTEPS)
      T11=I1/I*(FM10-THEI1*L)
      Z11=I2/I*(FM10-THEI1*L)
      T22=I1/I*(FM10-THEI2*L)
      Z22=I2/I*(FM10-THEI2*L)
      T33=I1/I*(FM20-THEI3*L)
      Z33=I2/I*(FM20-THEI3*L)
      T44=I1/I*(FM20-THEI4*L)
      Z44=I2/I*(FM20-THEI4*L)
      FX110=K**2/HT**2*(CONST1*COSH(G1)+CONSB1*SINH(G1))+A/E*
     @FMD110
      FX210=K**2/HT**2*(CONST2*COSH(G1)+CONSB2*SINH(G1))+A/E*
     @FMD110
      FX120=K**2/HT**2*(CONST2*COSH(G2)+CONSB2*SINH(G2))+A/E*
     @FMD120
      FX220=K**2/HT**2*(CONST3*COSH(G2)+CONSB3*SINH(G2))+A/E*
     @FMD120
      F11=K**2/HT**2*(CONST*COSH(G(IJ))+CONSB*SINH(G(IJ)))+A/E*FMD2(IJ)
      FAC=(A/E)*(I1/I*L-L1-DELTA)
      QX110=I2/I*FMD110+FAC*E/A*FX110
      QX210=I2/I*FMD110+FAC*E/A*FX210
      QX120=I2/I*FMD120+FAC*E/A*FX120
      QX220=I2/I*FMD120+FAC*E/A*FX220
      QX(IJ)=I2/I*FMD2(IJ)+FAC*E/A*F11
      SZ(IJ)=-I1/I*FMD1(IJ)-(I1/I*L-L1-DELTA)*R(IJ)
      SW(IJ)=-I2/I*FMD1(IJ)-(I2/I*L-L2+DELTA)*R(IJ)
C
C *** CALCULATION OF STRESSES
C
      SGMAA(IJ)=T(IJ)/AREA1+M1(IJ)*(C1-D1)/I1
      SGMAB(IJ)=T(IJ)/AREA1-M1(IJ)*D1/I1
      SGMAC(IJ)=-T(IJ)/AREA2+M2(IJ)*D2/I2
      SGMAD(IJ)=-T(IJ)/AREA2-M2(IJ)*(C2-D2)/I2
      IF(IJ.GT.1)THEN
      K2(IJ)=100.0*E/(A*L)*L*T(IJ)/FM(IJ)
      K1(IJ)=100-K2(IJ)
      ENDIF
C
C CALCULATION OF SLOPES AND LATERAL DEFLECTIONS
C
      IF(ISF.EQ.1)THETA=0.0
      IF(ISF.EQ.2)THETA=V0/KR
      ESD=A*L*HT**2/K**2
      IF(X(IJ).GT.X1)THEN
      DEL1=(X(IJ)-X1)*((CONST1-CONST2)*SINH(G1)+(CONSB1-CONSB2)*COSH
```

```
     @(G1))+(X(IJ)-X2)*((CONST2-CONST3)*SINH(G2)+(CONSB2-CONSB3)*
     @COSH(G2))
      DEL2=CONST1*(COSH(G1)-COSH(G(IJ)))+CONST2*(COSH(G2)-
     @COSH(G1))+CONSB1*(SINH(G1)-SINH(G(IJ)))+CONSB2*(SINH(G2)
     @-SINH(G1))+CONST3*(1.0-COSH(G2))+CONSB3*(G(IJ)-SINH(G2))
      DEL3=(CONST1-CONST2)*SINH(G1)+(CONSB1-CONSB2)*COSH(G1)
     @+(CONST2-CONST3)*SINH(G2)+(CONSB2-CONSB3)*COSH(G2)
      DEL4=-K*(CONST1*SINH(G(IJ))-CONSB3+CONSB1*COSH(G(IJ)))
      ENDIF
      IF(LEV(IJ).LE.LEV1)THEN
      DEL1=(X(IJ)-X2)*((CONST2-CONST3)*SINH(G2)+(CONSB2-CONSB3)*
     @COSH(G2))
      DEL2=CONST2*(COSH(G2)-COSH(G(IJ)))+CONST3*(1.0-COSH(G2))
     @+CONSB2*(SINH(G2)-SINH(G(IJ)))+CONSB3*(G(IJ)-SINH(G2))
      DEL3=(CONST2-CONST3)*SINH(G2)+(CONSB2-CONSB3)*COSH(G2)
      DEL4=-K*(CONST2*SINH(G(IJ))+CONSB2*COSH(G(IJ))-CONSB3)
      ENDIF
      IF(LEV(IJ).LE.LEV2)THEN
      DEL1=0.0
      DEL2=CONST3*(1.0-COSH(G(IJ)))+CONSB3*(G(IJ)-SINH(G(IJ)))
      DEL3=0.0
      DEL4=-K*(CONST3*SINH(G(IJ))-CONSB3*(1.0-COSH(G(IJ))))
      ENDIF
      Y(IJ)=1.0/(YM*I)*((1.0-ESD)*FMI2(IJ)+L/K*HT**2*DEL1+L/K**2
     @*HT**2*DEL2-ESD*HT**3*(UL*X(IJ)**2/(2.0*K**2)+TL*X(IJ)**3/
     @(3.0*K**2)))+THETA*X(IJ)*HT
      SLO(IJ)=1.0/(YM*I)*((1.0-ESD)*FMI1(IJ)+L/K*HT*DEL3
     @+L/K**2*HT*DEL4-ESD*HT**2*(UL*X(IJ)/K**2+TL*X(IJ)**2/K**2))+
     @THETA
C
C *** DISCRETISATION OF THE SYSTEM
C
C ** CALCULATION OF SHEAR FORCES AND AXIAL FORCES IN THE DISCRETE SET OF
C    BEAMS

      FMC=HT*(CL*(BOR4(IJ)-BOR1(IJ))/K+UL*(1.0-BOR1(IJ)/K)**2/2.0
     @-UL*(1.0-BOR4(IJ)/K)**2/2.0+TL*(1.0-BOR1(IJ)/K)**2
     @*(2.0+BOR1(IJ)/K)/3.0-TL*(1.0-BOR4(IJ)/K)**2*(2.0+BOR4(IJ)/K)/3.0
     @+2.0*TL/K**3*(BOR1(IJ)-BOR4(IJ)))
      FMC1=-UL*(BOR4(IJ)-BOR1(IJ))/K-TL*(BOR4(IJ)**2-BOR1(IJ)**2)/K**2
      IF(IJ.EQ.1)FMC1=-UL*(BOR4(IJ)-BOR1(IJ))/K-TL*(BOR4(IJ)**2-
     @BOR1(IJ)**2)/K**2+CL
      IF(LEV1.EQ.LEV(IJ).AND.IJ.NE.1)GOTO 50
      IF(LEV2.EQ.LEV(IJ).AND.IJ.NE.NSTEPS)GOTO 60
      SS2(IJ)=-(CONST*(COSH(BOR1(IJ))-COSH(BOR2(IJ)))+CONSB*(SINH
     @(BOR1(IJ))-SINH(BOR2(IJ)))+A/E*FMC)
      F1=E/A*(CONST*K/HT*(SINH(BOR1(IJ))-SINH(BOR2(IJ)))+CONSB*K/HT*
     @(COSH(BOR1(IJ))-COSH(BOR2(IJ)))+A/E*FMC1)
      IF(X1.EQ.1.0)SS2(IJ)=SS2(IJ)+VM1
      IF(X2.EQ.0.0)SS2(IJ)=SS2(IJ)+VM2
      GOTO 70
 50   SS2(IJ)=-(CONST1*(COSH(BOR1(IJ))-COSH(BOR2(IJ)))+CONSB1*(SINH
     @(BOR1(IJ))-SINH(BOR2(IJ)))+A/E*FMC)
     @-(CONST2*(COSH(BOR2(IJ))-COSH(BOR3))+CONSB2*(SINH(BOR2(IJ))-
     @SINH(BOR3)))+VM1
      F1=E/A*(CONST1*K/HT*(SINH(BOR1(IJ))-SINH(BOR2(IJ)))+CONSB1*K/HT*
     @(COSH(BOR1(IJ))-COSH(BOR2(IJ)))+A/E*FMC1)+E/A*(CONST2*K/HT*
     @(SINH(BOR2(IJ))-SINH(BOR3))+CONSB2*K/HT*(COSH(BOR2(IJ))-COSH
```

```
     @(BOR3)))
      GOTO 70
 60   SS2(IJ)=-(CONST2*(COSH(BOR1(IJ))-COSH(BOR2(IJ)))+CONSB2*(SINH
     @(BOR1(IJ))-SINH(BOR2(IJ)))+A/E*FMC)
     @-(CONST3*(COSH(BOR2(IJ))-COSH(BOR5))+CONSB3*(SINH(BOR2(IJ))-
     @SINH(BOR5)))+VM2
      F1=E/A*(CONST2*K/HT*(SINH(BOR1(IJ))-SINH(BOR2(IJ)))+CONSB2*K/HT*
     @(COSH(BOR1(IJ))-COSH(BOR2(IJ)))+A/E*FMC1)+E/A*(CONST3*K/HT*(SINH
     @(BOR2(IJ))-SINH(BOR5))+CONSB3*K/HT*(COSH(BOR2(IJ))-COSH(BOR5)))
 70   F2=I2/I*FMC1
      W(IJ)=F2+FAC*F1
      W(1)=F2+FAC*F1+SW(1)
C
C ** CALCULATION OF THE SHEARS IN WALLS
C
      IF(IJ.EQ.1)W2(IJ)=FMC1-W(IJ)
      IF(IJ.GT.1)W2(IJ)=W2(IJ-1)-W(IJ)+FMC1
      W1(IJ)=W2(IJ)+W(IJ)-FMC1
      IF(IJ.EQ.1)W1(IJ)=W2(IJ)
      IF(IJ.EQ.1)W4(IJ)=W(IJ)
      IF(IJ.GT.1)W4(IJ)=W4(IJ-1)+W(IJ)
      W3(IJ)=W4(IJ)-W(IJ)
      IF(IJ.EQ.1)W3(IJ)=W4(IJ)
C
C ** CALCULATION OF THE AXIAL FORCES IN WALLS
C
      IF(IJ.EQ.1)SS4(IJ)=SS2(IJ)
      IF(IJ.GT.1)SS4(IJ)=SS4(IJ-1)+SS2(IJ)
      SS3(IJ)=SS4(IJ)-SS2(IJ)
      IF(IJ.EQ.1)SS3(IJ)=SS4(IJ)
C
C ** CALCULATION OF MOMENTS IN WALLS
C
      IF(IJ.EQ.1)W6(IJ)=0.0
      IF(IJ.GT.1)W6(IJ)=W6(IJ-1)+W1(IJ)*HT/J
      IF(IJ.EQ.1)W7(IJ)=0.0
      IF(IJ.GT.1)W7(IJ)=W7(IJ-1)+W3(IJ)*HT/J
      SS5(IJ)=-SS3(IJ)*(L1+DELTA3(IJ))
      SS6(IJ)=-SS4(IJ)*(L1+DELTA3(IJ))
      SS7(IJ)=-SS3(IJ)*(L2-DELTA3(IJ))
      SS8(IJ)=-SS4(IJ)*(L2-DELTA3(IJ))
      MOM1(IJ)=W6(IJ)+SS5(IJ)
      MOM11(IJ)=SS6(IJ)+W6(IJ)
      MOM2(IJ)=W7(IJ)+SS7(IJ)
      MOM22(IJ)=SS8(IJ)+W7(IJ)
C
C ** ALTERNATIVE CALCULATION OF MOMENTS
C
      MOM3(IJ)=M1(IJ)+0.5*SS2(IJ)*(L1+DELTA3(IJ))
      MOM33(IJ)=M1(IJ)-0.5*SS2(IJ)*(L1+DELTA3(IJ))
      MOM4(IJ)=M2(IJ)+0.5*SS2(IJ)*(L2-DELTA3(IJ))
      MOM44(IJ)=M2(IJ)-0.5*SS2(IJ)*(L2-DELTA3(IJ))
C
 1       CONTINUE
C
      MOM33(1)=M1(1)-SS2(1)*(L1+DELTA3(1))
      MOM3(1)=MOM33(1)
      MOM44(1)=M2(1)-SS2(1)*(L2-DELTA3(1))
```

```
      MOM4(1)=MOM44(1)
      MOM4(NSTEPS)=M2(NSTEPS)+SS2(NSTEPS)*(L2-DELTA3(NSTEPS))
      MOM44(NSTEPS)=M2(NSTEPS)
      MOM3(NSTEPS)=M1(NSTEPS)+SS2(NSTEPS)*(L1+DELTA3(NSTEPS))
      MOM33(NSTEPS)=M1(NSTEPS)
C
      RMAX=-500.0E35
      SSMAX=-500.0E35
C
      DO 2 IJ=1,NSTEPS
C
      IF(R(IJ).GT.RMAX)RMAX=R(IJ)
      IF(RMAX.EQ.R(IJ))XMAX1=X(IJ)
      IF(SS2(IJ).GT.SSMAX)SSMAX=SS2(IJ)
      IF(SSMAX.EQ.SS2(IJ))XMAX2=X(IJ)
C
 2    CONTINUE
C
      CALL RESULT
C
      CLOSE(6)
      CLOSE(5)
      STOP
      END
C
      SUBROUTINE DATA
C
      COMMON/INPUT/YM,SM,CL,UL,TL,B,H,D1,D2,C1,C2,I1,AREA1,I2,AREA2,
     @IB,AB,J,IB1,AB1,IB2,AB2,X1,X2,ISF,KV,KR
      REAL I1,I2,IB,IB1,IB2,KV,KR
      OPEN(5,FILE=':GNCV65.HEIGH.DATA')
      REWIND(5)
      READ(5,*)YM,SM
      READ(5,*)CL,UL,TL
      READ(5,*)B,H
 19   FORMAT(1A3)
      READ(5,*)D1,D2
      READ(5,*)C1,C2
      READ(5,*)I1,AREA1,I2,AREA2
      READ(5,*)IB,AB
      READ(5,*)J
      READ(5,*)IB1,AB1,IB2,AB2
      READ(5,*)X1,X2
      READ(5,*)ISF
      IF(ISF.EQ.2)THEN
      READ(5,*)KV,KR
      WRITE(6,*)'FLEXIBLE FOUNDATIONS'
      WRITE(6,*)
      WRITE(6,20)'Kdelta = ',KV,',',' Kr = ',KR
 20    FORMAT(A9,E9.3,A1,A6,E9.3)
      ENDIF
      RETURN
      END
C
      SUBROUTINE RESULT
C
      REAL MOM1,MOM11,MOM2,
     @MOM22,K1,K2,M1,M2,K
```

```
     @,MOM3,MOM4,MOM33,MOM44,I1,I2,IB,IB1,IB2,KV,KR
      COMMON/INPUT/YM,SM,CL,UL,TL,B,H,D1,D2,C1,C2,I1,AREA1,I2
     @,AREA2,IB,AB,J,IB1,AB1,IB2,AB2,X1,X2,ISF,KV,KR
      COMMON/OUTPUT/NSTEPS,X(110),T(110),R(110),M1(110),M2(110),THEI2
     @,T22,Z22,THEI4,T44,Z44,S1(110),R1(110),T1(110),Z1(110),Y(110)
     @,Y1(110),SZ2(110),SW2(110),QX210,SZ1(110),SW1(110),QX220
     @,SZ(110),SW(110),QX(110),SLO(110),MOM1(110),MOM2(110),MOM11(110)
     @,MOM22(110),LEV(110),W(110),SS3(110),SS2(110),W1(110),W3(110),
     @SS4(110),W2(110),W4(110),MOM3(110),MOM33(110),MOM4(110),
     @MOM44(110),K1(110),K2(110),QX1(110),DELTA,GAMA1,GAMA2,RMAX
     @,XMAX1,RMIN,K,S,THETA,V0,LEV1,LEV2,SSMAX,XMAX2
      OPEN(6,FILE=':GNCV65.HEIGH.OUTPUT')
      CALL DATA
C
C *** OUTPUT RESULTS
C
      WRITE(6,*)
      WRITE(6,*)' A of 1st S.Beam ',' A of 2nd S.Beam'
     @,' I of 1st S.Beam ',' I of 2nd S.Beam '
      WRITE(6,21)AB1,AB2,IB1,IB2
      WRITE(6,*)
      WRITE(6,22)'B','d1','d2','h','J','K','delta/b'
 22    FORMAT(A2,4X,A4,4X,A4,2X,A4,2X,A4,2X,A3,4X,A7)
      WRITE(6,23)B,D1,D2,H,J,K,DELTA/B
 23    FORMAT(F3.1,4X,F4.2,4X,F4.2,2X,F4.2,1X,I4,2X,F5.2,4X,F4.2
     @,2X,A7)
      WRITE(6,*)
      WRITE(6,*)' A of 1st Wall   ',' A of 2nd Wall  '
     @,' I of 1st Wall   ',' I of 2nd Wall   '
      WRITE(6,21)AREA1,AREA2,I1,I2
 21   FORMAT(6X,E8.2,9X,E8.2,8X,E8.2,9X,E8.2)
      WRITE(6,*)
      WRITE(6,25)
      WRITE(6,*)
 25     FORMAT(' GAMA1',2X,'GAMA2',1X,'X1/H',2X,'X2/H',3X,'S:mm',4X,
     @'THETA',5X,'Y(H)',4X,'qmax',4X,'To',8X,'Mo')
      WRITE(6,26)GAMA1,GAMA2,X1,X2,S*1.0E3,THETA,Y(1)*1.0E3,
     @RMAX,T(NSTEPS),V0
 26       FORMAT(F6.3,1X,F6.3,1X,F4.2,2X,F4.2,2X,E7.1,2X,E7.1,2X,E7.1,
     @2X,F6.2,1X,E8.2,2X,E8.2)
      WRITE(6,*)
C
      WRITE(6,30)
 30   FORMAT(3X,'qmax',4X,'Xcor/H',5X,'Qmax',5X,'Xcor/H')
      WRITE(6,31)RMAX,XMAX1,SSMAX,XMAX2
 31    FORMAT(1X,E9.2,1X,E8.2,1X,E9.2,E9.2)
C
C ** CONTINUOUS CONNECTION RESULTS
C
      WRITE(6,*)
      WRITE(6,*)'CONTINUOUS CONNECTION RESULTS'
      WRITE(6,24)'X/H ','T','q','M1','M2'
 24    FORMAT(/1X,A4,4X,2(A3,8X),2(A4,7X),A8)
      DO 3 IJ=1,NSTEPS
      WRITE(6,32)X(IJ),T(IJ),R(IJ),M1(IJ),M2(IJ)
       IF(LEV1.EQ.LEV(IJ))WRITE(6,32)X(IJ),THEI2,R(IJ),T22,Z22
       IF(LEV2.EQ.LEV(IJ))WRITE(6,32)X(IJ),THEI4,R(IJ),T44,Z44
 32   FORMAT(F5.2,2X,E9.2,2X,E9.2,2X,E9.2,2X,E9.2,2X,E9.2)
```

```
 3     CONTINUE
       WRITE(6,35)'Snb','Y','S1','S2','n flow','Slope'
 35    FORMAT(/1X,A3,4X,A3,7X,2(A3,7X),A6,4X,A5)
       DO 5 IJ=1,NSTEPS
       WRITE(6,36)LEV(IJ),Y(IJ),SZ(IJ),SW(IJ),QX(IJ),SLO(IJ)
       IF(LEV1.EQ.LEV(IJ))THEN
       WRITE(6,36)LEV(IJ),Y(IJ),SZ(IJ),SW(IJ),QX210,SLO(IJ)
       ENDIF
        IF(LEV2.EQ.LEV(IJ))THEN
       WRITE(6,36)LEV(IJ),Y(IJ),SZ(IJ),SW(IJ),QX220,SLO(IJ)
       ENDIF
 36    FORMAT(1X,I2,2X,2(E9.2,2X),E8.2,1X,E8.2,1X,E8.2)
 5     CONTINUE
C
C ** DISCRETE RESULTS
C
       WRITE(6,*)
       WRITE(6,*)'DISCRETE RESULTS'
       WRITE(6,37) 'Snb','MOM1','MOM2'
       WRITE(6,40)(LEV(IJ),MOM1(IJ),MOM2(IJ),LEV(IJ),MOM11(IJ),MOM22(IJ)
      @,IJ=1,NSTEPS)
       WRITE(6,39)'Snb',' Nf','Tf',' Qf','S1f','S2f'
 39    FORMAT(/1X,A3,2X,A7,2X,A7,4X,A6,6X,A3,6X,A3)
       WRITE(6,42)(LEV(IJ),W(IJ),SS3(IJ),SS2(IJ),W1(IJ),W3(IJ),
      @LEV(IJ),W(IJ),SS4(IJ),SS2(IJ),W2(IJ),W4(IJ),IJ=1,NSTEPS)
 42    FORMAT(2(1X,I2,2X,2(E9.2,2X),E8.2,1X,E8.2,1X,E8.2/))
       WRITE(6,*)
        WRITE(6,*)'ALTERNATIVE MOMENTS'
       WRITE(6,37) 'Snb','MOM1','MOM2'
 37    FORMAT(/1X,A3,2X,2(A7,4X),A6,2X,A3,4X,A3,4X,A3,4X,A3)
       WRITE(6,40)(LEV(IJ),MOM3(IJ),MOM4(IJ),LEV(IJ),MOM33(IJ),MOM44(IJ)
      @,IJ=1,NSTEPS)
 40    FORMAT(2(1X,I2,2X,2(E9.2,2X)/))
 10    CONTINUE
       RETURN
       END
```

REFERENCES

1. **Fintel M, (chairman)** — 'Response of Buildings to Lateral Forces'. ACI Committee 442, J. Am. Concr. Inst. 1971 Vol. 68 Feb., pp 81-106.

2. **Coull A, and Stafford Smith B** — 'Structural Analysis of Tall Concrete Buildings'. Proc. Inst. Civ. Engrs. 1973, Vol. 55, Part 2., pp 151-166.

3. **Coull A** — 'Structural Design of Tall Concrete and Masonry Buildings. Methods of Analysis'. Second Century of the Skyscraper, Van Nostrand Reinhold co., New York, 1988., pp 921-944.

4. **Chitty L, and Wan W. J** — 'Tall Buildings Structures Under Wind Load'. Proc. 7th Int. Conf. for App. Mech., 1948, Vol. 1, Paper 22., pp 254-268.

5. **Beck H** — 'Contribution to the Analysis of Coupled Shear Walls'. J. Am. Concr. Inst, 1962, Vol. 59, No. 8, August., pp 1055-1070.

6. **Rosman R** — 'Approximate Analysis of Shear Walls Subject to Lateral Loads'. J. Am. Concr. Inst, 1964, Vol. 61., pp 717-732.

7. Rosman R — 'An Approximate Method of Analysis of Walls of Multistory Buildings'. Civil Engineering and Public Works Review (London), 1964, Vol. 59., pp 67-69.

8. Rosman R — 'Tables for the Internal Forces of Pierced shear walls Subject to lateral loads'. Bauingenieur-Praxis, Heft 66, W. Ernest and Sohn, Berlin, 1966. (in German and English).

9. Coull A, and Puri R. D — 'Analysis of Coupled Shear Walls of Variable Thickness'. Building Science, 1967, Vol. 2., pp 181-188.

10. Coull A, and Puri R.D — 'Analysis of Coupled Shear Walls of Variable Cross-Section'. Building Science, 1968, Vol. 2., pp 313-320.

11. Coull A — 'Interaction of Coupled Shear Walls with Elastic Foundations'. J. Am. Concr. Inst, Proceedings, 1971, Vol. 68, June., pp 457-461.

12. Coull A — 'Stiffening of Coupled Shear Walls Against Foundation Movements'. Structural Engineer, 1974, Vol. 52, No. 1, Jan., pp 23-26.

13. Coull A, and Stafford Smith B — 'Tall Buildings'. Proceedings of a Symposium on Tall buildings, University of Southampton, April 1966, Pergamon Press.

14. Coull A, and Choudhury J. R — 'Stresses and Deflection in Coupled Shear Walls'. J. Am. Conc. Inst. 1967, Vol. 64, No. 2, Feb., pp 65-72.

15. Coull A, and Choudhury J. R — 'Analysis of Coupled Shear Walls'. J. Am. Concr. Inst. 1967, Vol. 64, Sept., pp 587-593.

16. Coull A — 'Design of Connecting Beams in Coupled Shear Wall Structures'. J. Am. Concr. Inst, 1969, Vol. 66, March., pp 205-209.

17. Marshall M. G — 'The Analysis of Shear Walls Structures'. M.sc. Thesis, University of Waterloo, Ontario, 1968, Sept.

18. Pearce D. J, and Mathews D. D — 'An Appraisal of the Design of Shear Walls in Box Frame Structures'. Property Services Agency Report, Department of the Environment, 1973.

19. Ungureanu N — 'A New Structural Model for Shear Walls Analysis' International Symposium on Earthquake Structural Engineering, U.S.A, 1976, Aug., pp 1277-1291.

20. Schwaighofer J, and Microys H. F — 'Analysis of Shear Walls Using Standard Computer Programs'. J. Am. Concr. Inst, 1969, Vol. 66, Dec., pp 1005-1007.

21. Stafford Smith B — 'Modified Beam Method for Analysing Symmetrical Interconnected Shear Walls'. J. Am. Concr. Inst, 1970, Vol. 67, Dec., pp 977-980.

22. Michael D — 'The Effect of Local Wall Deformations on the Elastic Interaction of Cross Walls Coupled by Beams'. Proc. Symposium of Tall Buildings, University of Southampton, Pergamon Press, 1966, April., pp 253-270.

23. Bhatt P — 'Effect of Beam-Shear Wall Junction Deformations on the Flexibility of Connecting Beams'. Buildg. Sci, Pergamon Press, 1973, June, Vol. 8., pp 149-151.

24. Tso W. K, and Chan P. C. K — 'Flexible Foundation Effect on Coupled Shear Walls'. J. Am. Concr. Inst, 1972, Vol. 69, No. 9, Sept., pp 678-683.

25. Coull A, and Choo B. S — 'Stiffening of Laterally Loaded Coupled Shear Walls on Elastic Foundations'. Bldg and Environment., 1984, Vol. 19, No. 4., pp 251-256.

26. Chan H. C, and Kuang J. S — 'Effect of a Single Deep Beam on Twin Shear Walls with Rational Coupling'. Proc. Instn. Civ. Engrs, Part 2, 1988, Vol. 85, Sept., pp 503-515.

27. Deschapelles B — Discussion of a paper by, Beck H., 'Contribution to the Analysis of Coupled Shear Walls'. J. Am. Concr. Inst, Part 2, Vol. 59, 1963, March., pp 1993-1997.

28. Macleod I — 'Connected Shear Walls of Unequal Width'. J. Am. Concr. Inst, 1970, Vol. 67, May., pp 408-412.

29. Arvidsson K — 'Shear Walls With Door Openings Near the Edge of the Wall'. J. Am. Concr. Inst, 1974, Vol. 71, July., pp 353-357.

30. Tso W. K, A.M.ASCE and Chan H. B 'Dynamic Analysis of plane coupled shear walls' Journal of Engineering Mechanics Division, Proceedings of the American Society of Civil Engineers, 1971, Vol. 97, February., pp 33-48.

31. Chan H. C, and Kuang J. S 'Stiffened Coupled Shear Walls' Journal of Engineering Mechanics, ASCE, 1989, Vol. 115, No. 4, April., pp 689-703.